ANALYSIS OF SECONDARY CARBONATES FROM THE YOUNG LOESS-PALEOSOL SEQUENCES OF THE CARPATHIAN BASIN – ESPECIALLY REGARDING THEIR PALEOENVIRONMENTAL ROLE

Gabriella Barta

PHD DISSERTATION

2016

Eötvös Loránd University, Faculty of Science
Ph.D. school of Earth Sciences, Program of Geography and Meteorology

Head of the Ph.D. school of Earth Sciences: Dr. József Nemes-Nagy professor
Head of the doctoral program of Geography and Meteorology: Dr. Mária Szabó professor
Supervisor: Dr. Erzsébet Horváth habil. associate professor

Dedicated to the Quaternary Rebellz

1 Tartalom

1 TARTALOM 3

1. INTRODUCTION OF SECONDARY CARBONATES 7

2. SECONDARY CARBONATE TYPES 8

2.1. SYNSEDIMENTARY CLASSIFICATION 8

2.1.1. DIRECT ORGANIC/BIOGENIC ORIGIN 8

2.1.1.1. CRC 8

2.1.1.2. EBS 10

2.1.1.3. NFC 15

2.1.2. ABIOGENIC OR INDIRECT BIOGENIC ORIGIN 18

2.1.2.1. HC 18

2.2. POSTSEDIMENTARY CLASSIFICATION 20

2.2.1. ABIOGENIC OR INDIRECT BIOGENIC ORIGIN 20

2.2.1.1. CC, CC2 AND HC+CC 20

2.2.1.2. MACROSCALE SECONDARY CARBONATES 21

2.3. PROPOSITION FOR A CLARIFIED NOMENCLATURE – IN ORDER TO AVOID MISUNDERSTANDINGS 26

2.3.1. RHIZOLITH, AS A COLLECTIVE NOUN 26

2.3.2. MICRORHIZOLITHS VERSUS HYPOCOATINGS 29

2.3.3. PSEUDOMYCELIA/PSEUDOMYCELIUM – DESCRIPTIVE TERM FOR FIELD INVESTIGATIONS 29

2.4. OPTIONS FOR INTERPRETATION BASED ON THE MORPHOLOGY AND DISTRIBUTION OF SECONDARY CARBONATES 31

2.4.1. DUST ACCRETION 31

2.4.2. PEDOSEDIMENTARY ASPECTS 32

2.4.3. WHY IS MICROMORPHOLOGY SO IMPORTANT? 33

2.4.4. ROLE OF CERTAIN MICROSCALE SECONDARY CARBONATES 33

3. INTRODUCTION TO THE STABLE CARBON AND OXYGEN ISOTOPE COMPOSITION OF SECONDARY CARBONATES 35

3.1. GENERAL INFORMATION 35

3.2. INFLUENCING FACTORS OF THE STABLE ISOTOPE COMPOSITION: 36

3.2.1. EVAPORATION 37

3.2.2. SEASONAL CHANGES 37

3.2.3. PREFERENCES FOR THE USAGE OF LIGHTER ISOTOPES AND EFFECTS OF MICROBIAL REWORKING 37

3.2.4. VEGETATION DENSITY 38

3.2.5. SEDIMENTATION RATES 38

3.2.6. SOURCES OF CO2 38

3.2.7. POSSIBLE EFFECTS OF DISSOLUTION 39

3.2.8. QUESTIONS OF THE APPLICABILITY OF STABLE ISOTOPE SIGNALS 39

3.2.9. GUIDELINES FOR PRESENT WORK 40
3.3. KEY TO THE INTERPRETATION OF STABLE CARBON AND OXYGEN ISOTOPE VALUES 40
4. METHODS 42
4.1. SAMPLING METHODS 42
4.2. DETERMINATION OF STABLE CARBON AND OXYGEN ISOTOPE VALUES (Δ13C, Δ18O) 42
5. SITES AND SAMPLING 43
5.1. VERŐCE 43
5.1.1. GENERAL DESCRIPTION OF THE VERŐCE SEQUENCE 43
5.1.2. APPLIED METHODS FOR THE VERŐCE SEQUENCE 46
5.1.3. CHARACTERISTICS OF THE DIFFERENT SEDIMENTARY UNITS AND STABLE ISOTOPE SIGNALS OF HC 48
5.1.3.1. PALEOSOLS 48
5.1.3.1.1. VARIATIONS OF P4 PALEOSOL 48
5.1.3.1.1.1. P4 PALEOSOL IN VALLEY BOTTOM POSITION 48
5.1.3.1.1.2. P4 PALEOSOL DEVELOPED IN LOCAL TOP POSITION 49
5.1.3.1.1.3. P4 PALEOSOL SITUATED ON A PALEOSLOPE 50
5.1.3.1.2. P3 PALEOSOL 51
5.1.3.1.3. P2 PALEOSOL 52
5.1.3.2. LOESSES 53
5.1.3.2.1. VARIATIONS OF THE L5 LOESS 53
5.1.3.2.1.1. POSITION OF L5 UNDER THE PALEOSOL OF VALLEY BOTTOM POSITION 53
5.1.3.2.1.2. POSITION OF L5 UNDER THE PALEOSOL OF LOCAL TOP POSITION 54
5.1.3.2.2. THE L4 LOESS UNIT (UNIT C-10) 56
5.1.3.2.3. THE L3 LOESS UNIT (UNIT C-5) 56
5.1.3.3. TRANSITION ZONES 57
5.1.3.4. REWORKED LAYERS 58
5.1.4. STABLE ISOTOPE COMPOSITION OF CERTAIN SECONDARY CARBONATES 59
5.1.4.1. STABLE ISOTOPE COMPOSITION OF HC+CC AT VERŐCE 59
5.1.4.2. STABLE ISOTOPE COMPOSITION OF CC AT VERŐCE 60
5.1.4.3. STABLE ISOTOPE COMPOSITION OF CRC AT VERŐCE 61
5.1.4.4. STABLE ISOTOPE COMPOSITION OF EBS AT VERŐCE 62
5.2. PAKS 63
5.2.1. GENERAL DESCRIPTION OF THE PAKS SEQUENCE 63
5.2.2. METHODS AND GUIDELINES FOR THE ANALYSIS 66
5.2.3. DETAILED DESCRIPTION OF THE STABLE CARBON AND OXYGEN ISOTOPE VALUES 68
5.2.4. SIMILAR TENDENCIES 80

5.2.4.1. HC VERSUS BULK SAMPLES 80
5.2.4.2. HC VERSUS HC+CC 81
5.2.4.3. EBS VERSUS BULK SAMPLES 82
5.2.4.4. HC VERSUS EBS SAMPLES 82
5.2.5. POSSIBLE CONNECTIONS BETWEEN Δ13C AND Δ18O VALUES 82
5.2.6. POSSIBLE PALEOENVIRONMENTAL SIGNALS OF BULK SAMPLES 83
5.3. VILLÁNYKÖVESD 89
5.3.1. GENERAL DESCRIPTION OF THE VERŐCE SEQUENCE 89
5.3.2. METHODS AND GUIDELINES FOR THE ANALYSIS 96
5.3.3. DETAILED DESCRIPTION OF THE STABLE CARBON AND OXYGEN ISOTOPE VALUES 97
5.3.4. SIMILAR TENDENCIES 110
5.3.4.1. HC VERSUS BULK SAMPLES 111
5.3.4.2. HC VERSUS HC+CC 111
5.3.4.3. EBS VERSUS BULK SAMPLES 113
5.3.4.4. HC VERSUS EBS SAMPLES 113
5.3.5. POSSIBLE CONNECTIONS BETWEEN Δ13C AND Δ18O VALUES 114
5.3.6. POSSIBLE PALEOENVIRONMENTAL SIGNALS OF BULK SAMPLES 114
5.3.6.1. PALEOSOLS. 114
5.3.6.2. TRANSITION ZONES AND LOESS OF UNIT 18 AND UNIT 13 116
5.3.6.3. LOESS 116
5.3.7. POSSIBLE PALEOENVIRONMENTAL SIGNALS OF SECONDARY CARBONATES 117
5.3.7.1. HC 117
5.3.7.2. HC+CC 118
5.3.7.3. EBS 119
6. CONCLUSIONS 120
6.1. CHARACTERISTICS OF THE STUDIED LOESS-PALEOSOL SEQUENCES 120
6.1.1. CHARACTERISTICS OF PALEOSOLS 120
6.1.1.1. OBSERVATIONS IN THE CASE OF LOCAL PALEOSOL VARIATIONS 120
6.1.1.2. OBSERVATIONS CONCERNING DIFFERENT PALEOSOL TYPES OF THE SAME SEQUENCE 120
6.1.1.3. OBSERVATIONS OF PALEOSOLS BETWEEN DIFFERENT SEQUENCES 121
6.1.1.4. OBSERVATIONS FROM TRANSITION ZONES 122
6.1.1.5. OBSERVATIONS FROM LOESSES 124
6.2. OBSERVATIONS OF CERTAIN SECONDARY CARBONATES 125
6.2.1. THE ROLE OF SOIL-LIKE HC 125
6.2.2. APPLICABILITY OF HC+CC 125
6.2.3. THE ROLE OF EBS 126

6.3. QUESTIONS OF APPLICABILITY OF THE STABLE ISOTOPE SIGNALS OF BULK SAMPLES AND SECONDARY CARBONATES **127**

6.3.1. POSSIBILITIES OF APPLICATION **127**

6.3.2. DIFFICULTIES OF APPLICATION **128**

6.4. CONCLUDING THOUGHTS **128**

7. ACKNOWLEDGEMENTS **130**

8. REFERENCES **131**

9. SUMMARY IN ENGLISH **145**

10. SUMMARY IN HUNGARIAN ..... HIBA! A KÖNYVJELZŐ NEM LÉTEZIK.

11. APPENDIX **147**

1. Introduction of secondary carbonates

Secondary carbonates are sensitive paleoenvironmental indicators: not just their stable carbon and oxygen isotope composition provides information about former environmental conditions, but their morphology and distribution along the sequence (BECZE-DEÁK, J. et al. 1997). Primary carbonate content of loess derives from calcite and dolomite crystals, which are settling down contemporaneously with the mineral dust – and these crystals are responsible for the cementation of mineral grains during sedimentation (PÉCSI, M. 1990; PÉCSI, M. – RICHTER, G. 1996). Clay bridges play a role in the fixation of settling dust and in the impregnation of the matrix (CILEK, V. 2001), besides biological loess crusts (SMALLEY, I. et al. 2011). The formation of secondary carbonates is due to the vertical, horizontal or in situ resettlement of primary carbonates in the soil-sedimentary environment: this process is connected with the flow of bicarbonate solutions, biomineralization processes and the weathering of calcium-bearing minerals and mollusc shells (PÉCSI, M. 1990; GEREI, L. et al. 1995; BECZE-DEÁK, J. et al. 1997).

For my dissertation I set the following goals:

1) to introduce of the different secondary carbonates in a detailed way and provide the clarification of their nomenclature – the update of the terminology is crucial, since the appellations and definitions of the certain types are commonly confusing;
2) to collect secondary carbonate and bulk samples in high vertical resolution and analyse their stable carbon and oxygen isotope composition;
3) to draw conclusions from the stable isotope values and use them for paleoenvironmental reconstruction.

Sampling sites were chosen along a North-(North-Eastern) – South-(South-Western) transect, and contained the loess-paleosol sequences of Verőce, Paks and Villánykövesd. The main aim was to examine the stable carbon and oxygen isotope composition of the studied sequences and discover the stable isotope patterns among the different sedimentary units.

2. Secondary carbonate types

Secondary carbonate types are summarized on the 1. figure.

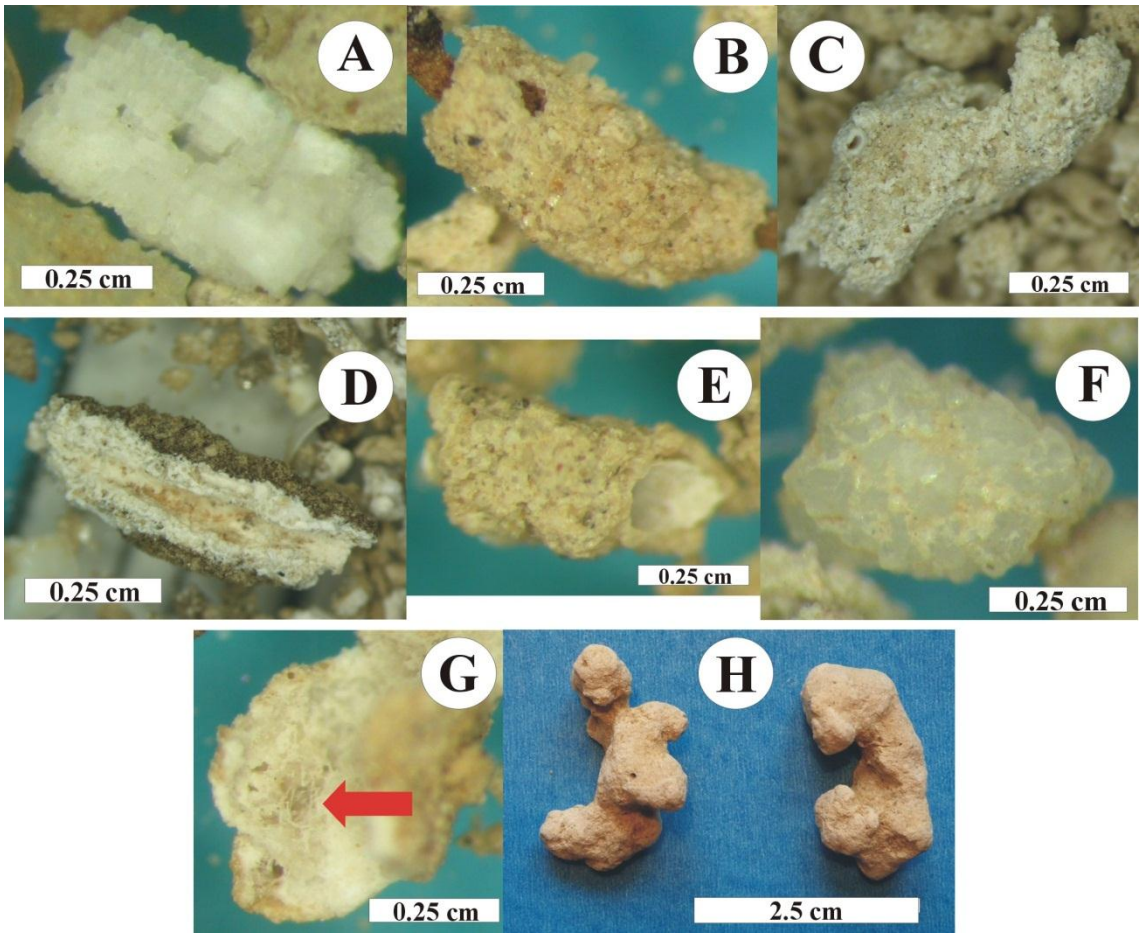

1. Figure: Secondary carbonate types: A – calcified root cells (CRC); B – hypocoating (HC); C – carbonate coating; D – CC2 subtype of carbonate coatings; E – the combined form of HC+CC; F – earthworm biospheroid (EBS); G – needle-fiber calcite (NFC, the red arrow is pointing on the fine needle network); H – loess dolls (BARTA, G. 2014)

2.1. Synsedimentary classification

2.1.1. Direct organic/biogenic origin

2.1.1.1. CRC

Origin of CRC and root calcification process

Calcified root cells (**CRC**) are bright white pore infillings (average diameter of 1 mm), which resulted from the biomineralization of roots, which belong mainly to grass species (JAILLARD, B. et al. 1991; BECZE-DEÁK, J. et al. 1997) (**Fig. 1. A**). These features are tracers of the former rhizosphere of the soil-sedimentary environment (BECZE-DEÁK, J. et al. 1997).

The term rhizosphere can be described through all the volume of soil, which is influenced by root activity. This special environment considers as well the attached

microbial biomass as mycorrhizal fungi or N-fixing bacteria (HINSINGER, P. 1998). The physical properties of the soil environment influence the transfer of molecular and ionic compounds, which may accumulate in the rhizosphere such as Ca or Mg (HINSINGER, P. 1998; HINSINGER, P. et al. 2006). Accumulation of Ca acts as a generator for carbonate precipitation around and inside the roots (BECZE-DEÁK, J. et al. 1997; MCCONNAUGHY, T.A. – WHELAN, J.F. 1997). Acidification enhances this process, which seems to be a well-functioning strategy for nutrient uptake (HINSINGER, P. 1998).

Nutrient uptake also depends on the pH of the rhizosphere, which is influenced by the respiration of the roots and related microorganisms (HINSINGER, P. et al. 2006). Changes in pH cause increase or decrease in the proton concentration, which is responsible for the dissolution or precipitation of soil minerals, such as carbonates (HINSINGER, P. et al. 2006). To summarize, different calcification processes can be distinguished (KOŠIR, A. 2004; DURAND, N. et al. 2010):

1) rhizosphere calcification (when carbonate precipitates in the surroundings of the root, causing cementated structures);

2) intracellular calcification (which causes **CRC structures**);

3) calcification of root-related organisms (such as fungi, turning into needle-fiber calcite - NFC - structures).

When cortical cells undergo calcification it enhances proton secretion in order to help the root to incorporate hardly available or less soluble nutrients from the rhizosphere (KOŠIR, A. 2004). Therefore such plants living on alkaline soils can choose calcification and carbonate excretion as a survival strategy (MCCONNAUGHY, T.A. – WHELAN, J.F. 1997). Calcification can by triggered by evaporation (MCCONNAUGHY, T.A. – WHELAN, J.F. 1997) and supported by the effect of fungal hyphae or certain soil bacteria (KLAPPA, C.F. 1980).

The main mass (95%) of the CRC originates through the calcium ion uptake by the plant, where the ions are absorbed within the cells first and then calcite precipitates (BECZE-DEÁK, J. et al. 1997). Recent stable isotope studies showed that calcite precipitation happened indeed within the cells and from fluids containing organic compounds (ŁĄCKA, B. et al. 2009). Outer cell walls also undergo biomineralization due to plasmolysis (BECZE-DEÁK, J. et al. 1997). The process of plasmolysis is connected to living plant cells and refers to the way, how these cells react to hyperosmotic stress (LANG, I. et al. 2014). When root tissues are calcified, it denotes protection against too high bicarbonate or calcium concentrations in the soil-sedimentary environment (KOŠIR,

A. 2004). Calcification occurs not solely during the life time of plants but may happen after their death: when decay starts with the release of certain proteins and sugars it is followed by calcite precipitation on the surface and in the inner part of the root cells (KLAPPA, C.F. 1980).

Morphological properties

CRC resemble the anatomical marks of the former cells and act as a pseudomorph (KLAPPA, C.F. 1980). CRC mean not just the conservation of cells, but the whole root structure and compose a straight or curving channel (in the mean length of 1 cm). This channel when it is cut into two halves shows a ring structure, which is built up of elongated or angular calcite crystals and a hollow part inside (JAILLARD, B. et al. 1991; BECZE-DEÁK, J. et al. 1997). Undisturbed tubes consist of layers of different cell shapes, which consist of the following from the outside of the whole structure towards the hollow part: tablets, polygons, ovoid-cylinders and tablets again (BECZE-DEÁK, J. et al. 1997). Cell size varies between 30-125 μm with averages of 60-80 μm (JAILLARD, B. et al. 1991). CRC consists of pure calcite or low-magnesium calcite (JAILLARD, B. et al. 1991; BECZE-DEÁK, J. et al. 1997).

Paleoenviromental indication

Presence of CRC indicates arid formation conditions (concerning at least the vegetation period), patchy character of former vegetation cover and also represent the carbonate content of the environment (BECZE-DEÁK, J. et al. 1997). CRC usually appears with hypocoatings (HC) together and both are thought to be the result of synsedimentary development (BECZE-DEÁK, J. et al. 1997; WANG, H. – GREENBERG, S.E. 2007). Redeposition and/or strong bioturbation are indicated by broken CRC structures, when individual cell crystals remain isolated in the matrix (BECZE-DEÁK, J. et al. 1997). Recently the formation of CRC became a characteristic of areas with Mediterranean moisture regime with warm and dry summers in arid areas (BECZE-DEÁK, J. et al. 1997).

2.1.1.2. EBS

General description

Earthworm biospheroids (EBS or sparitic biospheroids - BECZE-DEÁK, J. et al. 1997) are known among others as earthworm granules (DURAND, N. et al. 2010) or calcium carbonate granules (CANTI, M.G. – PIEARCE, T.G. 2003) (**Fig. 1. F**). EBS are

composed of biogenic $CaCO_3$, which is excreted by the calciferous glands of earthworms (e.g. DARWIN, C. 1882; CANTI, M.G. – PIEARCE, T.G. 2003). EBS resemble mostly mulberries, but sometimes irregular ones also appear (GAGO-DUPORT, L. et al. 2008). The less regular forms are described as remnants of broken granules (CANTI, M. 1998a). Based on the literature, the production of the most fully developed (and largest) EBS are connected to the species *Lumbricus terrestris* (known as common earthworm – United Kingdom, nightcrawler – North America), which is characterized by two pairs of calciferous glands and a pair of pouches (CANTI, M.G. – PIEARCE, T.G. 2003). It is also true, that since natural populations of earthworms contain juveniles and adults together, therefore the granules produced by adults are generally larger (LEE, M.R. et al. 2008a). The size of these biospheroids is generally between diameters of 0.5-2.5 mm (CANTI, M. 1998a; CANTI, M.G. – PIEARCE, T.G. 2003). Their surface can either be smooth or rough, but the reason for this division is not yet discovered (GAGO-DUPORT, L. et al. 2008).

The occurrence of EBS

EBS are usually found not only in loess-paleosol sequences, but in colluvial sediments as well and were discovered in archaeological sites (CANTI, M. 1998a), where granule concentrations tend to be higher on the surface of buried soil horizons (CANTI, M.G. – PIEARCE, T.G. 2003). EBS are also found in the castings of earthworms and in crotovinas (DARWIN, C. 1882; BECZE-DEÁK, J. et al. 1997). It is controversial whether EBS are always casted close to the surface (or on the surface of soils) or just underground: fossil findings are connected to the upper level of buried soils, while the recent experiments state that granules are casted underground (CANTI, M. 1998a). It is also sure that in general this species is able to till the deepest soil horizons as well (KOVÁCS A. 2010).

The role of calciferous glands in EBS production

Many theories and investigations are connected to the formation of EBS, since the presence of calcium compounds in the soil-sedimentary environment and organic matter both influence their excretion (ROBERTSON, J.D. 1936). Such organisms, which use the process of biomineralization, tend to develop own strategies for calcium uptake and storage – as well as earthworms (BRIONES, M.J.L. et al. 2008a). Functions of carbonate excretion are thought to be connected with the neutralization of gut pH and respiratory CO_2 (LEE, K.E. 1985; LEE, M.R. et al. 2008a), but may also be linked to some yet undiscovered metabolic processes (LEE, M.R. et al. 2008b). It seems that through the

neutralization of consumed humic acids, earthworms turn the litter more nutrious (BRIONES, M.J.L. et al. 2008b; KOVÁCS A. 2010). As summarized by LEE, K.E. (1985) and GAGO-DUPORT, L. et al. (2008), many options were introduced as an explanation, such as egg formation, buffering pH of blood or ionic and osmotic regulation of body fluids. Calciferous glands may act as a water regulator, which reduces water loss (BRIONES, M.J.L. et al. 2008b). The conversion of ingested calcium into carbonate in order to avoid the toxicity of the environment is also possible (WIECEK, C.S. – MESSENGER, A.S. 1972), since highly calcareous soils may be a threat for earthworms because of such toxic effects (CRANG, R.E. et al. 1968, BECZE-DEÁK, J. et al. 1997). Therefore the excretion of biospheroids may be the survival technique for earthworms in (highly) calcareous soil environments (BAL, L. 1977). Although different explanations are available, stable carbon isotope investigations of EBS showed connections with dietary uptake (KOENIGER, P. et al. 2014), where the mixing with atmospheric CO_2 and soil carbon were also a possible part of the formation (CANTI, M.G. 2009).

Size of granules and their production rates

Laboratory wormery experiments of CANTI, M. (1998a) showed that earthworms are able to produce 1-3 granules/worm weekly and based on this he calculated that at least 50-150 granules are excreted yearly. In weight the production rates are 0.8-2.9 mg/day for one exemplar (VERSTEEGH, E.A.A. et al. 2014). Rates tend to increase with soil pH according to the various investigations of LAMBKIN, D.C. et al. (2011). The growth of single calcite crystals within the EBS may reach the range of tens of micrometres per hour (as cited by LEE, M.R. et al. 2008a).

The function of the calciferous gland

DARWIN, C. (1882) already recognized, that when calciferous glands of earthworms are squeezed, pulpy white matter flows out with fine granular matter inside. As a result of ^{45}Ca tracer experiments it was shown that calcium is taken up from the earthworm via body fluids: the tracer was taken up promptly by the cells and was led to the gland cavity in order to start the accumulation of the biospheroid (NAKAHARA, H. – BEVELANDER, G. 1969).

The first step of EBS formation begins in the calciferous glands of earthworms, where the minute spherular crystals (1-8 μm) are produced. These crystals coalesce with each other in order to compose a larger spheroid (CANTI, M. 1998a). *Lumbricus* genus has a pair of oesophageal pouches, which are open to the oesophageal lumen and a pair

of glandular enlargements (Morren-type glands, KOVÁCS A. 2010): $CaCO_3$ suspension (milky fluid) is produced first by secretory cells in the glandular area, which is led forward to the oesophageal pouches to precipitate as amorphous calcium carbonate (ACC) and then as biospheroids (GAGO-DUPORT, L. et al. 2008).

As mentioned before, the first step of biomineralization is the excretion of the so-called colloidal 'milky fluid' (MF) – (BRIONES, M.J.L. et al. 2008a). 'Milky fluid' is composed of CO_2 dissolved in water and in the next step of its evolution carbonic anhydrase catalyses the formation of bicarbonate. Tiny spherulites are then formed in the MF, which are 1-5 μm in size. Amorphous calcium carbonate (ACC) will be stabilized from the 'milky fluid' under the presence of macromolecular constituents (BRIONES, M.J.L. et al. 2008a). ACC is the part of the protogranules and thus is a precursor of calcite crystal formation in the calciferous glands (GAGO-DUPORT, L. et al. 2008; LEE, M.R. et al. 2008a). Formation of ACC happens under the control of the earthworm: the transformation from ACC into biospheroids follows the Ostwald ripening process (GAGO-DUPORT, L. ET AL. 2008). During the Ostwald ripening process small sol particles and/or crystals are dissolved and redeposited on the surface of larger sol particles or crystals (MCNAUGHT, A.D. – WILKINSON, A. 1997), and during EBS formation this leads the precipitation process to proceed towards the direction of a more stable calcite form (GAGO-DUPORT, L. ET AL. 2008). ACC phase contains Mg, since Mg ions have higher hydration energy than Ca ions – in ACC Mg protects the phase from dehydration during the crystallization process (HODSON, M.E. et al. 2015). After biospheroids are excreted, they do not seem to have a biological role any more (GAGO-DUPORT, L. et al. 2008).

Morphological properties

Usually EBS are rounded to oval in shape with nearly smooth surfaces (DARWIN, C. 1882), their width is between 200-600 μm and length is generally 350-2500 μm, while mean weight is counted as 1.5 mg (BECZE-DEÁK J. et al. 1997; DURAND, N. et al. 2010). EBS are mainly composed of large single crystals (BRINZA, L. et al. 2013), which are loosely aggregated (BAL, L. 1977). In morphological sense EBS show overlapping with ooids (CANTI, M.G. 1998b), but the concept 'spherulite' may also be used for them since they are composed of radial or concentric crystal arrangements (CANTI, M.G. 1997).

Different internal structures of EBS can de distinguished: 1) dense and compact granule, showing mainly radial structure and few individual calcite layers; 2) composed

of numerous concentric rings and rich in silicate-inclusions, but contains larger void spaces and generally loosely packed (BRINZA, L. et al. 2013). In the first case EBS fabric mainly resembles a geode, since the radiating crystal structure encloses the central core as in a druse (BECZE-DEÁK J. et al. 1997; CANTI, M.G. 1998b)

Roughly radial patterns of outwards pointing elongated crystals are mixed with irregular crystallic infillings – as obtained by investigating thin sections (CANTI, M. 1998a). *Lumbricus terrestris* produces the lowest amount of intercrystalline cement within the EBS, while other earthworm species tend to have higher portions of it (CANTI, M.G. – PIEARCE, T.G. 2003). EBS generally contain ACC (amorphous calcium carbonate) inclusions up to ~20 vol% and ~30-300 μm in size, which show stromatolite-like patterns (LEE, M.R. et al. 2008a). In certain cases EBS are hollow in the central part (CANTI, M. 1998a). In other cases EBS may contain a quartz or feldspar core with a size of 50-300 μm (LEE, M.R. et al. 2008a). Since earthworms swallow small stones/minerals, which help them to mill their food (DARWIN, C. 1882), this helps the route of nutrients down the gut and then acts as a nucleation site for further calcite excretion (LEE, M.R. et al. 2008a).

During dissolution experiments of EBS the surface of single calcite crystals showed dissolution along their planes and there are no abrasion patterns or etching pits (LAMBKIN, D.C. et al. 2011). Gradual erosion of the surficial crystals of EBS may be connected partly to the effects of predation. When earthworms are consumed and digested by some bird species or even mammals, than EBS inside them seems to be quite tolerant to the HCl of stomach and shows only slight dissolution patterns (CANTI, M. 1998a).

Paleoenvironmental indication

Earthworms seem to be an important part of the biogeochemical cycles in the soil-sedimentary environment (LAMBKIN, D.C. et al. 2011), since they are responsible for the mixing of soil material and disassimilation of organic matter and also have a role in the aeration of soil (LEE, M.R. et al. 2008a). The calciferous gland of *Lumbricids* could be a CO_2-fixing organ, which sequesters CO_2 present in the soil atmosphere and metabolic-related CO_2 – and thus plays a great role in soil carbon dynamics (BRIONES, M.J.L. et al. 2008b). ^{13}C-labelling treatments showed that high CO_2 binding rate was characteristic of earthworm tissues and biospheroids (BRIONES, M.J.L. et al. 2008b).

The usage of EBS as a paleoclimate (especially paleotemperature) indicator has certain advantages as it shows wide temporal and spatial abundance and distribution,

while their $\delta^{18}O$ values are connected to both of soil temperature and composition of soil moisture/water (VERSTEEGH, E.A.A. et al. 2013; PRUD'HOMME, C. et al. 2016). According to BRINZA, L. et al. (2013), EBS could be used as a paleoproxy, since Sr substitutes into the biospheroids only with minimal modifications concerning the calcite structure.

During arid and/or intensely cold conditions earthworms are able to burrow deep down to 1-2.5 m, depending on other climatic conditions (DARWIN, C. 1882). As cited by PRUD'HOMME, C. et al. (2016), earthworm activity is strongly dependent on the season, which shows peaks during the spring and autumn time. Therefore earthworms are likely to excrete more biospheroids at higher temperatures, which is explained by more enhanced metabolic activities (VERSTEEGH, E.A.A. et al. 2014). During the Last Glacial period (in periglacial environments) the activity of earthworms was connected to the active layer in the thawing season possibly during the five warmest months of a year (PRUD'HOMME, C. et al. 2016).

In-situ characteristics of the soil-sedimentary environment can be gained through the morphological analysis of EBS, since redeposition breaks the granules and strong dissolution erodes the surface of composing crystals (BECZE-DEÁK J. et al. 1997). The fact of their presence and absence is also informative on sedimentation properties (BECZE-DEÁK, J. et al. 1997).

2.1.1.3. NFC

General description

Needle-fiber calcite (**NFC**) is a common compound of calcretes, calcareous soils, paleosols and partly loesses (VERRECCHIA, E.P. – VERRECCHIA, K.E. 1994; BECZE-DEÁK, J. et al. 1997; BAJNÓCZI, B. – KOVÁCS-KIS, V. 2006; BARTA, G. 2014) (**Fig. 1. G**). It can be found in recent periglacial environments as well (VILLAGRAN, X.S. – POCH, R.M. 2014). NFC are whole or partial infillings of interparticle pores, dissolution fractures or desiccation cracks (BAJNÓCZI, B. – KOVÁCS-KIS, V. 2006; DURAND, N. et al. 2010), and compose cotton-like meshes on ped surfaces and in earthworm channels (KHOKHLOVA, O.S. et al. 2001; KOVDA, I. et al. 2009). Humic zones (especially those of Chernozemic soils) offer high amount of organic matter and relative humid conditions with the continuous moisture support of capillary uplift. The most common appearance

of NFC is related to the transition zone from the humic horizon to C zone, in which they vanish gradually with the depth (BECZE-DEÁK, J. et al. 1997).

The calcite or low-magnesium calcite needles fill out the voids in different ways: as random meshes (after organic matter decayed in the void), convoluted forms (when breaking through mucous walls of mycelium bundles) or tangential forms (VERRECCHIA, E.P. – VERRECCHIA, K.E. 1994; DURAND, N. et al. 2010). During their formation nucleation is followed by the growth of calcite needles, which is due to the extraordinarily high degree of supersaturation of the parent solutions (BORSATO, A. et al. 2000; MILLIERE, L. et al. 2011).

They generally appear together with hypocoatings (HC) or are attached on the surface of calcified root cells (CRC), which refers to a connection with higher plants in the soil-sedimentary environment (BAJNÓCZI, B. – KOVÁCS-KIS, V. 2006; BARTA, G. 2014).

Origin and types of NFC

Various explanations are available for the origin of NFC, the reasons can be organic processes (such as fungal biomineralization) and physicochemical processes, which are generally independent from each other (BAJNÓCZI, B. – KOVÁCS-KIS, V. 2006). Still it may occur, that both processes worked together either supporting or inhibiting each other and causing the built up of the various morphologies (VERRECCHIA, E.P. – VERRECCHIA, K.E. 1994). Some hypothesis excludes that evaporation can be the reason of NFC formation, since the structural changes between needle lengthening and the angle of c axis cannot be linked solely to this effect (CAILLEAU, G. et al. 2009a). NFC reflect heterotrophic biogenic activity in the $CaCO_3$ cycle of the same environment and is in isotopic equilibrium with it, but different stable carbon and oxygen isotope signatures are connected to the different NFC morphologies (MILLIERE, L. et al. 2011).

NFC is used as a main concept for certain groups in terms of size and mineralogy (VERRECCHIA, E.P. – VERRECCHIA, K.E. 1994): 1) micro-rods (<2 μm long, <0.5 μm wide); 2) crystals (most common type, up to 100 μm length, 0.5-2 μm width); and 3) needles (30-1000 μm length, 2-20 μm width). Micro-rods indicate microorganic precipitation, when carbonate precipitation happened around an organic core (i.e. bacteria; LOISY, C. et al. 1999). Bacteria adapt themselves to various biogeochemical conditions in terrestrial environments, since their metabolism resembles a catalyst: they are able to increase the pH of the medium which leads to supersaturation of solutions and thus to calcite precipitation (ZHOU, J. – CHAFETZ, H.S. 2009a). Micro-rods appear commonly together with NFC (LOISY, C. et al. 1999).

Based on their morphology the following two groups can be built: 1) monocrystalline needles: M type (smooth, single micro-rods), MA type (smooth paired rods) and MB type (serrated-edged paired rods); and 2) polycrystalline chains (various combination of rhombohedral calcite joining together). Morphologies may be similar, but this does not necessarily mean genetic connections (VERRECCHIA, E.P. – VERRECCHIA, K.E. 1994). Monocystalline needles are connected to direct biological origin, while polycrystalline chains are the results of rapid evaporation and desiccation (VERRECCHIA, E.P. – VERRECCHIA, K.E. 1994; DURAND, N. et al. 2010). Since needle morphologies are quite complex, it was suggested by CAILLEAU, G. et al. (2009a), that the original term 'NFC' should be kept for the biogenic precipitation, while other types should be named as 'epitaxial forms of NFC'.

Formation of NFC is also possible through the degradation of certain shells: when physical factors, such as freeze-thaw are guiding the degradation, than the calcite prisms of the shell will be released as single needles (VILLAGRAN, X.S. – POCH, R.M. 2014). In this case original biomineralization is connected to the shell and needles are the consequence of general weathering and not considered as secondary carbonates in a strict sense (VILLAGRAN, X.S. – POCH, R.M. 2014).

NFC are often associated with nanofibres, which were formerly considered as precursors of NFC formation (CAILLEAU, G. et al. 2009b). The study of CAILLEAU, G. et al. (2009b) showed that nanofibres are likely templates for carbonate coating precipitation (or possibly for other carbonate forms as well).

Paleoenvironmental indication

Presence of NFC denotes that formerly decaying organic matter was available in the horizon, which was decomposed by fungi associated with higher plants (VERRECCHIA, E.P. – VERRECCHIA, K.E. 1994; BAJNÓCZI, B. – KOVÁCS-KIS, V. 2006). NFC is usually found in loess as well, where it indicates that enough moisture was available at least seasonally and saprophyte activity was possible (BECZE-DEÁK, J. et al. 1997). In many cases NFC forms during the early phase of pedogenesis (BAJNÓCZI, B. – KOVÁCS-KIS, V. 2006; DURAND, N. et al. 2010).

NFC are preserved until bioturbation and/or leaching are less intensive, which means that the presence of NFC may indicate the lack of leaching (weaker pedogenesis) and/or arid to semi-arid climatic conditions (VERRECCHIA, E.P. – VERRECCHIA, K.E. 1994; BECZE-DEÁK, J. 1997; BECZE-DEÁK, J. et al. 1997; BAJNÓCZI, B. – KOVÁCS-KIS, V. 2006).

2.1.2. Abiogenic or indirect biogenic origin

2.1.2.1. HC

General description

Hypocoatings (HC) are $CaCO_3$ impregnations around the pores of the soil/sediment matrix and around plant biogalleries, which consist of micritic to microsparitic crystals (**Fig. 1 B**). Generally their size is less than 1 cm in length, whereas diameter is in mm range (BECZE-DEÁK, J. et al. 1997; DURAND, N. et al. 2010). The presence of HC is mainly connected to the direct impregnation of the soil/sediment matrix and/or denotes the depletion of certain chemical compounds (BULLOCK, P. et al. 1985). Partial dissolution of hypocoatings may lead to the formation of quasi-coatings (DURAND, N. et al. 2010), which are thus not any more immediately joining the voids or pores (BULLOCK, P. et al. 1985).

Possible origin of hypocoatings

Two main hypothesis are connected to the formation of hypocoatings. One hypothesis connects their origin either to evaporation from calcium-rich solutions or to carbonate precipitation directly from the percolating solutions (BECZE-DEÁK, J. et al. 1997). Alteration of several desiccation and moisture cycles may also cause the formation of HC (as THOMPSON, T.L. et al. (1991) described micritic HC from waste heap of bauxite process).

The second main hypothesis is related to the metabolism of the roots. Since the CO_2 pressure is high in the vicinity of the roots and desiccating soil solutions also release CO_2, it all triggers relative rapid micritic crystallization. Root-suction effect presumably strengthens the precipitation process (WIEDER, M. – YAALON, D.H. 1982). Since root tips exert mechanical stress on the surrounding soil/sediment particles during their elongation, the bulk density in the vicinity of root will be enhanced (KAUTZ, T. et al. 2013). It effects the lateral transport of water and air around the root. Root tips release mucilage, which is responsible for the stability of root channels. Generally intense drying is characteristic of the root surroundings, which causes higher soil/sediment strength in the rhizosphere compared to the bulk matrix (KAUTZ, T. et al. 2013). HC formation may occur not just during the life of roots, but during their decay. When root decay begins, CO_2 levels become reduced in its vicinity and the root releases sugars and protein into the rhizosphere (causing alkalinity; KLAPPA, C.F. 1980). This process may

lead to calcite precipitation within the root cells ending up in CRC structures, which are preserved within the channel of HC (BECZE-DEÁK, J. et al. 1997). Parallels can be drawn to the formation and common occurrence of root tubules and root petrifications, which are introduced by KLAPPA, C.F. (1980). Root tubules seem to be equal to HC based on its formation criteria and since they consist of micritic (low-Mg) calcite cementation, which forms cylinders around former roots (KLAPPA, C.F. 1980; ZHOU, J. – CHAFETZ, H.S. 2009a). This pedofeature forms random or anastomosing structures, as HC also shows ramification (KLAPPA, C.F. 1980; BARTA, G. 2014).

Determination of hypocoatings in the literature

Certain parallels can be drawn between HC and the concept of 'microrhizolith', introduced by GOCKE, M. et al. (2014a). Their formation is connected mainly to grass species with shallow rooting depth. Generally rooting depth varies for temperate grassland as 2.6±0.2 m, whereas for tundra regions 0.5±0.1 m is characteristic. Recently in Mid Europe the average maximum rooting depth in grasslands seemed to be of 1.1 m (CANADELL, J. et al. 1996).

In certain cases the determination of hypocoatings is ambiguous in the literature. For instance hypocoatings are referred to as laminated carbonate accumulations, which are distributed inside the soil matrix (with diffuse boundaries) and along the soil pores (ZAMANIAN, K. et al. 2016). This definition seems to be mixed with the characteristics of carbonate coatings (CC), since HC are matrix impregnations of the soil/sediment matrix (BULLOCK, P. et al. 1985; BECZE-DEÁK, J. et al. 1997) and CC are carbonate precipitations or linings on the pore walls, not impregnations (HORVÁTH, E. et al. 2007; BARTA, G. 2011a). Hypocoatings were mentioned as rhizoliths and defined as coating of roots by ÚJVÁRI, G. et al. (2014) and radiocarbon dating showed values which proved that HCs are not synsedimentary features at the Dunaszekcső site. The determination of the HC sounds confusing in this case, since rhizoliths and carbonate coatings have different genetics. Based on Fig.3. in ÚJVÁRI, G. et al. (2014), they examined the exact HCs (and not rhizoliths or carbonate coatings). Partly on the images a thin calcite layer is visible on the inner channel wall of HCs, which may give hints that these features are a combined form of HC+CC (BARTA, G. 2014). Since CC counts as a postsedimentary feature, it may alter the signals of the encasing HC and lead to uncorrect age data. Further unclear or contradictory determinations of HC can be seen in **Appendix 7**.

Paleoenvironmental indication

Hypocoatings are found nowadays under arid to semi-arid climate and in areas with well fluctuating groundwater tables. Generally hypocoatings indicate a probably synsedimentary origin and dry formation conditions in the presence of patchy, shallow rooting vegetation (BECZE-DEÁK, J. et al. 1997; GOCKE, M. et al. 2014a). Their appearance together with calcified root cells may denote, that the plant responded differently for the environmental changes: root suction effect caused dense micritic impregnations, while the root itself underwent calcification (WIEDER, M. – YAALON, D.H. 1982; BECZE-DEÁK, J. et al. 1997). Hypocoatings may appear together with needle-fiber calcite, which denotes the influence of vegetation and the higher availability of organic matter (BECZE-DEÁK, J. et al. 1997).

The distribution and amount of hypocoatings and their combined form with carbonate coatings (HC+CC) denote relative dust accumulation velocities, the process of gradual accretion or pauses during sedimentation (BECZE-DEÁK, J. et al. 1997; BARTA, G. 2014). These properties offer the possibility to determine sedimentation phases in loess-paleosol sequences (BARTA, G. 2014).

2.2. Postsedimentary classification

2.2.1. Abiogenic or indirect biogenic origin

2.2.1.1. CC, CC2 and HC+CC

General properties

Precipitation of **carbonate coatings** (CC) is connected to the upward and downward percolating bicarbonate solutions and can happen any time after dust deposition (HORVÁTH, E. et al. 2007) (**Fig. 1 C**). Carbonate coatings are intrusive pedofeatures related to grains, aggregates and voids, especially occur in plant and animal biogalleries or biopores (BULLOCK, P. et al. 1985; ANTOINE, P. et al. 2001; STOOPS, G. 2003; HORVÁTH, E. et al. 2007). On the one hand the formation of carbonate coatings is unrelated to biological activity and can be formed by evaporation or mechanical transport, but on the other hand they are connected to biological activity, thus some coatings consist of certain needle-fiber calcite types or other microbial tubules (DURAND, N. et al. 2010).

Subtypes of carbonate coatings

Subtypes of carbonate coatings can be distinguished as the following (BARTA, G. 2011a; BARTA, G. 2014): 1) main type (marked with CC), which seems to be similar in

morphology to HC, but is grey to white in colour and consists of more homogeneous grains; 2) thin calcite tube, which may appear on the inner channel wall of HC thus composing the combined form of HC+CC (**Fig. 1 E**); 3) subtype marked by CC2, which composes a dense, chalky white accumulation and may be of paleocryogenic origin (**Fig. 1 D**).

The presence of powder-like, soft coatings and impregnations is characteristic of certain paleosols, as described by KOVDA, I. et al. (2009). These features may be linked to multiphase origin in connection to cyclical environmental changes (as cold-warm and/or wet-dry periods; KOVDA, I. et al. 2009). During the process of freezing dissolved salts (as calcium carbonate) will be dispersed in the ice mass. When sublimation of ice begins or gradual melting starts, these salts remain behind in pores or biogalleries in a quite high concentration. Meltwater or other percolating solutions may translocate them (CILEK, V. 2001). Such repeated cycles of freeze-thaw may be responsible for the formation of the CC2 subtype (BARTA, G. 2014).

Paleoenvironmental indication

The presence of CC and its subtypes indicate postdepositional alterations, which are connected to leaching or capillary uplift (HORVÁTH, E. et al. 2007). It is worth to mark, that leaching with multiphase character may not only lead to the formation of the CC main type, but to the development of (one or more) thin calcite tubes on the inner wall of CC channel (and possibly also of HC). This phenomena occurs especially under paleosol horizons, but other reasons may influence its formation, as topographical positions and thus a possible lateral inflow. In some cases the altering amount of CC corresponds with the altering size of loess dolls, which may refer to the intensity of the leaching front (BARTA, G. 2014).

2.2.1.2. Macroscale secondary carbonates

The category of macroscale secondary carbonates can be divided into the group of nodules and concretions. Such features belong to the nodules, which are not related to any natural surfaces or voids of the soil/sediment matrix (STOOPS, G. 2003) and are not present as infilling of preexistings cracks (SELLÉS-MARTÍNEZ, J. 1996). Morphology of nodules is acquired during growth (SELLÉS-MARTÍNEZ, J. 1996).

Development of concretions results in the precipitation of authigene minerals, which merge with the clastic compounds of the sediment matrix (SELLÉS-MARTÍNEZ, J. 1996).

In many cases they can be interpreted as cementations of the surrounding sediment matrix (SELLÉS-MARTÍNEZ, J. 1996), which preferably happens around cavity systems (SCHÄFTLEIN, S. 1996; DULTZ, S. – SCHÄFTLEIN, S. 1999).

The main morphological and formation properties of nodules and concretions are summarized in the upcoming subsections – in order to complete the introduction of secondary carbonate types. However, this present work lacks the broader introduction and analysis of their stable isotope compositions. The reason for this is that the differentiation of their crystal fabric, which would be crucial to rule out overprinting effects, was not among the aims of the dissertation. Stable isotope compositions can only be used for paleoenvironmental interpretation, when recrystallization effect is excluded.

Carbonate nodules

Formation and morphology

Nodules show a wide range of variations according to their internal texture or to their external morphology. Their presence and distribution is in connection with the stability of the enclosing soil/sediment structure and with precipitation-dissolution cycles (WIEDER, M. – YAALON, D.H. 1982; SELLÉS-MARTÍNEZ, J. 1996; STOOPS, G. 2003; DURAND, N. et al. 2010). Nodule formation is a physicochemical process, where the bicarbonate solutions have originally either meteoric or groundwater origin (BUDD, D.A. et al. 2002; ZHOU, J. – CHAFETZ, H.S. 2009b). Therefore carbonate nodules are usually found in 30-150 cm depth below the top of the bioturbated and leached zone (CERLING, T.E. – QUADE, J. 1990) - in many cases their appearance is strictly connected to a position beneath paleosols (SHUHUI, ZH. et al. 1987). Presence of clay minerals in the pore space may also promote calcification, through their absorbing habit (ZHOU, J. – CHAFETZ, H.S. 2009b).

Fabric of nodules can be divided into cracks and cavities and may contain recrystallized parts, these observations can be valid for concretions as well (DURAND, N. et al. 2010). Formation of cracks may be connected to desiccation and expansive growth (LEE, Y. – HISADA, K. 1999). In certain cases, these cracks are lined with manganese dendrites and Fe-oxide staining, especially those ones, which appear under Vertisols (MILLER, D.L. et al. 2007). Some randomly scattered skeletal grains, as quartz may also appear in the texture of nodules (DREES, L.R. – WILDING, L.P. 1987; LEE, Y. – HISADA, K. 1999).

Crystal size varies as followings: micritic (2-5 μm), microsparitic (5-15 μm) and sparitic (20-140 μm). Mottled texture is due to irregular variations of the above listed crystals. Microporosity can also be characteristic of the texture, especially between micritic crystals. Microsparitic linings generally occur on the wall of small voids within the nodule (BUDD, D.A. et al. 2002).

Categorization can be made among nodules on the basis of their formation stage. The following features occur especially in caliches – but may be characteristic of other sediment units as well (ZHOU, J. – CHAFETZ, H.S. 2009b). 1) Initial formation stage is categorized by soft, incipient nodules. These ones contain spherical to subspherical features in diameters of 3-8 mm. Their colour is creamy white and their structure is weakly cemented. Composing crystals are in the size of micrite to microsparite. 2) Intermediate stage and phase of accretionary growth is presented by partly lithified, chalky nodules. These features are usually found in alluvial-deltaic sediments, where they are formed in situ. Spherical to elongate morphology is characteristic of them, with size in diameters of 1-3 cm. Subtypes with homogeneous or concentric texture pattern can be distinguished. The latter type has a weakly cemented outer rim and a compact inner part. Desiccation cracks characterize them in certain cases, which have a starting point in the middle of the nodule. Composing crystals are in the size of micrite to microsparite. 3) Mature stage is signified by irregular, elongated hard nodules, in the size of 5-8 cm in diameter (in certain cases up to 12 cm). This feature can also be divided into a central part and an outer layer, but in this case the outer part is lithified as well. Appearance of desiccation cracks is common. Randomly distributed tiny holes are also characteristic of the texture. Micritic, microsparitic and sparitic crystal sizes are also common. This last feature shows many properties in common with concretions.

Effects of overprinting of stable isotopic signals

Nodules often suffer diagenetic alterations and lose their original paleoenvironmental signal, especially in environments with fluctuating groundwater table and in caliches (LEE, Y. – HISADA, K. 1999; DEUTZ, P. et al. 2001; BUDD, D.A. et al. 2002; MILLER, D.L. et al. 2007; ZHOU, J. – CHAFETZ, H.S. 2009b). Besides, seasonally infiltrating meteoric water may cause the (episodic or cyclical) alteration of wetting and drying events and lead to the same effects (BUDD, D.A. et al. 2002; MILLER, D.L. et al. 2007). Overprinting of paleoenvironmental signals is also possible, when soils remained stable

for a long time and thus they were exposed to certain climatic changes before their burial (DEUTZ, P. et al. 2001).

When nodule precipitates primary, than only micritic crystals are found in its texture and it lacks cements. Post-formation effects alter the original fabric and lead to the dissolution of the micritic crystals and development of microsparitic to sparitic crystals (BUDD, D.A. et al. 2002). Such nodules, which are compact, dense, non-layered and lack recrystallization can be considered to use for stable isotope analysis (SHUHUI, Z. et al. 1987).

Carbonate concretions

Carbonate concretions in general

The appearance of carbonate concretions is especially characteristic of the B_{Ca} and C_{Ca} horizons, which already suggests connections to the process of leaching and capillary uplift (ÁDÁM, L. et al. 1954, KÁDÁR, L. 1954; KRIVÁN, P. 1955; ST. ARNAUD, R.J. – HERBILLION, A.J. 1973; PÉCSI, M. 1993, JIAMAO, H. et al. 1997; KEMP, R.A. 1998). Horizon right below paleosols is a preferred spot, since the porosity of the sediment matrix differs from the soil (KÁDÁR, L. 1954, KEMP, R.A. 1995) and the partial pressure of CO_2 is lower (ST. ARNAUD, R.J. – HERBILLION, A.J. 1973). This latter effect leads to the supersaturation of solutions and thus to carbonate precipitation (ST. ARNAUD, R.J. – HERBILLION, A.J. 1973). Accretionary growth of concretions is guided by the later on infiltrating solutions, which provide additional carbonate to the system (PÉCSI, M. 1993, KEMP, R.A. 1998). Fluctuating groundwater table may also cause the formation of concretions. Such features may be flat or disc-shaped and denote the level of the rising groundwater table (KÁDÁR, L. 1954). Groundwater relations are also characteristic of concretions in sand (also in sandy horizons intercalating loess), where their shape resembles a cigar or teardrop and their position is parallel to the bedding (MACK, G.H. et al. 2000). Alluvial plains, which developed under arid to semi-arid climates, may contain another kind of concretion, the so-called Kankars. These are compact, hard and dark types, which are irregular in shape and larger than 5 cm in diameter. Kankars have in situ origin, possibly either due to diffusion in the soil/sediment matrix or to carbonate precipitation along voids (SEHGAL, J.L. – STOOPS, G. 1972).

Certain investigations highlight the role of fungal mycelium in the development of concretions. Since fungal mycelium in voids of the soil/sediment matrix releases CO_2

through respiration and liberates protons and organic acids, it triggers the process of calcification. This is especially characteristic of environments, where moist and arid conditions are changing cyclically (MASAPHY, S. et al. 2009).

Loess dolls

Different external appearance provides various associations for description, therefore carbonate concretions in loess-paleosol sequences may be called as **loess dolls** (**Fig. 1. H**). The original position of loess dolls is mainly vertical and show uneven distribution in the strata (KÁDÁR, L. 1954). Lag surface composed of loess dolls may remain in the sequence, when paleosols are translocated/totally eroded (KÁDÁR, L. 1954). Loess dolls accumulate not just right under paleosols, but in certain cases above them. As an effect of piping, loess wells and loess tunnels lead infiltrating meteoric water to the surface of the underlying (impermeable) paleosols, where carbonate precipitation may occur (BULLA, B. 1933).

Loess dolls are not made of pure carbonate, but may contain sand grains, clay and other non-calcareous particles in 30-40 weight% (LEACH, J.A. 1974; PÉCSI, M. 1993). Hydromorphic properties of soils influence the morphology of loess dolls underneath, such as the followings (DULTZ, S. – SCHÄFTLEIN, S. 1999): 1) mineral soils (e.g. Cambisols): rounded to elongated loess dolls with rough surface; and 2) hydromorphic soils (e.g. Gleysols) and well-developed soils (e.g. Chernozems): commonly contain protuberances on the smooth surface. The latter type may be characterized as 'glomerulus' (SEILACHER, A. 2001).

The structure of loess dolls may be (partly) hollow or compact (ÁDÁM, L. et al. 1954), but in both cases can be divided into an outer crust and a central core/void (SELLÉS-MARTÍNEZ, J. 1996). In certain cases the inner structure is concentrical, which presumes the process of diffusion as an important factor during growth (BERNER, R.A. 1968).

The inner structure represents the circumstances of precipitation, e.g. when carbonate precipitates around a cavity system of biogenic origin (DULTZ, S. – SCHÄFTLEIN, S. 1999; BARTA, G. 2011b). Root channels are presumed to be important in concretion formation, since in many cases loess dolls resemble root ramifications and in certain cases root remnants were found inside them (PÁVAI-VAJNA, F. 1909; SCHÄFTLEIN, S. 1996). These channels can be conduits for the percolating solutions (LEACH, J.A. 1974). Precipitation of carbonate can be effective in root cavity systems or around junction

points of roots, since these are well-exposed to air and here the partial pressure of CO_2 is lower (BLOCKHUIS, W.A. et al. 1968; SCHÄFTLEIN, S. 1996).

Inner structure of loess dolls may show the following patterns: 1) longitudinal and/or perpendicular cracks (developed into septarian cracks in certain cases); 2) carbonate accumulation around one or more condensation nucleus; and 3) the combination of both types (BARTA, G. 2011b). Cementation of hypocoatings may act as precipitation nucleus, as investigations of BARTA, G. (2011b) showed at the case of the Süttő sequence. This observation is also supported by the work of BLOCKHUIS, W.A. et al. (1968), who determined neocalcitans to be a first stage of nodule development in certain cases. These features seem to be equal to HC, based on their description and two images as Fig. 15. and Fig. 20. in BLOCKHUIS, W.A. et al. (1968). Description of neocalcitans is available in **Appendix 7**.

Loess dolls are concerned to reflect the multiphase evolution history of the carbonate profile development (KHOKHLOVA, O. et al. 2001; BARTA, G. 2011b).

2.3. Proposition for a clarified nomenclature – in order to avoid misunderstandings

The appearance of secondary carbonates is commonly documented during the field investigations, but in many cases they are not correctly determined due to disorder in the nomenclature (BARTA, G. 2011a). As guiding principle the paper of BECZE-DEÁK, J. et al. (1997) was used in my dissertation, since the introduced terms and concepts in the mentioned paper are exact on the one hand, and on the other hand their paleoeonvironmental role is also well expressed. In many cases different concepts are used for the same features, which make the literature of secondary carbonates ambiguous. On the other hand, some concepts are used as collective nouns, even though they determine exact subtypes. **Appendix 7** summarizes the collection and comparison of the different terms and types (re-organized and updated after BARTA, G. (2011a)). In the following sections a broader insight is given into certain important concepts, whereas their correct usage is also highlighted.

2.3.1. Rhizolith, as a collective noun

Rhizolith is a collective noun for such organo-sedimentary structures of higher plant species, which are connected to the preservation of roots (e.g. as encrustation by

secondary carbonates) and/or to mineral cementation structures which fill out the channels after the decay of roots (KLAPPA, C.F. 1980; CRAMER, M.D. – HAWKINS, H.-J. 2009; DURAND, N. et al. 2010; GOCKE, M. 2010). Cross section of rhizoliths is generally 0.1 to 20 cm in diameter, which decreases with the depth and may show branching characters (DURAND, N. et al. 2010). Central channel is not always pronounced (GOCKE, M. et al. 2014a). Rhizoliths may be referred to as slim fossil carbonate-filled roots as well (HUPUCZI, J. – SÜMEGI, P. 2010).

RICHTHOFEN, F. (1882) already described tubes in loess deposits, which are cemented with carbonate and strengthen the capillary structure of the strata. These features are positioned mostly vertically and often ramify. Since no data of size was available, it may be presumed that the description fits the criteria of rhizolith-like structures and/or possibly equivalent to hypocoatings on the small scale.

Investigations of GOCKE, M. et al. (2011) showed that the most part of rhizoliths appeared to lack postsegregational recrystallization, therefore they are suitable for radiocarbon dating. According to their data, the formation of rhizoliths could be relative fast and happen during the lifetime of roots or shortly thereafter. Formation of rhizoliths depend on such factors as water availability and transport mechanisms of Ca^{2+}, while the character of carbonate precipitation can appear to be unequal across the roots laterally and vertically (HUGUET, A. et al. 2013). Based on the assumptions of GOCKE, M. et al. (2011, 2014c), former root remnants are likely protected against total degradation by their encrustations as rhizoliths and in certain cases they may contain calcified root tissues as well. In some cases recent roots may grow through rhizoliths, which can either be due to the higher availability of nutrients from the decaying root tissues or to a possible flow path for percolating solutions (GOCKE, M. et al. 2014b). Presence of rhizoliths seems to confirm postsedimentary formation conditions (GOCKE, M. et al. 2014c).

ZAMANIAN, K. et al. (2016) mentions that rhizolith development is connected mainly to shrubs and trees, since the life cycle of grass species is too short. Under strongly calcareous circumstances some plants may precipitate $CaCO_3$ in the root cortical cells in order to avoid toxicity. As ZAMANIAN, K. et al. (2016) cites, this appearance is another type of rhizoliths named as calcified roots. One argument is forgotten by them in this determination, as calcified root cell structures may originate due to some other reasons and that they are connected in many cases to certain grass species (JAILLARD, B. et al. et al. 1991; BECZE-DEÁK, J. et al. 1997).

Appendix 7 summarizes also certain cases, when the collective term of rhizolith was used for other features, which may lead to confusions about the exact formation method of those types. It would be recommended to learn how to differentiate between them in order to gain more precise paleoenvironmental information. Certain other root-related features are listed here, which would help (field) descriptions, but cannot be linked to the microscale secondary carbonate types of **Appendix 7**:

- ***Rhizocretions*** are micritic mineral accumulations (usually low-Mg calcite), which encircle plant roots or fill up the channel part, where the root formerly led through (KLAPPA, C.F. 1980). This type may be equivalent with ***macro-hypocoatings***, which are carbonate accumulations along root channels and possess of equal thickness, as identified by BECZE-DEÁK, J. (1997).
- ***Rhizoconcretions*** are cylindrical concretions around decayed roots, which consist of quartz sand and/or carbonates (KLAPPA, C.F. 1980).
- ***Rhizomorph concretions*** are such accumulations around channels with root remnants, which are made up of three distinct layers: 1) micritic layer without skeleton inclusions present in the inner part of the structure; 2) transitional layer, which consists of micritic to microsparitic crystals; 3) sparitic layer with skeleton grains, which lacks biogenic parts. The different crystal size of the listed layers outwards denotes the decreasing influence of the root (WIEDER, M. – YAALON, D.H. 1982).
- ***Rhizomorphs*** resemble the structure of roots in a strict biological meaning, since they consist of dense masses of fungal hyphae (KLAPPA, C.F. 1980).
- ***Rhizolite*** is a rock, which contains the certain (structural, textural, fabric) properties of the activity or former activity of roots (KLAPPA, C.F. 1980).
- ***Root moulds*** are markers of the recently decayed roots. These tubular voids refer to the morphology of the former root channel system and also to the sufficient rigidity of the soil matrix, which prevented the structure from collapsing (KLAPPA, C.F. 1980; ZHOU, J. – CHAFETZ, H.S. 2009a).
- ***Root casts*** are infillings of root moulds with sediment, soil and/or certain kind of cements, which reflect the original structure, especially at the case of eolian sediments (KLAPPA, C.F. 1980; CRAMER, M.D. – HAWKINS, H.-J. 2009).
- ***Root petrifications*** are replacements of organic matter by mineral matter (calcite or silica), while original anatomical features remain preserved. Not just the

calcified cortex of roots can go under petrification, but root hairs as well (KLAPPA, C.F. 1980; DURAND, N. et al. 2010). In case of the calcified cortex of roots parallels can be drawn to calcified root cell structures (BARTA, G. 2011a).

2.3.2. Microrhizoliths versus hypocoatings

The term 'microrhizolith' was introduced by GOCKE, M. et al. (2014a,b), which concerns small rhizoliths with central channels in diameter ≤ 1mm. Microrhizoliths are often quite abundant and resemble mat-like accumulations (GOCKE, M. et al. 2014b) and their formation is connected to the presence of grasses or herbaceous plants, as well as to side roots of higher plant species (GOCKE, M. et al. 2014a). Microrhizoliths possess (nearly) synsedimentary character, as the rooting depth of their source vegetation is shallow. Synsedimentary origin seems to be proven by the synchronous trend of biopore abundance at the investigated sites by GOCKE, M. et al. (2014a). Biopores are concerned to be large, tubular pores in mainly vertical orientation, which may show certain degrees of branching and whose origin is connected to rooting or earthworm activity (PIERRET, A. et al. 2002). Microrhizoliths can be formed during all loess depositional phases and during initial to mature soil developmental phases (with the exception of Holocene soils), and likely less than one year time range is needed for them (GOCKE, M. et al. 2014a).

Microrhizoliths are described to differ from hypocoatings in formation timing and mechanism: according to GOCKE, M. et al. (2014a), microrhizoliths are encrustations of roots during their lifetime (or shortly thereafter), while hypocoatings are biopore impregnations with various origin (BECZE-DEÁK, J. et al. 1997). According to the images published (Fig.2. in GOCKE, M. et al. 2014a), 'F' shows besides rhizoliths soil-like hypocoatings, whereas 'G' in not unequivocal to sediment-like hypocoatings. Based on its grain composition and the given magnification of the image, it seems to be more of carbonate coating, which is mostly a postsedimentary feature (HORVÁTH, E. et al. 2007; BARTA, G. 2011a). Further analysis would be needed to divide it more certainly.

2.3.3. Pseudomycelia/pseudomycelium – descriptive term for field investigations

The usage of the term 'pseudomycelia/pseudomycelium' seems to be the most contradictory concept when we are about to determine secondary carbonates in loess-

paleosol sequences. Generally it tends to be the easiest way to describe secondary carbonate accumulations on the field, e.g. when one discovers white patches or tube-like forms on the excavated profile wall. However, it is not enough, when one considers going into more details about micromorphological marks.

Pseudomycelia/pseudomycelium occurs quite frequently in the literature, with the following connections (see as well **Appendix 7** for comparisons):

- Accumulations in gleyic layers as carbonate accumulations in the vicinity of oxidized root channels (ANTOINE, P. et al. 2009a), whereas the same study mentions the presence of carbonate concretions and calcified rootlets separately.
- Calcareous loess was described with the presence of pseudomycelium in ANTOINE, P. et al. (2001), where other features in the description were separated as followings: carbonate coatings of biopores; hypocoatings as secondary traces of rooting activity; occurrence of small loess dolls.
- Powdery, white calcite infillings of root channels in loess (CILEK, V. 2001); where its origin is hypothesised (and partly proven) to be connected to such carbonate precipitation, which are due to repeating freeze-thaw cycles. This description may have connection to CC2 type described by BARTA, G. (2014).
- Pseudomycels are abundant in the humus-rich „A" horizon of chernozem-like and drab or cinnamon soils (ZHONGLI, D. et al. 1993).
- Pseudomycelia is characteristic of modern chernozem soils generally, but its presence is separated from the occurrence of carbonate nodules and other soft spherical carbonate accumulations (MARKOVIĆ, S.B. et al. 2007).
- Pseudomycelium is concerned of secondary carbonate origin, which derives from the A and B horizons and accumulates below the Ck horizon along former root channels (KADEREIT, A. et al. 2010); the term is also separated from the presence of calcareous nodules.
- Granular structures (loose or moderate-large) with biopores are often conducted with carbonate pseudomycelia (TUNGSHENG, L. et al. 1996), which was divided from the dense and incomplete excremental infillings.
- Pseudomycelia occurs as loose cotton-like meshes on pore walls, ped surfaces and on the walls of earthworm channels (fine needles in length of 60 μm and diameter of 1 μm; KHOKHLOVA, O.S. et al. 2001; KOVDA, I. et al. 2009).

- Large and small rhizolith-like elongated carbonate features are often referred to in the literature as pseudomycelia. According to GOCKE, M. et al. (2014c), this term is mostly connected to abiotic processes among the references, whereas they offer the possibility of plant root derivation.
- Small, often branching carbonate accumulations (length of mm to few cm, diameter ≤1 mm), which are round in cross sections and show a holey centre are suggested to be analogues of rhizoliths were described formerly as pseudomycelia during field investigations (GOCKE, M. et al. 2014a). GOCKE, M. et al. (2014a) advise to cease this way of denomination and use therefore the term microrhizolith.
- Pseudomycels are referred to as hypocoatings by ZAMANIAN, K. et al. (2016), which are formed either from percolating solutions by rapid precipitation or from fluctuating groundwater table. Fast precipitation means that this accumulation form is quite young and forms within weeks to a month (ZAMANIAN, K. et al. 2016).
- Field description of pseudomycelia refers to hypocoatings (DURAND, N. et al. 2010).

As **Appendix 7** also summarizes pseudomycelia/pseudomycelium can stand among others for needle-fiber calcite or hypocoatings, etc. Previously VERRECCHIA, E.P. – VERRECCHIA, K.E. (1994) suggested that the usage of this term should be eliminated, on the grounds of its too general meaning.

'Pseudomycelium' may be used during field description, when the exact character of a secondary carbonate accumulation form cannot be determined more precisely. But for the deeper understanding of sequence development, detailed micromorphological investigations are needed, which require the usage of a clear nomenclature.

2.4. Options for interpretation based on the morphology and distribution of secondary carbonates

2.4.1. Dust accretion

Under the circumstances of dry grassland vegetation fine dust particles can be moved further lightly, because the movements of grass generate turbulence of air and sweeps away the particles. Nonetheless vegetation is able to trap the particles in the grain-size range of loess. Due to the relatively strong capillary forces, the deposited

grains will be protected against further transportation (CEGŁA, J. 1969). After dust particles are deposited on the surface, they infiltrate into the porous layer and root mat and mix with the organic matter (and dilute it). As dust accumulation continues, the boundary of the organic-mineral horizon migrates upwards. When dust fluxes are high enough, than soil development slows down and the duration of immature pedogenetic stages increase (EGER, A. et al. 2012).

Vegetation is an important factor in enabling long-term vertical accretion of depositing dust, since vegetation continues to grow upwards and trap even more grains (PYE, K. 1995). High sedimentation rates do not inhibit the expansion of vegetation, as it is also indicated by high biopore frequencies (GOCKE, M. et al. 2014b). This process remains effective, despite of high dust accumulation rates and inhibited pedogenic assimilation (JOHNSON, D.L. – WATSON-STEGNER, D. 1987; PYE, K. 1995).

2.4.2. Pedosedimentary aspects

Loess-paleosol sequences reflect the effects of interactions between the succession of pedogenesis and sedimentation. Loess units show the signs of syndepositional pedogenic alterations and its weak imprints as biochannels and preserved cryogenic structures. Therefore these horizons could be considered as pedosedimentary units (KEMP, R.A. 1999, 2001). According to CATT, J.A. (1990), loess sequences can be considered as pedocomplexes, since loess remains subjected to soil forming processes – even though dust accumulation changes the direction of soil forming processes (YAALON, D.H. – GANOR, E. 1973).

As dust deposition begins on the surface or when soil horizons are buried with freshly deposited sediments, then pedogenesis tries to keep pace with the rate of deposition (CATT, J.A. 1990). Dust accretion does not interrupt pedogenic processes (KUKLA, G.J. 1977), which may lead to the overthickening of the topmost soil horizons (CATT, J.A. 1990). Buried soil horizons may undergo different changes such as redistribution and recrystallization of existing minerals (e.g. formation of concretions or carbonate coatings; CATT, J.A. 1990).

Pedosedimentary aspect is supported by the fact, that loess organic matter is not restricted to the paleosol horizons, but is present in the sedimentary units below and above the soil horizons (GOCKE, M. et al. 2014b).

2.4.3. Why is micromorphology so important?

Pedosedimentary approach needs to get acquainted with the microstratigraphic relations within the studied sediments, therefore the types and abundance of micromorphological features (such as microscale secondary carbonates) should be determined (KEMP, R.A. 1999). Micromorphological features are keys to determine the characteristics of climate and environmental transitions, especially through the investigation of upper and lower boundaries of paleosols (KEMP, R.A. 1999).

2.4.4. Role of certain microscale secondary carbonates

Microscale secondary carbonates are sensitive indicators of paleoenvironmental changes: based on their genetic context and distribution pattern, information can be gained about dust deposition characteristics, environmental stability and leaching processes (BECZE-DEÁK, J. et al. 1997).

Pedogenic processes remain significant during dust deposition phases (KEMP, R.A. 1999). By these means biomineralization processes were always inherited as the microecosystem migrated upwards in the sequence as following the level of dust accumulation (CATT, J.A. 1990; BECZE-DEÁK, J. et al. 1997). The accumulation or absence of secondary carbonate features in the strata denotes the moisture regime of the environment and also the rates of dust accumulation (as dense or sparse, ephemeral vegetation cover was present; BECZE-DEÁK, J. et al. 1997; KEMP, R.A. 1999; MONGER, C.H. 2002).

Syndepositional pedogenic alterations remained traceable and were complemented by postsedimentary changes during loess-paleosol development in periglacial environments, where patchy vegetation cover was characteristic with short growing season species (BECZE-DEÁK, J. et al. 1997; KEMP, R.A. 2001).

Distribution of microscale secondary carbonates indicate the following environments:

- Uneven distribution is connected to gradual dust accumulation and patchy vegetation cover (BECZE-DEÁK, J. et al. 1997).
- Absence of dust accumulation or pause: the presence secondary carbonates is denser in comparison to the over- and underlying horizons. Non-leaching environments preserve microscale secondary carbonates in this form and no dissolution pattern is visible. In the case of a pause pedogenic processes may be

more intense and thus NFC in higher abundance may denote enhanced humic accumulations (CATT, J.A. 1990; BECZE-DEÁK, J. et al. 1997).

- Stability of environment is characterized by the presence of EBS, especially in higher amounts. Since the water establishment of earthworms' body is poorly developed, they need adequate moisture conditions. By these means their appearance denotes the absence of drastic changes in the water balance and indicate slow burial/sedimentation phases (BECZE-DEÁK, J. et al. 1997).
- Partially or totally dissolved secondary carbonates are characteristic of leaching environments. In case of total dissolution, secondary carbonates are absent in the sequence to a certain depth, which denotes the dynamics and intensity of leaching (BECZE-DEÁK, J. et al. 1997). Seasonally dry climates help the dissolution and redistribution of secondary carbonates: when a wet period follows a prolonged dry season and the strata is characterized of high pH values, dissolved carbonates will be translocated through leaching. Alternating illuvial clay layers and secondary carbonate accumulations are characteristic of such paleosols, which underwent repeatedly fluctuating rainfalls during their formation and later on (CATT, J.A. 1990). Especially cyclical changes in the moisture regime lead to multiphase leaching processes, where carbonate coatings develop in more generations and combine with other secondary carbonate types (as HC+CC, BARTA, G. 2014). Switch from leaching to non-leaching environment can also be traced, as secondary carbonates appear on both sides of the decalcification boundary (and in the decalcified matrix as well; BECZE-DEÁK, J. et al. 1997).
- Beginning of gradual dust accumulation is characterized again by the uneven distribution of secondary carbonates and thus also by limited biological activity (BECZE-DEÁK, J. et al. 1997).

3. Introduction to the stable carbon and oxygen isotope composition of secondary carbonates

3.1. General information

Stable isotopes are elements, which are characterized by unique atomic masses: isotope variations of a given element differ in the number of neutrons, but are equal in the number of protons (WEST, J.B. et al. 2006). During paleoenvironmental studies of secondary carbonates the ratio of the following isotope variations is usually determined: $^{12}C/^{13}C$ and $^{16}O/^{18}O$.

Precipitation of secondary carbonates results from the supersaturation of solutions, which is led by evaporation and decrease of partial pressure of CO_2 in the strata (CERLING, T.E. 1984). CO_2 derives partly from plant/soil biota respiration and decay of organic tissues and controls the process of precipitation (RETALLACK, G. 2001; LIU, W. et al. 2011). The stable isotopic composition of CO_2 will be preserved in the pedogenic calcite crystals (RETALLACK, G. 2001), since their formation is controlled by the isotopic composition of the solution, from which they precipitate and also by the temperature (DWORKIN, S.I. et al. 2005).

Carbon dioxide is removed from the atmosphere by plant leaves and is released again through respiration in the soil-sedimentary environment (WANG, H. – GREENBERG, S.E. 2007). Enhanced decay causes more effective oxidation, which means that reduced organic matter is converted into simpler compounds, such as CO_2. Higher CO_2 levels are additional to calcification (RETALLACK, G. 2001). Respired soil CO_2 is generally lighter isotopically, than CO_2 present in the atmosphere. Dominance of isotopically light CO_2 in the soil can be linked to low atmospheric partial pressure of CO_2, whereas high atmospheric partial pressure of CO_2 lead to the diffusion of isotopically heavy CO_2 compositions (RETALLACK, G. 2001). Secondary carbonates are considered to be in isotopic equilibrium with soil CO_2, which is dissolved in (soil) solutions (CERLING, T.E. 1984; FOX, D.L. – KOCH, P.L. 2004). Crystal lattice of carbonates incorporates the varying ratio of stable carbon isotopes (BOGUCKYJ, A.B. et al. 2006). No isotope exchange happens between CO_2 and H_2O after secondary carbonates are formed and when no recrystallization happens (RYSKOV, YA.G. et al. 1996). Based on the investigations of CERLING, T.E. – QUADE, J. (1993), the isotopic composition of secondary (pedogenic) carbonates should be constant below 25 cm depth in the soils. Generally only few soil types have carbonate precipitation within the uppermost 25 cm

depth, these types are developed mostly under desert climates or are in groundwater discharger zones (CERLING, T.E. – QUADE, J. 1993).

Irreversible oxidation of soil organic matter releases CO_2 (CERLING, T.E. et al. 1989). There are differences between the concepts of soil CO_2 and soil-respired CO_2: soil CO_2 means the gaseous phase filling up the pore space, while soil-respired CO_2 is equal to the flux of CO_2 throughout the soil medium. Soil CO_2 shows isotopic enrichment in comparison to soil-respired CO_2 (CERLING, T.E. et al. 1991). Partial pressure of CO_2 is higher in soils than in the atmosphere, which is due to root and animal respiration and to microbial oxidation of organic matter (CERLING, T.E. 1984).

Infiltration of rainwater equalizes CO_2 in the soil, which causes the (relative rapid) diffusion of CO_2 into the soil solution (HASINGER, O. et al. 2015). Therefore oxygen isotope composition of meteoric waters (and thus of secondary carbonates) are related to climatic effects, such as alterations of temperature (CERLING, T.E. 1984). Oxygen isotopic composition is effected not just by rain, but by other atmospheric precipitation forms, such as fog, hail and snow (MILLIERE, L. et al. 2011).

Carbon in secondary carbonates is primarily connected to atmospheric CO_2 and has the following sources: photosynthetic origin, decay of organic matter, root respiration and presence of dissolved inorganic carbon (HASINGER, O. et al. 2015). Plants follow one of the following photosynthetic pathways: 1) C_3: this variation includes mainly trees, shrubs, herbs and cool season grasses, which are characterized by $\delta^{13}C$ values between -25‰ and -32‰; 2) C_4: this type is mainly dominated by warm season grass species, which are adapted to water stress and high light conditions, and are characterized by $\delta^{13}C$ values between -10‰ to -14‰; and 3) CAM (Crassalacean acid metabolism): this way is typical for succulents and cacti, and is characterized by $\delta^{13}C$ values intermediate between C_3 and C_4 plants (CERLING, T.E. – QUADE, J. 1993).

3.2. Influencing factors of the stable isotope composition:

Stable isotope compositions of secondary carbonates have many influencing factors. Some of them are highlighted in the following section. An overview-table is also created (**Appendix 8**), which summarizes the main effects and orders them under the following categories: 1) shift towards more positive $\delta^{13}C$/ $\delta^{18}O$ values (enrichment in $^{13}C/^{18}O$); 2) shift towards more negative $\delta^{13}C$/ $\delta^{18}O$ values (depletion in $^{13}C/^{18}O$).

3.2.1. Evaporation

Soil water of meteoric origin may show alterations in isotopic composition, when 1) evaporation is strong in the upper soil horizon, which leads to isotopic enrichment; 2) mixing with infiltrating solutions happen, which are already evaporatively enriched; and 3) isotopically different water is added from the vadose zone (FOX, D.L. – KOCH, P.L. 2004). Evaporation is connected to rising temperatures and leads to increasing activity of Ca^{2+}, which is followed by the decrease of soil respiration rates and enhances water stress on plants and soil biota (BREECKER, D. 2010). Evaporation can be responsible for most of the water loss in case of high plant diversity. By these means a slight enrichment in the soil solutions may occur concerning $\delta^{18}O$ values (QUADE, J. et al. 1989).

3.2.2. Seasonal changes

Alteration of CO_2 partial pressure, composition of soil solutions, temperature and effects of microbial activity are changing during the year (CERLING, T.E. – QUADE, J. 1993). Seasonality is indicated by the possible fluctuations of CO_2 levels. Near-surface horizons are characterized by trace amounts of CO_2 and thus are enriched in ^{13}C, indicating the dominance of heavier carbon isotope composition. Higher amount of CO_2 is characteristic of deep-soil environments due to the effects of root and animal respiration. In this medium ^{13}C is more depleted and thus lighter carbon isotopic composition is peculiar (RETALLACK, G. 2001). Seasonal changes may cause shifts in the stable isotopic composition of soils/paleosols, since diffusion of CO_2 into the soil is effected by the changes of temperature (RETALLACK, G. 2001). Seasonal changes in the composition of meteoric water may affect the isotopic components of secondary carbonates as well, which precipitate from the infiltrating and percolating solutions (QUADE, J. et al. 1989).

3.2.3. Preferences for the usage of lighter isotopes and effects of microbial reworking

Isotopically lighter components are preferentially used during metabolic processes of organisms, since vibrational frequency of lighter ^{12}C isotope is higher than of heavier ^{13}C - by this means ^{12}C is more favourable for plants during photosynthesis (LIAN, B. et al. 2006; HASINGER, O. et al. 2015). Microbial reworking of organic matters also prefers the light isotopes, which may cause enrichment in the heavier isotopes in the soil

solutions – and thus influences the precipitation of further secondary carbonates (GALIMOV, E.M. 1990). As another effect, bacterial methanogenesis may lead to fractionation between soil CO_2 and methan, whereas the expanded methan migrates upwards and oxidizes into CO_2. This CO_2 is characterized by more negative isotopic values (ŁĄCKA, B. et al. 2009).

3.2.4. Vegetation density

Carbon content of biomass is strongly influenced by enhanced soil CO_2 during the growing season (CERLING, T.E. 1984). Therefore $\delta^{13}C$ values of secondary (pedogenic) carbonates reflect the vegetation density and the effectivity of biological activity (RAO, Z. et al. 2006). Vegetation density is higher especially under warmer and moister climatic conditions, thus preferably under interglacials (RAO, Z. et al. 2006). During this periods decomposition of organic matter is also enhanced, which causes the release of ^{13}C-depleted CO_2 and leads to the most negative $\delta^{13}C$ values also in the case of secondary carbonates (RAO, Z. et al. 2006; LIU, W. et al. 2011). Glacials are characterized of colder and more arid conditions with lower vegetation coverage and thus reduction in plant respired CO_2, which leads to more positive $\delta^{13}C$ values (RAO, Z. et al. 2006; CANDY, I. et al. 2012).

3.2.5. Sedimentation rates

Extremely low sedimentation rates (<1cm/1000 yr) may cause alterations in the stable isotopic composition, since effects of climatic changes cannot be ruled out during this long period. Higher sedimentation rates (>10 cm/1000 yr) preserve isotopic signals more effectively (CERLING, T.E. 1984).

3.2.6. Sources of CO_2

Carbon dioxide may derive from the following three components: 1) oxidation of the in situ organic matter; 2) tropospheric CO_2; and 3) dissolution of preceding carbon-bearing minerals. When all the three components coexist, than $\delta^{13}C$ values are more positive in comparison to scenarios, which do not contain the listed third component (SHELDON, N.D. – TABOR, N.J. 2009).

3.2.7. Possible effects of dissolution

Isotopic composition of secondary carbonates may be sensitive of partial dissolution effects (CERLING, T.E. 1984).

3.2.8. Questions of the applicability of stable isotope signals

- *Limitations of paleotemperature estimation*

Stable oxygen isotopic composition of secondary (pedogenic) carbonates may be applied for paleotemperature determination, as DWORKIN, S.I. et al. (2005) suggested. They considered certain petrographic criteria, which may limit the applicability of these features. DWORKIN, S.I. et al. (2005) excludes the usage of biogenic types (such as NFC, CRC) and only considers rhizomes and nodules. Rhizomes are also composed of micritic to microsparitic calcite grains, which may be hints on a possible relation to hypocoatings. DWORKIN, S.I. et al. (2005) suggest the application of these two types only in cases, when the composing crystals are not recrystallized. According to SHELDON, N.D. – TABOR, N.J. (2009), the method of DWORKIN, S.I. et al. (2005) does not consider the variability of $\delta^{18}O$ values among isothermal sites and lacks the effect of evaporation. SHELDON, N.D. – TABOR, N.J. (2009) suggest that it is better to avoid the usage of secondary carbonate $\delta^{18}O$ values for paleotemperature reconstructions.

Even though as an alternative solution, the stable isotope composition of EBS may be used for paleotemperature estimations, since it seems to be a closed system, which developed under environmentally controlled conditions (VERSTEEGH, E.A.A. et al. 2013, 2014; PRUD'HOMME, C. et al. 2016).

- *Consideration of standard deviations*

According to the literature, standard deviation for $\delta^{18}O$ is generally about 0.5‰ in the case of secondary carbonates. Greater standard deviations may indicate different formation conditions and mechanisms and/or climatic changes (CERLING, T.E. 1984).

- *Consideration of interpretation difficulties*

Stable isotopic composition of (unaltered and non-recrystallized) secondary carbonates can be used in order to determine vegetational histories, ecologic and climatic changes in soils and sediments, when they are examined carefully (CERLING, T.E. 1984; CERLING, T.E. – QUADE, J. 1993). When no considerable changes are present

along certain parts of the sequence, it may indicate that vegetation cover was not exposed to significant alterations (LASKAR, A.H. et al. 2010).

Stable oxygen isotope record of secondary carbonates may be used to recognize shifts in the temperature (ŁĄCKA, B. et al. 2009), but the isotopic signal may be overprinted, when the development of a certain horizon was exposed to several consequtive climatic and environmental changes (CERLING, T.E. 1984).

BOGUCKYJ, A.B. et al. (2006) pointed out the difficulties of stable isotope data interpretation. The main problem is (according to them), that certain features may have developed in various depths and probably indicate distinct climatic periods. Biominerals may go under isotopic alterations after the burial of the paleosols or sediment horizons, as due to significantly elevated temperatures (RETALLACK, G. 2001) or the effect of fluctuating ground water levels (BUDD, D.A. et al. 2002). The latter one may reset the original isotope signal, especially in carbonate nodules (BUDD, D.A. et al. 2002). As a hint of postsedimentary/postpedogenic alteration, the presence of sparry cements may denote the effects of microbial decay during the burial of the paleosol and thus alter the isotopic compositions (RETALLACK, G. 2001).

Regional changes also effect the connections between isotopic signals: secondary carbonates from the Western European region show no relationship between $\delta^{13}C$ and $\delta^{18}O$ values – but as an opposite, aridity seems to be a controlling factor in their stable isotope values in sequences from Southern Europe (CANDY, I. et al. 2012).

3.2.9. Guidelines for present work

- *Basis of selection*

Secondary carbonates were carefully examined on the basis of their morphological marks and genetic contexts. This method is essential to the analysis of their stable isotope composition, since significant differences (as few ‰) were shown between the isotope fractionation of the certain types at low temperatures (according to KIM, S.-T. – O'NEIL, J.R. 1997). Afterwards depth-dependent $\delta^{13}C$ and $\delta^{18}O$ value distribution was determined for the chosen sections.

3.3. Key to the interpretation of stable carbon and oxygen isotope values

As a key to the interpretation of stable carbon and oxygen isotope values of bulk and secondary carbonate samples, an overview-table was created (**Appendix 8**). This

synthesis matrix represents different paleoenvironmental indications, summarizes the main effects and orders them under the following categories: 1) shift towards more positive $\delta^{13}C$/ $\delta^{18}O$ values (enrichment in $^{13}C/^{18}O$); 2) shift towards more negative $\delta^{13}C$/ $\delta^{18}O$ values (depletion in $^{13}C/^{18}O$). This key was used during the interpretation of bulk and secondary carbonates of the Verőce, Paks and Villánykövesd sequences.

4. Methods

4.1. Sampling methods

Secondary carbonate samples were collected in 10 cm vertical resolution in bulk form. Wet sieving method was carried out on these samples by using a 500 μm sieve. Remaining material was washed with distilled water and then dried in an oven for an hour between 80-100°C. After this samples were examined under a binocular microscope. Types of secondary carbonates were distinguished based on their morphological properties, and the rest of the samples were also described. The quantity of certain secondary carbonates was also counted, when enough material was available (e.g. high amount of EBS for the Verőce and Paks sequences). Secondary carbonate analysis was carried out for the Verőce, Paks and Villánykövesd sequences.

Bulk samples were taken in 2 cm vertical resolution from the Paks and Villánykövesd sequences.

4.2. Determination of stable carbon and oxygen isotope values ($\delta^{13}C$, $\delta^{18}O$)

The same method was used as it was present in the common work with KOENIGER, P. et al. (2014). Stable isotope measurements were carried out by using a Thermo Finnigan Gasbench II for CO_2 processing and for the measurement a Thermo Finnigan Delta XP isotope ratio mass spectrometer was used in continuous flow mode in the Leibniz Institute of Applied Geophysics, Section S3. Sample preparation method was crushing and thus homogenizing the material with an agate pestle and mortar and react the remaining material with anhydrous phosphoric acid in Exetainer® vials after flushing headspace gas with helium. Aliquots of 1 mg were used from bulk samples, whereas different quantities were needed from secondary carbonates, as 250 μg from CRC and 400-450 μm from HC, HC+CC, CC, CC2 and EBS. Measured stable isotope compositions were normalized against the international standards of NBS-19 and L-SVEC. Isotope values were expressed against V-PDB (Vienna Peedee Belemnite) and given in per mil (‰) as δ values

$$\delta = (R_{SA}/R_S - 1) \times 10^3$$

where R is the isotope ratio $^{13}C/^{12}C$ or $^{18}O/^{16}O$ of sample R_{SA} or standard R_S.

5. Sites and sampling

5.1. Verőce

5.1.1. General description of the Verőce sequence

The Verőce loess-paleosol sequence is found in an abandoned brickyard in the vicinity of the Verőce village (Börzsöny Mountains, Hungary, BRADÁK, B. et al. 2014). The site location is on the left bank of River Danube, in the Visegrád Gorge (altitude of 130-155 m a.s.l., N47°49'46.0"; E19°02'33.6"). History of the area and former investigations are summarized in BRADÁK, B. et al. (2014). Profile description and notes presented together with the sedimentary units in **Appendix 4b**, based on BRADÁK, B. et al. (2014) and on common field work.

Depth (cm)			Description
110	**L2r**	**C-2**	Reworked material with intercalating pebbles; slightly stratified
140	**transition**	**C-3**	Transition zone to the underlying paleosol, but still part of the reworked sediment unit; less pebble intercalations
160	**P2**	**C-4**	Dark brown paleosol with root infillings (possibly of recent origin); frequently pebbles appear in root channels (possibly roots moved pebbles downwards)
300	**L3**	**C-5**	Loess unit with biogalleries, sediment mixing with pebbles
360	**L3r**	**C-6**	Transition zone to the underlying paleosol
380	**P3**	**C-7**	Upper horizon of dark brown paleosol, mixing with pebbles
400		**C-8**	Light brown coloured transition zone from the paleosol to the underlying sediment
450	**transition**	**C-9**	Transition zone, abundant in calcified root cells
460	**L4**	**C-10**	Loess unit, mixing with pebbles, abundant in calcified root cells

500	**L4r**	**C-11**	Slightly stratified reworked layer, contains loess-sand intercalations; mixing with pebbles	
600	**transition**	**C-12**	Transition zone to the underlying paleosol; sedimentary structure is less recognizable; colour gets darker brown downwards	
640	**P4**	**C-13**	**Paleosol in local top position**	Black paleosol with high clay content; do not show the characteristic properties of soil structure
670		**C-14**		Transition zone of the paleosol; dark brown to reddish brown in colour; contains biogalleries
700	**P4!/L5**	**C-15**	**Upper wall of paleoslope**	Boundary between the transition zone of paleosol and underlying loess, which is marked by the surface of a paleovalley. Carbonate accumulation zone (with loess dolls) is under the boundary and follows the slope of paleovalley.
760	**L5**	**C-16**	Loess	

Depth (cm)			**Description**	
210	**L4r**	**D-3**	Reworked horizon and transition to the underlying paleosol, which contains mixed loess – sandy loess – paleosol laminas and pebble lenses on its lowest part	
230	**P4**	**D-4**	**Paleodepression infill**	Black paleosol with slightly granular structure, which contains carbonate veins in cm thickness
290		**D-5**		Black-brown to brown paleosol (soil horizon), polyhedral structure with clay coatings. This horizon lacks the carbonate veins.
310				

artificial step

350	P4	D-6	Paleodepression infill	Black-brown paleosol horizon, which contains reddish biogalleries (source of infilling of biogalleries is the underlying soil horizon)
390		D-7		Reddish-brown transition zone of the paleosol, which contains pebbles
420		D-8		Reddish paleosol horizon
430		D-9		Lowest part of the reddish soil horizon
440	L5	D-10	Transition of paleosol/loess, which contains carbonate concretions and signs of carbonate migration	
450		D-11	Homogeneous, non-stratified loess horizon with continuous upper boundary to the transition zone; yellow-brown in colour	
490 520	A1	D-12	Greyish-brown sediment with continuous boundary to the above lying loess. More compact and clayey, contains higher portion of aleurite. Possibly developed under moist conditions, e.g. dust accumulation on the flood plain?	

Depth (cm)			Description	
190	Lr(?)	A-5	Paleosol in slope position	Reworked layer in greyish-brown colour, which contains a darker, brownish horizon.
200	P4	A-6		Transition zone to the upper horizon of the paleosol, colour transition from greyish-brown to black
210		A-7		Black paleosol with high amount of biogalleries
250		A-8		Dark brown paleosol horizon with high amount of biogalleries
290		A-9		

				Reddish-brown paleosol horizon, which contains less biogalleries (when compared to the upper paleosol horizons)
320		**A-10**		Lowest transition zone of paleosol to the underlying loess
350	**L5**	**A-11**	Loess horizon	

5.1.2. Applied methods for the Verőce sequence

Sedimentary units are ordered to main groups, as loess, paleosol, loess, transitional - reworked layer categories. Sedimentary units are presented from the lowest one towards the highest positions, as following the built-up of the sequence. Detailed secondary carbonate micromorphological description is available in **Appendix 1 (a-c)**, but certain important remarks and their indicative function are highlighted here. The $\delta^{18}O$ and $\delta^{13}C$ signals of HC were chosen for broader interpretation. This feature is thought to be synsedimentary and support the theory of the pedosedimentary development of the sequence (CATT, J.A. 1990; BECZE-DEÁK, J. et al. 1997) and may lack recrystallization effects (DWORKIN, S.I. et al. 2005). Mean $\delta^{18}O$ and $\delta^{13}C$ values of HC were calculated for the whole Verőce sequence and by these means an attempt was made for the interpretation of the fluctuating signals. Mean $\delta^{18}O$ is -8.83‰ (max. -6.30‰ and min. -12.17‰), while mean $\delta^{13}C$ is -8.76‰ (max. -5.53‰ and min. -10.47‰). Values shifted to the minimum direction are considered as more negative values, while values shifted towards the maximum direction are the more positive values. It means that more negative values are depleted in ^{13}C or ^{18}O, whereas more positive values are enriched in them. The sedimentary units are ordered into a matrix containing the main directions in **table 1**. Further information and references are present in **Appendix 8**, as well.

As other secondary carbonate types, HC+CC, CC, CRC and EBS were interpreted. The results of this analysis are not ordered to the sedimentary units, but are handled separately in subchapters because of their complexity.

Table 1: Stable isotope pattern of sedimentary units at Verőce

more negative $\delta^{13}C$ – depletion in ^{13}C	**more positive $\delta^{13}C$ – enriched in ^{13}C**

Trends obtained at Verőce site:	**Trends obtained at Verőce site:**

• *paleosols:*
  ○ 'local top position sequence' – P4
  ○ 'slope deposit' – P4 (except unit A-10)
  ○ P3 paleosol - reflects humid interglacial phase
  ○ P2 paleosol – lowest 1/3 part (both $\delta^{13}C$ and $\delta^{18}O$ values show the same behaviour regarding their trend)
• *loess layers:*
  ○ L5 overlaid by the well-developed paleovalley infill P4 paleosol - upper ½ part
  ○ Loess overlaid by the local top position P4 paleosol – upper ½ part (pedosedimentation effects are more characteristic upwards in this part: decreased dust accumulation rates and increasing vegetation cover)
• *redeposited layers:* L4r (C-11)
• *transition zones:* P3/L4 (C-9)
• *aleurite* – A1
	• *paleosols:*
	  ○ 'paleovalley infill, well developed paleosol' P4
	  ○ 'slope deposit' – P4, only unit A-10 (this subunit reflects the first stage of paleosol development)
	  ○ P2 paleosol – upper 2/3 part (both $\delta^{13}C$ and $\delta^{18}O$ values show the same behaviour regarding their trend)
	• *loess layers:*
	  ○ L5 overlaid by the well-developed paleovalley infill P4 paleosol - lowest ½ part
	  ○ L4
	• *redeposited layers:* L4r (C-11 and D-3); L2r
	• *transition zones:* P4/L4r (C-12); the boundary between L5 (overlaid by the well-developed paleovalley infill) and A1

more negative $\delta^{18}O$ – depletion in ^{18}O	**more positive $\delta^{18}O$ – enriched in ^{18}O**

Trends obtained at Verőce site:
• *paleosols:*
  ○ 'local top position sequence' – P4 (except unit C-12)
  ○ 'slope deposit' – P4 (except unit A-10)
  ○ P3 paleosol – reflects humid interglacial phase
  ○ P2 paleosol – lowest 1/3 part (both $\delta^{13}C$ and $\delta^{18}O$ values show the same behaviour regarding their trend)
• *loess layers:*
  ○ L5 overlaid by the well-developed paleovalley infill P4 paleosol – middle part
  ○ loess overlaid by the local top position P4 paleosol – upper ½ part
  ○ L4, L3
• *redeposited layers:* L4r (C-11)
• *transition zones:* P4/L4r transition (C-12); P3/L4 (C-9)
• *aleurite* – A1
	Trends obtained at Verőce site:
	• *paleosols:*
	  ○ 'paleovalley infill, well developed paleosol' P4
	  ○ 'local top position sequence' – P4, only unit C-12
	  ○ 'slope deposit' – P4, only unit A-10 (this subunit reflects the first stage of paleosol development)
	  ○ P2 paleosol – upper 2/3 part (both $\delta^{13}C$ and $\delta^{18}O$ values show the same behaviour regarding their trend)
	• *loess layers:*
	  ○ loess overlaid by the local top position P4 paleosol – lower ½ part
	  ○ L3
	• *redeposited layers:*
	  ○ L4r (D-3); L2r
	• *transition zones:* L2r/P2 (C-3); the boundary between L5 (overlaid by the well-developed paleovalley infill) and A1

5.1.3. Characteristics of the different sedimentary units and stable isotope signals of HC

General tendencies for HC are present in **Appendix 4b**, which sketch introduces the sedimentary unties as well.

5.1.3.1. Paleosols

5.1.3.1.1. Variations of P4 paleosol

5.1.3.1.1.1. P4 paleosol in valley bottom position

P4 paleosol in valley bottom position, profile D (P4-D, Units D-4, -5, -6, -7, -8):

The well-developed character and the thickness of the paleosol is possibly due to its paleogeomorphological position. Pedogenesis seemed to be continuous during dust accumulation or incorporation of reworked materials (BRADÁK, B. et al. 2014).

- *Synsedimentary/pedogenic secondary carbonate features:*
    - **Soil-like HC**. Leaching processes may be caused by the presence of recrystallized material in the inner channel part of HC (BRADÁK, B. et al. 2014).
    - **CRC**. Dissolution led to the erosion of the surficial cell layers, therefore presence of CRC is characteristic mostly in a weathered state. Such CRC were found in the subunit D-5, which seemed to have a decaying and party calcified section and a quite recent part. This latter observation raised the question, whether CRC was preserved in this state after burial or if it is formed recently from deep-rooting grasses. In this case it is questionable if it can be trusted to use as a paleoclimate indicator (BRADÁK, B. et al. 2014).
- *Postsedimentary/post-pedogenic secondary carbonate features:*
    - **CC**. Multichannel CC appeared in the subsection of D-9 and D-7 (BRADÁK, B. et al. 2014). This appearance may give hints on the multiphase leaching history of the paleosol (BARTA, G. 2014).
    - **Carbonate veins**. The upper 1 m part of the paleosol (subunit D-4) is characterized by the presence of carbonate veins. The length of these infillings varies between 12-15 cm, while its width is generally between 2-3 cm. The structure of carbonate veins can be divided into two main parts: 1) outer section of the vein infilling: porous, chalky white material, which

resembles the properties of CC; 2) inner section of the vein infilling: brownish-grey, compact material, which seems to be strongly recrystallized. These sections are joined together with a sharp boundary. Carbonate veins contained in some cases pebbles and CRC in their inner section, which give hints on the incorporation of the surrounding material during vein development (my interpretation part in BRADÁK, B. et al. 2014).

- *Stable isotope composition of HC (**Appendix 8.** contains the broader range of references)*
    - $\delta^{18}O$ and $\delta^{13}C$ values both are shifted mostly towards the direction of more positive values. The indication for $\delta^{18}O$ may reflect lower humidity and higher evaporation effect (e.g. CERLING, T.E. – QUADE, J. 1993). Valley bottom position possibly worked as a trap for downslope migrating solutions, where evaporation could have been enhanced on a seasonal basis. This could be especially characteristic of the near-surface zones (ŁĄCKA, B. et al. 2009). The $\delta^{13}C$ signal may indicate arid conditions with lower vegetation density and lower biological activity (e.g. CERLING, T.E. 1984). It may sound contradictory when it is compared with the development state of the paleosol. Other effects may have influenced $\delta^{13}C$ values, as the role of microbial decomposition. Since this paleosol horizon is well-developed and presence of organic matter is relevant, the decomposing effect of microorganisms was presumably more enhanced, which causes enrichment in ^{13}C in the soil environment (GALIMOV, E.M. 1990). Another effect could be related to the presence of closed forest canopy, which changes the properties of CO_2 in the local atmosphere and thus causes enrichment of ^{13}C in the plants and thus influences the composition of the soil-respired CO_2 (CERLING, T.E. – QUADE, J. 1993).

5.1.3.1.1.2. P4 paleosol developed in local top position

P4 paleosol developed in local top position, profile C (P4-C, Unit 13 and Unit 14):

This well-developed paleosol is characterized by separated pedological horizons, which extent is less than the P4 variation of the valley bottom position (BRADÁK, B. et al. 2014).

- *Synsedimentary/pedogenic secondary carbonate features:*

- **Soil-like HC**. This type was present throughout the whole paleosol (BRADÁK, B. et al. 2014).

- *Postsedimentary/post-pedogenic secondary carbonate features:*
  - The paleosol lacked other secondary carbonates and no hints were present on the effect of leaching or percolating solutions (***Appendix 1.a.***).
- *Stable isotope composition of HC (**Appendix 8.** contains the broader range of references)*
  - $\delta^{18}O$ and $\delta^{13}C$ values are mainly shifted towards the direction of more negative values, but $\delta^{18}O$ moved towards the positive direction in two cases. The more negative values $\delta^{18}O$ are connected to possibly higher moisture content and thus reflect more negligible evaporation - with the exception of the more positive two values (e.g. ALAM, M.S. et al. 1997). The $\delta^{13}C$ signal indicated enhanced vegetation and soil development under moister conditions, which pointed out on an interglacial phase (e.g. RAO, Z. et al. 2006). These observations sound partly contradictory, since various geomorphological positions are marked by different moisture conditions. By this means, local aridity should be more enhanced for soils related to top positions in comparison to soils found in valley positions (JENNY, H. 1994). However, stable carbon and oxygen isotope signals show the opposite trend in this case.

5.1.3.1.1.3. P4 paleosol situated on a paleoslope

P4 paleosol situated on a paleoslope, profile A (P4-A, Units A-6, -7, -8, -9, -10):

Variation of the P4 paleosol developed in paleoslope position, therefore its pedogenic horizons were less noticeable. Its uppermost part was covered by and mixed with sediment and paleosol laminas, which referred to active reworking along the former slope surface (BRADÁK, B. et al. 2014).

- *Synsedimentary/pedogenic secondary carbonate features:*
  - **Soil-like HC**. Its presence was not characteristic of every subhorizon.
- *Postsedimentary/post-pedogenic secondary carbonate features:*
  - **CC**. Occurrence of the main type was quite common.

- *Stable isotope composition of HC (**Appendix 8.** contains the broader range of references)*
    - $\delta^{18}O$ and $\delta^{13}C$ values in the upper subunits of A-6 to A-9 are mainly shifted towards the direction of more negative values and show similar properties as described for the P4 developed in local top position. Subunit A-10 is different, since $\delta^{18}O$ and $\delta^{13}C$ are both shifted to the direction of more positive values. Generally it seems to be more connected to lower vegetation densities, less humid environment and higher evaporation rates (e.g. CERLING, T.E. 1984). It can also be connected to the slow built-up of the paleosol, where this subunit reflects the effects of the first stage. The question is raised, whether slopeward migrating solutions show an effect on the values.

5.1.3.1.2. P3 paleosol

P3 paleosol (Unit C-7 and C-8) shows continuous accretion from the underlying loess horizon (BRADÁK, B. et al. 2014). Micromorphological analysis of the whole samples after the wet sieving process showed mixing sedimentary and pedogenic properties (based on the grain compositions and structure of aggregates).

- *Synsedimentary/pedogenic secondary carbonate features:*
    - **Soil-like HC**. Soil-like HC was present, partly in the form of HC+CC, which show postsedimentary/postpedogenic character.
- *Postsedimentary/post-pedogenic secondary carbonate features:*
    - **CC**. Main type of CC appeared along the whole paleosol unit. In one case it was hard to differentiate it from CRC, it resembled one of its latter type, which underwent a strong degree of dissolution.
    - **Pendants**. Presence of pendants on pebbles was quite common along the paleosol (BRADÁK, B. et al. 2014).
- *Stable isotope composition of HC (**Appendix 8.** contains the broader range of references)*
    - $\delta^{18}O$ and $\delta^{13}C$ values are mainly shifted towards the more negative values, which may reflect a more humid interglacial phase with high vegetation densities (e.g. RAO, Z. et al. 2006).

5.1.3.1.3. P2 paleosol

P2 paleosol (Unit C-4) developed on the L3 loess unit and is characterized by large number of biogalleries (BRADÁK, B. et al. 2014). In the uppermost part of the paleosol the signs of the beginning of the sedimentation period could be traced according to the micromorphological investigations.

- *Synsedimentary/pedogenic secondary carbonate features:*
    - **Soil-like HC**. This type was present along this paleosol horizon.
    - **NFC**. Preserved only in the inner channel of a HC and CC as well (BRADÁK, B. et al. 2014).
- *Postsedimentary/post-pedogenic secondary carbonate features:*
    - **CC**. Appearance of CC is not just in the form of the main type, but as thin calcite tubes and in the form of powdery white accumulations.
    - **Concretions**. Small concretions appear in the lowest horizons of the soil, according to the ***Appendix1.a..***
- *Stable isotope composition of HC (**Appendix 8.** contains the broader range of references)*
    - $\delta^{18}O$ and $\delta^{13}C$ values show a shift towards more positive values on the upper and lowest part of the paleosol. Almost in all cases the values move together, which means, that if $\delta^{18}O$ is shifted towards one direction, than $\delta^{13}C$ values is shifted towards the same. It may reflect a strong connection. The lowest and upmost part of the paleosol is mostly characterized by more arid conditions, less vegetation density and enhanced evaporation effects (e.g. CERLING, T.E. 1984). However the values of the middle section refer to a shift towards a slightly more humid environment with denser vegetation properties (e.g. QUADE, J. et al. 1989). It is also possible, that paleosol development started under arid conditions than due to climate change, a more humid period begun. By the end of the interglacial period climate shifted again towards aridity, which are reflected in the isotopic compositions of HC.

5.1.3.2. Loesses

5.1.3.2.1. Variations of the L5 loess

5.1.3.2.1.1. Position of L5 under the paleosol of valley bottom position

Position of L5 loess (Unit D-9, -10, -11) and A1 aleurite (Unit D-12) under P4-D paleosol of valley bottom position:

- *Synsedimentary secondary carbonate features:*
  - **HC**. Sediment-like HC was present in these units.
  - **EBS**. The highest amount of EBS occurred in the L5 loess of both positions and their quantitative distribution can be considered as a correlative link between the subunits of D-11, D-10 and C-16. Increasing tendency of EBS was shown from the A1 unit, throughout the whole L5 until it reached the boundary of the P4 paleosol (BRADÁK, B. et al. 2014). This great amount may refer to the increasing stability of the surface and leads towards the soil developmental phase (BECZE-DEÁK, J. et al. 1997).
  - **CRC**. CRC was present along the L5 unit, but not continuously (***Appendix 1.b.***). Their colour was bright white and the multiple cell layers were visible under the binocular microscope (BRADÁK, B. et al. 2014).
- *Postsedimentary secondary carbonate features:*
  - **Carbonate concretions**. Concretions occurred in two parts of the profile. Once in the carbonate accumulation zone of P4 and second at ~510 cm depth in the A1 unit. This latter case appeared beneath a 2-3 cm thick reddish layer (BRADÁK, B. et al. 2014). Since the presence of concretions denotes the former stability of the surface (KEMP, R.A. 1995), this layer may slightly refer to the presence of former (possibly) weak pedogenetic process. Although the possible effects of ground water fluctuations also cannot be ruled out. Loess dolls were in all cases elongated in their longitudinal axis (BRADÁK, B. et al. 2014).
- *Stable isotope composition of HC (**Appendix 8.** contains the broader range of references)*
  - $\delta^{18}O$ values are shifted towards more negative values upwards from the middle part of the profile, which showed same tendency with $\delta^{13}C$ values. $\delta^{13}C$ values are only more positive on the lowest part of L5. More negative values of $\delta^{13}C$ indicated slightly denser vegetation cover and thus may be

connected to the pedosedimentary profile development (e.g. CATT, J.A. 1990; RAO, Z. et al. 2006). The boundary of the underlying A1 to L5 (Units D-12 and D-11) is indicated by more positive $\delta^{18}O$ and $\delta^{13}C$ values, reflecting a slight shift to more arid conditions (e.g. KAAKINEN, A. et al. 2006).

- The A1 aleurite (Unit D-12) unit is mainly characterized by more negative $\delta^{18}O$, which could indicate moister conditions (e.g. ALAM, M.S. et al. 1997). Above and below the mentioned thin reddish layer the character of the stable isotope composition changed. Upwards from this layer both $\delta^{13}C$ and $\delta^{18}O$ values shifted towards more negative values, referring to more humid conditions with denser vegetation (e.g. PENDALL, E. – AMUNDSON, R.G. 1990; CERLING, T.E. – QUADE, J. 1993). The question was raised, whether it could be a possible remnant of a weak (and/or eroded) paleosol, whose development was suppressed by accumulating dust.

5.1.3.2.1.2. Position of L5 under the paleosol of local top position

Position of L5 loess (C-15, -16) under P4-C paleosol of local top position:

- *Synsedimentary secondary carbonate features:*
  - **HC**. HC was present both in soil-like and sediment-like appearances in the subunit of C-16 (BRADÁK, B. et al. 2014). Soil-like HCs show a possible connection with the presumed slowing down of dust accumulation, where pedogenic processes were even less suppressed due to climate change (CATT, J.A. 1990; BRADÁK, B. et al. 2014).
  - **EBS.** The amount of EBS was very high under both P4 variations (top and paleovalley; BRADÁK, B. et al. 2014), which indicate the stability of the environment and thus support the pedosedimentary aspect of the profile development (BECZE-DEÁK, J. et al. 1997; KEMP, R.A. 1999). This stability denoted the possible slowing down of dust deposition and a stable moisture regime (BECZE-DEÁK, J. et al. 1997).
  - **CRC.** Dissimilar amounts of CRC of L5 also gave hints of the differing moisture conditions obtaining between the P4 variations of the top position and paleovalley. CRC was present in higher amounts under P4 of the top

position, which may indicate that the environment was more arid during the dust deposition phase (BECZE-DEÁK, J. et al. 1997), or at least that water content was drained more effectively. This aridity may reflect a seasonal basis to the variations (QUADE, J. et al. 1989).

- *Postsedimentary secondary carbonate features:*
    - **Carbonate concretions**. Field investigation showed a special topographical position between P4-C paleosol and the underlying L5 loess. Left from the middle point of the section wall (right under P4-C) the deposition of P4-C was horizontal on L5, but from the middle point towards the right direction the boundary showed downhill characteristics. Through this observation, the uppermost part of valley hang was caught along the subunit C-15. Loess dolls were found not just under the horizontal position, but as a lining of the valley hang boundary. These loess dolls were in all cases elongated in their longitudinal axis and one of them had crescent morphology (BRADÁK, B. et al. 2014). They marked not just the carbonate accumulation zone of P4, but the route of the migrating bicarbonate solutions. These solutions start to move from the upslope position in the direction of the downslope, along which route carbonate possibly precipitates in the form of concretions (SCHARPENSEEL, H.W. et al. 2000; MONGER, C.H. 2002). At the Verőce site the top position caused the modification of the pathway of the leaching front and led the solutions to flow in the direction of the connecting valley slope.
- *Stable isotope composition of HC (**Appendix 8.** contains the broader range of references)*
    - The $\delta^{18}O$ signal is shifted towards the more positive values right under the boundary of the paleoslope and along the sediment unit. This shift may indicate more arid conditions and thus reflect the role of evaporation (e.g. CERLING, T.E. – QUADE, J. 1993). The $\delta^{13}C$ values show fluctuations and are slightly shifted to more negative values towards the direction of P4 paleosol. This may draw parallels to the pedosedimentary profile development, since vegetation was even more characteristic and dense when the shift in the climate system was reached (e.g. BECZE-DEÁK, J. et al. 1997; RAO, Z. et al. 2006). It is also strengthened by the presence of soil-like HC.

5.1.3.2.2. The L4 loess unit (Unit C-10)

- *Synsedimentary secondary carbonate features:*
  - **Sediment-like HC**. This feature is present along the whole loess unit.
  - **EBS**. EBS is present almost along the whole unit, except the last 10 cm.
- *Postsedimentary secondary carbonate features:*
  - No signs of postsedimentary effects were present.
- *Stable isotope composition of HC (**Appendix 8.** contains the broader range of references)*
  - L4 is characterised by $\delta^{13}C$ values, which are mostly shifted towards the more positive direction. This denotes possibly sedimentary conditions and less dense vegetation cover, which belong to the general loessic characteristics. $\delta^{18}O$ values show the opposite trend in certain cases, which may denote slightly enhanced humidity.

5.1.3.2.3. The L3 loess unit (Unit C-5)

- *Synsedimentary secondary carbonate features:*
  - **Sediment-like HC** and **soil-like HC**. The latter type was present on the lowest half of the unit, which may strengthen the pedosedimentary theory (CATT, J.A. 1990; BECZE-DEÁK, J. et al. 1997).
  - **EBS.** EBS was present throughout the whole unit, in upwards decreasing amount.
- *Postsedimentary secondary carbonate features:*
  - **CC**. Besides the main type, some chalky white powdery accumulations were also present.
  - **Concretions**. They were present only in small size range (see ***Appendix 1.a.*** for details). The appearance of these concretions was not compact and cemented, as loess dolls used to be. They were not compact, but seemed to be strongly impregnated (BRADÁK, B. et al. 2014). In one case they resembled the structure of cemented CCs or HCs.
- *Stable isotope composition of HC (**Appendix 8.** contains the broader range of references)*

- L3 showed similar trend to L4 based on the $\delta^{13}C$ values, but showed upwards increasing tendencies and indicated less enhanced vegetation cover. The $\delta^{18}O$ values were shifted towards the more negative directions, which may either be connected to enhanced humidity on a seasonal basis (e.g. QUADE, J. et al. 1989). The negative $\delta^{18}O$ values become even less negative upwards in the unit. This may refer to the effects of development on L3r (see below), which was impacted by sheetwash processes and thus showed higher proportions of migrating solutions.

5.1.3.3. Transition zones

Transition zones were differentiated between loess/reworked loesses and paleosol horizons, as follows: C-12 (overlying of P4), C-9 (below P3) and C-3 (overlying of P2).

- *Synsedimentary secondary carbonate features:*
  - **Sediment-like HC**. High amount of this feature was found in the subunit of C-12, which counts as the upper transition zone of the local top P4 paleosol. The pedogenic phase was even more suppressed by the increasing dust accumulation rates, but the present microecosystem was still active and therefore it tried to keep pace with dust settlement. Since the switch from soil development to dust accretion was presumably slow, the biomineralized products, as HC remained in the sediment relative abundant (CATT, J.A. 1990; BECZE-DEÁK, J. et al. 1997; BRADÁK, B. et al. 2014). C-9 and C-3 contained only low amount of HC, but the wet sieved samples were characterized by both of sediment and soil properties (according to the micromorphological description, see ***Appendix 1.a.***).
- *Stable isotope composition of HC (**Appendix 8.** contains the broader range of references)*
  - The transitions showed different patterns according to their stable isotope compositions. As a continuation of the $\delta^{18}O$ values observed in P4, the transition zone C-12 shows almost the same negative values (which slightly increase upwards). $\delta^{13}C$ values seem also to follow the pattern of P4 as staying in the more positive direction. Similarities with P4-C may refer to the above mentioned effect (presence of high amount of HC in C-15), as soil development to dust accretion happened gradually (e.g. BECZE-DEÁK, J. et al. 1997).

- C-9 was characterized by more negative $\delta^{13}C$ and $\delta^{18}O$ values, which are similar to the isotopic pattern of P3 paleosol. The values presented here may already be the first signs of the climatic change towards the interglacial phase (e.g. RAO, Z. et al. 2006).
- Both $\delta^{13}C$ and $\delta^{18}O$ values showed shifts towards the more positive direction in the case of C-3. This indicates that the paleosol development phase was ended and transition begun towards conditions, which are more typical of dust deposition (as lower vegetation density and decreasing humidity).

5.1.3.4. Reworked layers

- *Synsedimentary secondary carbonate features:*
  - **Soil-like HC**. The reworked layers of L4r (C-11, D-3), L3r (C-6) and L2r (C-2) contained soil-like HC. Though these samples showed detrital characteristics, the soil-like HCs were whole and non-detrital (only with the exception of L4r in D-3). This observation raised the following two possibilities: 1) HC formed after the translocation process ended; or 2) translocation was really slow and during this process the formation of HC was simultaneous. For instance, HC found in L3r is composed of strongly mixed up materials and seems to be the impregnation of loess, sand and soil at the same time. This may strengthen the second hypothesis (BRADÁK, B. et al. 2014).
  - **EBS**. Presence of EBS was quite common in the reworked layers. Most of them were whole and non-detrital. Broken EBS was found in L4r (C-11), which gave hints on the reworking effects (BECZE-DEÁK, J. et al. 1997; BRADÁK, B. et al. 2014) and strengthened the characteristics of the field observations. The breakage revealed the inner structure of the EBS, which possessed a central core with radially arranged crystals (BRADÁK, B. et al. 2014).
- *Postsedimentary secondary carbonate features:*
  - **Cement layer.** The boundary between L4r (D-3) and P4 valley bottom paleosol was characterized by a thin carbonate cement layer. This soft cement material was compacted only locally and formed small concretion-like features with loose structure (BRADÁK, B. et al. 2014).

- *Stable isotope composition of HC (**Appendix 8.** contains the broader range of references)*
    - In the case of L4r (C-11) both $\delta^{13}C$ and $\delta^{18}O$ signals are on the more negative side of the mean value, but they shift gradually towards the positive direction upwards in the layer. Possibly vegetation was still present at the beginning of the reworking phase, which led to the negative values (e.g. QUADE, J. et al. 1989). As reworking was more effective, it may have slowly repelled parts of the vegetation cover and thus caused the presented shift in the values for the remaining HC. Reworking and possible sheetwash influenced the infiltration and migration of solutions and this means it cannot be ruled out, that the evaporative effects were possibly higher in the near-surface. This may lead to the more positive $\delta^{18}O$ values upwards in the layer (e.g. ŁĄCKA, B. et al. 2009).
    - L4r in the D-3 subunit is characterized by more positive $\delta^{13}C$ and $\delta^{18}O$ values. This layer covers the P4 paleosol and still denotes the paleogeomorphological position of the valley bottom. Possibly sheetwash processes happened along the paleoslope, which were characterized by high amount of infiltrating solutions. These dense, bicarbonated solutions may have led to the formation of the above mentioned cement layer on the lower boundary of the unit. These two factors may be connected with stronger evaporative effects, which led to enrichment in ^{18}O (e.g. CERLING, T.E. – QUADE, J. 1993) and low biological productivity ending up in the enrichment of ^{13}C (e.g. CERLING, T.E. 1984).
    - $\delta^{13}C$ and $\delta^{18}O$ values in L2r are mostly located on the more positive side of the mean value, but show a fluctuating habit even more towards the negative direction of the mean value.

5.1.4. Stable isotope composition of certain secondary carbonates

5.1.4.1. Stable isotope composition of HC+CC at Verőce

Mean values of HC+CC were calculated for the Verőce section as -8.99‰ for $\delta^{13}C$ (max. -8.45‰ and min. -9.79‰) and -9.46‰ for $\delta^{18}O$ (max. -6.73‰ and min. -10.62‰), based on the following units: D-3, -4, -5, -9, -10, -11 and Unit A-5, -9.

HC+CC is a combined form, where CC is present as a thin calcite tube on the inner channel wall of HC. The special characteristic of the feature is that HC is thought to be of synsedimentary origin, whereas the presence of CC on its inner channel wall is due to postsedimentary precipitation (BARTA, G. 2011a; BARTA, G. 2014).

The availability of HC+CC was not continuous along the Verőce sequence. Some remarks were made only according to the L5-D layer. This horizon contained HC and HC+CC as well and their $\delta^{13}C$ and $\delta^{18}O$ values were compared to each other. The difference was determined as follows: 0.02‰ to 0.51‰ for $\delta^{13}C$ and 0.06‰ to 0.85‰ for $\delta^{18}O$. The curves of HC and HC+CC seemed to follow the same tendency upwards in the sequence (**Appendix 4.e.*)***. This observation may denote the application possibilities of HC+CC signals. In all cases the habit of the inner calcite tube should be determined in order to rule out multiple tube formation and thus more complex leaching connections.

5.1.4.2. Stable isotope composition of CC at Verőce

Mean values of CC were calculated for the Verőce section as -8.83‰ for $\delta^{13}C$ (max. -7.03‰ and min. -10.15‰) and -10.00‰ for $\delta^{18}O$ (max. -7.91‰ and min. -12.03‰), based on the following units: D-4, -5, -6, -7, -8, -9; Unit A-8, -9, -11; and Units C-3, -4,-5,-6,-8,-9.Main type of CC was analysed, which denotes postsedimentary/postpedogenic leaching processes (HORVÁTH, E. et al. 2007).

$\delta^{13}C$ values of CC show similar tendency and range to the curves of HC in profile C. This observation may raise the following hypothesis: leaching may have happened parallel to the sequence development, or shortly after the built up of the sedimentary units. The ground for it may be that $\delta^{13}C$ had the same source in both cases and therefore denoted that the available organic matter had alike properties during the formation of HC and CC as well.

Less similarities to HC are shown in the case of $\delta^{18}O$ values and trends seem to be opposite to each other, with the exception of L3-C. This may be connected to the above presented hypothesis (as leaching may have happened parallel to the sequence development) and complemented with the possibility, that the source of leaching could have been connected to seasonal differences during sequence built-up (and thus not just to the vegetation period).

Stable isotopes signals of P4-A paleosol variation of the paleoslope situation are complicated to compare to those of HC. Shift towards the more negative $\delta^{18}O$ values may be interpreted as the consequence of leaching. As this sequence is in slope position, the infiltrating solutions derived not just directly from the meteoric water, but from slopeward sheetwash. Moisture conditions may be influenced by seasonal changes and thus by rhapsodic storm events as well.

Comparison of CC and HC in the case of P4-D (valley bottom position) was only available in a narrower horizon, where $\delta^{13}C$ values seemed to move towards the same direction, whereas $\delta^{18}O$ values showed the opposite trend. This may have similar reasons, as introduced for profile C. In the lowest parts of P4-D paleosol no data of HC was available. Valley bottom position may be responsible for the more effective collection of infiltrating solutions and enhance the amount of leaching (also on seasonal basis). This may cause shift of $\delta^{18}O$ values towards the more negative direction.

5.1.4.3. Stable isotope composition of CRC at Verőce

Mean values of CRC were calculated for the Verőce section as -24.29‰ for $\delta^{13}C$ (max. -15.28‰ and min. -33.21‰) and -14.19‰ for $\delta^{18}O$ (max. -10.28‰ and min. -17.04‰). Presence of CRC denotes in situ formation characteristics according to BECZE-DEÁK, J. et al. (1997).

An attempt was made to order those sedimentary units into the created matrix (as seen in **Appendix 8.**), which contained CRC (**Table 2**). Shifts were determined in comparison to the calculated mean values. It also has to be considered, that due to their formation process, the values of CRC are strongly influenced by biomineralization processes and therefore they are characterized by more negative values than HC (e.g. KOENIGER, P. et al. 2014).

Table 2: General tendencies of CRC at the Verőce site

more negative $\delta^{13}C$ – depletion in ^{13}C	**more positive $\delta^{13}C$ – enrichment in ^{13}C**

• *aleurite* – A1
• *loess layer:*
  ○ L5 under P4 of local top position
	• *loess layer:*
	  ○ L5 under P4 of valley bottom position
	  ○ L3
	• *paleosol:*

	○ P4 of valley bottom position
more negative $\delta^{18}O$ – depletion in ^{18}O	**more positive $\delta^{18}O$ – enrichment in ^{18}O**
• *aleurite* – A1 • *loess layer*: ○ L5 under P4 of valley bottom position ○ L5 under P4 of local top position	• *loess layer:* ○ L3 • *paleosol*: ○ P4 of valley bottom position

L5-C in local top position showed more negative $\delta^{13}C$ values compared to the L5-D version under the P4-D paleosol of valley bottom position. $\delta^{13}C$ values of HC showed slight shifts towards the negative direction upwards in the layer (towards P4-C), as it was introduced in the section dealing with HC values for L5-C: certain parallels may be drawn between the values of HC and CRC in the frame of the pedosedimentary profile development (BECZE-DEÁK, J. et al. 1997; RAO, Z. et al. 2006).

Both $\delta^{13}C$ and $\delta^{18}O$ values of CRC from P4-D paleosol are shifted towards the more positive direction. These CRC showed slightly dissolved surfaces, as being in the strongly leached paleosol. Dissolution and possible recrystallization on the former surface may influence the isotopic signal. The composition of infiltrating solutions may be different according to the climatic conditions, since leaching happens not just continuously during paleosol development, but also later on.

5.1.4.4. Stable isotope composition of EBS at Verőce

Mean values of EBS were calculated for the Verőce section as -12.90‰ for $\delta^{13}C$ (max. -9.82‰ and min. -14.82‰) and -8.17‰ for $\delta^{18}O$ (max. -1.46‰ and min. -12.41‰). Analysed EBS were whole and not broken ones, which refer to in situ formation characteristics according to BECZE-DEÁK, J. et al. (1997).

$\delta^{13}C$ values showed fluctuations between the above listed maximum and minimum values, without showing a clear trend (**Appendix c-d.**). Some EBS sampled from the same depth showed such values, which moved towards to opposite direction. Therefore the curves were similar to a zigzag pattern. Earthworm activity strongly depends on the season, as cited by PRUD'HOMME, C. et al. (2016), which may denote that the EBS values of the Verőce sequence also reflect the spring-autumn formation period. Dietary

uptake of earthworms strongly influences the $\delta^{13}C$ values of EBS (CANTI, M.G. 2009; KOENIGER, P. et al. 2014), especially during periods with higher temperatures, which enhance metabolic activites (VERSTEEGH, E.A.A. et al. 2014). By this means seasonality may cause the scattering of values in zigzag pattern, as influencing the availability of organic matter in the system. Possibly the type of vegetation may be an influencing factor on the availability of organic matter, e.g. the $\delta^{13}C$ values of EBS from the L2r-C layer reflect a slight shift towards the less negative values. During the reworking phase vegetation was probably not that effective, which affected the availability of organic matter.

$\delta^{18}O$ values show a zigzag pattern along the profile C and D. In the case of profile C the amplitude of the shifts is especially large in the case of the P4-C paleosol. Amplitudes seem to narrow slightly upwards in the profile, or at least the range of the values is smaller (as in L2r-C). It is complicated to compare or synchronize the values of EBS to the values of HC. It also has to be considered, that shifts of the $\delta^{18}O$ values may be due to seasonal changes, as the body fluids of earthworms are connected to the composition of the soil moisture (VERSTEEGH, E.A.A. et al. 2013; PRUD'HOMME, C. et al. 2016). A possible summer aridity and lower water availability may cause extreme shifts to ^{18}O enrichment, since earthworms can produce biospheroids quite rapidly (1-3 EBS/worm/week as proven by CANTI, M. 1998).

As an additional effect it should also be considered, that earthworms may burrow down to more than 1 m, depending on the climatic conditions (DARWIN, C. 1882), which may cause mixing among the values. The zone of fluctuating ground water and the depth of soil frost both influences the life range of earthworms.

5.2. Paks

5.2.1. General description of the Paks sequence

The Paks Brickyard sequence is one of the most detailed loess-paleosol sequences in Hungary, which was also examined in boreholes and thus an almost 60 m thick sequence was revealed (PÉCSI, M. 1993). A detailed overview of the former investigations and of stratigraphic units is given in HORVÁTH, E. – BRADÁK, B. (2014). Currently THIEL, C. et al. (2014) updated the chronostratigraphic frame of the Paks sequence by the application of post-IR IRSL dating methods. In my dissertation I

investigated the same profile after the information of THIEL, C. (personal communication), which made comparisons easier. Coordinates of the Paks sequence were as N46°38'24" and E18°52'24", 135 m a.s.l. Field description of secondary carbonate appearances was formerly described by KÁSA, I. (2010), but no sampling was carried out by her.

Depth (cm)	Unit	Description
10	**Unit 1**	**Loess** – colour of the unit was pale grey to yellow between 10-420 cm, whereas the lowermost part between 430-550 cm was pale yellow without greyish shade. Granular structure was common for the unit and no signs of stratification were observed. Manganese was abundant in the profile, whereas Fe spots were common between 10-210 cm and between 350-420 cm. Manganese appeared also as lining along root channels (between 165-180 cm). Signs of carbonate migration were present in two horizons: between 165-180 cm – in the form of a weak calcified layer; between 275-320 cm – in the form of carbonate spots. Presence of biochannels was common between 430-520 cm.
560	**Unit 2**	**Partly stratified loess** – pale brown colour and the abundance of manganese was characteristic of this unit. Biochannels appeared frequently.
610	**Unit 3**	**Stratified loess** – brown colour with the presence of manganese. The whole unit was stratified and biochannels appeared frequently.
690	**Unit 4**	**Loess with red bands** – pale yellow colour was characteristic of this unit, which was mixing with reddish calcified material between 700-750 cm. Calcified spots appeared in this mixed material in the diameter of 0.5-1 cm.
750	**Unit 5a**	**Soil-like loess a)** – brownish colour and loose, granular structure was characteristic of this unit, which showed similarities to soils. Presence of manganese was common.
765	**Unit 5b**	

		Soil-like loess b) – paler brown colour in comparison to Unit 5a. Appearance of Mn and Fe was common. This horizon seemed to show similarities to soils. Certain brownish spots with granular structure were observed, which reflected the colour of the overlying Unit 5a – but no crotovinas were visible.
790	**Unit 6**	**Reddish band** – this unit was reddish brown in colour and had compact, hard structure. Mn and Fe were present
800	**Unit 7**	**Loess** – pale yellow colour was characteristic of this homogeneous loess unit. Mn and Fe were observed, where this latter one was present in high amount.
830	**Unit 8a**	**Sediment/soil transition** – pale brown to yellowish colour between **830-882 cm**. Three subhorizons were distinguished: 1. between 830-851 cm: granular structure; common appearance of crotovinas and calcified spots; 2. between 851-865 cm: granular structure; lack of crotovinas; lower amount of calcified spots; 3. between 865-882 cm: pale brown colour, which turned upwards to yellowish. Mn was present as root channel lining. Crotovinas of different size were observed (larger ones in the length of 5 cm and many small coin-sized ones). This subhorizon was strongly bioturbated.
	Unit 8b	**Sediment/soil transition** – brown to orange yellow colour between **882-915 cm**. Mn and Fe were common. Crotovinas were observed in different size (larger ones in the length of 5 cm and many small coin-sized ones).
	Unit 8c	**Sediment/soil transition** – light brown colour between **915-929 cm**, which turned orange yellow downwards. Mn was common, especially as root channel lining. Small crotovinas were also observed.
	Unit 8d	**Sediment/soil transition** – chocolate brown to ligher brown colour between **929-938 cm**. Mn was common. Crotovinas appeared with loessic infilling in diameters of 4-5 cm.
940	**Unit 9**	**Chocolate brown paleosol** – which was identified as the

		‘Basaharc Double 1’ paleosol in the Hungarian loess stratigraphy system (THIEL, C. et al. 2014). Three subhorizons were distinguished: 1. between 938-972 cm: transitional habit in brown colour, which was partly mixing with chocolate brown colour. Presence of manganese was common. Signs of clay migration appeared in the form of clay coatings on ped surfaces. Crotovinas had loessic or orange yellow infilling. Their length varied between 7-8 cm, whereas their width was between 4-5 cm. 2. between 972-983 cm: stronger transition was observed to chocolate brown colour. Mn was common. Crotovinas had chocolate brown to orange yellow infilling. 3. between 983-997 cm: chocolate brown soil. Mn was common. Crotovinas were mostly coin-sized.
1000 1020	**Unit 10**	**Soil/sediment transition** – brown colour. The presence of Mn was common in the carbonate accumulation zone, where small carboante concretions and calcified spots were also common. Crotovinas were coin-sized and had chocolate brown or loessic infilling.

5.2.2. Methods and guidelines for the analysis

Sampling frequency for general bulk samples was in 2 cm vertical resolution. For the separation of secondary carbonates, bulk samples of 100 g were needed in 10 cm vertical resolution (as following the method described in BARTA, G. 2014). EBS were available in exceptionally high amount along the sequence (see **Appendix 5.i.** and **Appendix 2.**). In those horizons, where it was possible, 10 EBS samples were taken for stable isotope analysis. Each sample was individually crushed, weighted and measured. It was not easy to determine the exact fluctuation tendencies from the curves of all measurements together, therefore a composite curve was made based on the mean values of each horizon. Highest amount of EBS was observed in Unit 1 at the following depths: 4.40 m; 3.70-3.00 m and 2.50-1.70 m (**Appendix 5.i.**).

Amount of EBS (pieces)			
Unit 1	1222	Unit 8	24
Unit 2	35	*Unit 8 a)*	*4*
Unit 3	89	*Unit 8 b)*	*17*

Unit 4	87	*Unit 8 c)*	*0*
Unit 5	20	*Unit 8 d)*	*3*
Unit 6	0	Unit 9	13
Unit 7	0	Unit 10	24
In total:		**1514**	

Mean values were calculated for the analysis of the certain units. Different groups were divided among the bulk values, based on the curves and their value range (**Appendix 5.a**):

- loess group 1): this group contained Unit 1 (loess), Unit 2 (partly stratified loess) and Unit 3 (stratified loess). Mean values were as -0.47‰ for $\delta^{13}C$ and -4.00‰ for $\delta^{18}O$.
- loess group 2): this group contained Unit 4 (loess with red bands), Unit 5 (soil-like loess), Unit 7 (loess) and based on the similar value range also Unit 6 (reddish band) was ordered here. Mean values were as -2.14‰ for $\delta^{13}C$ and -4.63‰ for $\delta^{18}O$.
- soil/sediment transitions and paleosol: this group contained Unit 8 and Unit 10 as soil/sediment transition horizons, and Unit 9 as chocolate brown paleosol. Mean values were as -7.97‰ for $\delta^{13}C$ and -7.23‰ for $\delta^{18}O$.

Mean values were calculated for those secondary carbonates, which were relative abundant along the sequence and showed depth-dependent tendencies:

- HC: -4.26‰ as mean $\delta^{13}C$ value and -6.21‰ as mean $\delta^{18}O$ value.
- HC+CC: -4.68‰ as mean $\delta^{13}C$ value and -6.46‰ as mean $\delta^{18}O$ value.
- EBS: -12.09‰ as mean $\delta^{13}C$ value and -6.57‰ as mean $\delta^{18}O$ value.
- CRC: -12.80‰ as mean $\delta^{13}C$ value and -10.32‰ as mean $\delta^{18}O$ value.
- CC2: -8.03‰ as mean $\delta^{13}C$ value and -8.24‰ as mean $\delta^{18}O$ value.

The examined sedimentary units were ordered into the composed matrix (as introduced on **Appendix 8.**): when values are shifted from the mean value towards the minimum direction, it is considered as ‘more negative values’ – whereas those values, which are shifted towards the maximum direction are referred as ‘more positive values’. Depth-dependent tendencies of the stable carbon and oxygen isotope curves were described as bulk samples, HC, HC+CC and EBS. Since only lower amounts of CRC and CC2 were available in the sequence, therefore no tendencies were distinguished for their stable isotope values. Curves were divided in many cases into different cycles.

Description and analysis was made from the lowest unit (Unit 10) towards the uppermost unit (Unit 1), in order to follow the built-up of the sequence.

5.2.3. Detailed description of the stable carbon and oxygen isotope values

Bulk loess (Unit 1), partly stratified loess (Unit 2) and stratified loess (Unit 3), with the following mean values: -0.47‰ for $\delta^{13}C$ and -4.00‰ for $\delta^{18}O$ (**Appendix 5.c-d)**.

more negative $\delta^{13}C$ – depletion in ^{13}C	**more positive $\delta^{13}C$ – enrichment in ^{13}C**
Unit 3 – cycle a): the value of -0.87‰ at 6.64 m belonged to the more negative direction. The uppermost value of cycle d) belonged also here, as -0.72‰ at 6.10 m.	**Unit 3** – the following cycles were differentiated for this unit: • cycle a) between 6.80-6.64 m: upwards decreasing tendency with larger amplitude fluctuations. Value range was -0.87‰ and +0.14‰. • cycle b) between 6.64-6.42 m: values showed increasing tendency with fluctuations. One of the fluctuations had large amplitude, whereas two were smaller. • cycle c) between 6.42-6.32 m: values showed decreasing tendency until 6.40 m (-0.52‰) and switched for increasing tendency. The uppermost point of the cycle was the highest value for Unit 3 as +0.23‰ at 6.32 m. • cycle d) between 6.32-6.10 m: values showed decreasing tendency towards the mean value, with fluctuations of larger amplitude.
Unit 2 – the following cycles belonged here: • cycle a): the lowest peak at 6.00 m as -0.97‰. • cycle b): the lowest peak at 5.82 m as -1.19‰. • cycle d) between 5.68-5.60 m: the cycle begun with a large amplitude shift towards the more negative direction and reached the value of -1.53‰ at 5.68 m. Increasing tendency begun upwards in the unit, but showed fluctuations of larger amplitude. Two	**Unit 2** – the following cycles were differentiated for this unit: • cycle a) between 6.08-6.00 m: values seemed the be the continuation of the underlying Unit 3. Increasing tendency was characteristic until 6.02 m, than a larger amplitude fluctuation shifted the values towards the more negative direction. • cycle b) between 6.00-5.82 m: the cycle started with a large amplitude fluctuation towards the higher values, than the tendency switched back to

high peaks were at 5.66 m (-1.21‰) and at 5.62 m (-0.70‰).	decreasing habit with smaller amplitude fluctuations. The last fluctuation had large amplitude and ended up in the more negative direction. • cycle c) between 5.82-5.68 m: large amplitude fluctuation begun towards the more positive direction and showed increasing tendency until 5.72 (-0.19‰). Smaller low peak occurred at 5.74 m, which coincided with the mean value.
Unit 1 – the following cycles were distinguished: • cycle a) between 5.58-5.02 m: slightly increasing tendency upwards, with zigzag pattern fluctuations among the range of -1.18‰ to -0.25‰. Larger shift started from 5.00 m towards the more positive direction. • certain peaks of cycle c), especially the low peaks at 3.66 m (-0.59‰), 3.65 m (-0.74‰), 3.50 m (-0.65‰) and at 3.46 m (-0.82‰). • cycle e) between 1.80-1.42 m: this cycle started and finished in the more positive direction. First decreasing tendency was characteristic, which switched to increasing. Zigzag pattern was characteristic of the fluctuations. Value range was within -1.95‰ and -0.10‰. The lowest peaks were -19.95‰ at 1.72 m and -1.32‰ at 1.48 m. • certain parts of cycle f): the two lowest peaks belonged to the more negative direction, as -0.76‰ at 1.38 m and -0.84‰ at 1.06 m. • cycle g), uppermost part between 0.98-0.74 m: gradual decrease continued with smaller fluctuations. Value range was within -4.08‰ and -3.20‰. • cycle h) between 0.74-0.10 m: generally decreasing tendency was characteristic of this cycle. The pattern of fluctuations showed smaller and larger amplitude shifts within the range of -2.45‰ and -1.44‰. Highest peak was -1.44‰ at 0.44 m.	**Unit 1** – the following cycles were distinguished: • cycle b) between 5.02-4.30 m: values were present within the range of -0.25‰ and +0.53‰ and showed zigzag pattern fluctuations upwards in the unit. Slightly increasing tendency was characteristic until the highest peak of 4.62 m (+0.53‰), which was followed by slightly decreasing tendency. • cycle c) between 4.00-3.30 m: fluctuation of larger amplitude was present in this cycle. Upwards from 3.30 m decreasing tendency begun with zigzag pattern fluctuations until the lowest peak of 3.46 m (-0.82‰). It was followed by increasing tendency, again with zigzag pattern until 4.00 m. The range of values was within -0.82‰ and +0.44‰. • cycle d) between 3.30-2.40 m: this cycle started with decreasing tendency until the lowest peak of -0.41‰ at 2.88 m. From this value the tendency switched for increase until +0.10‰ at 2.40 m. The decreasing and increasing patterns were both characterized by zigzag fluctuations of different amplitude. The range of values was among -0.41‰ and +0.44‰. • certain peaks of cycle e), as -0.10‰ at 1.80 m, -0.44‰ at 1.68 m and -0.22‰ at 1.42 m. • cycle f) between 1.42-0.98 m: the same tendency was characteristic of this cycle as of cycle e), but within a

	different range (-0.86‰ and +0.19‰). • cycle g), lowermost part between 0.98-0.88 m: the values showed gradual decrease until they reached the mean value. The range was within -3.44‰ and -2.97‰.
more negative $\delta^{18}O$ – depletion in ^{18}O	**more positive $\delta^{18}O$ – enrichment in ^{18}O**
Unit 3 – the following cycles were distinguished for this unit: • cycle a) between 6.80-6.70 m: decreasing tendency was observed with fluctuations of large amplitude. Value range was -3.93‰ and -4.39‰. • cycle b) between 6.70-6.54 m: increasing tendency was observed. It begun with large amplitude fluctuations and high peaks as -4.03‰ at 6.66 m and -4.10‰ at 6.62 m. Values showed gradual increase from 6.60 m towards the more positive direction. • cycle d) between 6.48-6.36 m: decreasing tendency started towards the more negative direction with certain fluctuations. Tendency was gradual between 6.40-6.36 m. • cycle e) between 6.36-6.10 m: this cycle started with a larger amplitude shift towards the more positive direction, until 6.32 m. Afterwards the tendency switched for decrease. Decrease was gradual, with the exception of two smaller high peaks as -4.04‰ at 6.22 m and -4.03‰ at 6.18 m.	**Unit 3** – the following cycles belonged to the more positive direction: • cycle a): the first value at 6.80 (-3.96‰) and two high peaks of the large amplitude fluctuations (-3.93‰ at 6.76 m and -3.96‰ at 6.72 m) belonged to the more positive direction. • cycle c) between 6.54-6.48 m: values represented only slight increase within the small range of -3.96‰ and -3.93‰. • cycle d): the lowermost value as -3.93‰ at 6.48 m belonged here and the high peak of -3.89‰ at 6.44 m. • cycle e): the high peak of -3.80‰ at 6.32 m belonged here.
Unit 2 – the following cycles were distinguished: • cycle a) between 6.08-6.02 m: this cycle seemed to be the closure of the tendency, which begun in cycle e) of **Unit 3**. The uppermost value of **Unit 3** was -4.41‰ at 6.10 m. This could	**Unit 2** – only one value of cycle a) belonged to the more positive direction, as -3.91‰ at 6.02 m.

be counted as the lowest peak of a large fluctuation, which switched for increasing tendency in **Unit 2**. • cycle b) between 6.02-5.80 m: this cycle begun with a larger shift towards the more negative direction, to -4.31‰ at 6.00 m. Upwards increasing tendency was general, but with the presence of fluctuations. The two lowest peaks were -4.42‰ at 5.86 m and the same at 5.82 m. • cycle c) between 5.80-5.68 m: gradually decreasing tendency was observed with one smaller fluctuation. This latter one was present in the small high peak of -4.31‰ at 5.72 m. Range of decrease was -4.09‰ and -4.83‰. • cycle d) between 5.68-5.60 m: increasing tendency begun towards the mean value, with a low peak at 5.62 m (-4.80‰). **Unit 1** – the following cycles were distinguished: • cycle a) between 5.58-4.86 m: decreasing tendency was characteristic of the cycle, with zigzag pattern fluctuations within the range of -5.05‰ and -3.30‰. Lowest peak was at 5.44 m (-5.05‰). The values were present on the more positive direction from 5.06 m, upwards in this section part. • cycle c) between 4.00-3.30 m: decreasing tendency was characteristic of the cycle, with zigzag pattern fluctuations within the range of -4.51‰ and -3.38‰. Lowest peak was at 3.42 m (-4.51‰). Upwards from this point increasing tendency started towards the more positive direction. • certain parts of cycle d): among others the lowest peak belonged here as -4.22‰ at 2.80 m. • certain parts of cycle e): among others the lowest peak belonged here as -5.22‰ at 1.68 m. • certain parts of cycle f): values	**Unit 1** – the following cycles were distinguished: • certain parts of cycle a) belonged here, upwards from 5.06 m to 4.86 m. • cycle b) between 4.86-4.30 m: slightly decreasing tendency was observed towards the mean value, within the range of -4.09‰ and -3.30 ‰. • certain parts of cycle c) belonged here, as the lowermost values between 4.00-3.82 m and the uppermost values between 3.34-3.30 m. • cycle d) between 3.30-2.40 m: values showed slight decrease upward in this section part, towards the mean value. Zigzag fluctuation pattern was common within the range of -4.22‰ and -3.38‰. • cycle e) between 1.80-1.22 m: upwards increasing tendency was characteristic of this cycle. The zigzag pattern fluctuations showed one large amplitude shift with a low peak in the more negative direction. The value range was within -5.22‰ and -3.37‰. • cycle f) between 1.22-1.00 m: fluctuation started with gradually decreasing tendency until the low peak

between 1.12-1.02 m belonged here, with the lowest peak of -4.30‰ at 1.02 m. • cycle g), uppermost part between 0.74-0.10 m: the upwards decreasing tendency continued upwards within the range of -4.76‰ and -4.00‰. Two lowermost peaks were at 0.48 m and 0.14 m.	at 1.02 m (-4.30‰), than it switched for increase towards the more positive direction. The value range was within -4.30‰ and -3.03‰. • cycle g), lowermost part between 1.00-0.74 m: values showed decreasing tendency towards the mean value, with small fluctuations within the range of -4.08‰ and -2.97‰.

Loess with red bands (Unit 4), soil-like loess (Unit 5), reddish band (Unit 6) and loess (Unit 7), with the following mean values: -2.14‰ for $\delta^{13}C$ and -4.63‰ for $\delta^{18}O$ (**Appendix 5.e**).

more negative $\delta^{13}C$ – depletion in ^{13}C	**more positive $\delta^{13}C$ – enrichment in ^{13}C**
The curves of **Unit 7** and **Unit 6** could be connected to each other, which showed an upwards increasing tendency towards the mean value. Three low peaks occurred, as -3,53‰ at 8.06 m, -3.86‰ at 8.00 m and -3.47‰ at 7.94 m. The uppermost value of **Unit 6** exceeded the mean value towards the more positive direction (-1.90‰ at 7.90 m). **Unit 5** – between 7.84-7.64 m decreasing tendency was present, which switched to gradual increase and showed the following low peaks: -3.20‰ a 7.80 m, -3.39‰ at 7.74 m and -2.87‰ at 7.68 m. **Unit 4** – one part of cycle b) belonged to the more negative direction, as between 7.26-7.16 m.	The increasing tendency of **Unit 6** continued in the lowermost part of **Unit 5**, until 7.86 m (-1.32‰) – afterwards it changed for decreasing habit. **Unit 5** – between 7.64-7.50 m: increasing pattern started from 7.64 m, which continued in **Unit 4**. High peaks in **Unit 5** were at 7.60 m (-0.90‰) and at 7.54 m (-0.70‰). **Unit 4** – the following cycles were present in this unit: • cycle a) between 7.48-7.30 m: this cycle was the continuum of **Unit 5**. Increasing tendency towards the more positive values was characteristic of this cycle, with two smaller and one larger low peaks (-1.14‰ at 7.46 m, -2.3‰ at 7.38 m and -1.56‰ at 7.34 m). • cycle b) between 7.30-7.14 m: this cycle started with decreasing tendency, where the amplitude of fluctuations was growing until it reached the lowest peak at 7.16 m (-2.95‰).

	• cycle c) between 7.14-6.90 m: the values showed generally increasing tendency towards the more positive direction with larger amplitude fluctuations. Lowest peak was -2.02‰ at 7.04 m, whereas the two highest peaks were at 7.00 m (-0.32‰) and at 6.94 m (-0.27‰).
more negative $\delta^{18}O$ – depletion in ^{18}O	**more positive $\delta^{18}O$ – enrichment in ^{18}O**
Unit 7 – gradual increase was characteristic of this unit towards the mean value, with the following two small high peaks: -4.79‰ at 8.18 m and -4.71‰ at 8.10 m.	**Unit 4** – the following cycles were characteristic of this part: • cycle b) between 7.28-7.14 m: values shifted first towards the more negative direction, than tendency switched for increase from 7.20 m upwards. Two low peaks were the followings: -5.33‰ at 7.20 m and -5.33‰ at 7.16 m. • cycle d) between 7.02-6.90 m: increasing tendency was present until 6.92 m (-3.94‰) with smaller low peaks of 6.98-6.96 m. The uppermost value of -4.31‰ (6.90 m) was shifted towards the mean value. •
Unit 6 – this unit was the continuum of **Unit 7** and showed gradual increase from the more negative direction towards the more positive direction with one low peak at 7.94 m as -4.90‰. **Unit 5** – values were present mainly along the mean value, but showed small fluctuations in both of the more positive and more negative directions. Range of fluctuation was between -4.87‰ and -4.18‰**.** **Unit 4** – two cycles were present with values mainly along the mean value, as followings: • cycle a) between 7.48-7.28 m: small fluctuations were present in the range of -4.78‰ and -4.26‰. This cycle was the continuum of **Unit 5**. • cycle c) between 7.14-7.02 m: small fluctuations were present in the range of -4.84‰ and -4.40‰.	

Transition zones (Unit 8 and Unit 10) and chocolate brown paleosol (Unit 9, 'Basaharc Double 1'), with the following mean values: -7.97‰ for $\delta^{13}C$ and -7.23‰ for $\delta^{18}O$ (**Appendix 5.f**).

more negative $\delta^{13}C$ – depletion in ^{13}C	more positive $\delta^{13}C$ – enrichment in ^{13}C
Unit 9 – chocolate brown paleosol: the uppermost part is characterized as cycle d), between 9.48-9.40 m. This cycle showed gradual transition towards the more negative direction (without fluctuations). **Unit 8** – transition zone showed the following cycles: • cycle a) between 9.38-9.20 m: decreasing tendency switched to increasing tendency towards the mean value. The range of fluctuation was -12.37‰ and -8.09‰. Three low peaks were divided as at 9.36 m (-12.37‰), at 9.30 m (-11.64‰) and at 9.24 m (-11.12‰). • cycle b) between 9.20-8.86 m: decreasing tendency switched to increasing tendency towards the mean value. Mean value was exceeded during the cycle. The range of fluctuation was -10.88‰ and -6.40‰. Three low peaks occurred, as at 9.18 m (-8.53‰), at 9.12 m (-10.88‰) and at 9.02 m (-10.05‰). • cycle d) between 8.62-8.52 m: increasing tendency occurred in the range of -9.72‰ and -8.15‰. One fluctuation was present in the tendency, with the high peak of -8.15‰ at 8.56 m.	**Unit 10** – transition zone: values showed decreasing tendency towards the mean value, with the presence of one low peak (-6.46‰ at 10.06 m). **Unit 9** – chocolate brown paleosol: division made into the following cycles: • cycle a) between 9.98-9.86 m: almost gradual decreasing tendency with the presence of one high peak (-7.47‰ at 9.90 m). This cycle seemed to be the continuation of the underlying Unit 10. • cycle b) between 9.86.9.68 m: gradually increasing values. • cycle c) between 9.68-9.48 m: gradually decreasing values, which met the mean value at the uppermost part of the cycle. Fluctuations of smaller range were present. **Unit 8** – transition zone showed the following cycles: • cycle c) between 8.86-8.62 m: decreasing tendency was shown with small range fluctuations (-6.40‰ and -6.93‰) until 8.70 m. From 8.70 m decrease was gradual, exceeded the mean value towards the more negative direction. Uppermost point of the cycle was -9.72‰ at 8.62 m. • cycle e) between 8.52-8.30 m: gradually increasing tendency, which started from the more negative direction, than exceeded the mean value at 8.48 m depth and continued towards the more positive direction. The value range was -8.69‰ and -4.63‰.
more negative $\delta^{18}O$ – depletion in ^{18}O	**more positive $\delta^{18}O$ – enrichment in ^{18}O**
Unit 9 – chocolate brown paleosol, the	**Unit 10** – transition: values showed

following cycles were divided: • cycle b) between 9.80-9.72 m: increase towards the more positive values started from 9.80 m. One high peak was observed at 9-74 m as -6.82‰. **Unit 8** – transition zone showed the following cycles: • cycle a) between 9.38-9.18 m: the cycle started with decrease until 9.36 m (-9.08‰) and switched to gradual increase towards the mean value – and exceeded it. Range of the values was -9.08‰ and -7.10‰. • cycle b) between 9.18-8.86 m: gradual decrease was shown until the low peak of -9.18‰ at 9.10 m. Gradual increase started until 8.86 m and thus the mean value was exceeded towards the more positive direction. Value range was -9.18‰ and .6.18‰. • cycle d) between 8.72-8.62 m: the cycle started with increasing tendency towards the high peak of -6.76‰ at 8.70 m. It continued in decrease until 8.62 m (-8.31‰). The value range was -8.31‰ and -6.76‰. • cycle e) between 8.62-8.30 m lower part, until 8.52 m: gradual increase was characteristic of the cycle and the uppermost value exceeded the mean value. The value range was -8.31‰ and -7.04‰.	slightly decreasing tendency towards the mean value, with the presence of one low peak at 10.08 m (-7.04‰). **Unit 9** – chocolate brown paleosol, the following cycles were divided: • cycle a) between 9.98-9.80 m: decreasing tendency with small fluctuations towards the more negative direction. Values were present along the mean value between 9.86-9.82 m. • cycle c) between 9.72-9.40 m: values were present mainly along the mean value, but showed three small high peaks as -6.93‰ at 9.68 m, -6.86‰ at 9.58 m and -7.00‰ at 9.50 m. **Unit 8** - transition zone showed the following cycles: • cycle c) between 8.86-8.72 m: the cycle started with increase until 8.80 m (-6.05‰), then switched to gradual decrease until 8.72 m (-7.53‰), where the mean value was exceeded towards the more negative direction. The value range was -7.53‰ and -6.05‰. • cycle e) between 8.64-8.30 m upper part, above 8.52 m: gradual increase towards the more positive direction continued among -7.04‰ and -5.44‰. One low peak occurred at 8.46 m as -6.90‰.

Hypocoatings (**Appendix 5.g)**

more negative $\delta^{13}C$ – depletion in ^{13}C	**more positive $\delta^{13}C$ – enrichment in ^{13}C**
Unit 10 – transition unit showed upwards slightly decreasing habit. **Unit 9** – the chocolate brown paleosol was represented only by one value at 9.70 m as -7.45‰.	**Unit 7** – this unit was represented by two values, one in the more positive direction and the other slightly exceeded the mean value in the more negative direction. **Unit 3 and 2** represented one cycle, where

Unit 8 – this transition was characterized by zigzag pattern fluctuations with a generally increasing tendency towards the mean value. The lowest peak was at 8.60 m (-10.10‰). **Unit 5** – generally decreasing tendency was characteristic of this unit within the range of -4.17‰ and -8.04‰. **Unit 4** – this unit seemed to be the continuum of **Unit 5**, but with values fluctuating within a smaller range (-8.03‰ and -6.92‰). Certain low peaks of **Unit 1** belonged to the more negative direction, as -6.97‰ at 5.00 m, -4.87‰ at 3.10 m, -5.68‰ at 2.60 m and lower ones between 1.70-0.30 m.	decreasing tendency begun from 6.50 m (-0.82‰) until the low peak at 5.70 m (-5.25‰). Tendency shifted towards the more positive direction and reached 5.50 m (-1.92‰). This was marked by cycle a). The uppermost part of **Unit 2** (5.50-5.40 m) was connected to **Unit 1** (5.40-3.30 m) and together represented one larger cycle – cycle b). The uppermost point of the cycle was +1.62‰ at 3.30 m. The lowest peak was -6.97‰ at 5.00 m, which was followed by increasing tendency (with zigzag fluctuations). **Unit 1** was divided into the following cycles: • cycle c) between 3.30-2.20 m: one larger amplitude oscillation was present in the range of -5.68‰ and +1.62‰. This oscillation had slightly decreasing character. • cycle d) between 2.20-0.80 m: the range of oscillation was smaller than in the above lying cycle, as of -4.87‰ and -0.97‰. • cycle e) upwards from 0.80 m until 0.30 m: decreasing tendency, with fluctuations. Value range was of -0.97‰ and -5.83‰.
more negative $\delta^{18}O$ – depletion in ^{18}O	**more positive $\delta^{18}O$ – enrichment in ^{18}O**
Unit 10 – the values of this transition zone showed gradual decrease towards the paleosol within the range of -7.37‰ and -8.15‰. **Unit 9** – the chocolate brown paleosol was only represented by one value (-8.24‰ at 9.70 m), quite close to the uppermost value of **Unit 10**. **Unit 8** – this transition zone showed increasing tendency towards the mean value with large amplitude fluctuations within the range of -11.33‰ and -6.84‰.	**Unit 7** – this unit was only represented by two values, relative close to each other (as -5.26‰ and -5.33‰). **Unit 3 and 2** represented one cycle between 6.60-5.50 m. Upwards decreasing tendency was characteristic of them with a double low peak in the more negative direction. This was marked by cycle a). The uppermost part of **Unit 2** (5.50-5.40 m) was connected to **Unit 1** (5.40-3.80 m) and together represented one cycle – cycle b). The tendency was upwards increasing

Unit 5 – upwards decreasing tendency was characteristic of the unit within the range of -5.81‰ and -9.24‰. The cycle started in the more positive direction and shifted towards the more negative side. **Unit 4** – this unit represented one fluctuation with increasing tendency within the range of -8.25‰ and -9.86‰. **Unit 4** may be in connection with **Unit 5**. Low peaks of **Unit 3 and 2** belonged to the more negative direction, as -6.81‰ at 6.10 m and -7.29‰ at 5.70 m. Low peaks of **Unit 1** belonged to the more negative direction, as -7.47‰ at 5.00 m, -7.50‰ at 3.10 m, -7.03‰ at 2.60 m, -7.22‰ at 1.00 and -6.76‰ at 0.40 m.	with one low peak. **Unit 1** – division of cycles: • cycle c) between 3.80-2.90 m: generally decreasing tendency was characteristic of this cycle, with large amplitude oscillations. The highest peak was +0.96‰ at 3.30 m. The range of fluctuations was within -7.50‰ and +0.96‰. • cycle d) between 2.90-0.80 m: the general tendency was increasing with different amplitude fluctuations within the range of -7.22‰ and -3.31‰. • cycle e) between 0.80-0.30 m: decreasing tendency was observed with fluctuations of smaller amplitude. Value range was within -3.31‰ and -6.02‰.

HC+CC

more negative $\delta^{13}C$ – depletion in ^{13}C	**more positive $\delta^{13}C$ – enrichment in ^{13}C**
Unit 4 **Unit 5** **Unit 1** – cycle d) between 0-90-0-40 m: decreasing tendency of larger amplitude within the range of -7.11‰ and -3.51‰.	**Unit 1** – the following cycles were distinguished: • cycle a) between 5.20-3.90 m: increasing tendency within the value range of -5.17‰ and -2.20‰. • cycle b) between 3.90-3.10 m: decreasing tendency, with high peak at 3.30 m. • cycle c) between 3.10-0.90 m: decreasing tendency within the value range of -4.99‰ and -3.15‰.
more negative $\delta^{18}O$ – depletion in ^{18}O	**more positive $\delta^{18}O$ – enrichment in ^{18}O**
Unit 5 **Unit 4** **Unit 3** **Unit 2** **Unit 1** – the following two cycles were distinguished:	**Unit 1** – the following two cycles belonged to the more positive direction: • cycle b) between 3.10-1.60 m: increasing tendency was characteristic of this cycle with two high peaks (2.10 m and 1.80 m). Value range was within -7.35‰ and -4.80‰.

• cycle a) between 5.20-3.10 m: decreasing tendency was characteristic within the value range of -7.35‰ and -4.83‰. Two high peaks occurred, one at 3.90 m and the other at 3.30 m. • cycle d) between 0.50-0.40 m: decreasing tendency was characteristic of this cycle within the value range of -8.54‰ and -6.33‰.	• cycle c) between 1.60-0.50 m: increasing tendency was observed with high peak at 0.80 m. Value range was within -6.83‰ and -5.29‰.

Earthworm biospheroids (**Appendix 5.h)**

more negative $\delta^{13}C$ – depletion in ^{13}C	**more positive $\delta^{13}C$ – enrichment in ^{13}C**
Unit 8 – the decreasing tendency continued in the uppermost part of **Unit 8**, between 8.70-8.40 m. The value range for the whole **Unit 8** was within -10.67‰ and -15.84‰. Two low peaks of **Unit 4** belonged to the more negative direction, as -12.96‰ at 7.10 m and -13.60‰ at 6.80 m. **Unit 3** – this unit could be counted as the continuum of **Unit 4** and represented upwards (gradually) increasing values. The uppermost part was connected to **Unit 2** and thus represented a low peak (-12.82‰ at 5.90 m) in upwards increasing tendency. The highest point of the cycle was -11.56‰ at 5.50 m. The uppermost value of **Unit 2** (-13.18‰ at 5.40 m) was counted as the part of the first **Unit 1** cycle. **Unit 1** – between 5.30-1.50 m the values moved close to the mean value and showed slight oscillations towards both directions. Most of the oscillations peaks were in the more negative direction. Some higher peaks were present in the more positive direction. When the larger low and high peaks are not counted, than the	**Unit 10** – both values of the transition zone were close to the mean value. **Unit 9** – upwards increasing tendency was shown in the chocolate brown paleosol. One low peak was observed close to the mean value, as -11.91‰ at 9.50 m. **Unit 8** – lowest part between 9.00-8.80 m showed upwards decreasing tendency with one high peak at 8.90 m (-10.67‰). **Unit 5 and 4** were connected and together they represented an upwards decreasing tendency with smaller fluctuations within the range of -10.97‰ and -13.60‰. Highest peak of **Unit 2** belonged to the more positive direction, as -11.56‰ at 5.50 m. Certain high peaks of **Unit 1** belonged to the more positive direction, as -6.53‰ at 5.10 m, -10.62‰ at 2.50 m and -11.55‰ at 1.50 m. In **Unit 1**, between 1.50-0.10 m the lowermost two values and the uppermost one seemed to be quite close to each other, whereas the cycle showed between them fluctuations. Low peak was in the more

value range was within -13.18‰ and -11.55‰. Low peak of **Unit 1** at 0.40 m (-13.01‰) belonged to the more negative direction.	negative direction, whereas high peak belonged to the more positive side (-11.04‰ at 0.20 m).
more negative $\delta^{18}O$ – depletion in ^{18}O	**more positive $\delta^{18}O$ – enrichment in ^{18}O**
Unit 10 – both values of the transition zone were close to each other (as -7.84‰ and -8.02‰). **Unit 9** – the values of the chocolate brown paleosol showed upwards decreasing tendency with one high peak at 9.60 m (-6.99‰). **Unit 8** – lowermost part between 9.00-8.70 m started with a decreasing phase towards the low peak of -10.86‰ at 8.90 m, then switched to increase upwards in the unit. Low peaks of **Unit 3** belonged to the more negative direction as -7.56‰ at 6.60 m, -7.04‰ at 6.40 m and -7.93‰ at 6.00 m. One low peak of **Unit 2** belonged to the more negative direction as -7.17‰ at 5.80 m. **Unit 1** – the following cycles were differentiated: • between 3.30-2.70 m: decreasing tendency was present with smaller fluctuations of zigzag pattern within the range of -6.34‰ and -7.55‰. • between 2.70-1.60 m: increasing tendency started with fluctuations of larger amplitude. Low peak was present at 2.50 m (-8.96‰). The high peak was part of the more positive direction, as -4.95‰ at 2.50 m.	**Unit 8** – uppermost part between 8.70-8.40 m belonged to the increasing phase. **Unit 5** was represented by two values, which seemed to show increasing tendency toward the lowermost value of **Unit 4**. **Unit 4** showed upwards decreasing tendency with fluctuations within the range of -3.55‰ and -6.70‰. **Unit 3** – slightly increasing tendency was characteristic upwards in this unit. Fluctuations were within the range of -7.93‰ and -4.79‰. **Unit 2** – this unit showed fluctuations in smaller range (when compared to **Unit 3**) and slightly decreasing tendency. Value range was -7.17‰ and -5.93‰. **Unit 1** – the following cycles were differentiated: • between 5.30-4.70 m: one larger fluctuation was present with the high peak of -3.53‰ at 5.10 m. General tendency was increase. • between 4.70-3.30 m: increasing tendency continued with fluctuations of larger amplitude. Value range was within -7.85‰ and -4.72‰. Values were present in both of the more negative and more positive direction. • between 1.60-0.10 m: increasing tendency continued upwards with larger fluctuations. High peak was observed at 2.00 m as -4.95‰, whereas the low peak was part of the

	more negative direction, as -8.95‰ at 0.40 m.

5.2.4. Similar tendencies

The examined stable carbon and oxygen isotope curves were compared to each other and showed similarities in certain cases, as it can be seen below:

5.2.4.1. HC versus bulk samples

- Comparison of bulk and HC curves - **δ^{13}C**. HC curve showed similarities with the following units and/or cycles:
  - *loess group 1)*: Unit 3 – bulk c)-d) cycles were similar to HC cycle a); Unit 2 – bulk c)-d) cycles were similar to HC cycle a); Unit 1 – bulk a)-b) cycles were similar in tendency to HC cycles a)-b), bulk c) cycle was similar to HC cycle b), bulk d) cycle was similar to HC cycle c), bulk e)-g) cycles were similar to HC cycle d) and bulk h) cycle was similar to HC cycle e).
  - *loess group 2)*: Unit 4 – bulk c) cycle was similar to the HC curve.
  - *soil/sediment transition and paleosol*: Unit 10; Unit 8 – bulk cycles b)-e) were similar to the HC curve.
- Comparison of bulk and HC curves - **δ^{18}O**. HC curve showed similarity with the following units and/or cycles:
  - *loess group 1)*: Unit 3 – bulk cycle a) showed similarities between 6.30-6.10 m depth. Bulk Unit 1 tendency was similar to the HC curve, with the following remarks: the amplitude of the shift towards the more positive direction between 3.50-3.30 m (bulk cycle a)/b) boundary) was quite large for both sample types. The tendency of another larger shift (bulk d) cycle) was the same, just sample depth was a little bit shifted off: range of shift was between 1.02-1.00 m for bulk samples, whereas 1.00-0.80 m for HC samples.
  - *soil/sediment transition*: Unit 10; Unit 8 – upwards from the depth of 9.10 m.

5.2.4.2. HC versus HC+CC

- Comparison of HC and HC+CC values in general: Difference between the $\delta^{13}C$ and $\delta^{18}O$ values was calculated for those units and horizons, which contained both of these features. It was possible to calculate maximum and minimum differences, when enough samples were available – as for Unit 1and Unit 5a. The other units, as Unit 2 and Unit 3 contained only one sample, whereas the other units of the sequence lacked HC+CC. The mean difference of $\delta^{13}C$ values was 1.55‰, whereas the mean difference for $\delta^{18}O$ was 1.24‰.The maximum difference among $\delta^{13}C$ values was 4.21‰, whereas the minimum was 0.13‰. The maximum difference for $\delta^{18}O$ values was greater, as 6.37‰, whereas the minimum was 0.02‰. The **Table 3** contains the calculations:

Table 3: Calculated differences between HC and HC+CC

	$\delta^{13}C$ (VPDB ‰)				**$\delta^{18}O$ (VPDB ‰)**			
	Max	**Min**	**Mean**	**SD Mean**	**Max**	**Min**	**Mean**	**SD Mean**
Unit 1	4,21	0,13	1,71	*0,00*	6,37	0,02	1,40	*0,01*
Unit 2			1,27	*0,00*			1,11	*0,00*
Unit 3			0,40	*0,00*			0,19	*0,00*
Unit 5a	0,99	0,39	0,69	*0,00*	0,60	0,11	0,36	*0,05*

- Comparison of HC and HC+CC curves - **$\delta^{13}C$**. Mean values were slightly different, as -4.26‰ for HC and -4.68‰ for HC+CC. The calculated mean difference among HC and HC+CC values was 1.55‰. Comparison showed the following connections:
    - *loess group 1)*: Unit 1 – tendency of the two curves was similar, but the amplitude of fluctuations was larger for HC.
- Comparison of HC and HC+CC curves - **$\delta^{18}O$**. Mean values were slightly different, as -6.21‰ for HC and -6.46‰ for HC+CC. The calculated mean difference among HC and HC+CC values was 1.24‰. Comparison showed the following connections:
    - *loess group 1)*: Unit 1 – similar tendency and amplitude of fluctuations was shown between the two curves. As a remark, one high peak of the HC curve was connected to a fluctuation with exceptionally large amplitude at 3.30 m.

5.2.4.3. EBS versus bulk samples

- Comparison of bulk and EBS curves - **δ^{13}C**. HC curve showed similarities with the following units and/or cycles:
    - *loess group 1)*: Unit 3; Unit 1 – bulk c) cycle between 4.20-3.40 m showed similarities.
    - *loess group 2)*: Unit 5; Unit 4.
    - *soil/sediment transition*: Unit 8 – bulk cycle b)-c).
- Comparison of bulk and EBS curves - **δ^{18}O**. HC curve showed similarity with the following units and/or cycles:
    - *loess group 1)*: Unit 3 between 6.60-6.10 m; Unit 1 – bulk cycles b)-c) and e)-f) coincided with the EBS curve.
    - *loess group 2)*: Unit 7.
    - *soil/sediment transition and paleosol*: Unit 10; Unit 9; Unit 8.

5.2.4.4. HC versus EBS samples

- Comparison of HC and EBS curves - **δ^{13}C**. EBS curve showed similarities with the following units and/or cycles:
    - *loess group 1)*: Unit 3; Unit 2; Unit – similarities only with HC cycle b) between 4.90-4.30 m. Remarks to Unit 3: the tendency was similar to each other, but HC curve showed fluctuations of large amplitude, whereas tendency of EBS curve was relative gradual.
    - *loess group 2)*: Unit 5.
- Comparison of HC and EBS curves - **δ^{18}O**. EBS curve showed similarity with the following units and/or cycles:
    - *loess group 1)*: Unit 2; Unit 1 – similarities with HC cycle d) between 3.50-2.00 m and with HC cycle e) upwards from 0.40 m.
    - *loess group 2)*: Unit 4.
    - *soil/sediment transition*: Unit 10; Unit 8.

5.2.5. Possible connections between δ13C and δ18O values

Linear regression was calculated for each unit and for each component (as bulk samples and certain secondary carbonates). The coefficient of determination (R^2) and

the steepness of the slope were plotted on the same graph. The main aim was to determine the strength of connection between $\delta^{13}C$ and $\delta^{18}O$. Table 4 summarizes those connections, which were worth to compare.

Strong connection ($R^2 \geq 0.70$)			
HC	soil-like loess	Unit 5	R^2=0.94
	stratified loess	Unit 3	R^2=0.93
	partly stratified loess	Unit 2	R^2=0.99
Bulk	soil/sediment transition	Unit 8 - in general	R^2=0.80
		Unit 8 a) (field)	R^2=0.70
		Unit 8 b) (field)	R^2=0.95
		Unit 8 d) (field)	R^2=0.76
	reddish band	Unit 6	R^2=0.87
	loess with red bands	Unit 4	R^2=0.75
	modern soil	Unit 1	R^2=0.76
Moderate connection ($0.5 < R^2 < 0.70$)			
HC	soil/sediment transition	Unit 10	R^2=0.62
		Unit 8 - in general	R^2=0.69
		Unit 8 b) (field)	R^2=0.64
	loess	Unit 1	R^2=0.69
Bulk	soil/sediment transition	Unit 8 b) (field)	R^2=0.64
	partly stratified loess	Unit 2	R^2=0.64
No connection ($R^2 \sim 0.00$)			
EBS	stratified loess	Unit 3	R^2=0.00
	partly stratified loess	Unit 2	R^2=0.00
Bulk	soil/sediment transition	Unit 10	R^2=0.00
	loess	Unit 7	R^2=0.00
	soil-like loess	Unit 5	R^2=0.00

5.2.6. Possible paleoenvironmental signals of bulk samples

Soil/sediment transition and paleosol.

Unit 10

The $\delta^{13}C$ and $\delta^{18}O$ curves of the transition zone Unit 10 showed similarities only in the upper halves of the curves, as between 10.04-10.00 m. This similar tendency had

decreasing habit towards the above lying paleosol. No connection was shown between $\delta^{13}C$ and $\delta^{18}O$ according to the determination coefficient (R^2).

Unit 9

The chocolate brown paleosol of Unit 9 was ordered the upper member of the 'Basaharc Double' pedocomplex, since exactly the same sequence wall was chosen and sampled, which is present in the work of THIEL, C. et al. (2014). Former sampling spots for luminescence dating were still visible on the field. According to the measurements of THIEL, C. et al. (2014), the 'Basaharc Double' pedocomplex was clearly linked to the MIS 7 interglacial phase (THIEL, C. et al. 2014).

The $\delta^{13}C$ and $\delta^{18}O$ curves showed similarities only in the case of one cycle: cycle d) of $\delta^{13}C$ and showed similar tendency to the uppermost part of cycle c) of $\delta^{18}O$. No connection was present among $\delta^{13}C$ and $\delta^{18}O$ values, according to the determination coefficient (R^2). The values of Unit 9 showed gradual transition towards the Unit 8 transition zone. As a striking difference, the values of Unit 8 were shifted towards more negative values with large amplitude, whereas the values of Unit 9 were present in a smaller range and lacked such "radical" shifts. This difference may indicate that Unit 9 developed under moderately humid conditions with balanced water household (as $\delta^{18}O$ values were present within a small range). Vegetation cover was possibly less dense and had more opened character, which influenced the $\delta^{13}C$ values not to shift toward the extremely negative direction (e.g. QUADE, J. et al. 1989, see general **Appendix 8.**). The large shift of the transition zone, especially regarding the $\delta^{13}C$ values may be connected to higher vegetation densities in Unit 8 due to the transitional habit: as climate changed and dust accumulation rates were slowly increasing and therefore the microecosystem had more adequate niche and kept pace with the dust accumulation rates (CATT, J.A. 1990; BECZE-DEÁK, J. et al. 1997). By this means climatic fluctuations may have played an important role in the development of the transition zone

Unit 8

Four different horizons were distinguished for Unit 8, as it is shown in the descriptive **Appendix 2**. Differentiation was made based on the colour and signs of bioturbation (as the various appearance of crotovinas). The subunits, which were described on the field showed certain connections with $\delta^{13}C$ and $\delta^{18}O$ cycles. Unit 8d was connected to the lower part of cycle a) of $\delta^{13}C$ and $\delta^{18}O$ curves, whereas Unit 8c was connected to the upper part of cycle a) of $\delta^{13}C$ and $\delta^{18}O$ curves. Unit 8b belonged to

cycle b) of $\delta^{13}C$ and $\delta^{18}O$ curves, whereas Unit 8a was part of the cycles c)-e) of $\delta^{13}C$ and $\delta^{18}O$ curves.

The $\delta^{13}C$ and $\delta^{18}O$ curves of Unit 8 showed similarities in the tendencies and the distinguished cycles coincided. Strong connection was determined between $\delta^{13}C$ and $\delta^{18}O$ for Unit 8, especially for the subunits as Unit 8a, 8c and 8d. Moderately strong connection was characteristic of the subunit 8b.

The general tendency of both $\delta^{13}C$ and $\delta^{18}O$ curves was increasing towards the more positive direction upwards in the sequence. This habit also drew the attention to the comparison with field observations and to the structure of subunits. Unit 8d was the part of the transition zone, which was connected directly to the upper zone of the Unit 9 paleosol. This subunit showed generally the more negative $\delta^{13}C$ values, when compared to the other subunits. This may mean that vegetation density was still relative high in the transition zone. The microecosystem still had enough ecological niche and kept pace easier with the accumulating dust (according to CATT, J.A. 1990 and BECZE-DEÁK, J. et al. 1997). Signs of bioturbation, as the presence of crotovinas, were common for subunit 8d. Subunit 8c showed the same characteristics according to the $\delta^{13}C$ values, but here the size of crotovinas changed and got smaller. The $\delta^{13}C$ curve of subunit 8b was already shifted towards the more positive direction and showed gradually increasing tendency upwards from 9.10 m. The colour of this subunit turned more to brown and orange yellow and showed mainly coin-like, small crotovinas. The uppermost subunit 8a also showed generally increasing tendency, which was turned to be more gradual upwards from 8.64 m. The colour of the subunit turned upwards from brownish to pale brown and yellow, whereas the structure became even more granular. The $\delta^{18}O$ curves were similar in tendency to the $\delta^{13}C$ curves and showed in some cases fluctuations of smaller amplitude. $\delta^{18}O$ values showed also increasing tendency upwards in Unit 8 and thus indicated that possibly less humid conditions were present upwards in the transition zone, when compared to the lowermost subunit 8d.

Loess group 2).

Unit 7 to Unit 4

THIEL, C. et al. (2014) agreed on that the sequence is not a continuous record and this lacks loess deposits from MIS 4 and MIS 5, therefore Unit 4 and Unit 5 could be ordered to the MIS 3. The field description of THIEL, C. et al. (2014) mentioned strong reworking above the 'Basaharc Double 1' paleosol, with the presence of several

crotovinas. The bioturbated habit of the sediment may have led to a smaller degree of luminescence age overestimation and thus raised the possibility, that loess (Unit 7) above 'Basaharc Double 1' paleosol was connected to MIS 6 and not MIS 7.

The $\delta^{13}C$ and $\delta^{18}O$ tendencies in Unit 7 showed opposite habits and therefore no connection was present among them (according to R^2). The $\delta^{13}C$ and $\delta^{18}O$ curves of Unit 5 showed different tendencies and no connection according to the determination coefficient (R^2): values of $\delta^{13}C$ showed fluctuations of large amplitudes, whereas the values of $\delta^{18}O$ were present within a quite small range. The $\delta^{13}C$ and $\delta^{18}O$ curves of Unit 4 showed similar tendencies to each other: cycle a) and b) of $\delta^{13}C$ were similar to cycle a) and b) of $\delta^{18}O$, whereas cycle c) of $\delta^{13}C$ was similar to cycle c)-d) of $\delta^{18}O$. Shifts in the tendency of $\delta^{13}C$ were characterized by larger amplitude.

Strong bioturbation was characteristic of for all of the units, but especially for Unit 6.THIEL, C. et al. (2014) considered the reddish band of Unit 6 to be the remnant of an eroded soil. It was not mentioned, whether THIEL, C. et al. (2014) linked the erosion to in situ characteristics or to erosion-transport-accumulation from a nearby location. The $\delta^{13}C$ and $\delta^{18}O$ curves showed similar tendencies for Unit 6 and strong connection was characteristic of them according to the determination coefficient (R^2).

When the units from Unit 7 to Unit 4 are connected, they show increasing tendency towards the more positive values. Shifts of larger amplitude were present in the increasing tendency. Upwards in these units the $\delta^{13}C$ values indicated changes in the vegetation density, as vegetation cover possibly got lower and more opened (e.g. ALAM, M.S. et al. 1997, see **Appendix 8**). This alteration was possible not connected with significant changes in the moisture conditions, as $\delta^{18}O$ values were present within a small range and lacked extreme large fluctuations.

Loess group 1).

Unit 1

According to the data of THIEL, C. et al. (2014), the most part of Unit 1 was connected to pre-LGM and LGM (Last Glacial Maximum) loess sedimentation, whereas the main part of Unit 1 was formed during MIS 3. The uppermost samples between 1.10-3.20 m correlated with MIS 2 and referred to the so-called Greenland Interstadial phase to the termination of the Younger Dryas (THIEL, C. et al. 2014). The absence of paleosol development during MIS 3 was explained by THIEL, C. et al. (2014) with the following possible reasons: 1) erosion; and 2) paleotopographic position may have

functioned as a local sediment trap, which prevented significant soil formation due to the higher accumulation rates.

The comparison of $\delta^{13}C$ and $\delta^{18}O$ curves showed similarities along Unit1: cycles from a) to d) were parallel to each other in tendencies, whereas the upper 1.80 m of the unit showed some differences. $\delta^{13}C$ curve was divided into more cycles as from e) to h), whereas $\delta^{18}O$ curve was divided into three cycles as from e) to g). Not just the tendencies showed similarities, but the pattern and amplitude of shifts (e.g. on the boundary of cycle a)/b) or cycle d)/e)). The connection among $\delta^{13}C$ and $\delta^{18}O$ was strong, based on the determination coefficient (R^2).

Traces of carbonate migration were observed during the field description, which showed certain connections to the stable $\delta^{13}C$ and $\delta^{18}O$ values. Carbonate spots were present between 3.20-2.75 m, which coincided with the shift towards the more negative direction in cycle d), lowest half (both for $\delta^{13}C$ and $\delta^{18}O$). Weak calcified layer was present between 1.80-1.65 m, which coincided with cycle e) of the $\delta^{13}C$ curve (range of shift was within -1.95‰ and -0.10‰) and with the lower half of cycle e) of the $\delta^{18}O$ curve (range of shift was within -5.22‰ and -3.37‰). Presence of carbonate migration signs refers to more effective infiltration and possible leaching, which could be linked to enhanced moisture conditions (at least periodically) and thus to the shift towards the more negative direction for both $\delta^{13}C$ and $\delta^{18}O$ values (based on e.g. ALAM, M.S. et al. 1997).

Both $\delta^{13}C$ and $\delta^{18}O$ curves showed shifts of larger amplitude on the boundary of certain cycles: between 5.04-4.96 m – boundary of cycle a)/b); between 3.46-3.38 m – boundary of cycle c)/d); between 2.42-1.68 m – boundary of cycle d)/e); and between 0.98-0.74 m, which was the boundary of cycle g)/h) for $\delta^{13}C$ and the boundary of cycle f)/g) for $\delta^{18}O$. Along these boundaries the value range altered significantly.

During field description no discordance or signs of erosion were observed for Unit 1, but the mentioned shifts of the stable isotope values may indicate former erosion and thus hiatus in the sequence. Field description showed enhanced presence of biochannels between 5.50-4.30 m in Unit 1, but no other signs of strong bioturbation were present on the field. Micromorphological description of the wet sieved samples showed signs of bioturbation in some other cases, as the sample seemed to be partly detrital and composed of grain and aggregate mixture of different colour and habit – as between 5.40-5.20 m, 4.40-4.30 m, 4.20-3.80 m and 2.60-2.00 m. Micromorphological description showed not just the signs of bioturbation, but the presence of larger soil

aggregates for the depth of 5.40-5.30 m and 4.20-3.80 m. This appearance gave hints on a possible slight humus accumulation zone or at least on the presence of enhanced organic matter – and thus strengthened the pedosedimentary sequence development theory (according to CATT, J. A. 1990; BECZE-DEÁK, J. et al. 1997). The presence of exceptionally high EBS amounts at 4.40 m, between 3.70-3.00 m and 2.50-1.70 m also strengthened the role of bioturbation. The depth of enhanced bioturbation seemed to precede and prepare the significant shifts within the $\delta^{13}C$ and $\delta^{18}O$ curves at the cycle boundaries. Certain graduality was shown in the tendencies between the cycle boundaries, except of the boundary of d)/e) which lacked sampling in 60 cm thickness due to the excavation of profiles. The observed graduality may be connected to possible continuous effects of bioturbation, which begun before the shift started in more enhanced level and possibly continued on a less enhanced level until the new cycle started.

Unit 3 and Unit 2

Both of Unit 3 and Unit 2 showed similarities among their $\delta^{13}C$ and $\delta^{18}O$ curves. The curves of Unit 2 could be connected continuously to the curves of Unit1, without shifts of large amplitude. Cycles of $\delta^{13}C$ and $\delta^{18}O$ were the same for Unit 2. In the case of Unit 3, $\delta^{13}C$ showed shifts of larger amplitude in Unit 3 (cycle b)-c) for $\delta^{13}C$), whereas tendency of $\delta^{18}O$ remained more gradual (cycle c)-d) for $\delta^{18}O$). The connection among the cycle was the following: cycle a) and the lower part of b) of $\delta^{18}O$ was similar to cycle a) of $\delta^{13}C$; the upper part of cycle b) and cycle c) of $\delta^{18}O$ were similar to cycle b) of $\delta^{13}C$; cycle d) of $\delta^{18}O$ was similar to cycle c) of $\delta^{13}C$; and cycle e) of $\delta^{18}O$ was similar to cycle d) of $\delta^{13}C$. The connection between $\delta^{13}C$ and $\delta^{18}O$ values seemed to be moderately strong based on the determination coefficient (R^2).

Both of Unit 3 and Unit 2 showed the signs of bioturbation and contained soil-aggregates according to the micromorphological description, whereas biochannels of higher amount were present under field circumstances. Unit 2 was partly stratified, whereas Unit 3 was completely stratified, which may be connected to reworking processes, where enhanced bioturbation may have played an important role.

$\delta^{13}C$ values of Unit 3 and Unit 2 were both present along the mean value, or mainly shifted towards the more negative direction and thus seemed to represent slightly denser vegetation cover and thus the presence of slightly enhanced organic matter – when compared to Unit 1 between 5.00-2.40 m. $\delta^{18}O$ values were present in the more negative direction, showing similarities in range with the a), c) and g) cycles of Unit 1. And thus

possibly represented slightly more humid conditions, when compared to the other cycles of Unit 1.

5.3. Villánykövesd

5.3.1. General description of the Verőce sequence

The Villánykövesd Brickyard sequence is located on the Middle-Western part of the Nyárád-Harkányi Plain and can be characterized by the following coordinates: 45°52'47"N and 18°26'16"E, 122 m a.s.l. (ÚJVÁRI, G. 2004; DUDÁS, N. 2012). The Villánykövesd Brickyard sequence seemed to be worth for further investigations, since former paleoecological studies showed significant submediterranean climatic effects in this region based on malacological investigations (HUM, L. et al. 2006): the climatic conditions were relative mild and humid during the Middle and Late Pleistocene in the South-Eastern Transdanubia, and this region had a "green corridor" function for the refugium areas during the climatic oscillations of the Pleistocene (HUM, L. 2001).

Former studies of the sequence were made in the fields of sedimentology and malacology, e.g. as ÚJVÁRI, G. (2004), HUM, L. (2006), HUM, L. et al. (2006) and DUDÁS, N. (2012). Based on these works, three different parts of the brickyard were studied:

1) HUM, L. (2006) and HUM, L. et al. (2006) investigated apparently the inactive part of the brickyard and excavated a 17.5 m thick profile, which seemed to be continuous after the cleaning of the wall. The height of the profile was 124 m a.s.l. They determined the 'Mende Base', the 'Basaharc Lower' and the 'Mende Upper 1' paleosols on the basis of sedimentological and malacological investigations. Other sedimentary units presented in other, more complex loess sections were eroded in the case of the Villánykövesd sequence and HUM, L. et al. (2006) presumed that not the original thickness of the horizons was preserved in every case. The Villánykövesd sequence lacked those cold and aridity tolerant species, which are generally markers of strong cooling climatic periods. The malacological findings of HUM, L. et al. (2006) strengthened the presence of the submediterranean effect, which is characteristic of the South-Eastern Transdanubian area. HUM, L. et al. (2006) ordered the most part of the section to the Middle Pleistocene (based on former sedimentological investigations in

HUM, L. 2006) and therefore criticized the paper of ÚJVÁRI, G. (2004), who connected the section with the Upper Pleistocene.

2) ÚJVÁRI, G. (2004) also chose the inactive part of the brickyard for his sedimentological and malacological investigations. The excavated profiles were in the vicinity of the profile of HUM, L. et al. (2006), but 10-15 m further on the left side (ÚJVÁRI, G., *personal communication*). A 10.60 m thick profile was cleaned and divided into three main parts: lowermost 3.60 thick section, middle part in 4.40 thickness and the uppermost section in 3.60 m. The presence of a pedogene horizon connects the middle and lower sections, but the direct link is missing between the middle and uppermost parts.
3) DUDÁS, N. (2012) chose the active part of the brickyard for her MSc thesis, in which she connected the general sedimentological description with carbonate content analysis and colour determination (according to the Munsell colour chart).

In the present work the same parts of the brickyard were investigated and sampled as presented in DUDÁS, N. (2012). According to her work, the following five profiles were excavated in the area of the brickyard and marked on the EOV sheet extract: 1-3) profiles A, B and C were parts of the active brickyard (SW exposure); 4) profile D was excavated on the SE exposed side wall of the brickyard; and 5) profile E was part of the inactive part of the brickyard (SW exposure). The profiles were connected on the basis of levelling and thus a 9 m thick quasi-continuous sequence was made by DUDÁS, N. (2012). The recent soil, which is on the top of profile A, was eliminated from the composite. This composite profile was complemented by the Munsell colour determination, but lacked the exact depths ordered to the profile parts.

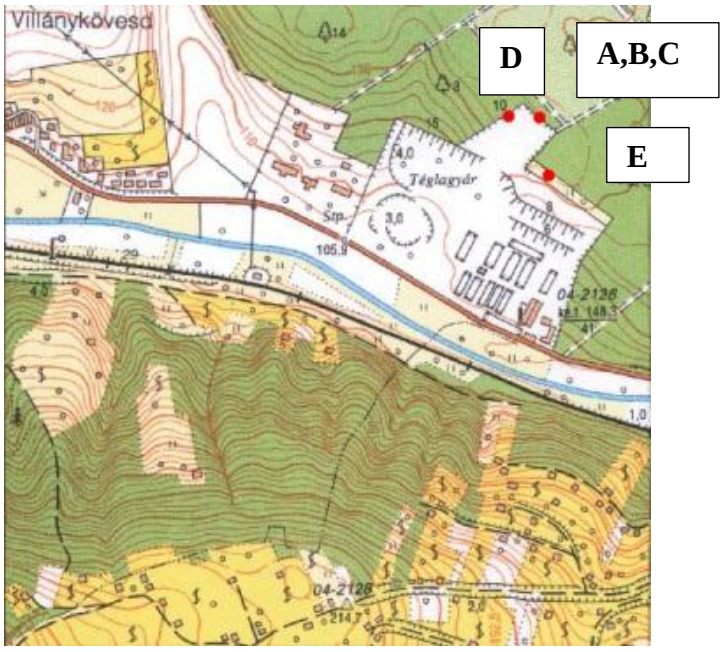

Fig.: EOV sheet extract of Villánykövesd site, with the sampoled profiles

New composite profile was made in the present work, which shows the depth values in m and orders the sequence into units. Division of the sequence was based on the detailed field description of DUDÁS, N. (2012) and own investigations – as it is presented on sequence sketch and in the **Appendix 3**.

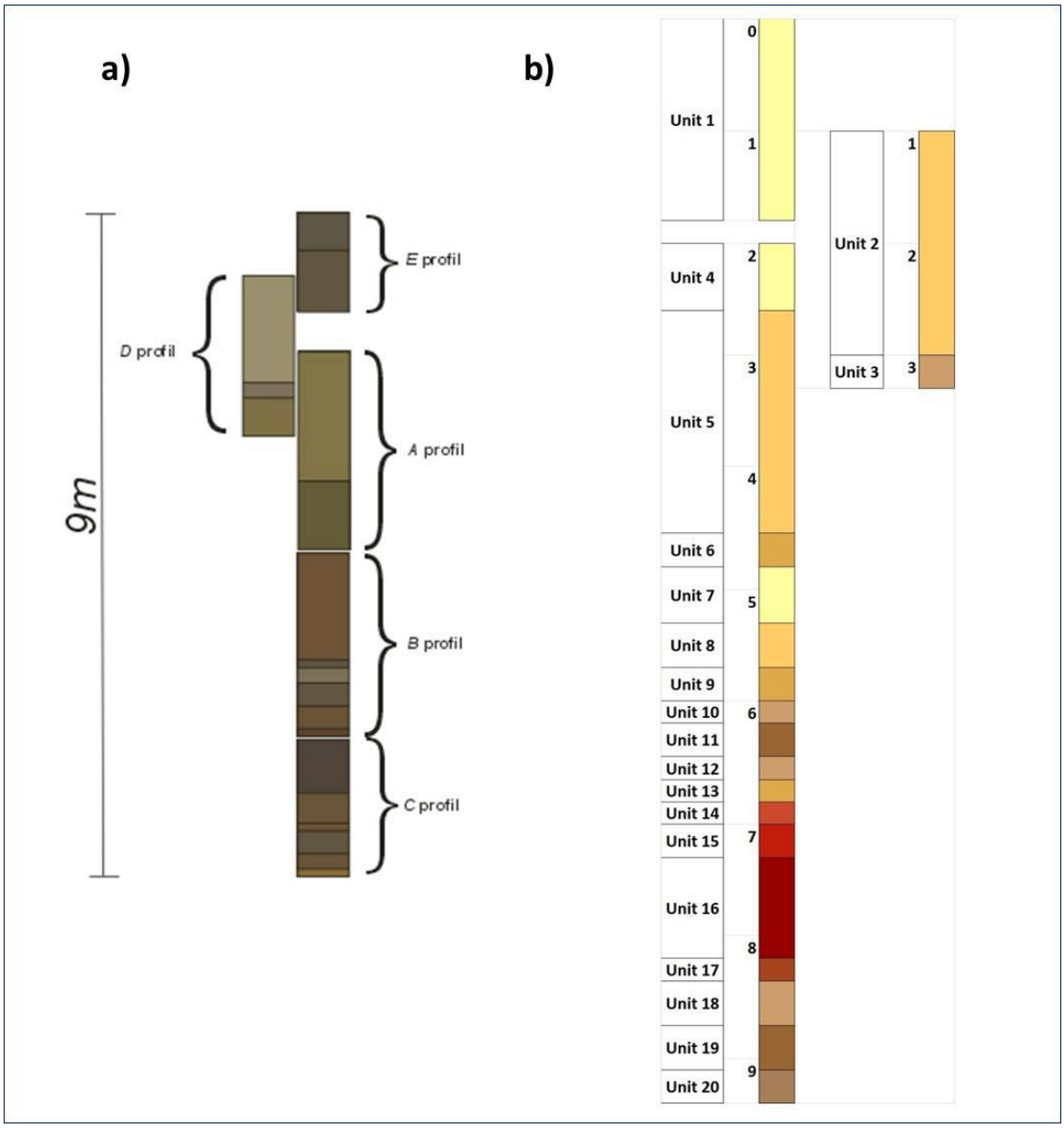

a) Composite profile based on levelling and Munsell colour determination by DUDÁS, N. (2012); b) updated composite profile ordered in to units by BARTA, G., present work.**

Detailed sequence description, based on DUDÁS, N. (2012) and own investigation:

Profile E:

Depth (cm)		Description
0	**Unit 1**	**Loess** – pale greyish-yellow in colour. This wall was in an extremely dried out state during the sampling, but its structure was granular. The quite homogeneous loess contained only few Mn spots in the diameter of 0.5-1 mm.

170		

Profile D:

Depth (cm)		Description
102	**Unit 2**	**Loess** – structure of loess was granular. This unit could be divided into the following two subunits: • a) 102-245 cm: colour was pale yellowish brown. The uppermost part of the subunit contained rounded carbonate concretions in the diameter of 0.5 cm. Presence on Mn was especially characteristic between 136-150 cm. • b) 245-286 cm: colour was pale brown. Presence of Mn is characteristic of the whole subunit. ~10 pieces of small loess dolls appeared between 245-264 cm and ~20 pieces between 264-286 cm.
300 320	**Unit 3**	**Loess** – colour was pale brown to greyish, whereas the structure was granular. Presence of Mn could be traced along the whole unit. Loess dolls appeared in higher amount until 315 cm depth, while below this depth the amount decreased.

Profile A:

Depth (cm)		Description
200	**Unit 4**	**Loess** – pale grey to yellow in colour. Rounded loess dolls appeared in diameter of 2-8 cm below 230 cm. Below 230 cm Mn showed high abundance and was associated with Fe spots below 240 cm. The following properties were observed according to the structure: • 200-240 cm: structure seemed platy and less massive; • 240-255 cm: massive granular structure.
260	**Unit 5**	**Loess** – brownish-yellow colour, which was partly divided by reddish stains. Mn and Fe spots were abundant along the unit.

		The structure changed upwards: between 300-450 cm it was granular, while in the uppermost section (260-300 cm) it was more massive.
460 480	**Unit 6**	**Loess** – darker brownish-yellow with massive structure. This unit is rich in Mn and Fe spots and abundant in crotovinas.

Profiles B and C:

Depth (cm)		Description
480	**Unit 7**	**Loess** – pale yellow to light yellow in colour and granular in structure.
530	**Unit 8**	**Sediment/soil transition** – dark yellow colour and slightly granular structure.
570	**Unit 9**	**Sediment/soil transition** – yellow-brown in colour and slightly granular in structure.
600	**Unit 10**	**Sediment/soil transition** – brown in colour. Friability of structure changed to ~30%.
620	**Unit 11**	**Dark brown paleosol** – granularity of structure is only ~30%. Mn spots appeared only scarcely. Small carbonate concretions were present in the diameter of 1 cm.
650	**Unit 12**	**Soil/sediment transition** – lighter brown colour than the above lying paleosol. The granularity of the structure is only ~30%. Transitional habit was also shown by the presence of crotovinas. 'More generation crotovinas' also appeared, which were firstly filled out with dark material (possibly from the above lying paleosol) and then mixed with lighter brown/yellow material due to further reworking.
660	**Unit 13**	**Loess** – yellow-brown in colour. The granularity of structure was about ~30%.

680	**Unit 14**	**Sediment/soil transition** – light reddish brown in colour. The granularity of the structure was about ~30%.
700	**Unit 15**	**Paleosol – reddish brown horizon** – massive soil structure.
730	**Unit 16**	**Paleosol – dark reddish brown horizon** – massive soil structure. Mn spots were observed below 756 cm. The signs of clay migration were observed on the field between 761-810 cm. Crotovinas had two different appearances: 1) between 756-795 cm they were characterized by loess infilling; 2) between 795-810 cm the crotovinas were coin-sized and contained orange coloured infilling (colour was possibly connected to bacterial effects).
810	**Unit 17**	**Soil/sediment transition** – lighter brown colour and massive structure. Mn was present along the unit and signs of clay migration were also observed. Coin-sized crotovinas were present with the same infilling patterns as in Unit 16. Loess dolls were present in diameter of 2 cm, close to the upper boundary of the unit.
830	**Unit 18**	**Loess** – light brown colour mixing with grey shade. Structure was massive. The lowest part of the unit showed slight signs of clay migration (as clay coatings on ped surfaces). Less crotovinas were present in comparison to Unit 17, their infilling was darker (presumably deriving from the underlying paleosol) and lined by Mn. Only few loess dolls were present.
870	**Unit 19**	**Dark greyish brown paleosol** – massive soil structure, which showed the signs of clay migration. Calcified root cell structures appeared commonly and were concentrated in some parts. Larger, rounded, dark brown crotovinas (in diameter of 1.2 cm) were mixing with small light brown coloured ones (mm size range) between 869-898 cm. Their orientation was mainly vertical. Between 898-910 cm the pattern of the crotovinas was different: the larger ones were light coloured, whereas the small ones were dark (possible effect of the presence of Mn).
910 930	**Unit 20**	**Soil/sediment transition** – middle light brown colour with slightly greyish shade. Structure was massive and signs of clay migration were common. Calcified root cell structures appeared commonly and were concentrated in some parts. The amount of

		crotovinas increased upwards in the unit – but they were present in smaller amount compared to the paleosol. Mainly larger, elongated crotovinas were observed with dark brown or light brown coloured infilling.

5.3.2. Methods and guidelines for the analysis

Sampling frequency for general bulk samples was in 2 cm vertical resolution. For the separation of secondary carbonates, bulk samples of 100 g were needed in 10 cm vertical resolution (as following the method described in BARTA, G. 2014). Sampling was carried out during two field campaigns. No bulk samples were taken from Unit 1 for bulk stable isotope analysis, since the section wall was extremely dried out during the second field campaign and it could not be sampled. Only secondary carbonate measurements are available from Unit 1. Bulk stable isotope data are not available from Unit 15 and Unit 17 due to analytical error during the measurement.

Mean values were calculated for the analysis of the certain units. Different groups were divided among the bulk values, based on the curves and their value range:

- bulk loess samples from Unit 2 to Unit 7: -3.01‰ as mean $\delta^{13}C$ value and -5.56‰ as mean $\delta^{18}O$ value.
- bulk transition zones, including the loesses of Unit 13 and Unit 18: -9.53‰ as mean $\delta^{13}C$ value and -8.64‰ as mean $\delta^{18}O$ value.
- bulk paleosol samples of Unit 11, Unit 15-16 and Unit 19: -10.06‰ as mean $\delta^{13}C$ and -8.54‰ as mean $\delta^{18}O$.

Mean values were calculated for those secondary carbonates, which were relative abundant along the sequence and showed depth-dependent tendencies:

- HC: -8.41‰ as mean $\delta^{13}C$ value and -7.16‰ as mean $\delta^{18}O$ value.
- HC+CC: -8.96‰ as mean $\delta^{13}C$ value and -7.23‰ as mean $\delta^{18}O$ value.
- EBS: -12.33‰ as mean $\delta^{13}C$ value and -7.47‰ as mean $\delta^{18}O$ value.

The examined sedimentary units were ordered into the composed matrix (as introduced on **Appendix 8.**): when values are shifted from the mean value towards the minimum direction, than it is considered as ‘more negative values’ – whereas those values, which are shifted towards the maximum direction are referred as ‘more positive values’. Depth-dependent tendencies of the stable carbon and oxygen isotope curves were described for bulk samples, HC, HC+CC and EBS. Curves were divided in many

cases into different cycles. Description and analysis was made from the lowest unit (Unit 20) towards the uppermost unit (Unit 1), in order to follow the built-up of the sequence.

5.3.3. Detailed description of the stable carbon and oxygen isotope values

Bulk loess samples – without Unit 13 and Unit 18 – **Appendix 6d**

more negative $\delta^{13}C$ – depletion in ^{13}C	**more positive $\delta^{13}C$ – enrichment in ^{13}C**
Unit 7 – gradually increasing tendency was observed from -5.48‰ (5.28 m), which started from the underlying Unit 8 transition zone and continued towards the mean value. Certain lower peaks were still characteristic of the curve (-5.70‰ at 5.26 m; -4.47‰ at 5.00 m and .3.88‰ at 4.82 m). **Unit 2** – Unit 2 is the gradual continuum of the underlying Unit 3, but on the more negative side of the mean value. Between 3.00-1.80 m the values stayed close to the mean value (-2.02‰ to -4.65‰). Some smaller more positive peaks occurred between 2.20-2.60 m, with one larger at 2.34 m as -2.02‰. Upwards in the section from 1.80 m the values left the range of the mean value and shifted significantly towards more negative values (as between -4.18‰ and -7.56‰).	**Unit 5** – this unit could be divided into three cycles based on the values: • cycle a): lowest part between 4.56-3.84 m (maximum value as -1.69‰ and minimum as -2.75‰). Gradually increasing tendency towards the more positive values, but with the presence of the following low peaks: -2.26‰ at 4.54 m; -2.40‰ at 4.42 m; -2.59‰ at 4.28 m; -2.75‰ at 4.14 m. The high peak of the increasing tendency was -1.22‰ at 4.12 m. Afterwards the values decreased gradually until 3.96 m (-1.72‰) and switched back to increasing tendency again until 3.84 m (-0.91‰). • cycle b): middle part between 3.84-3.08 m (maximum value as -0.98‰ and minimum as -3.09‰). This cycle begun with decreasing tendency which switched into increasing habit again, whereas certain low peaks occurred as: -3.08‰ at 3.58 m, -3.19‰ at 3.36 m and -4.30‰ at 3.00 m (these exceeded the mean value towards the more negative direction) and -2.59‰ at 3.12 m. • cycle c): uppermost part between 3.08-2.60 m (maximum value as -1.34‰ and minimum value as -4.30‰). Zigzag pattern was characteristic of this part, divided into the following four "zigzags": 1) 3.08-2.94 m; 2) 2.94-2.86 m; 3) 2.86-2.74 m; 4) 2.74-2.70 m. The uppermost part of the curve showed decreasing

	tendency towards the mean value between 2.74-2.60 m. Mean value was exceeded only in the case of the lowest peak: -4.30‰ at 3.00 m. **Unit 4** – upper part; peaks in the more positive direction, which turn backwards towards the more negative values on the uppermost part • cycle a) between 2.58-2.26 m: gradually increasing values from -2.77‰ towards -1.16‰ with one high peak at 2.56 m (-2.06‰) and one low peak at 2.32 m (-2.39‰). • cycle b) between 2.26-2.18 m: switch from decrease towards increase was present in one zigzag with a low peak at 2.20 m, which met the mean value. • cycle c) between 2.18-2.00 m: generally decreasing values, with one low peak at 2.04 m, which met the mean value. **Unit 3** – the values range between -1.95‰ to -3.50‰ and move on the more positive side of the mean value. Certain lower peaks exceed the mean value towards the more negative direction (-3.18‰ at 3.64 m, -3.08‰ at 3.58 m, -3.29‰ at 3.54 m and -3.23‰ at 3.04 m) – and so did the uppermost value as well with -3.50‰ at 3.00 m.
The profile containing Unit 2 and Unit 3 are parts of profile D, in the left section of the brickyard; whereas Unit 4 and Unit 5 are in the middle section of the brickyard, as part of profile A. Connection between the different profiles was made based on their recent topographical position by DUDÁS, N. (2012). Therefore different sedimentary units are connected to the same height and are presented as parallel curves.	
more negative $\delta^{18}O$ – depletion in ^{18}O	**more positive $\delta^{18}O$ – enrichment in ^{18}O**
Unit 7 – lowest part of Unit 7 showed increasing tendency towards the mean value, as from -6.50‰ (5.28 m) to -5.48‰ (5.06 m). Unit seemed to be the gradual continuum of the underlying Unit 8 transition zone.	**Unit 7** - upper part of the Unit 7 exceeded the mean value and showed fluctuating tendency between -5.50‰ (5.06 m) and -5.29‰ (4.80 m). The highest peak was at 4.88 m with -4.88‰. The general tendency had decreasing habit towards the mean value.

Unit 5 – two parts of this unit showed larger shift towards the more negative direction. • cycle c) with the low peak of -6.21‰ at 3.58 m (as presented in the right column of the present table); • cycle e) among others, the low peak with -6.53‰ at 3.00 m. **Unit 4** – lower half of the unit belonged to the more negative direction, as following: 2.58-2.34 m: generally increasing values towards the mean value, with small zigzag patterns. One high peak occurred at 2.56 m (-5.45‰), which exceeded the mean value towards the more positive direction. **Unit 3** – this unit could be divided into three parts, as: • cycle a) between 3.68-3.60 m: gradually increasing tendency with one low peak at 3.64 m (-7.12‰). • cycle b) between 3.60-3.48 m: switch from decrease to increase in the form of a double zigzag. Two low peaks as at 3.58 m (-9.12‰) and at 3.54 m (-8.76‰), and one high peak at 3.56 m (-7.37‰). • cycle c) between 3.48-3.36 m: same characteristics as at b), but the zigzag pattern had smaller amplitude. Two low peaks at 3.44 m (-7.43‰) and at 3.40 m (-7.65‰), one high peak at 3.42 m (-7.15‰). • cycle d) between 3.34-3.10 m: slight increase, where the curve showed only small fluctuations and values met the mean value. • cycle e) between 3.10-3.04 m: shift towards the more negative direction, with one zigzag pattern. High peak at 3.02 m (-5.35‰), which exceeded the mean value. **Unit 2** – continuum of Unit 3, where the values mostly moved in the more negative side, but still close to the mean value. • cycle a) between 2.98-2.46 m: values	**Unit 5** – this unit can be divided into the following cycles: • cycle a) between 4.56-4.28 m: values varied between -5.31‰ and -4.52‰ and the curve had zigzag pattern towards the direction of the mean value. • cycle b) between 4.26-3.66 m: larger shift from cycle a) towards the more positive direction, which is shown through the range of the values (between -5.11‰ and -4.34‰). The zigzag pattern showed upwards a slight decreasing habit towards the mean value. • cycle c) between 3.64-3.46 m: one large "zigzag" fluctuation toward the more negative direction and back to the more positive direction, with the low peak of -6.21‰ at 3.58 m. • cycle d) between 3.44-3.10 m: values varied between the range of -5.68‰ and -4.93‰ and showed zigzags of larger amplitude. Two low peaks exceeded the mean value (at 3.20 and 3.12 m). • cycle e) between 3.10-2.60 m: values showed gradually decreasing tendency towards the mean value. Larger low peak occurred at 3.00 m depth (-6.53‰). Upwards from this depth the values were present close to the mean value in both of the more negative and more positive directions. **Unit 4** – upper half of the unit belonged to the more positive direction, as followings: • cycle a) between 2.32-2.26 m: increasing habit with zigzag pattern and two low peaks (-6.22‰ at 2.32 m and -5.53‰ at 2.28 m). • cycle b) between 2.26-2.18 m: switch from decrease towards increase in zigzag pattern with a low peak at 2.20 m (-5.80‰), which exceeded the mean value. • cycle c) between 2.18-2.00 m: gradually decreasing tendency upwards in the unit, towards the mean

tended to move towards the mean value with different amplitude zigzag patterns. • cycle b) between 2.46-2.30 m: switch from increasing towards decreasing values in zigzag pattern. One low value at 2.42 m (-6.21‰) and one high value at 2.34 m (-4.96‰), which exceeded the mean value. • cycle c) between 2.30-1.90 m: upwards the decreasing tendency switched towards increasing habit, with low peaks at 2.12 m (-6.00‰) and 2.08 m (-6.22‰). • cycle d) between 1.90-1.42 m: values were shifted mostly towards the more negative direction and showed fluctuations in zigzag pattern.	value. One low peak was characteristic at 2.04 m (-5.91‰). **Unit 2** – uppermost part; where the values oscillate with small peaks both on the more negative and on the more positive side Cycle b) between 2.38-2.28 m. • cycle e) between 1.42-1.00 m: increasing tendency, where values were mostly present in the more positive direction. The tendency showed fluctuations in zigzag patterns of different amplitude in the range of -6.09‰ and -5.20‰.

Bulk samples from the transition zones and loess of Unit 13 and Unit 18 – **Appendix 6.e.**

more negative $\delta^{13}C$ – depletion in ^{13}C	**more positive $\delta^{13}C$ – enrichment in ^{13}C**
Unit 20 – this unit was divided into the following cycles: • cycle a) between 9.52-9.34 m: increasing tendency was shown with two low peaks (-12.54‰ at 9.50 m and -12.91‰ at 9.42 m) and one high peak of -10.16‰ at 9.44 m. • cycle b) between 9.34-9.28 m: slight gradual decrease, which switches into increase at 9.30 m. • cycle c) between 9.28-9.14 m: decreasing tendency with zigzag fluctuations, which switched back to increasing habit from 9.18 m. • cycle d) between 9.16-9.10 m: slight increase towards the mean value. **Unit 20** showed gradual transition towards the paleosol of **Unit 19**. **Unit 18** – two cycles were differentiated, as followings:	**Unit 13** – the following cycles were distinguished: • cycle b) between 6.72-6.66 m is characterized by one zigzag fluctuation and high peak at 6.68 m (-8.50‰). • cycle c) means the depth between 6.66-6.60 m, where the values were present in a really small range (between -8.98‰ and -9.15‰). **Unit 12** – values showed decreasing habit toward the mean value from 6.58 m to 6.50 m, with one high peak at 6.54 m (-8.34‰). **Unit 10** – two cycles were present in Unit 10: • cycle a) between 6.18-6.02 m in the value range of -7.69‰ and -7.78‰, where the values showed slight increase until 6.08 m, than started to

• cycle a) between 8.68-8.52 m: values were present mainly along the mean value, with one small high peak at 8.64 m (-9.20‰) and one small low peak at 8.60 m (-9.96‰). • cycle b) between 8.52-8.44 m: decreasing tendency was present, with one low peak at 8.46 m (-11.35‰). **Unit 18** showed gradual transition towards the paleosol of Unit 16. **Unit 14** – three cycles were divided in this unit, as: • cycle a) between 6.98-6.94 m: decreasing tendency from -10.63‰ to -12.44‰. • cycle b) between 6.94-6.86 m: increasing tendency from -12.44‰ to –11.25 ‰. • cycle c) between 6.68-6.80 m: one zigzag fluctuation towards the mean value with the low peak of -12.76‰ at 6.84 m. **Unit 13** – between 6.78-6.72 m cycle a) was characteristic, which showed gradually increasing values towards the mean value. **Unit 9** – cycle b) was characteristic of 5.82-5.70 m with fluctuating values, but generally decreasing habit. One high peak exceeded the mean value at 5.76 m (-8.11‰), whereas two low peaks remained on the more negative side (5.74 m and 5.78 m). **Unit 8** – the lowest part of the unit can be mentioned as cycle a) between 5.68 m (-10.37‰) and 5.48 m (-6.28‰). Values showed gradual increase towards the mean value with one low peak at 5.62 m (-12.09‰).	decrease; • cycle b) between 6.02-6.00 m, where increase started again. **Unit 9** – between 5.98-5.82 m gradually decreasing tendency was characteristic and marked by cycle a). The uppermost value met the mean value. **Unit 8** – two more cycles could be divided in Unit 8: • cycle b) between 5.48-5.42 m, which showed gradually increasing tendency and one low peak at 5.46 m (-6.96‰). • cycle c) was characteristic of 5.42-5.30 m, where the values showed only slight fluctuations between -4.81‰ and -5.64‰.
more negative $\delta^{18}O$ – depletion in ^{18}O	**more positive $\delta^{18}O$ – enrichment in ^{18}O**
Unit 20 – the following cycles were differentiated in this unit: • cycle a) between 9.54-9.44 m: the	**Unit 18 –** cycle a) between 8.68-8.52 m showed values in the smaller range of -7.53‰ and -6.89 m, with one high peak

general tendency was increasing towards the mean value (between -9.10‰ and -8.76‰).

- cycle b) between 9.44-9.34 m: this cycle started and ended with the mean value and had two low peaks (-10.63‰ at 9.42 m and -10.09‰ at 9.36 m).
- cycle c) between 9.34-9.18 m: generally decreasing tendency with zigzag fluctuations of different amplitude.
- cycle d) between 9.18-9.10 m: increasing tendency was shown towards the mean value.

Unit 18 – cycle b) between 8.52-8.44 m showed values with decreasing tendency.

Unit 14 – two cycles were divided, as followings:

- cycle a) between 6.98-6.88 m: increasing character towards the mean value with a high peak at 6.96 m (-10.26‰) and a low peak at 6.92 m (-11.24‰).
- cycle b) between 6.88-6.80 m: one zigzag fluctuation with upwards increasing character. low peak at 6.84 m (-12.28‰).

Unit 13 – gradual increase was characteristic of 6.78-6.68 m, where the mean value was exceeded (cycle a)).

Unit 9 – cycle a) was characteristic of 5.98-5.78 m, which showed gradually decreasing habit towards the mean value. One zigzag appeared with low peak at 5.90 m (-7.65‰).

Unit 8 – two cycles were differentiated:

- cycle a) between 5.68-5.60 m with gradually decreasing values;
- cycle b) between 5.60-5.48 m with gradually increasing values towards the mean value. In the latter case the range of values was -11.89‰ to -8.10‰, which means that the mean value was exceeded.

(8.64 m, -6.89‰) and one low peak (8.60 m, -7.43‰).

Unit 13 – two cycles were differentiated:

- cycle b) means the zigzag pattern between 6.68-6.64 m with the low peak of -8.13‰ at 6.66 m.
- cycle c) showed gradual decrease between 6.64-6.60 m in the small range of -7.40‰ to -7.63‰.

Unit 12 – values showed slight increase from 6.58 m to 6.54 m, than decrease toward the mean value was characteristic again.

Unit 10 – generally increasing tendency was characteristic of Unit 10 (6.18-6.00 m) with value range of -7.24‰ and -6.90‰. One small low peak appeared at 6.14 m as -7.22‰ and one small high peak at 6.06 m as -6.61‰.

Unit 9 – cycle b) was characteristic of the depth 5.78-5.70 m, where the lowest and uppermost values met the mean value. One high peak occurred at 5.76 m (-8.06‰), and one low peak at 5.72 m (-9.38‰).

Unit 8 – one cycle was characteristic of the more positive direction as cycle c) between 5.48-5.30 m. This showed increasing tendency, with two low peaks (5.46 m and 5.38 m), which met the mean value.

Bulk paleosol samples – **Appendix 6f**

more negative $\delta^{13}C$ – depletion in ^{13}C	**more positive $\delta^{13}C$ – enrichment in ^{13}C**
Unit 16 – the following cycles were characteristic of this unit: • cycle a) between 8.14-8.04 m: values showed increasing tendency between -11.90‰ and -12.19‰. • cycle b) between 8.04-7.94 m: increasing tendency continued with zigzag fluctuations. High peak at 8.02 (-11.36‰) and low peak at 8.00 m (-12.67‰). • cycle c) between 7.94-7.72 m: gradual increase with fluctuations of only small amplitude. Small high peak at 7.86 m (-10.83‰) and small low peak at 7.82 m (-11.08‰). The uppermost part of the cycle met the mean value. • cycle d) between 7.72-7.60 m: one larger amplitude fluctuation towards the mean value. Low peak at 7.66 m (-11.96‰).	**Unit 19** – the following cycles were differentiated in this unit: • cycle a) between 9.08-8.96 m: values moved along the mean value with the exception of one high peak at 9.00 (-9.03‰). • cycle b) between 8.96-8.80 m: gradually increasing tendency. • cycle c) between 8.80-8.74 m: decreasing tendency started with a fluctuation. Low peak at 8.76 m met the mean value. • cycle d) between 8.74-8.70 m: decreasing tendency upwards in the unit. **Unit 11** – the following two cycles were differentiated: • cycle a) between 6.48-6.34 m: increasing tendency in the range of -9.47‰ and -9.41‰. • cycle b) between 6.34-6.20 m: increasing tendency continued in the range of -9.47‰ and -7.99‰.
more negative $\delta^{18}O$ – depletion in ^{18}O	**more positive $\delta^{18}O$ – enrichment in ^{18}O**
Unit 16 – the following cycles were differentiated for this unit: • cycle a) between 8.14-7.88 m: upwards increasing tendency, which is presented in zigzag fluctuations of different amplitude. Range was between -11.42‰ and -9.42‰.	**Unit 19** – the following cycles were present in the unit: • cycle a) between 9.08-9.02 m: gradual increase between -8.39‰ and -7.98‰. • cycle b) between 9.02-8.84 m: increasing tendency continued with the exception of the lowermost zigzag

• cycle b) between 7.88-7.74 m: increasing tendency continued in the range of -8.37‰ and -9.42‰. The uppermost value exceeded the mean value. • cycle c) between 7.74-7.60 m: switch from decreasing values towards increasing habit was shown through zigzag pattern. Low peak at 7.66 m (-9.96‰). The uppermost value exceeded the mean value.	fluctuation. Low peak at 9.00 (-8.88‰). • cycle c) between 8.84-8.80 m: decreasing tendency. • cycle d) between 8.80-8.70 m: increasing tendency again with one low peak at 8.76 m (-8.02‰). **Unit 11** – between 6.48-6.20 m the values showed increasing tendency. Between 6.44-6.34 m zigzag fluctuation appeared with small amplitude.

Hypocoatings

more negative $\delta^{13}C$ – depletion in ^{13}C	**more positive $\delta^{13}C$ – enrichment in ^{13}C**
Loess: **Unit 18, Unit 7, Unit 5, Unit 2, Unit 1** *Transition zone*: **Unit 20; Unit 8** (between 5.50-5.40 m) *Paleosol*: **Unit 19** Gradually increasing tendency was obtained from the transition of **Unit 20**, towards the paleosol of **Unit 19** and continuously in the loess of **Unit 18**. The only exception was between the first two values at 9.30-9.10 m, where decreasing was characteristic. **Unit 7** showed upwards increasing tendency and exceeded the mean value towards the more positive direction. **Unit 2**: between 2.00-1.10 m the values tended to shift towards the more negative direction. The amplitude of fluctuations became smaller, as the decreasing tendency continued upwards.	*Loess*: **Unit 13, Unit 5, Unit 3, Unit 2** *Transition zone*: **Unit 14, Unit 10, Unit 9;** lowest and uppermost part of **Unit 8** *Paleosol*: **Unit 16, Unit 15, Unit 11** Only the **Units 10, 9 and 8** showed certain kind of graduality: their curves can be connected to each other and thus show a zigzag pattern. High peak is at 5.80 m (-4.85‰). Two low values were present, as at 6.00 m (-8.26‰) and at 5.40 m (-9.10‰). **Unit 3** could be linked to **Unit 2**, as the possible beginning of the fluctuating pattern of **Unit 2**. **Unit 2**: between 2.80-2.00 m the values are present mostly in the more positive direction with more high peaks than lower ones. Lower peaks exceed the mean value.

Unit 1: between 1.60-1.30 m the values showed decreasing tendency, which changed to slight increase. Values between 1.10-0.50 m showed almost the same value. the uppermost value was shifted towards the mean value.	
Unit 5 showed largely fluctuating habits in the range of -10.43‰ and -4.94‰. The amplitude of fluctuations was smaller only between 2.90 m and 2.60 m, where it was mostly in the range of the mean value. Low peaks were at 4.40 m (-10.43‰), at 4.00 (-9.28‰), at 3.50 (-9.73‰) and at 3.10 m (-10.36‰).High peaks were at 4.10 m (-6.35‰), at 3.70 (-8.10‰, close to the mean value) and at 3.30 (-4.94‰).	
more negative $\delta^{18}O$ – depletion in ^{18}O	**more positive $\delta^{18}O$ – enrichment in ^{18}O**
Loess: **Unit 18, Unit 13, Unit 7, Unit 5** (2.70-2.60 m), **Unit 3, Unit 2, Unit 1** *Transition zone*: **Unit 20, Unit 12, Unit 9, Unit 8** (between 5.50-5.40 m) *Paleosol*: **Unit 19, Unit 11** The values of **Unit 20, 19 and 18** could be connected to each other in the pattern of fluctuations. Lowest peak was present in **Unit 20** at 9.10 m (-8.87‰), whereas the two high peaks reached the mean value: 8.70 m (**Unit 19**) and 8.50 m (**Unit 18**). **Unit 13**: uppermost value belonged here (-7.94‰ at 6.60 m). **Unit 11**: uppermost value belonged here (-7.57‰ at 6.30), close to the value of **Unit 12**. **Unit 8** showed the same habit, as in the case of $\delta^{13}C$: the middle two values belonged to the more negative side. **Unit 7**: between 5.20-5.00 m, where the values showed upwards decreasing habit and then switched to increasing tendency (towards the mean value). **Unit 5**: between 2.70-2.60 m values	*Loess*: **Unit 13, Unit 7** (4.90 m), **Unit 6, Unit 5, Unit 2, Unit 1** (0.40 m) *Transition*: **Unit 14, Unit 10,** lowest and uppermost part of **Unit 8** *Paleosol*: **Unit 16, Unit 15, Unit 11** The values of **Unit 16** shifted towards the mean value, whereas the tendency of the curve changed within the paleosol and tended to move towards the more positive values. The uppermost value of **Unit 16** (-5.00‰ at 7.00 m) could be connected to the transition zone of **Unit 14**, which was continued in **Unit 13**. **Unit 11**: lowermost value belonged here (-5.01‰ at 6.40 m). **Unit 8** showed the same habit, as in the case of $\delta^{13}C$: the lowest (5.60 m) and uppermost (5.30 m) values belonged to the more positive side. **Unit 7**: uppermost value at 4.90 m (-6.83‰) belonged here. **Unit 5**: between 5.40-3.60 m and between 3.10-2.70 m belonged here. Fluctuations of smaller amplitude were characteristic in the range of -6.24‰ and -7.61‰. Between

belonged here with decreasing habit. **Unit 1**: between 1.60-0.80 m the values moved along the mean value, with the exception of a low peak at 1.40 m (-7.99‰). Between 0.80-0.40 m one larger fluctuation was present in zigzag pattern with the low peak of -8.24‰ (at 0.70 m).	3.60-3.10 m the values moved along the mean value. **Unit 1**: the uppermost value as -6.76‰ (0.40 m) belonged here.
Unit 2 showed fluctuating tendency with low peaks in the more negative direction and high peaks in the more positive direction. The range of the values was -9.87‰ and -7.04‰. The uppermost part of **Unit 2** (1.30-1.10 m) showed shift towards the more positive direction.	

HC+CC – **Appendix 6h**

more negative $\delta^{13}C$ – depletion in ^{13}C	**more positive $\delta^{13}C$ – enrichment in ^{13}C**
Loess: **Unit 5** (3.40-2.90 m), **Unit 2** (2.40-1.90 m), **Unit 1** **Unit 5**: one zigzag fluctuation was characteristic of Unit 5 between 3.40-2.90 m, which started with decreasing tendency and continued in increasing towards the mean value. Low peak at 3.20 m (-10.53‰). **Unit 2**: between 2.40-1.90 m the tendency begun with increasing towards the mean value. Values were present mostly along the mean value, but in the uppermost part shift occurred again towards the more negative values. Uppermost value was -9.92‰ at 1.90 m. **Unit 1**: three small cycles could be connected to this unit, as a) 1.60-1.50 m with increasing tendency towards the mean value; b) 1.50-0.80 m, where decreasing tendency switched to increasing again with the lowest point of -10.10‰ at 1.20 m; c) 0.80-0.40 m, same	*Loess*: **Unit 7**, **Unit 5** (3.80-3.40 m and 2.90-2.70 m), **Unit 3**, **Unit 2** (2.90-2.40) *Transition zone*: **Unit 12**, **Unit 9**, **Unit 8** *Paleosol*: **Unit 15**, **Unit 11** **Unit 8**: decrease towards the mean value from 5.60 m (-7.39‰). **Unit 7** was represented only by one value (-8.59‰ at 5.20 m), which seemed to fit the tendency of **Unit 8**. **Unit 5**: gradual decrease towards the mean value from 3.80 m (-6.37‰) to 3.40 (-8.90‰). Than between 2.90-2.70 m slight shift towards the more positive direction again. **Unit 3**: the values are close to the mean value and seemed to connected to the tendency of Unit 2 upwards in the section. **Unit 2**: tendency of **Unit 3** continued in Unit 2. Between 2.90 m (-8.60‰) and 2.40

characteristics as for cycle b), the low peak was at 0.60 m with -10.03‰.	(-9.25‰) increasing tendency turned into decreasing and exceeded the mean value towards the more negative direction.
more negative $\delta^{18}O$ – depletion in ^{18}O	**more positive $\delta^{18}O$ – enrichment in ^{18}O**
Loess: **Unit 3**, **Unit 2**, **Unit 1** (1.60 m, 0.70-0.40 m) *Transition*: **Unit 9**, **Unit 8** (5.40 m) **Unit 8**: low peak of the zigzag fluctuation belonged to the more negative direction from the mean value (-7.98‰ at 5.40 m). **Unit 3**: the values of this unit seemed to be connected to **Unit 2**. When **Unit 3** and **Unit 2** are combined, two cycles could be distinguished. Cycle a) between 3.10-2.60 m, which showed decreasing tendency with lowest values almost at the same range (3.00-2.80 m). Cycle b) between 2.60-2.00 m showed decreasing tendency, which turned to increasing again and met the mean value at 2.00 m. The uppermost value of **Unit 2** was shifted towards the more negative direction again (-7.64‰ at 1.90 m). **Unit 1**: the value of -8.08‰ at 1.60 m belonged to the more negative direction, but the increasing tendency of this part started from this point. – The uppermost part of **Unit 1**, between 0.70-0.40 m belonged also in this direction. Zigzag fluctuation pattern was shown, with low peak at 0.60 m (-8.37‰). This pattern pointed out on increasing tendency again.	*Loess*: **Unit 7**, **Unit 1** (1.50-0.70 m) *Transition*: **Unit 12**, **Unit 8** (5.60 m and 5.30 m), **Unit 5** *Paleosol*: **Unit 15**, **Unit 11** **Unit 15** was represented by only one value, which met the mean value at 7.20 m. **Unit 8**: fluctuation with zigzag pattern was characteristic of this unit, where two values belonged here (-6.80‰ at 5.60 m and -6.91‰ at 5.30 m). **Unit 7** was represented by only one value at 5.20 m (-6.39‰), which seemed to be the continuation of the tendency in **Unit 8**. **Unit 5**: upwards increasing tendency was present in this unit, with zigzag fluctuation pattern. Low peaks were at 3.20 m (-7.21‰) and at 2.90 m (-6.67‰); high peak was observed at 3.00 m (-6.38‰). **Unit 1**: between 1.50-0.90 m generally increasing tendency was characteristic, with certain fluctuations in the range of -7.57‰ and -6.51‰. Between 0.90-0.70 m decreasing was characteristic towards the mean value.

Earthworm biospheroids – **Appendix 6i**

more negative $\delta^{13}C$ – depletion in ^{13}C	**more positive $\delta^{13}C$ – enrichment in ^{13}C**

Loess: **Unit 13, Unit 7*** (5.20 m, 5.00 m), **Unit 5** (3.30-3.00 m), **Unit 3, Unit 4, Unit 2** (2.40-1.90 m)**, **Unit 1*****

Transition zone: **Unit 20** (9.30 m), **Unit 14, Unit 12, Unit 10, Unit 8** (only 5.50 m)

Paleosol: **Unit 19** (only 8.70 m), **Unit 16, Unit 15, Unit 11** (6.40-6.30 m)

Unit 16, 14 and 13 were almost in the same range (-13.17 and -13.70‰, and -13.03‰ and -12.63‰, respectively). When these units and **Unit 15** were connected, than a zigzag fluctuation pattern could be observed with an upwards decreasing tendency and low peak at 7.10 m (-14.80‰).

The transition horizon of **Unit 12** is represented by one value (-12.47‰ at 6.50 m), which was fallen into the range of the lower part of **Unit 11**.

The values of **Unit 11** were within a small range (close to -12.50‰), whereas the above lying transition zone of **Unit 10** was shifted towards the more negative values.

Unit 8 was characterized by a zigzag pattern fluctuation, where the low peak belonged to the more negative direction (-13.23‰ at 5.50 m).

The uppermost part of **Unit 5** belonged to the more negative direction, as values at 3.30 m (-13.69‰) and at 3.00 m (-13.84‰).

Unit 4 showed decreasing tendency with zigzag pattern and low peak at 2.40 m (-15.10‰) and high peak at 2.20 m (-13.66‰).

Unit 2: the values of **Unit 2** showed a large shift from the more positive direction towards the more negative direction (and thus exceeded the mean value). After the shift the values showed increasing

Loess: **Unit 18, Unit 7*** (5.10 m, 4.90 m), **Unit 6, Unit 5** (4.30-3.40 m), **Unit 2** (2.90-2.40 m)**, **Unit 1*****

Transition zone: **Unit 20** (9.20-9.10 m), **Unit 9, Unit 8**

Paleosol: **Unit 19, Unit 11** (6.20 m)

The tendency of **Unit 20, 19 and 18** seemed to be connectible in the form of a zigzag fluctuation pattern (with varying amplitude). High peaks were almost the same: -10.72‰ at 9.20 m, -10.76‰ at 8.80 m and -10.72‰ at 8.40 m.

One value of **Unit 11** was present in the more positive direction, close to the mean value at 6.20 m (-12.14‰).

The tendency of **Unit 9** seemed to be the continuation of **Unit 10**, as showing increasing habit upwards in the section.

The tendency of **Unit 9** seemingly continued in **Unit 8**, which was characterized by a zigzag pattern fluctuation. Values at 5.60 m, 5.40 m and 5.30 m belonged to the more positive direction.

Unit 6 seemed to be the continuation of the tendency presented in **Unit 7**. The lowermost and uppermost value met the mean value, whereas a high peak was obtained at 4.60 m (-11.37‰).

Unit 5 could be linked to the fluctuating habit of **Unit 6**. Increasing tendency was observed until 3.40 m (-10.87‰), with small amplitude fluctuations in the range of -12.03‰ and -10.87‰. Above this a larger shift begun towards the more negative direction.

Unit 2: the values between 2.90-2.40 m belonged to the more positive direction. Fluctuation of the values showed zigzag pattern, with low peak at the mean value

character back to the mean value again (between 2.40-1.90 m).**	and a large amplitude high peak at 2.40 m (-9.37‰). Decrease happened upwards in the unit above 2.40 m, with a shift of large amplitude towards the more negative direction.
*__Unit 7__: this unit seemed to be the continuation of **Unit 8** with zigzag fluctuation pattern. Low peaks were present in the more negative direction as at 5.20 m (-12.55‰) and at 5.00 m (-12.93‰). High peaks were in the more positive direction: one with larger amplitude at 5.10 m (-10.02‰) and a smaller one at 4.90 m (-12.12‰). **__Unit 2__: between 1.90-1.10 m fluctuations were present on both sides of the mean value in the range of -10.97‰ and -13.73‰. Tendency of the fluctuations ended in decreasing values between 1.20-1.10 m. ***__Unit 1__: the whole unit was characterized by large amplitude fluctuations between 1.60-0.40 m. Lowest peak was at 1.30 m (-13.94‰), whereas the highest peak was at 1.20 m (-9.34‰). The uppermost value was present in the more negative direction.	
more negative $\delta^{18}O$ – depletion in ^{18}O	**more positive $\delta^{18}O$ – enrichment in ^{18}O**
Loess: **Unit 18, Unit 7*, Unit 6** (4.60-4.50 m)*, **Unit 5** (4.40-3.70 m), **Unit 3** (3.10 m)**, **Unit 2****, **Unit 1***** *Transition*: **Unit 20, Unit 9*** (5.80-5.70 m), **Unit 8** (5.30 m)*, *Paleosol*: **Unit 19, Unit 16** (7.30 m), **Unit 11** (6.40 m and 6.20 m) Upwards increasing tendency was characteristic of **Unit 20, 19 and 18** through the connection of the curves. This tendency contained zigzag fluctuations, which amplitude got smaller upwards. Lowest peak occurred at 8.90 m (-10.96‰), while the highest one was at 8.30 m (-7.29‰). Values in **Unit 11** showed one zigzag fluctuation, beginning in the more negative direction, but with a high peak in the more positive direction (-6.71‰ at 6.30 m). Values of **Unit 5** between 4.40-3.70 m belonged to the more negative direction.	*Loess*: **Unit 13, Unit 7** (only 5.00 m)*, **Unit 6** (4.80 m)*, U**nit 5** (3.70-3.00 m), **Unit 3** (3.00 m)**, **Unit 4, Unit 2****, **Unit 1***** *Transition*: **Unit 14, Unit 12, Unit 10, Unit 9** (5.90 m)*, **Unit 8** (5.60-5.40 m)* *Paleosol*: **Unit 16** (7.40 m), **Unit 15, Unit 11** (6.30 m) Shift towards the more positive direction was obtained through the comparison of **Unit 16** and **Unit 15** (the two horizons of the same paleosol). This was also characteristic of the upper transition zone of the paleosol, as **Unit 14**. Values shifted back towards the mean value in the case of **Unit 13** and **Unit 12**. Upper part of **Unit 5**, between 3.70-3.00 m belonged to the more positive direction. Gradual increase was obtained until 3.30 m (-4.59‰), where direction changed and became decreasing.

Gradually decreasing tendency was shown until 3.90 m, where it changed for increase and shifted with larger amplitude towards the mean value.	
*__Unit 9, 8 and 7__ could be connected the each other, and thus they reflected large amplitude fluctuations between the more negative and more positive direction. Range of fluctuation was -10.08‰ and -5.63‰. The presented tendency continued in **Unit 6** with smaller amplitude fluctuation. **__Unit 2__ and **Unit 3**: these two units could be linked to each other to be the part of larger amplitude fluctuations. Peaks of this fluctuating pattern were present in both (more positive and more negative) sides, within the range of -10.23‰ and -4.79‰. When the positions of the high peaks were taken into account, these marked the mostly increasing tendency of **Unit 2**. ***__Unit 1__: values of Unit 1 showed larger amplitude fluctuations in the range of -10.48‰ and -4.26‰. Most values were present in the more negative direction. General tendency seemed to have decreasing habit.	

Calcified root cells

Presence of CRC was not really characteristic of the Villánykövesd Brickyard sequence. Pure samples were found in Unit 2, 6 and 9, whereas the combination of HC+CRC was found in Unit 5. Five samples were described from Unit 2 in the range of -28.47‰ to -31.18‰ for $\delta^{13}C$ and -14.80‰ and -16.12‰ for $\delta^{18}O$. The other samples showed higher values, as -25.62‰ for $\delta^{13}C$ and -11.84‰ for $\delta^{18}O$ in Unit 6, and -9.14‰ for $\delta^{13}C$ and -8.64‰ for $\delta^{18}O$.

Carbonate coatings

Only four CC samples were found in the sequence: two pieces of CC in Unit 17, and one-one in Unit 18 and Unit 20. Mean values for $\delta^{13}C$ were -10.14‰ and -7.88‰ for $\delta^{18}O$, respectively.

5.3.4. Similar tendencies

The examined stable carbon and oxygen isotope curves were compared to each other and they showed similarities in certain cases, as it can be seen below:

5.3.4.1. HC versus bulk samples

- Comparison of bulk and HC curves - **δ^{13}C**. HC curve showed similarities with the following units and/or cycles:
    - *palesols*: similarity with Unit 19, cycle b).
    - *transition zones*: similarity with Unit 13 cycle a)-b); Unit 7; Unit 4 cycle a)-b); Unit 2. In the case of Unit 4, cycle b) showed two low peaks for the bulk sample, whereas only one low peak was characteristic of HC – but the tendency of curves was the same. Unit 2 showed the same decreasing tendency for both, the larger shift towards the more negative direction started from 1.80 m in the case of the bulk curve and from 1.70 m in the case of the HC curve.
- Comparison of bulk and HC curves - **δ^{18}O**. HC curve showed similarity with the following units and/or cycles:
    - *paleosols*: similarity with Unit 19 b)-d).
    - *transition zones*: similarity with Unit 20 c)-d); Unit 8. In the latter case similarity was present only in the case of cycle c) between 5.40-5.30 m.
    - *loess*: Unit 18 b); Unit 5 c) and e); Unit 3 e); Unit 2 b)-e). Unit 5 cycle c) was similar to the low peak of HC at 3.60 m.

5.3.4.2. HC versus HC+CC

- Comparison of HC and HC+CC values in general: Difference between the δ^{13}C and δ^{18}O values was calculated for those units and horizons, which contained both of these features. It was possible to calculate maximum and minimum differences, when enough samples were available – as for Unit 1, 2, 3, 5 and 8. The other units contained one or two HC+CC samples, or lacked it. The mean difference of δ^{13}C values was 0.67‰, whereas the mean difference for δ^{18}O was 0.58‰. The maximum difference among δ^{13}C values was 2.67‰, whereas the minimum was 0.01‰. δ^{18}O values showed smaller difference, as a maximum of 0.71‰, whereas the minimum was 0.00‰ (which means equality between the values). The table contains the calculations:

	δ13C (VPDB ‰)				**δ18O (VPDB ‰)**			
	Max	**Min**	**Mean**	**SD Mean**	**Max**	**Min**	**Mean**	**SD Mean**
Unit 1	1,06	0,01	**0,31**	*0,00*	1,24	0,04	**0,52**	*0,01*
Unit 2	2,09	0,02	**0,88**	*0,00*	1,67	0,14	**0,69**	*0,00*

Unit 3	2,47	0,06	**1,18**	*0,00*	1,20	0,15	**0,57**	*0,00*
Unit 4			**0,06**	*0,00*			**1,20**	*0,00*
Unit 5	2,67	0,10	**0,75**	*0,00*	1,41	0,00	**0,35**	*0,01*
Unit 7			**0,52**	*0,00*			**0,76**	*0,00*
Unit 8	1,08	0,25	**0,63**	*0,01*	0,41	0,23	**0,31**	*0,00*
Unit 9			**0,86**	*0,01*			**0,00**	*-0,86*
Unit 11			**0,97**	*0,00*			**1,71**	*0,00*
Unit 12			**0,19**	*0,00*			**0,90**	*0,01*
Unit 15			**0,63**	*0,04*			**0,87**	*0,05*

- Comparison of HC and HC+CC curves - **δ^{13}C**. Mean values were slightly different, as -8.41‰ for HC and -8.96‰ for HC+CC. The calculated mean difference among HC and HC+CC values was 0.67‰. Comparison showed the following connections:
    - *paleosols*: similar tendencies were observed for Unit 15 and Unit 11.
    - *transition zones*: similar tendencies with Unit 12 and Unit 8. In the latter case the tendency was the same, but HC+CC values were slightly shifted towards the more negative direction.
    - *loess*: similar tendencies with certain parts of Unit 5; Unit 3; certain parts of Unit 2 and Unit 1. As a remark to Unit 5, both curves met and showed the same increasing tendency between 3.20-2.70 m. The tendency was the same between 3.80-3.20 m, but the curves did not fit perfectly, because lower sampling resolution was available for HC+CC. The same decreasing tendency was observed for Unit 2 between 2.80-1.90 m, but HC showed larger amplitude fluctuations within the range of -9.54‰ and -7.04‰, whereas the fluctuations of the HC+CC curve were in smaller range, as -9.92‰ and -8.21‰.

- Comparison of HC and HC+CC curves - **$\delta^{18}O$**. Mean values were almost the same, as -7.16‰ for HC and -7.23‰ for HC+CC. The calculated mean difference among HC and HC+CC values was 0.58‰. Comparison showed the following connections:
    - *transition zones*: similar tendency with Unit 8 and Unit 9.
    - *loess*: only certain similarity was shown with Unit 2. For instance value range and tendency was differing in the following case: between 2.90-1.90 m the value range for HC+CC was within -8.17‰ and -7.28‰ and values showed only slight fluctuations, whereas the fluctuations of HC showed large amplitude within the range of -8.08‰ and -5.61‰.

5.3.4.3. EBS versus bulk samples

- Comparison of EBS and bulk curves - **$\delta^{13}C$**. EBS curve showed similarity with following units and/or cycles:
    - *paleosols*: similarity with Unit 19 b)-c); Unit 11 b).
    - *transition zones*: similarity with Unit 8 a)-b).
    - *loess*: similarity with Unit 13 b)-c); Unit 7 (tendency is the same, but larger amplitude fluctuations for EBS); Unit 3.
- Comparison of EBS and bulk curves - **$\delta^{18}O$**. EBS curve showed similarity with following units and/or cycles:
    - *paleosols*: Unit 19 b)-d).
    - *transition zones*: Unit 14 b); Unit 10 (upper part between 6.10-6.00 m); Unit 9 a)-b)
    - *loess*: Unit 13 a) and partly b); Unit 7 (between 5.20-4.90 m); Unit 5 a)-b); Unit 3 e); Unit 2 b)-d).

5.3.4.4. HC versus EBS samples

- Comparison of HC and EBS curves - **$\delta^{13}C$**. Similarity was shown in the case of following units:
    - *paleosols*: Unit 15.
    - *transition zones*: Unit 14; Unit 10; Unit 9; Unit 8.
    - *loess*: Unit 18; Unit 13; Unit 5 (between 4.50-3.30 m); certain parts of Unit 2.

- Comparison of HC and EBS curves - **$\delta^{18}O$**. Similarity was shown in the case of following units:
    - *paleosols*: Unit 19; Unit 16-15.

5.3.5. Possible connections between δ13C and δ18O values

Linear regression was calculated for each unit and for each component (as bulk samples and certain secondary carbonates). The coefficient of determination (R^2) and the steepness of the slope were plotted on the same graph. The main aim was to determine the strength of connection between $\delta^{13}C$ and $\delta^{18}O$. Table summarizes those connections, which were worth to compare.

Strong connection ($R^2 \geq 0.70$)				**Moderate connection ($0.5 < R^2 < 0.70$)**			
				EBS	Transition	Unit 20	R^2=0.62
EBS	Transition	Unit 9	R^2 =0.75			Unit 8	R^2=0.69
HC	Transition	Unit 20	R^2=0.94	Bulk	Transition	Unit 20	R^2=0.61
		Unit 9	R^2=1.0			Unit 9	R^2=0.61
		Unit 8	R^2=0.84		Paleosol	Unit 16	R^2=0.69
	Paleosol	Unit 19	R^2=0.71	**No connection (R^2 ~ 0.00)**			
	Loess	Unit 18	R^2=0.81	EBS	Paleosol	Unit 19	R^2=0.00
Bulk	Transition	Unit 8	R^2=0.89			Unit 11	R^2=0.00
	Loess	Unit 18	R^2=0.88		Loess	Unit 4	R^2=0.00
		Unit 13	R^2=0.77	HC	Loess	Unit 4	R^2=0.00
		Unit 7	R^2=0.86	Bulk	Loess	Unit 2	R^2=0.02

5.3.6. Possible paleoenvironmental signals of bulk samples

5.3.6.1. Paleosols.

Three different paleosols were present in the studied part of the Villánykövesd Brickyard sequence: Unit 11 – as dark brown paleosol; Unit 16 – paleosol, dark reddish brown paleosol (with Unit 15, as reddish brown horizon of the same paleosol); and Unit 19 – dark greyish brown paleosol. The mentioned paleosols showed differences according to both of the $\delta^{13}C$ and $\delta^{18}O$ curves. Unit 11 and Unit 19 were both shifted towards the more positive direction, whereas the values of Unit 16 were present in more negative direction. This arrangement could point out on the differences between the

paleosol developmental phases. Possibly more enhanced vegetation cover and more moister conditions were characteristic of Unit 16 in comparison to the other two paleosols. The shift towards both of more negative $\delta^{13}C$ and $\delta^{18}O$ values indicates enhanced vegetation cover and higher available humidity (e.g. ALAM, M.S. et al. 1997; RAO, Z. et al. 2006 – see more details in the interpretation matrix, **Appendix 8**). Higher vegetation density may mean more closed vegetation habit, compared to the paleosols of Unit 11 and Unit 19.

AAR age determination method was carried out on mollusc samples from Unit 11 and Unit 16 by OCHES, E.A. – MCCOY, W.D. – KAUFMAN, D. (*personal communication, unpublished data*). The preliminary AAR results connected Unit 11 to the paleosol S2 of the Chinese stratigraphy system and thus to the MIS 7 interglacial phase. This may strengthen the correlation of Unit 11 to the 'Basaharc Double' pedocomplex. Independent age control provided data about the above lying loess units. Post-IR IRSL luminescence dating was carried out on samples from Unit 5 (3.40-3.30 m), which gave 168±22 ka age as result (NOVOTHNY, Á., *personal communication, unpublished data*). This part of Unit 5 belonged presumably to the MIS 6 glacial stage, which was followed by the MIS 7 interglacial and thus with the development of the 'Basaharc Double 1' paleosol.

During the investigation of the inactive brickyard, ÚJVÁRI, G. (2004) also localized the 'Basaharc Double' pedocomplex. Through malacological investigations ÚJVÁRI, G. (2004) determined low sedimentation rates, moderately humid conditions and opened vegetation cover during soil development. Based on malacostratigraphy, the pedocomplex could be linked to the *Helicopsis striata* subzone, which made a more clear connection to 'Basaharc Double'. This information is important for the understanding of the stable isotope values: the presented properties strengthen the reason, why are both carbon and oxygen isotope values shifted towards the more positive direction. The more positive direction means changes in the moisture regime: when Unit 16 was characterized by more humid conditions, than Unit 11 is only moderately humid in comparison (based on the observations of ÚJVÁRI, G. 2004).

The question was raised whether both parts of the 'Basaharc Double' pedocomplex were present in the current sequence. The investigation of the main Basaharc brickyard sequence showed 0.2-0.8 m loess intercalation between the double paleosol (PÉCSI, M. – HAHN, GY. 1987). In the current sequence 0.18 m thick loess intercalation was found (when the two transition zones, as Unit 12 and Unit 14 are not taken into account),

which may show parallels to the appearance in the main Basaharc sequence. Although the stratigraphical position may indicate that Unit 16 could be parallel to 'Basaharc Double 2', there are some reasons, which may not strengthen the idea. One reason is, that AAR investigations were carried out on mollusc samples from Unit 16, which gave an uncertain result as the paleosol is connected to S3 of the Chinese stratigraphy system and thus to MIS 9 and to the 'Basaharc Lower' paleosol (OCHES, E.A. – MCCOY, W.D. – KAUFMAN, D., *personal communication, unpublished data*). The soil structure of Unit 11 and Unit 16 is also different: Unit 11 showed granular structure, whereas Unit 16 had massive soil structure and indicated higher soil developmental stage. The general appearance of 'Basaharc Double 1-2' refers to weak to moderate soil development, whereas 'Basaharc Lower' paleosol is strongly developed and shows compact structure (as summarized by HORVÁTH, E. – BRADÁK, B. 2014). The stable carbon and oxygen isotope composition of Unit 11 and Unit 16 indicated significant differences between the past paleoenvironmental conditions, as in the availability of moisture and the habit of vegetation coverage. Different vegetation densities were indicated especially by the stable carbon isotope values: Unit 11 and Unit 19 seemed to have lower vegetation density and thus more opened vegetation cover, whereas Unit 16 was characterized by higher densities and more closed vegetation cover. This may indicate that Unit 16 was part of a warmer interglacial phase, when compared to Unit 11 and Unit 19 (based on RAO, Z. et al. 2006; CANDY, I. et al. 2012).

5.3.6.2. Transition zones and loess of Unit 18 and Unit 13

The tendency of both $\delta^{13}C$ and $\delta^{18}O$ showed the same pattern. The transition between the paleosols and towards the loess of Unit 7 was continuous upwards in the sequence – with tendencies towards the more negative or more positive direction. Gradual transition towards phases with moderate humidity and possibly more opened vegetation cover were present in Unit 20, Unit 14, Unit 12 and Unit 8 cycle b)-c). Transition to more humid conditions and possibly more closed vegetation cover were characteristic of Unit 18, Unit 9 and Unit 8 cycle a).

5.3.6.3. Loess

Different patterns were characteristic of $\delta^{13}C$ and $\delta^{18}O$ curves in the case of the loess units. According to $\delta^{13}C$ and $\delta^{18}O$ values, Unit 7 seemed to continue the shift towards the more positive values, as towards moderately humid/arid conditions and lower, more

opened vegetation densities – which were possibly more characteristic of dust deposition

The $\delta^{13}C$ curves of Unit 5 and Unit 3showed similarities in value range until ~3.00 m. Upwards in the sequence there were slight differences between the tendencies of Unit 5+4 (profile A) and Unit 3+2 (profile D). According to the $\delta^{18}O$ values, Unit 5+4 (profile A) and Unit 2 (profile D) showed similarities in range and tendency, with the exception of Unit 3. Unit 3 showed the same low peak at 3.58 m as Unit 5, but the value was in different range (as -9.12‰ for Unit 3 and -6.21‰ for Unit 5). The observations of both $\delta^{13}C$ and $\delta^{18}O$ values raised the question, whether paleotopographical position could play a role in the differentiation of values. Top, slope or valley bottom positions may be characterized by slightly dissimilar vegetation pattern and different water holding capacities.

The tendencies of the $\delta^{13}C$ and $\delta^{18}O$ curves showed differences for Unit 2. Gradual, but large shift towards the more negative direction was characteristic of $\delta^{13}C$ values from 1.80 m upwards in the section, whereas $\delta^{18}O$ values showed a larger shift towards the more positive direction upwards from 1.42 m (on the boundary of cycle d)-e)). No discordance or any signs of erosion were observed in Unit 2 on the field, but the mentioned shifts of the stable isotope values - especially the case of $\delta^{13}C$ - may indicate missing horizons. The graduality of the larger shift may be connected to the continuous effects of bioturbation, which homogenized the matrix during dust accumulation and the built-up of the sequence. Bioturbation seemed to "hide" the signs of former erosion. As a sign of effective bioturbation the structure of loess was granular in whole Unit 2.

5.3.7. Possible paleoenvironmental signals of secondary carbonates

5.3.7.1. HC

Gradual transition towards the mean value and thus towards the more positive direction was observed in the case of $\delta^{13}C$ and $\delta^{18}O$ curves of Unit 20, Unit 19 and Unit 18. According to the determination coefficient (R^2), strong connections were characteristic of these units. The tendency of curves present for Unit 19 showed certain similarities with bulk samples in the case Unit 19 cycle b) (both for $\delta^{13}C$ and $\delta^{18}O$ values) and with EBS in the case of Unit 19 cycles b)-d) (just for $\delta^{18}O$). $\delta^{13}C$ and $\delta^{18}O$ signals were still present in the more negative direction, which may strengthen the idea of the presence of

enhanced vegetation and available organic matter under (at least seasonally) moister conditions (see **Appendix** 8. for explanations).

The $\delta^{13}C$ values Unit 15-16 and Unit 11 paleosol were present in the more positive direction, which may indicate less enhanced vegetation cover (or aridity, see general **Appendix 8** for explanations). The $\delta^{18}O$ signals were present in the more positive direction or close to the mean value in the more negative direction. This may show less humid conditions, when compared to the values of Unit 20-18.

The observations of Unit 15-16 seemed to be contradictory when compared to the interpretation of bulk Unit 16 values. The possibility was raised whether such phenomenon is connected to certain characteristics of the vegetation cover. Unit 16 paleosol was interpreted to be developed under moister conditions and more closed vegetation cover and its bulk values reflected the effects of the produced biomass in total (as connected to grass species, herbs, shrubs and trees). But HC is thought to be developed under around grass species, which are connected to surfaces dominated by opened steppe vegetation (e.g. BECZE-DEÁK, J. et al. 1997). It could be possible, that the stable isotope composition of HC was connected to patches of opened vegetation and/or reflect the seasonality.

The highest scattering of $\delta^{13}C$ values was observed in Unit 5, which seemed to be atypical for loess in the case of the Villánykövesd Brickyard sequence when compared to the other loess units of the section. $\delta^{18}O$ did not seem to have such large amplitude fluctuations.

The $\delta^{13}C$ values of Unit 2 and Unit 1 showed upwards decreasing tendencies (with the exception of the uppermost value at 0.40 m). Shift towards the more negative direction may indicate slightly higher densities (e.g. LIU, W. et al. 2011, see **Appendix 8** for more details), which may be connected to the decrease of dust accumulation rates. When dust accumulation rates get lower and sedimentation slows down, the microecosystem has broader ecological niche and their biomineralized products will reflect the presence of more enhanced organic matter and the effects of higher CO_2 levels in the strata (CATT, J.A. 1990; BECZE-DEÁK, J. et al. 1997).

5.3.7.2. HC+CC

The comparison of $\delta^{13}C$ curves of HC+CC and HC showed more similarities, since the HC components of both features were formed in the same soil/sediment matrix and reflected synsedimentary effects. Difference was characteristic of the $\delta^{18}O$ curves,

which may reflect the postsedimentary formation effect of the CC component. Similarity of $\delta^{18}O$ curves of HC+CC and CC may indicate contemporaneous and/or repeated infiltration or leaching during the sedimentation phase. Dissimilar $\delta^{18}O$ curves may indicate infiltration or leaching processes, which happened after the sedimentation phase and derived from meteoric water of other stable isotope composition. It should be taken into account, that the Villánykövesd area was under the influence of submediterranean effects (as presented e.g. in HUM, L. 2001 and HUM, L. et al. 2006), which had local influence on the composition of meteoric water and thus effected isotopically the infiltrating solutions.

5.3.7.3. EBS

The tendencies of $\delta^{13}C$ and $\delta^{18}O$ curves showed similarities to the bulk and HC curves in certain cases. Coincidence was present in tendency with the transition zone of Unit 8 concerning bulk and HC $\delta^{13}C$ curves. Certain similarity with both HC and bulk curves was present for $\delta^{13}C$ in the case of Unit 19 and Unit 11: although the tendency was mainly the same, the values of Unit 19 were present in the more positive direction, whereas values of Unit 11 were in the more negative direction. Similarity with bulk $\delta^{18}O$ of Unit 19 cycle b)-d) showed values and tendency in the same (more negative) direction. The transition zones of Unit 14, Unit 10 and Unit 9 showed also similarities with both HC and bulk curves of $\delta^{18}O$.

Strong or moderately strong connection was shown between $\delta^{13}C$ and $\delta^{18}O$ values, based on the determination coefficient (R^2) for the transition zones of Unit 20, Unit 9 and Unit 8. No connection was shown between $\delta^{13}C$ and $\delta^{18}O$ in the case of Unit 19 and Unit 11 paleosols, although similar tendencies were present with bulk and HC curves for these units. Two possibilities should be considered: 1) bioturbation was possibly more enhanced in these paleosols and especially in their transition zones; and 2) the life range of earthworms was possibly larger according to the submediterranean climatic influence (as introduced by HUM, L. 2001 and HUM, L. et al. 2006), thus it lowered the zone of soil frost. Earthworms may have consumed soil/organic matter of slightly different stable carbon isotope composition during their bioturbating “route” in the strata.

6. Conclusions

6.1. Characteristics of the studied loess-paleosol sequences

6.1.1. Characteristics of paleosols

6.1.1.1. Observations in the case of local paleosol variations

Paleosols may have locally different appearances due to their paleotopographic position. Such case was discovered for the Verőce sequence (BRADÁK, B. et al. 2014), where the paleosol variations developed in valley bottom, paleoslope and local top positions. These variations of the P4 paleosol contained HC, which was characterized by different stable carbon and oxygen isotope values.

The valley bottom paleosol showed such $\delta^{18}O$ and $\delta^{13}C$ values, which were shifted towards the more positive direction, whereas the stable isotope values of HC in the case of the local top paleosol variation showed shifts towards the more negative direction. The paleosol variation, which was developed in paleoslope position, showed both tendencies. The stable carbon and oxygen isotope values of HC were applicable to show fine differences between the development of these paleosol variations at the Verőce sequence, as in the comparison of vegetation densities and evaporative effects.

6.1.1.2. Observations concerning different paleosol types of the same sequence

Stable carbon and oxygen isotope values of bulk samples were applicable to show different characteristics in value range and tendencies among the paleosol - as it was observed at the Villánykövesd Brickyard sequence. The $\delta^{13}C$ and $\delta^{18}O$ values suggested that paleosol Unit 16 was developed under more humid conditions and under higher vegetation densities, whereas the paleosols of Unit 19 and Unit 11 denoted aridity and lower vegetation densities. A comparison method was applied to refine the interpretation of the observed tendencies. Based on AAR data (OCHES, E.A. – MCCOY, W.D. – KAUFMAN, D., *personal communication, unpublished data*), Unit 11 paleosol was recognized as a member of the 'Basaharc Double' pedocomplex – which made possible to consider the malacological observations of ÚJVÁRI, G. (2004), who studied a different part of the brickyard, but localized and investigated the mentioned pedocomplex. Malacological analysis showed that Unit 11 developed under moderately humid conditions and opened vegetation cover. This information strengthened the explanation of stable isotope values for Unit 11 and refined the presumed aridity factor to moderately humid. Since value range and tendencies were similar to those of Unit 19,

the development of Unit 19 paleosol was characterized by the same properties as of Unit 11.

The $\delta^{13}C$ values of HC showed the same tendencies for Unit 11, as it was presented by the bulk values. The same shift towards the more positive direction was characteristic of Unit 16 – based on the $\delta^{13}C$ values of HC, which sounds contradictory when compared to the bulk values. The possibility was raised whether such phenomenon is connected to certain characteristics of the vegetation cover. Unit 16 paleosol was interpreted to be developed under moister conditions and more closed vegetation cover and its bulk values reflected the effects of the produced biomass in total (as connected to grass species, herbs, shrubs and trees). But HC is thought to be developed under around grass species, which are connected to surfaces dominated by opened steppe vegetation (e.g. BECZE-DEÁK, J. et al. 1997). It could be possible, that the stable isotope composition of HC was connected to patches of opened vegetation and/or reflect the seasonality.

6.1.1.3. Observations of paleosols between different sequences

The studied three sequences, as Verőce, Paks and Villánykövesd followed a North-(North-Eastern) – South-(South-Western) transect. Comparison of sites had certain difficulties, since these sequences were quasi-continuous and the sedimentological units were not overlapping in the time range of formation in every case. As a connecting link, the 'Basaharc Double 1' (BD1) paleosol was recognized in the Paks and Villánykövesd sequences. 'Basaharc Double 1' paleosol at Paks was characterized by decreasing $\delta^{13}C$ and $\delta^{18}O$ values of bulk samples towards the more negative values upwards in the paleosol, whereas the same paleosol in the Villánykövesd sequence showed gradually increasing values towards the more positive direction. The calculated mean values for both paleosol versions showed similarities in the $\delta^{18}O$ value (as -7.16‰ for BD1 at Paks and as -7.67‰ for BD1 at Villánykövesd), but the mean $\delta^{13}C$ was different (as -7.52‰ for BD1 at Paks and as -9.05‰ for BD1 at Villánykövesd). The development of both paleosols were characterized by moderately humid conditions based on the $\delta^{18}O$ values, but regionally differences were shown in the tendency of the $\delta^{18}O$ curves. During the development of BD1 paleosol at Villánykövesd, it tended to shift from the moderately humid conditions towards the direction of aridity – as indicated by the increasing tendency of the $\delta^{18}O$ curve. The development of BD1 paleosol at Paks showed the opposite tendency, it tended to show a slight shift towards the humid direction from the

moderately humid conditions. The $\delta^{13}C$ values indicated opened vegetation cover for both BD1 variations, but the difference in the tendencies suggested that BD1 variation at Villánykövesd tended to develop under even more opened vegetation coverage, whereas the BD1 variation at Paks showed the opposite and tended to develop under slightly more closed vegetation cover. The difference of the exact values and value ranges could possibly be connected to paleosol development in different topographical positions, to differences in exposure or may reflect regional variations of the local flora and thus available organic matter.

6.1.1.4. Observations from transition zones

Transition zones were present in two different positions within the sequences: 1) above the paleosols (as sediment/soil transition), where the influence of sedimentation had an important role; and 2) below the paleosols (as soil/sediment transition), which were mainly caused by bioturbation effects.

The transition zones showed different patterns according to their stable isotope composition within the studied sequences. In the C-12 transition zone at the Verőce site (the overlying of the P4-C paleosol of local top position) the $\delta^{18}O$ values of HC were present almost in the same negative range, as those of the P4-C paleosol - but with slightly increasing tendency upwards. The $\delta^{13}C$ values of HC also seemed to follow the pattern of P4-C paleosol, as staying in the more positive direction – also with slightly increasing tendency upwards. These similarities suggested that the transition from the paleosol towards dust accretion happened gradually (e.g. BECZE-DEÁK, J. et al. 1997). The C-3 transition zone (overlying of P2-C) at the Verőce site showed the same prominent tendency, as both $\delta^{13}C$ and $\delta^{18}O$ values tended to shift towards the more positive direction. These tendencies indicated transition in the paleoenvironmental conditions, as indicating that the vegetation cover changed its habit (transition to lower vegetation density) and as indicating that the moisture conditions changed as well (transition from humid towards moderately humid or arid). Different pattern was characteristic of the C-9 transition zone (underlying of P3-C) at the Verőce site, as both $\delta^{13}C$ and $\delta^{18}O$ values of HC shifted towards the more negative direction and showed similarities to the stable isotope composition of P3-C. These tendencies of HC were possibly the first signs of the climatic change towards the interglacial phase (e.g. RAO, Z. et al. 2006), since dust accretion rates were probably lowered, vegetation cover

became more enhanced and more available organic matter were present in the strata as a forerunner of soil development (e.g. BECZE-DEÁK, J. et al. 1997).

Two transition zones were present at the Paks sequence: Unit 8 was overlying of the 'Basaharc Double 1' paleosol and Unit 10 was found beneath BD1. The underlying Unit 10 showed gradual transition towards the BD1, but the $\delta^{13}C$ and $\delta^{18}O$ curves showed similarities in tendency only in the uppermost half and no connection was shown between them. The lack of connection may be caused by effects of bioturbation, which mixed the sediment with the material of the paleosol. Signs of bioturbation were also present in the form of crotovinas. The $\delta^{13}C$ and $\delta^{18}O$ values of HC followed the upwards decreasing tendency of the bulk curve, but the $\delta^{13}C$ and $\delta^{18}O$ values of HC showed moderate connection. Moderate connection was possible, since HC has synsedimentary characteristics and reflected the formation conditions and not the effects of bioturbation. Unit 8 (overlying of BD1 paleosol) was characterized by similar tendencies of $\delta^{13}C$ and $\delta^{18}O$ values, which showed upwards increasing habit with large fluctuations. Unit 8 could be divided into four subunits based on the field observations, which showed certain coincidence with the determined cycles of the stable isotope curves of bulk and HC samples. Bulk samples of Unit 8 showed strong connections between $\delta^{13}C$ and $\delta^{18}O$ values, whereas $\delta^{13}C$ and $\delta^{18}O$ values of HC and the bulk samples of the subhorizon Unit 8b showed moderate connections. The pattern of $\delta^{13}C$ and $\delta^{18}O$ HC curves showed the same high amplitude fluctuations. Especially since the connections between $\delta^{13}C$ and $\delta^{18}O$ of bulk and HC samples were quite strong, therefore both tendencies of stable isotope values suggested a larger amplitude climatic shift during the transition.

The bulk samples of the Villánykövesd transition zones showed gradual, continuous tendencies towards the overlying paleosols and loesses. Connections between $\delta^{13}C$ and $\delta^{18}O$ of bulk and HC samples were strong or moderately strong in many of these zones. Transitions, which were overlyings of paleosols showed different patterns: Unit 14 (overlying of Unit 15-16 paleosol) referred to a transition towards moderately humid conditions and more opened vegetation cover, whereas Unit 10 (the overlying of Unit 11 paleosol, 'Basaharc Double 1') represented possibly a transition towards more humid conditions and more closed vegetation cover. It has to be considered, that bulk stable isotope compositions of those transitions, which are underlyings of paleosols (as Unit 20 and Unit 12) can be influenced by bioturbation effects and thus reflect partly connections to the stable isotope composition of the paleosols.

6.1.1.5. Observations from loesses

The shift of bulk and HC $\delta^{13}C$ values towards the more positive direction was characteristic of loess units, especially in L4-C and L3-C at Verőce site, Unit 7 at Villánykövesd site and Units 7, -5, -4 at Paks site. This tendency referred to a shift towards moderately humid or arid conditions with lower vegetation densities. The more opened vegetation coverage can be linked to the patchy vegetation habit, which was characteristic of dust deposition and loess formation (e.g. BECZE-DEÁK, J. et al. 1997).

Larger amplitude shifts of $\delta^{13}C$ and $\delta^{18}O$ bulk values were characteristic of Unit 1 at the Paks sequence. Based on the curves and fluctuations of $\delta^{13}C$ and $\delta^{18}O$ values, Unit 1 was ordered into certain cycles. The boundary of cycles indicated the large amplitude shifts, where the stable isotope values altered significantly on both sides of the boundary. Connection between bulk $\delta^{13}C$ and $\delta^{18}O$ values was strong, whereas $\delta^{13}C$ and $\delta^{18}O$ values of HC showed moderate connection. No signs of erosion or missing horizons were recognizable on the field and this loess unit seemed to be macroscopically homogeneous and continuous, however, the larger shifts indicated possibly missing horizons. The presented shifts were large, but gradual, which may indicate the followings: after a possible erosion event dust accumulation and the built-up of the sequence continued and was contributed by the continuous effects of bioturbation. Bioturbation mixed and homogenized the freshly accreted dust and freshly produced organic matter with the buried horizon and thus seemed to hide the signs of the former erosion. Hiatuses were recognized in Unit 1 by the luminescence dating results of THIEL, C. et al. (2014).

The tendencies of bulk $\delta^{13}C$ and $\delta^{18}O$ values showed differences in Unit 2 of the Villánykövesd sequence. No connection was present among the bulk $\delta^{13}C$ and $\delta^{18}O$ values. Gradual, but large shifts towards the negative direction were characteristic of $\delta^{13}C$ values upwards from 1.80 m, whereas $\delta^{18}O$ values showed the opposite tendency (shift towards the more positive direction) upwards from 1.42 m. This observation could possibly be explained in the same way, as in the former paragraph for Paks: bioturbation mixed possibly the freshly accumulated material and produced organic matter with the buried horizon and thus hide the signs of former hiatus. Enhanced bioturbation was visible along whole Unit 2 on the field. The Villánykövesd sequence contains possibly more hiatuses, since not all paleosols were present in the site suggested in the

Hungarian loess stratigraphy (based on own investigation and former studies as ÚJVÁRI, G. 2004 and HUM, L. et al. 2006).

6.2. Observations of certain secondary carbonates

6.2.1. The role of soil-like HC

Reworked layers of the Verőce sequence contained whole, non-detrital soil-like HC, which was possibly formed in the following ways: 1) formed after the translocation process ended; or 2) the translocation process was slow enough and the formation of HC was simultaneous with the process. For instance, HC found in L3r is composed of a strongly mixed up materials and seems to be the impregnation of loess, sand and soil at the same time. (BRADÁK, B. et al. 2014).

Soil-like HC was found in loess units as well. For instance the Unit L5-C at the Verőce site contained soil-like HC besides the sediment-like ones in its uppermost part, below the P4-C paleosol of local top position. This appearance was guided by the presence of higher amount of EBS and CRC, which also indicated the stability of the former surface. Possibly the dust accumulation rates started to decrease towards the interglacial phase and organic matter accumulation became denser, according to the theory of the pedosedimentary profile development (e.g. BECZE-DEÁK, J. et al. 1997). The higher availability of organic matter led to the different appearance of HC, which was marked as soil-like HC, since it formed through the impregnation of the available matrix. The $\delta^{13}C$ values of HC were shifted towards the more negative direction, which may indicate that the vegetation cover became more dense until the soil developmental phase begun (e.g. RAO, Z. et al. 2006).

6.2.2. Applicability of HC+CC

The $\delta^{13}C$ and $\delta^{18}O$ values and tendencies of HC and HC+CC features were compared to each other and different observations were made. The calculations for the Verőce site showed only slight differences, the values showed almost the same. The tendency of HC+CC curves followed the same tendency as of HC along the sequence. Although the calculated differences for the Paks site were slightly larger, the tendencies of HC+CC were similar to those of HC, also concerning the amplitude of fluctuations.

In the case of the Villánykövesd sequence the comparison of $\delta^{13}C$ curves of HC+CC and HC showed similarities, which is due to the general fact that HC components of

both features were formed in the same soil/sediment matrix and reflected synsedimentary effects. The comparison of $\delta^{18}O$ curves showed two different characteristics: 1) tendencies were similar between HC and HC+CC, which may indicate contemporaneous and/or repeated infiltration or leaching during the sedimentation phase; and 2) tendencies were different, which may reflect the postsedimentary formation effect of the CC component. In the latter case the infiltration or leaching processes happened after the sedimentation phase and derived from meteoric water of other stable isotope composition.

Certain conclusions may be drawn. Based on the observations it is possible that the analysis of the relationship between HC and HC+CC is not functioning well in the Southern regions of Hungary, since this area was under the influence of submediterranean effects (as it was presented for Villánykövesd by HUM, L. 2001 and HUM, L. et al. 2006). This submediterranean effect had local influence on the composition of meteoric water and on the amount of infiltrating water – and thus effected isotopically the infiltrating solutions and the formation of the CC lining on the inner channel wall of HC. The stable carbon isotope composition of the HC component of HC+CC remained mainly unaltered, since it formed below the same surface and under the same circumstances as the synsedimentary HC.

6.2.3. The role of EBS

High amount of EBS denotes the stability of the environment and the former surface (BECZE-DEÁK, J. et al. 1997). The presence of EBS in increasing amount towards the P4 paleosol versions of the Verőce sequence was characteristic of the L5-C and L5-D units. These EBS were whole and non-detrital, which denotes that they lacked the effects of translocation (BECZE-DEÁK, J. et al. 1997). Especially when higher amount of EBS in a horizon is connected with higher amount of CRC and HC, or when soil-like HC is also present – it strengthens the theory that the surface became more stable, whereas dust accumulation rates were decreasing and the microecosystem had a more adequate niche in the sediment. This appearance may lead to the formation of humus accumulation zones, which can be the first step during soil development.

The $\delta^{13}C$ and $\delta^{18}O$ curves of EBS were not unequivocal to interpret in every case, although they showed similarities to bulk and HC values. The general observation was that $\delta^{13}C$ and $\delta^{18}O$ curves of EBS showed a zigzag fluctuation pattern. This pattern of

$\delta^{13}C$ values was in between a range, which mostly reflected the dietary habits and uptake of the earthworms (KOENIGER, P. et al. 2014), therefore it was complicated to connect it with the values of other samples. Tendencies of $\delta^{18}O$ were more applicable for usage similar to the other secondary carbonates, since it reflects the composition of the meteoric water (e.g. CERLING, T.E. 1984).

Strong or moderately strong connection was shown between $\delta^{13}C$ and $\delta^{18}O$ values of EBS for the following transition zones of the Villánykövesd sequence: Unit 20, Unit 9 and Unit 8, whereas the transition zones of Verőce and Paks lacked this connection.

No connection was shown between $\delta^{13}C$ and $\delta^{18}O$ of EBS in the case of Unit 19 and Unit 11 paleosols of the Villánykövesd sequence, although similar tendencies were present with bulk and HC curves for these units. Two possibilities should be considered: 1) bioturbation was possibly more enhanced in these paleosols; and 2) the life range of earthworms was possibly larger according to the submediterranean climatic influence (as introduced by HUM, L. 2001 and HUM, L. et al. 2006), thus it lowered the zone of groundwater level and soil frost. Earthworms may have consumed soil/organic matter of slightly different stable carbon isotope composition along their bioturbation route in the strata.

6.3. Questions of applicability of the stable isotope signals of bulk samples and secondary carbonates

6.3.1. Possibilities of application

The stable carbon and oxygen isotope composition of bulk and secondary carbonate samples seemed to be applicable for the analysis of individual sequence development.

Larger amplitude shifts of bulk $\delta^{13}C$ and $\delta^{18}O$ values indicated the possibility of hiatuses in such loess units, which seemed to be relatively homogeneous and lacked signs of erosion based on field observations. These shifts were characterized by gradual tendencies, which possibly indicated the effects of continuous bioturbation: bioturbation mixed and homogenized the freshly accreted dust and freshly produced organic matter with the buried horizon and thus seemed to hide the signs of the hiatuses.

In the case of the analysed three loess-paleosol sequences, certain similarities and fluctuations were observed in the $\delta^{13}C$ and $\delta^{18}O$ curves of bulk and secondary carbonate samples in certain cases, which were divided into small cycles. For a deeper understanding on the habit of these cycles and their paleoenvironmental role other

proxies would be useful – as the examination of magnetic susceptibility or further malacogical studies.

6.3.2. Difficulties of application

The comparison of stable isotope data between loess-paleosol sequences of different geographical localities can be complicated. On the one hand, regionally different climatic conditions cause differences in the amount and stable isotope composition of meteoric water and thus also lead to the alterations of the water household characteristics – which influences locally the stable isotope composition both of bulk and secondary carbonate samples. On the other hand, regionality influences both the flora and fauna elements and type of vegetation cover and thus the availability of organic matter in the strata – which will also be reflected in the stable isotope composition both of bulk and secondary carbonate samples among the localities.

Topographic position is also an important influencing factor, as it was shown in the case of the three paleosol variations at the Verőce site. Each of the paleosol variations of P4 were located in another position, as local top, paleoslope and valley bottom situations. These variations were characterized by different stable isotope patterns and tendencies according to the composition of analysed secondary carbonate types.

It was difficult to synchronize stable isotope curves in the case of certain secondary carbonates, because some other factors were important to consider. Such as in the case of EBS, in which the dietary uptake influenced $\delta^{13}C$ values (KOENIGER, P. et al. 2014). During interpretation it should also be taken into account, that the $\delta^{18}O$ values of EBS were possibly also influenced by seasonal changes of local meteoric water and thus of available soil moisture (VERSTEEGH, E.A.A. et al. 2013; PRUD'HOMME, C. et al. 2016).

6.4. Concluding thoughts

The stable carbon and oxygen isotope composition of bulk and secondary carbonate samples is a descriptive proxy, which provides an outline to the development history of the sequence. It seems that the method in itself is applicable in only fortunate cases, but more frequently it is needed to combine this method with other proxies (e.g. with malacological investigations, as it was introduced for the Villánykövesd sequence by ÚJVÁRI, G. 2004).

The method in itself is not advised to use for the correlation of loess-paleosol sequences from different localities. However, it is seems to be applicable for the comparison of paleoenvironmental signals of such horizons, which were correlated formerly by using luminescence dating or AAR methods – or when specific marker horizons are present. It is always important to take paleotopographic positions into account during the application of the method.

Stable isotope analysis as a proxy is different from other ones (e.g. from magnetic susceptibility), since the results reflect local paleoenvironmental changes and cannot be effectively expanded on a regional basis – at least in the case of the studied loess-paleosol sequences of the Carpathian Basin.

Stable carbon isotopes are used to determine the characteristics of the former vegetation cover (as low or high vegetation density was present) and thus the availability of organic matter in the system, whereas stable oxygen isotope compositions denote the changes of the former moisture regime and refer to the presence or absence of strong evaporation (e.g. CERLING, T.E. 1984, ALAM, M.S. et al. 1997, LIU, W. et al. 2011).

The applicability of the stable isotope analysis method for bulk samples and secondary carbonates could be improved when the following two thoughts are considered: during the interpretation of signals other proxies should be used as well, especially regarding the analysis of different amplitude fluctuations in the $\delta^{13}C$ and $\delta^{18}O$ curves; and several profiles should be excavated and analysed at the same location, which makes possible the recognition of paleotopography and help the understanding of different stable isotope patterns.

7. Acknowledgements

I would like to say thank you to my supervisor, Erzsébet Horváth, who was helping me until the very last moment. I owe thanks to Manfred Frechen and thus to the Leibniz Institute for Applied Geophysics, Section S3, who made me possible to carry out all the stable analysis measurements and who welcomed me during all my stay in Hannover. I say thank you also to Paul Königer, Astrid Jaeckel, Sonja Riemenschneider, Christine Thiel, Detlev Klosa and all the members of Section S3. I thank my colleagues for the support, as Balázs Bradák, Ágnes Novothny, Tamás Végh, Klaudia Kiss, Veronika Iván, Fatima Eisam Eldeen, Judit Szabó, Tamás Biró, Márton Deák, Mátyás Árvai and Balázs Kohán. I am grateful for the help with the field work, especially for István Milinkó, Balázs Vígh, Viktória Csiki, Balázs Csatai, Nikolett Dudás, Attila Csernátoni and Árpád Székely. I am thankful for the support of my friends, especially for the motivation, as Nikoletta Kovács, Gabriella Heidrich, Emőke Fodor, Tamás Toplak, Viola Pfening, Krisztina Dobos, András Egyed, and the Havasi Gyopár. I say thank you to my Mother and to my two favourite cousins, Erzsébet Pataki and Zsuzsanna Pataki. I hope I haven't forgotten anybody... And Quaternary Rebellz rock!

8. References

ALAM, M.S. – KEPPENS, E. – PAEPE, R. 1997. The use of oxygen and carbon isotope composition of pedogenic carbonates from Pleistocene palaeosols in NW Bangladesh, as palaeoclimatic indicators. *Quaternary Science Reviews 16*, pp. 161-168.

ANTOINE, P. – ROUSSEAU, D.-D. – ZÖLLER, L. – LANG, A. – MUNAUT, A.-V. – HATTÉ, C. – FONTUGNE, M. 2001. High-resolution record of the last Interglacial-glacial cycle in the Nussloch loess-palaeosol sequences, Upper Rhine Area, Germany. *Quaternary International 76/77*, pp. 211-229.

ANTOINE, P. – ROUSSEAU, D.-D. – MOINE, O. – KUNESCH, S. – HATTÉ, C. – LANG, A. – TISSOUX, H. – ZÖLLER, L. 2009a. Rapid and cyclic aeolian deposition during the Last Glacial in European loess: a high-resolution record from Nussloch, Germany. *Quaternary Science Reviews 28*, pp. 2955-2973.

ÁDÁM, L. – MAROSI, S. – SZILÁRD, J. 1954. A paksi löszfeltárás. *Földrajzi Közlemények 78/3*, pp. 239-254. ("The loess sequence of Paks", in Hungarian)

BAJNÓCZI, B. - KOVÁCS-KIS, V. 2006: Origin of pedogenic needle-fiber calcite revealed by micromorphology and stable isotope composition – a case study of a Quaternary paleosol from Hungary. *Chem. Erde - Geochem. 66*, pp. 203-212.

BAL, L. 1977: The formation of carbonate nodules and intercalary crystals in the soil by the earthworm *Lumbricus rubellus*. *Pedobiologia 17*, pp. 102-106.

BARTA, G. 2011a. Secondary carbonates in loess-paleosoil sequences: a general review. *Central European Journal of Geosciences 3/2*, pp. 129-146.

BARTA, G. 2011b. The structure of loess dolls – a case study from the loess-paleosoil sequence of Süttő, Hungary. *Journal of Environmental Geography 4/1-4*, pp. 1-10.

BARTA, G. 2014. Paleoenvironmental reconstruction based on the morphology and distribution of secondary carbonates of the loess-paleosol sequence at Süttő, Hungary. *Quaternary International 319*, pp. 64-75.

BECZE-DEÁK, J. 1997. Study of secondary $CaCO_3$ in the frame of geopedological research and reconstruction of the environment evolution of the last interglacial – early glacial sequence at the Wallertheim Site (Rheinhessen – Germany). *PhD Thesis*, University of Gent, Belgium, 1997

BECZE-DEÁK, J. - LANGOHR, R. - VERRECCHIA, E.P. 1997. Small scale secondary $CaCO_3$ accumulations in selected sections of the European loess belt. Morphological

forms and potential for paleoenvironmental reconstruction. *Geoderma 76*, pp. 221-252.

BERNER, R.A. 1968. Rate of concretion growth. *Geochimica et Cosmochimica Acta 32*, pp. 477-483.

BLOCKHUIS, W.A. - PAPE, TH. - SLAGER, S. 1968. Morphology and distribution of pedogenic carbonate in some Vertisols of the Sudan. *Geoderma 2*, pp. 173-200

BOGUCKYJ, A.B. – ŁANCZONT, M. – ŁĄCKA, B. – MADEYSKA, T. – ZAWIDSKI, P. 2006. Stable isotopic composition of carbonates in Quaternary sediments of the Skala Podil'ska sequence (Ukraine). *Quaternary International 152-153*, pp. 3-13.

BORSATO, A. – FRISIA, S. – JONES, B. – VAN DER BORG, K. 2000: Calcite moonmilk: crystal morphology and environment of formation in caves in the Italian Alps. *Journal of Sedimentary Research 70/5*, pp. 1179-1190.

BRADÁK, B. – KISS, K. – BARTA, G. – VARGA, GY. – SZEBERÉNYI, J. – NOVOTHNY, Á. – SZALAI, Z. – MÉSZÁROS, E. – MARKÓ, A. 2013. Lokális talajváltozatok a verőcei téglagyár környezetében – a Pécsi-féle löszrétegtan nyitott kérdései. (Local variations of paleosols in the brick-yard of Verőce – questions of Pécsi's loess-stratigraphy). *Földrajzi Közlemények 137/3*, pp. 312-322. (in Hungarian, abstract is available in English)

BRADÁK, B. – KISS, K. – BARTA, G. – VARGA, GY. – SZEBERÉNYI, J. – JÓZSA, S. – NOVOTHNY, Á. – KOVÁCS, J. – MARKÓ, A. – MÉSZÁROS, E. – SZALAI, Z. 2014. Different paleoenvironments of Late Pleistocene age identified in Verőce outcrop, Hungary: Preliminary results. *Quaternary International 319*, pp. 119-136.

BRINZA, L. - QUINN, P.D. - SCHOFIELD, P.F. - MOSSELMANS, J.F.W. - HODSON, M.E. 2013: Incorporation of strontium in earthworm-secreted calcium carbonate granules produced in strontium-amended and strontium-bearing soil. *Geochimica et Cosmochimica Acta 113*, pp. 21-37.

BRIONES, M.J.I. - LÓPEZ, E. - MÉNDEZ, J. - RODRÍGUEZ, J.B. - GAGO-DUPORT, L. 2008a: Biological control over the formation and storage of amorphous calcium carbonate by earthworms. *Mineralogical Magazine 72(1)*, pp. 227-231.

BRIONES, M.J.I. - OSTLE, N.J. - PIEARCE, T.G. 2008b: Stable isotopes reveal that the calciferous gland of earthworms is CO_2-fixing organ. *Soil Biology & Biochemistry 20*, pp. 554-557.

BUDD, D.A. – PACK, S.M. – FOGEL, M.L. 2002. The destruction of paleoclimatic isotopic signals in Pleistocene carbonate soil nodules of Western Australia. *Palaeogeography, Palaeoclimatology, Palaeoecology 188*, pp. 249-273.

BULLA, B. 1933. Morfológiai megfigyelések magyarországi löszös területeken. *Földrajzi Közlemények 61/7*-8, pp. 169-201. ("Morphological observations on the loess covered areas of Hungary"; in Hungarian)

BULLOCK, P. – FEDOROFF, N. – JONGERIUS, A. – STOOPS, G. 1985. Handbook for soil thin section description. Waine Research Publications, Wolderhampton, 150 p.

CAILLEAU, G. - VERRECCHIA, E.P. - BRAISSANT, O. - EMMANUEL, L. 2009a: The biogenic origin of needle fibre calcite. *Sedimentology 56*, pp. 1858-1875.

CAILLEAU, G. – DADRAS, M. – ABOLHASSANI-DADRAS, S. – BRAISSANT, O. – VERRECCHIA, E.P. 2009b: Evidence for an organic origin of pedogenic calcitic nanofibres. *Journal of Crystal Growth 311*, pp. 2490-2496.

CANADELL, J. – JACKSON, R.B. – EHLERINGER, J.R. – MOONEY, H.A. – SALA, O.E. – SCHULZE, E.-D. 1996. Maximum rooting depth of vegetation types at the global scale. *Oecologia 108*, pp. 538-595.

CANDY, I. – ADAMSON, K. – GALLANT, C.E. . WHITFIELD, E. – POPE, R. 2012. Oxygen and carbon isotopic composition of Quaternary meteoric carbonates from western and southern Europe: Their role in paleoenvironmental reconstruction. *Palaeogeography, Palaeoclimatology, Palaeoecology 326-328*, pp. 1-11.

CANTI, M.G. 1997. An investigation of microscopic calcareous spherulites from herbivore dungs. *Journal of Archeological Science 24*, pp. 219-231.

CANTI, M. 1998a. Origin of calcium carbonate granules found in buried soils and Quaternary deposits. *Boreas 27*, pp. 275-288

CANTI, M.G. 1998b. The micromorphological identification of faecal spherulites from archeological and modern materials. *Journal of Archeological Science 25*, pp. 435-444.

CANTI, M.G. 2009. Experiments on the origin of ^{13}C in the calcium carbonate granules produced by the earthworm *Lumbricus terrestris*. *Soil Biology and Biochemistry 41*, pp. 2588-2592.

CANTI, M.G. - PIEARCE, T.G., 2003: Morphology and dynamics of calcium carbonate granules produced by different earthworm species. *Pedobiologia 47*, pp. 511-521.

CATT, J.A. 1990. Paleopedology manual. *Quaternary International 6*, pp. 1-95.

CEGŁA, J. 1969. Influence of Capillary Ground Moisture on Eolian Accumulation of Loess. *Loess Letter 13*, 1985, pp. 3-4.

CERLING, T.E. 1984. The stable isotopic composition of modern soil carbonate and its relationship to climate. *Earth Planetary Science Letters 71*, pp. 229-240.

CERLING, T.E. – QUADE, J. – WANG, Y. – BOWMAN, R. 1989. Carbon isotopes in soils and palaeosols as ecology and palaeoecology indicators. *Nature 341*, pp. 138-139.

CERLING, T.E. – SOLOMON, D.K. – QUADE, J. – BOWMAN, J.R. 1991. On the isotopic composition of carbon in soil carbon dioxide. *Geochimica et Cosmochimica Acta 55*, pp. 3403-3405.

CERLING, T.E. - QUADE, J. 1993. Stable carbon and oxygen isotopes in soil carbonates. In: SWART, P.K. - LOHMANN, K.C. - MCKENZIE, J. - SAVIN, S. (Eds.): Climate Change in Continental Isotopic Records, *Geophysical Monograph 78*, AGU, pp. 217–231.

CILEK, V. 2001. The loess deposit of the Bohemian Massif: silt provenance, palaeometeorology and loessification processes. *Quaternary International 76/77*, pp. 123-128.

CRAMER, M.D. – HAWKINS, H.-J. 2009. A physiological mechanism for the formation of root casts. *Palaeogeography, Palaeoecology, Palaeoclimatology 274*, pp. 125-133.

CRANG, R.E. - HOLSEN, R.C. - HITT, J.B. 1968: Calcite production in mitochondria of earthworm calciferous glands. *Bioscience 18*, pp. 299-301.

DARWIN, C. 1882: The Formation of Vegetable Mould Through the Action of Worms, with Observations on Their Habits (*corrected*). John Murray, London.

DEUTZ, P. - MONTANEZ, I.P. - MONGER, H.C. - MORRISON, J. 2001. Morphology and isotope heterogeneity of Late Quaternary pedogenic carbonates: Implications for paleosol carbonates as paleoenvironmental proxies. *Palaeogeography, Palaeoclimatology, Palaeoecology 166*, pp. 293-317.

DREES, L.R. - WILDING, L.P. 1987. Micromorphic record and interpretations of carbonate forms in the Rolling Plains of Texas. *Geoderma 40*, pp. 157–175.

DUDÁS, N. 2012. A Villánykövesdi téglagyár lösz-paleotalaj sorozatának vizsgálata. MSc thesis, ELTE TTK, Budapest

DULTZ, S. - SCHÄFTLEIN S. 1999. Carbonate und Gips in Konkretionen in Böden aus Löß *Mitteilungen der Deutschen Bodenkundlichen Gesellschaft 91/3*, pp. 1379-1382. ("Carbonate and gypsum concretions in soils developed on loess"; in German)

DURAND, N. - MONGER, H.C. - CANTI, M.G. 2010: Calcium carbonate features. In: STOOPS, G. - MARCELINO, V. - MEES, F. (EDS.), Interpretation of micromorphological features of soils and regoliths. *Elsevier 2010*, pp. 149-194. (DOI: 10.1016/B978-0-444-53156-8.00009-X)

DWORKIN, S.I. – NORDT, L. – ATCHLEY, S. 2005. Determining terrestrial paleotemperatures using the oxygen isotopic composition of pedogenic carbonate. *Earth and Planetary Science Letters 237*, pp. 56-68.

EGER, A. - ALMOND, P.C. - CONDRON, L.M. 2012. Upbuilding pedogenesis under active loess deposition in a super-humid, temperate climate – quantification of deposition rates, soil chemistry and pedogenic thresholds. *Geoderma 189-190*, pp. 491-501.

FOX, D.L. – KOCH, P.L. 2004. Carbon and oxygen isotopic variability in Neogene paleosol carbonates: constraints on the evolution of the C_4-grasslands of the Great Plains, USA. *Palaeogeography, Palaeoclimatology, Palaeoecology 207*, pp. 305-329.

GAGO-DUPORT, L. - BRIONES, M.J.I. - RODRÍGUEZ, J.B. - COVELO, B. 2008: Amorphous calcium carbonate biomineralization in the earthworm's calciferous gland: Pathways to the formation of crystalline phases. *Journal of Structural Biology 162*, pp. 422-435.

GALIMOV, E.M. 1990. Biogeochemistry of stable carbon isotopes. *Mitteilungen aus dem Geologisch-Paläontologischen Institut der Universität Hamburg*, Heft 69, pp. 9-20.

GOCKE, M. 2010. Pedogenic carbonates in loess – formation rates, formation conditions and source apportionment assessed by isotopes and molecular proxies. PhD Thesis, University of Bayreuth, Germany, 176 p.

GOCKE, M. – PUSTOVOYTOV, K. – KÜHN, P. – WIESENBERG, G.L.B. – LÖSCHER, M. – KUZYAKOV, Y. 2011. Carbonate rhizoliths in loess and their implications for paleoenvironmental reconstruction revealed by isotopic composition: $\delta^{13}C$, ^{14}C. *Chemical Geology 283*, pp. 251-260.

GOCKE, M. – GULYÁS, S. – HAMBACH, U. – JOVANOVIĆ, M. – KOVÁCS, G. – MARKOVIĆ, S.B. – WIESENBERG, G.L.B. 2014a. Biopores and root features as new

tools for improvig paleoecological understanding of terrestrial sediment-paleosol sequences. *Palaeogeography, Palaeoclimatology, Palaeoecology 394*, pp. 42-58.

GOCKE, M. – HAMBACH, U. – ECKMEIER, E. – SCHWARK, L. – ZÖLLER, L. – FUCHS, M. – LÖSCHER, M. – WIESENBERG, G.L.B. 2014b. Introducing an improved multi-proxy approach for paleoenvironmental reconstruction of loess-paleosol archives applied on the Late Pleistocene Nussloch sequence (SW Germany). *Palaeogeography, palaeoclimatology, Palaeoecology 410*, pp. 300-315.

GOCKE, M. – PETH, S. – WIESENBERG, G.L.B. 2014c. Lateral and depth variation of loess organic matter overprint related to rhizoliths – Revealed by lipid molecular proxies and X-ray tomography. *Catena 112*, pp. 72-85.

HASINGER, O. – SPANGENBERG, J.E. - MILLIÈRE, L. – BINDSCHEDLER, S. – CAILLEAU, G. – VERRECCHIA, E.P. 2015. Carbon dioxide in scree slope deposits: A pathway from atmosphere to pedogenic carbonate. *Geoderma 247-248*, pp. 129-139.

HAYS, P.D. - GROSSMAN, E.L. 1991. Oxygen isotopes in meteoric calcite cements as indicators of continental paleoclimate. *Geology* 19, pp. 441–444.

HINSINGER, P. 1998: How do plant roots acquire mineral nutrients? Chemical processes involved in the rhizosphere. *Advances in Agronomy 64*, pp. 225-265.

HINSINGER, P. – PLASSARD, C. – JAILLARD, B. 2006: Rhizosphere: A new frontier for soil biogeochemistry. *Journal of Geochemical Exploration 88*, pp. 210-213.

HODSON, M.E. - BENNING, L.G. - DEMARCHI, B. - PENKMAN, K.E.H. - RODRÍGUEZ-BLANCO, J.D. - SCHOFIELD, P. - VERSTEEGH, E.A.A. 2015: Biomineralisation by earthworms – an investigation into the stability and distribution of amorphous calcium carbonate. *Geochemical Transactions 16/4* DOI 10.1186/s12932-015-0019-z

HORVÁTH, E. - BRADÁK, B. - NOVOTHNY, Á. - FRECHEN, M. 2007. A löszök paleotalajainak rétegtani és környezetrekonstrukciós jelentősége. *Földrajzi Közlemények* CXXXI/LV (4), pp. 389-406 (in Hungarian).

HORVÁTH, E. – BRADÁK, B. 2014. Sárga föld, lősz, lösz: Short historical overview of loess research and litostratigraphy in Hungary. *Quaternary International 319*, pp. 1-10.

HUGUET, A. – GOCKE, M. – DERENNE, S. – FOSSE, C. – WIESENBERG, G.L.B. 2013. Root-associated branched tetraether source microorganisms may reduce estimated paleotemperatire in subsoil. *Chemical Geology 356*, pp. 1-10.

HUM, L. 2001. Délkelet-Dunántúli lösz-paleotalaj sorozatok keletkezésének rekonstrukciója őslénytani vizsgálatok alapján. *Földrajzi Közlöny 131/1-2*, pp. 235-251. (in Hungarian with English abstract)

HUM, L. 2006. Ciklikus klímaváltozások kimutatása dél-magyarországi pleisztocén rétegsorok üledéktani, geokémiai és őslénytani vizsgálatai alapján. Kutatási zárójelentés, OTKA K-035139, Szeged. 24 p. (http://real.mtak.hu/81/1/35139_ZJ1.pdf) (OTKA research report in Hungarian)

HUM, L. – HORVÁTH, Z. – LINKAI, I. 2006. A villánykövesdi téglagyár pleisztocén képződményei (Pleistocene deposits in the Villánykövesd brickyard). Táj, környezeti és társadalom, SZTE Éghajlattani és Tájföldrajzi Tanszék, Természeti Földrajzi és Geoinformatikai Tanszék, Szeged, pp. 305-314. (in Hungarian with English abstract)

HUPUCZI, J. – SÜMEGI, P. 2010. The Late Pleistocene paleoenvironment and paleoclimate of the Madaras section (South Hungary), based on preliminary records from mollusks. *Central European Journal of Geosciences 2/1*, pp. 64-70.

JAILLARD, B. - GUYON, A. - MAURIN, A.F. 1991: Structure and composition of calcified roots, and their identification in calcareous soils. *Geoderma 50*, pp. 197-210.

JENNY, H. 1994. Factors of soil formation – A System of Quantitative Pedology. Dover Publications, Inc., New York.

JIAMAO, H. – KEPPENS, E. – TUNGSHENG, L. – PAEPE, R. – WENYING, J. 1997. Stable isotope composition of the carbonate concretion in loess and climate change. *Quaternary International 37*, pp. 37–43.

JOHNSON, D.L. - WATSON-STEGNER, D. 1987. Evolution model of pedogenesis. *Soil Science 143/5*, pp. 349-366.

KAAKINEN, A. – SONNINEN, E. – LUNKKA, J.P. 2006. Stable isotope record in paleosol carbonates from the Chinese Loess Plateau: Implications for late Neogene paleoclimate and paleovegetation. *Palaeogeography, Palaeoclimatology, Palaeoecology 237*, pp. 359-369.

KÁDÁR, L. 1954. A lösz keletkezése és pusztulása. *MTA Társadalmi-Történeti Tudományok osztályának közleményeiből 4/3-4*, pp. 109-114. ("The origin and denudation of loess", in Hungarian)

KADEREIT, A. – KÜHN, P. – WAGNER, G.A. 2010. Holocene relief and soil changes in loess-covered areas of south-western Germany: The pedosedimentary archives of Bretten-Bauerbach (Kraichgau). *Quaternary International 222*, pp. 96-119.

KÁSA, I. 2010. A paksi téglagyári löszfeltárás másodlagos karbonátjainak leíró bemutatása. MSc Thesis. 71 p.

KAUTZ, T. – AMELUNG, W. – EWERT, F. – GAISER, T. – HORN, R. – JAHN, R. – JAVAUX, M. – KEMNA, A. – KUZYAKOV, Y. – MUNCH., J.-C. – PÄTZOLD, S. – PETH, S. – SCHERER, H.W. – SCHLOTER, M. – SCHNEIDER, H. – VANDERBORGHT, J. – VETTERLEIN, D. – WALTER, A. – WIESENBERG, G.L.B. – KÖPKE, U. 2013. Nutrient acquisition from arable subsoils in temperate climates. *Soil Biology & Biochemistry 57*, pp. 1003-1022.

KEMP, R.A. 1995. Distribution and genesis of calcitic pedofeatures within a rapidly aggrading loess-paleosol sequence in China. *Geoderma 50*, pp. 197-210.

KEMP, R.A. 1998. Role of micromorphology in paleopedological research. *Quaternary International* 51/52, pp. 133-141.

KEMP, R.A. 1999. Micromorphology of loess-paleosol sequences: a record of paleoenvironmental change. *Catena 35*, pp. 179-196.

KEMP, R.A. 2001. Pedogenic modification of loess: significance for palaeoclimatic reconstructions. *Earth-Science Reviews 54*, pp. 145-156.

KHOKHLOVA, O.S. - SEDOV, S.N. - GOLYEVA, A.A. - KHOKHLOV, A.A. 2001. Evolution of Chernozems in the Northern Caucasus, Russia during the second half of the Holocene: carbonate status of paleosols as a tool for paleoenvironmental reconstruction. *Geoderma* 104, pp. 115-133.

KIM, S.-T. – O'NEIL, J.R. 1997. Equilibrium and nonequilibrium oxygen isotope effects in synthetic carbonates. *Geochimica et Cosmochimica Acta 61/16*, pp. 3461-3475.

KLAPPA, C.F. 1980: Rhizoliths in terrestrial carbonates: classification, recognition, genesis and significance. *Sedimentology 27*, pp. 613-629.

KOENIGER, P. – BARTA, G. – THIEL, C. – BAJNÓCZI, B. – NOVOTHNY, Á. – HORVÁTH, E. – TECHMER, A. – FRECHEN, M. 2014. Stable isotope composition of bulk and secondary carbonates from the Quaternary loess-paleosol sequence in Süttő, Hungary. *Quaternary International 319*, pp. 38-49.

KOŠIR, A. 2004: *Microcodium* revisited: root calcification products of terrestrial plants on carbonate-rich substrates. *Journal of Sedimentary Research 74/6*, pp. 845-857.

KOVÁCS A. 2010: A földigiliszták családja (Lumbricidae). In: DR. KOVÁCS A. – PÁLFIA ZS. – DR. PÉCZELY P. – DR. RÉZ G. – DR. SASS M. – DR. ZBORAY G.: *Összehasonlító anatómiai praktikum I.* DR. ZBORAY G. (szerk.). Nemzeti Tankönyvkiadó, Budapest, pp. 131-143.

KOVDA, I. - SYCHEVA, S. - LEBEDEVA, M. - INOZEMTZEV, S. 2009: Variability of carbonate pedofeatures in a loess-paleosol sequence and their use for paleoreconstructions. *Journal of Mountain Science 6 (2)*, pp. 155-161.

KRIVÁN, P. 1955. A közép-európai pleisztocén éghajlat tagolása és a paksi alapszelvény. *Magyar Állami Földtani Intézet Évkönyv 9/3*, pp. 363-512. (" The division of the Pleistocene climate of Central Europe and the base sequence of Paks"; in Hungarian)

KUKLA, G.J. 1977. Pleistocene Land-Sea Correlations I. Europe. *Earth-Science Reviews 13*, pp. 307-374.

ŁĄCKA, B. – ŁANCZONT, M. – MADEYSKA, T. 2009: Oxygen and carbon stable isotope composition of authigenic carbonates in loess sequences from the Carpathian margin and Podolia, as a palaeoclimatic record. *Quaternary International 198*, pp. 136-151.

LANG, I. – SASSMAN, S. – SCHMIDT, B. – KOMIS, G. 2014. Plasmolysis: Loss of Turgor and Beyond. *Plants 3*, pp. 583-593.

LAMBKIN, D.C. - GWILLIAM, K.H. - LAYTON, C. - CANTI, M.G. - PIEARCE, T.G. - HODSON, M.E. 2011: Production and dissolution rates of earthworm-secreted calcium carbonate. *Pedobiologia – International Journal of Soil Biology 54*, pp. 119-129.

LASKAR, A.H. – SHARMA, N. – RAMESH, R. – JANI, R.A. – YADAVA, M.G. 2010. Paleoclimate and paleovegetation of Lower Narmada Basin, Gujarat, Western India, inferred from stable carbon and oxygen isotopes. *Quaternary International 227*, pp. 183-189.

LEACH, J.A. 1974. Soil structures preserved in carbonate concretions in loess. *Quarterly Journal of Engineering Geology 7*, pp. 311-314.

LEE, K.E. 1985: Earthworms – Their Ecology and Relationship with Soils and Land Use Academic Press, Sydney. 411 p.

LEE, M.R. - HODSON, M.E. - LANGWORTHY, G. 2008a: Earthworms produce granules of intricately zoned calcite. *Geology 36(12),* pp. 943-946.

LEE, M.R. - HODSON, M.E. - LANGWORTHY, G. 2008b: Crystallization of calcite from amorphous calcium carbonate: earthworms show the way. *Mineralogical Magazine 72(1),* pp. 257-261.

LEE, Y. - HISADA, K. 1999. Stable isotopic composition of pedogenic carbonates of the Early Cretaceous Shimonoseki Subgroup, western Honshu, Japan. *Palaeogeography Palaeoclimatology Palaeoecology 153*, pp. 127–138.

LIAN, B. – HU, Q. – CHEN, J. – JI, J. – TENG, H.H. 2006. Carbonate biomineralization induced by soil bacterium *Bacillus megaterium*. *Geochimica et Cosmochimica Acta 70*, pp. 5522-5535.

LIU, W. – YANG, H. – SUN, Y. – WANG, X. 2011. $\delta^{13}C$ Values of loess total carbonate: A sensitive proxy for Asian summer monsoon in arid northwestern margin of the Chinese loess plateau. *Chemical Geology 284*, pp. 317-322.

LOISY, C. - VERRECCHIA, E.P. - DUFOUR, P. 1999: Microbial origin for pedogenic micrite associated with a carbonate paleosol (Champagne, France). *Sedimentary Geology 126*, pp. 193-204.

MACK, G.H. - COLE, D.R. - TREVIÑO, L. 2000. The distribution and discrimination of shallow, authigenic carbonate in the Pliocene-Pleistocene Palomas Basin, southern Rio Grande rift. *Geological Society of America Bulletin 112*, pp. 643-656.

MARKOVIĆ, S.B. – OCHES, E.A. – MCCOY, W.D. – FRECHEN, M. – GAUDENYI, T. 2007. Malacological and sedimentological evidence for "warm" glacial climate from the Irig loess sequence, Vojvodina, Serbia. *Geochemistry Geophysics Geosystems 8/9*, Q09008, doi:10.1029/2006GC001565 12 p.

MASAPHY, S. - ZABARI, L. - PASTRANA, J. - DULTZ, S. 2009. Role of fungal mycelium in the formation of carbonate concretions in growing media – an investigation by SEM and synchroton-based X-ray tomographic microscopy. *Geomicrobiology Journal 26*, pp. 442-450.

MCCONNAUGHEY, T.A. – WHELAN, J.F. 1997: Calcification generates protons for nutrient and bicarbonate uptake. *Earth-Science Reviews 42,* pp. 95-117.

MCNAUGHT, A.D. – WILKINSON, A. (editors) 1997. IUPAC. Compendium of Chemical Terminology, 2nd edition (the "Gold Book"). Blackwell Scientific Publications, Oxford. XML on-line corrected version: http://goldbook.iupac.org

(2006-) created by NIC, M. - JIRAT, J. – KOSATA, B., updates compiled by JENKINS, A. ISBN 0-9678550-9-8 and doi:10.1351/goldbook.O04348.

MILLER, D.L. - MORA, C.I. - DRIESE, S.G. 2007. Isotopic variability in large carbonate nodules in Vertisols: Implications for climate and ecosystem assessments. *Geoderma 142*, pp. 104-111.

MILLIERE, L. – HASINGER, O. – BINDSCHEDLER, S. – CAILLEAU, G. – SPANGENBERG, J.E. – VERRECCHIA, E.P. 2011: Stable carbon and oxygen isotope signatures of pedogenic needle fibre calcite. *Geoderma 161*, pp. 74-87.

MONGER, C.H. 2002. Pedogenic carbonate: links between biotic and abiotic $CaCO_3$. In: *Proc. 17th World Congress of Soil Science*, 14-21, August, Bangkok, Thailand. pp. 897-1 to 897-9.

NAKAHARA, H. - BEVELANDER, G. 1969: An electron microscope and autoradiographic study of the calciferous glands of the earthworm Lumbricus terrestris. *Calc. Tiss. Res. 4*, pp. 193-201.

PÁVAI-VAJNA, F. 1909. Az Erdélyrészi Medence löszfoltjairól. *Magyar Királyi Intézet Évi Jelentései 25*, pp. 200-221. ("About the loess covered areas of the Transylvanian Basin"; in Hungarian)

PÉCSI, M. 1990: Loess is not just the accumulation of dust. *Quaternary International* 7-8, pp. 1-21.

PÉCSI, M. 1993. Negyedkor és löszkutatás. Akadémiai Kiadó, Budapest. 376 p. ("Quaternary and loess research"; in Hungarian)

PÉCSI, M. – HAHN, GY. 1987. Paleosol stratotypes in the Upper Pleistocene Loess at Basaharc, Hungary. *Catena Supplement 9*, pp. 95-102.

PÉCSI, M. - RICHTER, G. 1996. Löss. Herkunft - Gliederung - Landschaften. Annales of Geomorphology 98. Gebrüder Bornträger, Berlin, Stuttgart.

PENDALL, E. - AMUNDSON, R.G. 1990. The stable isotope chemistry of pedogenic carbonate in an alluvial soil from the Punjab, Pakistan. *Soil Science* 149, pp. 199-211.

PIERRET, A. – CAPOWIEZ, Y. – BELZUNCES, L. – MORAN, C.J. 2002. 3D reconstruction and quantification of macropores using X-ray computed tomography and image analysis. *Geoderma 106*, pp. 247-271.

PRUD'HOMME, C. - LÉCUYER, C. - ANTOINE, P. - MOINE, O. - HATTÉ, C. - FOUREL, F. - MARTINEAU, F. - ROUSSEAU, D.-D. 2016: Paleotemperature reconstruction during

the Last Glacial from $\delta^{18}O$ of earthworm calcite granules from Nussloch loess sequence, Germany. *Earth and Planetary Science Letters 442*, pp. 13-20.

PYE, K. 1995. The nature, origin and accumulation of loess. *Quaternary Science Reviews 14*, pp. 653-667.

QUADE, J. - CERLING, T.E. - BOWMAN, J.R. 1989. Systematic variations in the carbon and oxygen isotopic composition of pedogenic carbonate along elevation transects in the southern Great Basin, United States. *Geol. Soc. Am. Bull.* 101, pp. 464–475.

RAO, Z. – ZHU, Z. – CHEN, F. – ZHANG, J. 2006. Does $\delta^{13}C_{carb}$ of the Chinese loess indicate past C_3/C_4 abundance? A review on stable carbon isotopes of the Chinese loess. *Quaternary Science Reviews 25*, pp. 2251-2257.

RETALLACK, G. 2001. Soils of the past – An introduction to paleopedology (2nd edition). Blackwell Science, 404 p.

RICHTHOFEN, F. von 1882. On the mode of origin of the loess. Geological Magazine Series 2, 9, pp. 293-305.

ROBERTSON, J.D. 1936: The function of the calciferous glands of earthworms. *Journal of Experimental Biology 13*, pp. 279-297.

RYSKOV, YA.G. - MERGEL, S.V. - KOVDA, I.V. - MORGUN, YE.G. 1996. Stable isotopes of carbon and oxygen as an indicator of the formation conditions of soils carbonates. *Eurasian Soil Science* 28/6, pp. 1–14.

SCHARPENSEEL, H.W. - MTIMET, A. - FREYTAG, J. 2000. Soil inorganic carbon and global change. In: LAL, R. - KIMBLE, J.M. - ESWARAN, H. - STEWART, B.A. (Eds.). Global climate change and pedogenic carbonates. Lewis Publishers, London, 27-42.

SCHÄFTLEIN, S. 1996. Genese und Struktur von Lößkindln in Böden unterschiedlicher Hydromorphie. Thesis. University of Hannover, Germany. ("Genesis and structure of loess dolls from soils with different hydromorphic properties"; in German)

SEHGAL, J.L. - STOOPS, G. 1972. Pedogenic calcite accumulation in arid and semi-arid regions of the Indo-Gangetic alluvial plain of Erstwhile Punjab (India) – their morphology and origin. *Geoderma 8*, pp. 59–72.

SEILACHER, A. 2001. Concretion morphologies reflecting diagenetic and epigenetic pathways. *Sedimentary Geology 143*, pp. 41-57.

SELLÉS-MARTÍNEZ, J. 1996. Concretion morphology, classification and genesis. *Earth-Science Reviews 41*, pp. 177-210.

SHELDON, N.D. - TABOR, N.J. 2009. Quantitative paleoenvironmental and paleoclimatic reconstruction using paleosols. *Earth-Science Reviews 95*, pp. 1-52.

SHUHUI, ZH. - YANG, W. – CHENGYE, CH. 1987. Studies on the stable isotopes in carbonates in Luochuan Loess Section: Applicability of the Ca daduies as paleoclimate indicators, pp. 283-290. In: TUNGSHENG, L. (Editor-in-Chief): Aspects of Loess Research, China Ocean Press, p. 447.

SMALLEY, I.- MARKOVIĆ, S.B. - SVIRČEV, Z. 2011. Loess is [almost totally formed by] the accumulation of dust. *Quaternary International 240*, 4-11.

ST. ARNAUD, R.J. - HERBILLON, A.J. 1973. Occurrence and genesis of secondary magnesium-bearing calcites in soils. *Geoderma 9*, pp. 279–298.

STOOPS, G. 2003. Guidelines for analysis and description of soil and regolith thin sections. Soil Science Society of America, Madison, USA

THIEL, C. – HORVÁTH, E. – FRECHEN, M. 2014. Revisiting the loess/palaeosol sequence in paks, Hungary: A post-IR IRSL based chronology for the 'Young Loess Series'. *Quaternary International 319*, pp. 88-98.

THOMPSON, T.L. - HOSSNER, L.R. - WILDING, L.P. 1991. Micromorphology of calcium carbonate in bauxite processing waste. *Geoderma 48*, pp. 31-42.

TUNGSHENG, L. – ZHENGTANG, G. – NAIQIN, W. – HOUYUAN, L. 1996. Prehistoric vegetation on the Loess Plateau: steppe or forest? *Journal of Southeast Asian Earth Sciences 13/3-5*, pp. 341-346.

ÚJVÁRI, G. 2004. A Villánykövesdi Téglagyár rétegsorának malakofaunája. *Malakológiai Tájékoztató 22*, pp. 39-49. (in Hungarian with English abstract)

ÚJVÁRI, G. – MOLNÁR, M. – NOVOTHNY, Á. – PÁLL-GERGELY, B. – KOVÁCS, J. – VÁRHEGYI, A. 2014. AMS ^{14}C and OSL/IRSL dating of the Dunaszekcső loess sequence (Hungary): chronology for 20 to 150 ka and implications for establishing reliable age-depth models for the last 40 ka. *Quaternary Science Reviews 106*, pp. 140-154.

VILLAGRAN, X.S. – POCH, R.M. 2014: A new form of needle-fiber calcite produced by physical weathering of shells. *Geoderma 213*, pp. 173-177.

VERRECCHIA, E.P. - VERRECCHIA, K.E. 1994: Needle-fiber calcite: a critical review and a proposed classification. *Journal of Sedimentary Research A64/3*, pp. 650-664

VERSTEEGH, E.A.A. - BLACK, S. - CANTI, M.G. - HODSON, M.E. 2013: Earthworm-produced calcite granules: A new terrestrial palaeothermometer? *Geochimica et Cosmochimica Acta 123*, pp. 351-357.

VERSTEEGH, E.A.A. - BLACK, S. - HODSON, M.E. 2014: Environmental controls on the production of calcium carbonate by earthworms. *Soil Biology & Biochemistry 70*, pp. 159-161.

WANG, H. - GREENBERG, S.E. 2007: Reconstructing the response of C_3 and C_4 plants to decadal-scale climate change during the late Pleistocene in southern Illinois using isotope analyses of calcified rootlets. *Quaternary Research 67*, pp. 136-142.

WEST, J.B. - BOWEN, G.J. - CERLING, T.E. - EHLERINGER, J.R. 2006. Stable isotopes as one of nature's ecological orders. *TRENDS in Ecology and Evolution 21/7*, pp. 408-414.

WIECEK, C.S. - MESSENGER, A.S. 1972: Calcite contributions by earthworms to forest soils in Northern Illinois. *Soil Science of America Proceedings 36*, pp. 478-480.

WIEDER, M. – YAALON, D.H. 1974. Effect of matrix composition on carbonate nodule crystallization. *Geoderma 11*, pp. 95-121.

WIEDER, M. - YAALON, D.H. 1982. Micromorphological fabrics and developmental stages of carbonate nodular forms related to soil characteristics. *Geoderma* 28, pp. 203-220.

YAALON, D.H. - GANOR, E. 1973. The influence of dust on soils during the Quaternary. *Soil Science 116/3*, pp. 146-155.

ZAMANIAN, K. – PUSTOVOYTOV, K. – KUZYAKOV, Y. 2016. Pedogenic carbonates: Forms and formation processes. *Earth Science Reviews* (accepted manuscript), DOI: 10.1016/j.earscirev.2016.03.003;

ZHONGLI, D. – RUTTER, N. – TUNGSHENG, L. 1993. Pedostratigraphy of Chinese Loess Deposits and Climatic Cycles in the Last 2.5 Myr. *Catena 20*, pp. 73-91.

ZHOU, J. – CHAFETZ, H.S. 2009a. Biogenic caliches in Texas: The role of organisms and effect of climate. *Sedimentary Geology 222*, pp. 207-225.

ZHOU, J. - CHAFETZ, H.S. 2009b. The genesis of late Quaternary caliche nodules in Mission Bay, Texas: stable isotope compositions and paleoenvironmental interpretation. *Sedimentology* 56, pp. 1392-1410.

9. Summary in English

Analysis of secondary carbonates from the young loess-paleosol sequences of the Carpathian Basin – especially regarding their paleoenvironmental role
-English summary

Gabriella Barta

In my dissertation I used the morphological and stable carbon and oxygen isotope analysis of secondary carbonates in order to define paleoenvironmental changes. Stable isotope compositions were determined of bulk loess/paleosol samples as a complementary method. Sampling sites were chosen along a North-(North-Eastern) – South-(South-Western) transect and contained the loess-paleosol sequences of Verőce, Paks and Villánykövesd. The main aim of the study was to examine the stable carbon and oxygen isotope composition of the studied sequences and discover the stable isotope patterns among the different sedimentary units.

The nomenclature of secondary carbonates was ambiguous in many cases, as certain concepts were used incorrectly. Since the analysis of secondary carbonates requires a consistent nomenclature to make possible the comparison of research works in the topic, therefore a clarified nomenclature was set up.

The analysis of secondary carbonates and bulk samples provided interesting information about the development of loess-paleosol sequences. The importance of different paleotopographic positions connected to local paleosol variations were highlighted by the comparison of stable carbon and oxygen isotope compositions of hypocoatings at the Verőce site, which resulted in different isotope patterns according to the different paleotopographic positions. Comparison was made among different paleosols in the same sequence on the basis of bulk stable carbon and oxygen isotope compositions in order to discover differences among the paleoenvironmental conditions in which they developed. The stable isotope pattern of the 'Basaharc Double 1' paleosol was compared between the Paks and Villánykövesd sites, in order to discover fine paleoenvironmental differences among the two localities. Over- and underlying transition zones of paleosols showed different patterns as well. Bulk isotope compositions were applicable for the recognition of possible hiatuses in the loess-paleosol sequences. It was discovered, that the appearance of soil-like hypocoatings strengthened the theory of pedosedimentary sequence evolution at the Verőce site. The applicability of HC+CC was proven for the Paks and Verőce sites, whereas it was denied for the Villánykövesd section due to regional differences.

As a summary, the stable carbon and oxygen isotope compositions of bulk and secondary carbonate samples were applicable for the description of relative environmental changes and individual sequence development – but the results were only comparable with other sequences, when other proxies or absolute dating results were available.

A Kárpát-medence fiatal löszeiben látható másodlagos karbonátok vizsgálata, különös tekintettel azok környezetjelző szerepére

Barta Gabriella

Disszertációmban a másodlagos karbonátok morfológiai és stabil szén és oxigén izotóp összetételének elemzését használtam fel őskörnyezeti változások megismeréséhez. Bulk (teljes) lösz-paleotalaj minták stabil izotóp összetételének meghatározását is alkalmaztam kiegészítő módszerként. A mintavételi helyek kijelölése egy észak-(északkelet) – dél-(délnyugat) átló mentén történt és a következő lösz-paleotalaj feltárásokat tartalmazta: Verőce, Paks és Villánykövesd. A fő cél az volt, hogy ezen feltárásokban a stabil izotóp összetétel elemzése mellett az egyes szedimentációs egységek izotóp mintázata is meghatározásra kerüljön.

A másodlagos karbonátok nevezéktana sok esetben nem egyértelmű, vagyis bizonyos fogalmakat helytelen módon alkalmaznak. Mivel a másodlagos karbonátok vizsgálata átlátható nevezéktant igényel, mely lehetővé teszi az összehasonlítást a különböző tudományos munkák között, így egy letisztázott terminológia került bevezetésre.

A másodlagos karbonátok és bulk minták elemzése érdekes információkkal járult hozzá a lösz-paleotalaj szelvények fejlődésének megismeréséhez. A különböző paleotopográfiai helyzetek szerepének fontossága kiemelhetővé vált, különösen a hozzájuk kötődő paleotalaj változatok felület alatti bevonatainak stabil szén és oxigén izotóp összetételének elemzésével a Verőce szelvényben. A különböző paleotopográfiai helyzetben megőrződött paleotalajok felület alatti bevonatai eltérő izotópos mintázatokat mutattak. Különböző paleotalajok őskörnyezeti összehasonlítása egy szelvényen belül is lehetséges volt a bulk stabil szén és oxigén izotóp összetétel elemzésének segítségével, így meghatározhatóvá vált, hogy egymáshoz képest ezek a paletalajok milyen őskörnyezeti körülmények között keletkeztek. A „Basaharc Dupla 1” paleotalaj stabil izotóp értékeinek őskörnyezeti szemléletű összehasonlítása lehetséges volt a Paks és Villánykövesd szelvények között. Bulk minták és felület alatti bevonatok stabil izotóp összetétele eltérő mintázatot mutatott a paleotalajok feküjében és fedőjében jelenlévő átmeneti zónák között. A bulk minták stabil szén és oxigén izotóp értékei alapján lehetségessé vált a lösz-paleotalaj sorozatokban található esetleges hiátusok jelenlétének kimutatása. A talajos-jellegű felület alatti bevonatok jelenléte megerősítette a pedoszedimentációs szelvényfejlődés elméletét a Verőce szelvény kapcsán. A HC+CC típus alkalmazhatósága bizonyításra került a Paks és Verőce szelvények kapcsán, míg elvetésre került a Villánykövesd szelvény kapcsán regionális eltérések miatt.

Összefoglalásképp elmondható, hogy a bulk és másodlagos karbonát minták stabil szén és oxigén izotóp összetétele alkalmazható viszonylagos környezeti változások kimutatására és egyéni szelvényfejlődés ábrázolására – de eredményeinek felhasználhatósága a szelvények közötti összehasonlításban csak akkor válik alkalmazhatóvá, ha más proxik illetve abszolút koradatok is a rendelkezésünkre állnak.

10. Appendix

Appendix

1. Micromorphological description of wet sieved samples from the Verőce sequence
    a. Profile C
    b. Profile D
    c. Profile A
2. Micromorphological description of wet sieved samples from the Paks sequence
    a. Profile A
    b. Profile B
    c. Profile C
    d. Profile D
    e. Profile E
3. Micromorphological description of wet sieved samples from the Villánykövesd sequence
    a. Profile E
    b. Profile D
    c. Profile A
    d. Profiles B and C
4. Verőce
    a. Mean values of secondary carbonates at the Verőce section
    b. Tendencies of HC at the Verőce sequence, including site description (figure designed by BALÁZS BRADÁK)
    c. EBS curves of Verőce – profile C
    d. EBS curves of Verőce – profile D
    e. HC+CC curves of Verőce – profile D
    f. CRC curves of Verőce – profile C
    g. CRC curves of Verőce – profile C
5. Paks
    a. Mean values for bulk samples from the Paks sequence
    b. Bulk samples of Paks
    c. Bulk samples of Paks – Unit 1,2,3
    d. Bulk samples of Paks – Unit 2,3
    e. Bulk samples of Paks – Unit 4,5,6,7
    f. Bulk samples of Paks – Unit 8,9,10
    g. Hypocoatings of Paks
    h. Earthworm biospheroids of Paks
    i. Amount of EBS at Paks
6. Villánykövesd
    a. Mean values of bulk samples from the Villánykövesd sequence
    b. Mean values of secondary carbonates in the Villánykövesd sequence
    c. Bulk values of Villánykövesd
    d. Bulk values of Villánykövesd – loess units
    e. Bulk values of Villánykövesd – transition units + Unit 13 loess + Unit 18 loess
    f. Bulk values of Villánykövesd – paleosols
    g. Hypocoatings of Villánykövesd
    h. HC+CC of Villánykövesd
    i. Earthworm biospheroids of Villánykövesd
7. Applied terminology of microscale secondary carbonates based on BECZE-DEÁK, J. et al. (1997) and updated after BARTA, G. (2011a)
8. Synthesis matrix for the interpretation of stable isotope values

1. Micromorphological description of wet sieved samples from the Verőce sequence

a. Profile C:

Depth (cm)			HC	HC+CC	CC	CRC	EBS	Other remarks
110	L2r	C-2	+	+	-	-	2	• sedimentary transition zone, partly detrital • small minerals and pebbles • small concretions (length=1.3 cm; width=0.8cm): origin is partly connected to the cementation of coatings; concretions integrate pebbles • calcified filaments (not NFC)
120			+	+	-	-	4	• sedimentary transition zone • soil-like HC • **pendant** on pebbles • charcoal
130			+	+	-	+	4	• sedimentary transition zone: mixture of loess + soil • partly detrital sample • **pendant** on pebbles • CRC with partly dissolved surface • presence of Mn
140	transition	C-3	+	+	-	-	2	• sedimentary transition zone: mixture of loess + soil • partly detrital sample • **pendant** on pebbles • mollusc shell fragment
150			+	+	-	-	3	• transition zone, grains reflecting more the colour of soil
160	P2	C-4	+	+	+	-	-	• transition zone, grains reflecting more the colour of soil • soil-like HC • CC as calcite tube
170			+	+	+	-	5	• sample structure still reflects a mixture of sediment + soil • soil-like HC • CC chalky white

180			+	+	+	-	4	• sample structure still reflects a mixture of sediment + soil • soil-like HC – some covered by NFC network • CC chalky white, powdery • charcoal • mollusc shell fragment
190			+	-	+	-	-	• sample structure still reflects a mixture of sediment + soil • CC chalky white, powdery
200			+	+	+	-	3	• sample structure still reflects a mixture of sediment + soil • presence of Mn • CC chalky white, powdery + contains NFC network • mollusc shell fragment
210			-	+	+	-	-	• soil aggregates: colour is dark brown with orange • presence of Mn • CC chalky white, powdery
220			-	+	+	-	3	• soil aggregates • charcoal
230		C-4	+	+	+	-	8	• soil aggregates • HC containing NFC network
240			+	-	+	-	2	• soil aggregates: colour is dark brown with orange • presence of pebbles • HC containing NFC network • CC chalky white, powdery, but partly resembles dissolved CRC, partly contains NFC network • charcoal
250			-	+	+	-	-	• soil aggregates: colour is dark brown with orange • presence of pebbles • presence of Mn • CC chalky white, powdery

								• concretions in cracks: length=4cm; width=0.8-2cm: not so compact; channel leads through it • charcoal
260			-	-	+	-	-	• detrital soil aggregates • small pebbles • presence of Mn • CC chalky white, powdery (lacks channel)
270			+	-	+	-	-	• detrital soil aggregates • small pebbles • seems to be a transition zone • CC chalky white, powdery + contains NFC network
280			+	-	+	-	**1**	• detrital soil aggregates • small pebbles • seems to be a transition zone • soil-like HC • small concretion: length=2cm; width=0.6-1.5cm – contains opened-up channels (possibly formed through the cementation of coatings) • CC chalky white, powdery, but partly resembles dissolved CRC
300	**L3**	**C-5**	+	-	+	-	**1**	• sedimentary sample • presence of Mn, Fe • 4 small concretions in the size of 1-1.5cm – structure: impregnated, but not recrystallized (formation possibly through coating cementation) • CC main type
310			+	-	+	+	**4**	• sedimentary sample, but contains soil aggregates • small concretion: length=1.2 cm; width=0.3-0.7cm – cemented coatings

								• CC: chalky white, powdery
320			+	+	+	-	**4**	• sedimentary sample, but contains soil aggregates • soil-like HC • CC: chalky white, powdery with channel
330			+	-	+	-	**5**	• sedimentary sample, but contains soil aggregates • signs of transition • soil-like HC, partly contains NFC network in its channel • chalky white CC, resembling dissolved CRC
360	**L3r**	**C-6**	-	+	-	-	**9**	• sedimentary sample, but contains soil aggregates • signs of transition • soil-like HC+CC • high amount of minerals
370			+	-	-	-	**2**	• transition zone • mostly soil aggregates, less sedimentary properties • soil-like HC
380	**P3**	**C-7**	+	-	-	-	**2**	• transition zone • soil aggregates • **pendant** on pebble
390			+	+	+	-	-	• soil with small aggregates • aggregates are partly detrital • soil-like HC, HC+CC • CC resembles dissolved CRC • **pendant** on pebble
400		**C-8**	+	-	+	-	-	• soil • small pebbles + **pendants** • presence of Mn • inner channel of HC contains recrystallized material • CC main type
410			-	-	+	-	-	• soil • small pebbles • CC main type

420		C-8	+	-	-	-	-	• soil mixing with sedimentary properties • lighter in colour
430			-	-	-	-	1	• soil mixing with sedimentary properties • aggregates are partly detrital • lighter in colour
450	transition	C-9	-	-	-	-	1	• soil aggregates in light colour mixing with sedimentary properties • mollusc shell fragment
455			+	-	-	-	5	• soil aggregates in light colour mixing with sedimentary properties
460	L4	C-10	+	-	-	-	6	• sedimentary with soil aggregates • partly detrital • small pebbles
470			+	-	-	-	5	• sedimentary properties, but really typical of loess • small pebbles
480			+	-	-	-	4	• sedimentary with soil aggregates • partly detrital
490			+	-	-	-	-	• mixture of soil and sediment • partly detrital • possible signs of bioturbation? • presence of Mn
500	L4r	C-11	+	-	-	-	5	• detrital mixture of soil and sediment • signs of bioturbation or translocation
510			-	-	-	-	-	• detrital mixture of soil and sediment • signs of bioturbation or translocation
520			-	-	-	-	-	• detrital mixture of soil and sediment • signs of bioturbation or translocation • aggregate colour refers more to soil
530			+	-	-	-	4	• soil with some sedimentary marks
540			+	-	-	-	-	• soil/sediment transition • translocation effects?
550			+	-	+	-	9	• soil/sediment transition • translocation effects?

								• small pebbles • CC main type
560			+	-	-	-	-	• soil aggregates
570		C-11	+	-	-	-	-	• soil aggregates in colour of brown and orange • partly sedimentary character • soil-like HC • signs of clay migration • signs of carbonate migration
580			+	-	-	-	**2**	• soil/sediment mixture • soil-like HC • transition?
580			+	-	-	-	-	• soil/sediment mixture • transition?
590	transition	C-12	+	+	-	-	**2**	• soil/sediment mixture
600			+	-	-	-	**5**	• soil aggregates are dominant, but presence of sedimentary properties
610			+	-	-	-	**2**	• soil aggregates are dominant, but presence of sedimentary properties • small pebbles
620			+	-	-	-	-	• soil aggregates • high amount of HC
630			+	-	-	-	-	• soil aggregates • high amount of HC
640	P4	C-13	+	-	-	-	-	• dark brown soil aggregates • partly shows transition to the upper horizon • soil-like HC
650			+	-	-	-	-	• dark brown soil aggregates • soil-like HC
660			+	-	-	-	-	• dark brown soil aggregates – clayey and well-cemented • no signs of carbonate migration • soil-like HC
670		C-14	+	-	-	-	-	• dark brown soil aggregates and transition to reddish brown aggregates • soil-like HC
680			+	-	-	-	-	• soil aggregates dominantly in reddish

								brown colour
690		**C-14**	**+**	**-**	**-**	**-**	**-**	• reddish brown soil aggregates • partly detrital aggregates • small pebbles
700	**L5 (directly under P4 and not along the paleovalley slope)**		**+**	**-**	**-**	**7**	**23**	• loess sample • presence of Mn • sediment-like HC • mollusc shell fragment
710			**+**	**-**	**-**	**59**	**11**	• loess sample • contains cemented aggregates with opened-up channels (not soil aggregates) • sediment-like HC • mollusc shell fragment
720			**+**	**-**	**-**	**20**	**20**	• loess sample • low amount of soil aggregates – slight hints of soil development or stable environmental conditions • sediment-like HC • mollusc shell fragment
730		**C-15**	**+**	**-**	**-**	**12**	**16**	• loess sample • low amount of soil aggregates – slight hints of soil development or +stable environmental conditions • sediment-like HC • mollusc shell fragment
740			**+**	**-**	**-**	**41**	**16**	• loess sample • low amount of soil aggregates – slight hints of soil development or stable environmental conditions • presence of Mn • small concretion: length=1.2cm; width=0.7cm - few channel openings on the surface • sediment-like HC • mollusc shell fragment
750	**L5**	**C-16**	**+**	**-**	**-**	**5**	**39**	• loess sample • low amount of soil

760		**C-16**						aggregates – slight hints of soil development or stable environmental conditions • presence of Mn • sediment-like and soil-like HC • charcoal? • mollusc shell fragment

b. <u>Profile D:</u>

Depth (cm)			**HC**	**HC+CC**	**CC**	**CRC**	**EBS**	**Other remarks**
210	**L4r**	**D-3**	+	-	-	-	-	• detrital HC • soil/sediment transition • small pebbles • compact carbonate concretions in length=1cm; width=0.8cm
220			+	-	+	-	-	• detrital HC • few CC, main type (signs of carbonate migration) • soil/sediment transition • compact concretions as above
230	**P4**	**D-4**	+	-	+	-	-	• 1 pc of HC: opened up channel filled out with recrystallized material • CC, main type as sign of carbonate migration • soil aggregates dominate, but with certain sedimentary properties • components of a well-developed carbonate vein
240			+	-	+	-	-	• CC preserved as mould on a soil aggregate • soil aggregates
250			+	-	+	-	-	• soil aggregates • carbonate pellets
260			+	-	+	-	-	• 1 pc of HC with more channel openings • carbonate sheets • fragments of a carbonate vein • soil aggregates

270		D-4	+	-	+	-	-	• few HC • carbonate sheets • soil aggregates
280			+	-	+	+	-	• fragments of the carbonate vein • soil aggregates
290		D-5	+	-	+	+	-	• soil aggregates (partly detrital)
300			+	+	-	+	-	• HC with NFC network in the inner channel • soil aggregates
310			+	-	+	+	-	• soil aggregates

350	P4	D-6	-	-	+	-	-	• soil aggregates • small pebbles • carbonate sheets • carbonate cover on aggregates
360			-	-	+	-	-	• CC: main type, partly opened up with recrystallized inner channel infilling • detrital soil aggregates – signs of bioturbation?
370			-	-	-	-	-	• soil aggregates • small pebbles
380			-	-	+	-	-	• CC: main type, but partly recrystallized showing desiccation cracks • charcoal • soil aggregates • small pebbles
390		D-7	-	-	+	-	-	• CC as calcite tube • soil aggregates • small pebbles • carbonate cover on aggregates
400		D-8	-	-	+	-	-	• CC as calcite tube • soil aggregates • small pebbles • carbonate cover on aggregates
410			-	-	+	-	-	• CC as recrystallized calcite tube • soil aggregates • small pebbles • carbonate cover on aggregates
420	L5	D-9	-	-	+	-	-	• CC main type with more channel openings

								• soil aggregates in lighter colour • small pebbles
430		**D-9**	**-**	**+**	**-**	**-**	**-**	• mollusc shell fragment • soil aggregates in lighter colour • transition characteristics between soil/loess • small pebbles
440		**D-10**	**+**	**+**	**-**	**-**	**1**	• whole mollusc + shell fragments • transition characteristics between soil/loess • small carbonate concretions: 10 pcs (length=0.8-9cm; width=0.5-5cm)
450		**D-11**	**+**	**+**	**+**	**4**	**15**	• HC contains NFC network in the inner channel • CC as calcite tube • mollusc shell fragment • loess sample
460			**+**	**+**	**(+)**	**4**	**39**	• mollusc shell fragment • loess sample • signs of bioturbation • small carbonate concretion (length=0.8cm; width=0.6cm)
470			**+**	**+**	**+**	**+**	**34**	• mollusc shell fragment • loess sample with soil aggregates • signs of bioturbation?
480			**+**	**-**	**+**	**13**	**36**	• mollusc shell fragment • loess sample with soil aggregates • signs of bioturbation or aggrading characteristics?
490	**A1**	**D-12**	**+**	**-**	**-**	**3**	**16**	• mollusc shell fragment • loessic sample + soil aggregates
500			**+**	**-**	**-**	**-**	**22**	• mollusc shell fragment • loessic sample + soil aggregates
510			**+**	**-**	**-**	**1**	**24**	• mollusc shell fragment • loessic sample + soil aggregates
520			**+**	**-**	**-**	**1**	**66**	• mollusc shell fragment • loessic sample + soil aggregates

Additional remarks to Unit D-12:

- at 510 cm depth: reddish layer was visible on the field in 1-2 cm thickness. Small carbonate concretions were present below this layer. Above the horizon a crotovina was observed, which was filled up with material in the same colour as the horizon.

c. Profile A:

Depth (cm)			HC	HC+CC	CC	CRC	EBS	Other remarks
190	Lr(?)	A-5	+	+	-	-	-	• charcoal? • Mn spheroids
200	P4	A-6	-	-	+	-	-	• CC main type • Mn spheroids
210		A-7	-	-	-	-	-	• Mn spheroids
220			+	-	+	-	-	• CC main type • Mn spheroids
230			+	-	+	-	-	• CC main type • Mn spheroids
240			-	-	-	-	-	• signs of carbonate migration on soil aggregates • Mn spheroids • decaying root partly 'manganified'
250		A-8	-	-	-	-	-	• Mn spheroids • decaying root partly 'manganified'
260			-	-	+	-	-	• CC main type • Mn spheroids • decaying root partly 'manganified'
270			-	-	+	-	-	• CC main type • charcoal • Mn spheroids
280			-	-	+	-	-	• CC main type • Mn spheroids
290		A-9	+	-	+	-	-	• CC main type • charocoal • Mn spheroids
300			-	-	-	-	-	• signs of carbonate migration on soil aggregates • Mn spheroids • decaying root partly 'manganified'
310			-	-	+	-	-	• CC main type • signs of carbonate migration on soil

		A-9						aggregates • charcoal? • Mn spheroids • decaying root partly ‘manganified’
320		**A-10**	**+**	**-**	**-**	**-**	**-**	• Mn spheroids • decaying root partly ‘manganified’
330			**+**	**-**	**-**	**-**	**-**	• Mn spheroids
340			**+**	**-**	**-**	**-**	**-**	• charcoal? • Mn spheroids
350	**L5**	**A-11**	**-**	**-**	**-**	**-**	**-**	• carbonate ‘roses’ • Mn spheroids

2. Micromorphological description of wet sieved samples from the Paks sequence

a. Profile A

Depth (cm)		HC	HC+CC	CC	CRC	EBS (pcs)	Other remarks
10	Unit 1	-	-	-	-	3	• small concretion, which can be snapped by a clip – not classical one, seems to be a first phase type • soil aggregates • recent root in the pre-phase of calcification – original tissue is visible besides the calcified cells
20		+	-	-	-	1	• aggregates • small concretion
30		+	+	-	-	1	• no special remarks
40		+	+	-	-	-	• calcite crust on the inner channel wall of HC+CC is hardly cemented
50		+	+	-	-	1	• aggregates • broken HC remnants
60		+	+	-	-	1	• aggregates
70		+	+	-	+	-	• fragile, well-developed CRC which contains more cell layers • HC occurred with decayed root remnants
80		+	+	-	-	-	• no special remarks
90		+	-	-	-	-	• no special remarks
100		+	-	+	-	-	• CC occurred as calcite tube
110		+	+	-	-	1	• no special remarks
120		-	+	-	-	-	• no special remarks
130		-	-	+	-	-	• CC main type
140		+	-	-	-	10	• EBS are well-developed and whole • mollusc shell fragments • whole sample is granular
150		+	+	-	-	31	• whole molluscs + shell fragments
160		+	+	-	-	17	• whole molluscs + shell fragments
170		+	+	-	-	55	• whole molluscs + shell fragments
180		+	+			50	• large HC, well-developed, characteristic loess type HC • whole molluscs + shell fragments
190		+	-	-	-	53	• well-developed, characteristic loess type HC • whole mollusc + shell fragments
200		+	+	-	-	39	• sample shows mixed pattern: may refer for slight soil development and/or bioturbation? • whole molluscs + shell fragments

b. Profile B

Depth (cm)		HC	HC+CC	CC	CRC	EBS (pcs)	Other remarks
240	Unit 1	+	-	+	-	54	• presence of Mn • CC occurred as calcite tube • whole molluscs + shell fragments • sample seems to be mostly detrital: possible signs of bioturbation
250		+	-	-	-	58	• presence of Mn • certain EBS seems to be broken • sample seems to be mostly detrital: possible signs of bioturbation
260		(+)	-	-	-	49	• presence of Mn • whole molluscs + shell fragments • no whole HC, just broken • sample seems to be mostly detrital: possible signs of bioturbation
270		-	-	+	-	7	• CC as calcite tube • sample seems to be mostly detrital
280		+	-	-	-	7	• no special remarks
290		+	-	-	-	9	• presence of Mn
300		-	+	-	-	79	• whole molluscs + shell fragments
310		+	-	-	-	41	• whole mollusc
320		+	-	-	-	39	• only few whole HC • aggregates • mollusc shell fragments
330		+	+	-	-	50	• whole mollusc • sample shows the general properties of a loess sample
340		+	+	-	-	80	• presence of Mn • whole molluscs
350		+	+	-	-	51	• mollusc shell fragments
360		+	+	-	-	74	• whole molluscs + shell fragments
370		+	+	-	-	86	• molluscs shell fragments
380		+	+	-	-	5	• less EBS compared to the above lying horizons + smaller in size • sample characteristics are similar to those of a weakly developed soil horizon and/or strong bioturbation
390		+	-	-	-	4	• sample characteristics are similar to those of a weakly developed soil horizon and/or strong bioturbation
400		+	-	-	+	12	• EBS have generally elongated morphology • whole mollusc • sample characteristics are similar to those of a weakly developed soil horizon and/or strong bioturbation
410		+	+	-	-	5	• sample characteristics are similar to

							those of a weakly developed soil horizon and/or strong bioturbation
420		+	+	-	+	21	• EBS have generally elongated morphology • broken CRC • sample characteristics are similar to those of a weakly developed soil horizon and/or strong bioturbation

c. Profile C:

Depth (cm)		HC	HC+CC	CC	CRC	EBS (pcs)	Other remarks
430	Unit 1	-	-	-	+	27	• certain EBS with elongated morphology • soil aggregates • signs of bioturbation, proofs of earthworm activity in the sample structure (aggregate discs)
440		+	-	-	+	58	• presence of Mn • HC in ring structure; broken CRC • whole molluscs + shell fragments • soil aggregates • signs of bioturbation, proofs of earthworm activity in the sample structure (aggregate discs)
450		-	-	-	+	29	• whole molluscs + shell fragments • soil aggregates
460		+	-	-	+	14	• soil aggregates • calcite disc of *Arion* sp.
470		+	-	-	(+)	7	• broken CRC
480		+	-	-	-	12	• no special remarks
490		+	-	-	-	25	• no special remarks
500		+	+	-	(+)	23	• broken CRC • whole molluscs + shell fragments
510		+	-	-	(+)	6	• broken CRC • mollusc shell fragments • high amount of small minerals
520		+	+	-	++	15	• presence of Mn in the inner channel of HC • relative high amount of CRC: signs of dissolution, opened-up channels, partly Mn cover • mollusc shell fragments • signs of bioturbation, proofs of earthworm activity in the sample structure (aggregate discs)
530		-	+	-	+	5	• soil aggregates • presumably weak signs of soil development or humus accumulation

							• signs of bioturbation, proofs of earthworm activity in the sample structure (aggregate discs)
540		+	-	-	+	3	• soil aggregates • presumably weak signs of soil development or humus accumulation • proofs of earthworm activity in the sample structure (aggregate discs)
550		+	+	-	(+)	5	• presence of Mn also in the inner channel of HC • certain EBS with elongated morphology • broken CRC • soil aggregates + soil properties • whole molluscs + shell fragments
560	Unit 2	+	-	-	-	6	• presence of Mn in the inner channel of HC • soil aggregates + soil properties • one small concretion with crack pattern on the surface
570		+	-	-	-	3	• soil aggregates + soil properties • whole molluscs + shell fragments
580		+	-	-	-	9	• HC is more compact and strongly cemented • whole mollusc + shell fragments • soil aggregates + soil properties
590		+	-	-	-	7	• mollusc shell fragments • soil aggregates + soil properties
600		+	-	-	-	10	• whole mollusc + shell fragments • soil aggregates + soil properties • proofs of earthworm activity in the sample structure (aggregate discs)
610	Unit 3	+	+	-	-	8	• mollusc shell fragments • soil aggregates + soil properties
620		+	-	-	-	21	• mollusc shell fragments • soil aggregates + soil properties
630		+	-	-	-	19	• presence of Mn in the inner channel of HC • mollusc shell fragments • presence of charcoal • soil aggregates + soil properties
640		+	-	-	-	16	• **presence of CC2 (chalky white)** • mollusc shell fragments • soil aggregates + soil properties
650		+	-	-	-	7	• mollusc shell fragments • soil aggregates + soil properties • proofs of earthworm activity in the sample structure (aggregate discs)
660		+	-	-	-	9	• presence of Mn on the inner channel of HC • whole mollusc + shell fragments

670		+	-	-	-	**9**	• **presence of CC2 (chalky white)** • presence of Mn on the inner channel of HC • mollusc shell fragments

d. Profile D:

Depth (cm)		HC	HC+CC	CC	CRC	EBS (pcs)	Other remarks
690		-	+	-	-	**6**	• EBS also occurs broken • soil aggregates and soil properties • signs of bioturbation
700		+	-	-	(+)	**16**	• broken CRC • **presence of CC2 (chalky white)** • soil aggregates + soil properties • signs of bioturbation
710	**Unit 4**	+	-	-	(+)	**9**	• whole molluscs + shell fragments • broken CRC; colour of feature is towards the direction of transparent
720		+	-	-	+	**15**	• whole molluscs + shell fragments
730		+	-	-	+	**21**	• CRC are not always whole; higher amount as compared to the above lying horizon • morphology of EBS is quite diverse • whole mollusc + shell fragments
740		+	+	-	+	**20**	• whole mollusc + shell fragments
750	**Unit 5a**	+	+	-	-	**20**	• mollusc shell fragments
760		+	-	-	-	-	• sample properties: granular; possible signs of bioturbation • soil aggregates
770	**Unit 5b**	+	-	-	-	-	• sample properties: granular; possible signs of bioturbation • soil aggregates
780		-	-	-	-	-	• proofs of earthworm activity in the sample structure (aggregate discs) • soil aggregates • seems to be strongly bioturbated
790	**Unit 6**	-	-	-	-	-	• no signs of the reddish colour in the prepared sample • proofs of earthworm activity in the sample structure (aggregate discs) • soil aggregates • seems to be strongly bioturbated
800	**Unit 7**	+	-	-	-	-	• presence of Mn in the inner channel of HC • proofs of earthworm activity in the sample structure (aggregate discs) • soil aggregates • seems to be strongly bioturbated
810		+	-	-	-	-	• proofs of earthworm activity in the

							sample structure (aggregate discs) • soil aggregates • seems to be strongly bioturbated

e. Profile E:

Depth (cm)		HC	HC+CC	CC	CRC	EBS (pcs)	Other remarks
830	Unit 8a	-	-	-	-	-	• soil aggregates, strongly cemented
840		-	-	-	-	-	• sample shows loess characteristics but contains soil aggreates
850		+	-	-	-	1	• presence of Mn on the inner channel of HC • soil aggregates
860		+	-	-	-	-	• proofs of earthworm activity in the sample structure (aggregate discs) • soil aggregates
870		+	-	-	-	-	• presence of Mn on the inner channel of HC • soil aggregates
880		+	-	-	-	3	• calcite disc of *Arion* sp. • soil aggregates
890	Unit 8b	+	-	-	-	2	• HC containing NFC network in the inner channel • presence of Mn on the inner channel of HC • soil aggregates • mollusc shell fragments
900		+	-	-	-	8	• presence of Mn on the inner channel of HC • EBS appeared with holey centre • mollusc shell fragments
910		+	-	-	-	7	• presence of Mn on the inner channel of HC • colour of HC reflects soil properties ("soil-like HC") • soil aggregates in brown colour
920	Unit 8c	+	-	-	-	-	• presence of Mn on the inner channel of HC • soil aggregates in brown colour
930	Unit 8d	+	-	+	-	3	• presence of Mn on the inner channel of HC • soil aggregates in brown colour
940	Unit 9	+	-	-	+	-	• presence of Mn on the inner channel of HC • really thin CRC
950		+	-	-	-	5	• presence of Mn on the inner channel of HC
960		-	-	-	-	4	• carbonate concretion (length=1cm; width=0.6-0.7cm): not so easy to break

							• broken and relatively flat EBS • large, cemented soil aggregates
970		-	-	+	-	**2**	• carbonate concretion (length=1cm; width=0.8cm): relatively soft, easy to break • other signs of carbonate migration: soil aggregates are strongly cemented • carbonate aggregates, breakable by clip
980		+	-	+	-	**2**	• other signs of carbonate migration: soil aggregates are strongly cemented • carbonate aggregates, breakable by clip
990		+	-	+	-	-	• carbonate concretions: 1) length=1cm; width=0.6-0.8cm; soft, easy to break 2) length=1cm; width=1cm; surface contains small channel openings, which refer to former root channels 3) length=0.9cm; width=0.5-0.9cm; same characteristics as of 2) 4) length=0.5cm; width=0.5 cm
1000		+	-	+	-	**11**	• presence of Mn on the inner channel of HC • whole mollusc + shell fragments • soil aggregates • sample shows transition characteristics to loess in grain composition and colour
1010	**Unit 10**	+	-	+	-	**13**	• presence of Mn on the inner channel of HC • EBS are mainly grain cover attached to their surfaces • EBS are large in size • whole molluscs + shell fragments • soil aggregates • sample shows transition characteristics to loess in grain composition and colour

3. Micromorphological description of wet sieved samples from the Villánykövesd sequence

a. Profile E:

Depth (cm)		HC	HC+CC	CC	CRC	EBS	Other remarks
40	Unit 1	+	+	-	-	+	• large EBS • sample structure: loessic
50		+	+	-	-	+	• large EBS, high amount • sample structure: loessic
60		-	+	-	(+)	+	• large EBS, certain EBS are elongated • HC+CC seems to be compact, shows signs of strong carbonate migration + more generations of calcite tubes in the inner channel • HC containing remains of CRC • sample structure: loessic
70		+	+	-	-	+	• some EBS are elongated • sample structure: loessic
80		+	+	-	-	+	• extreme large EBS • sample structure: loessic
90		+	+	-	-	+	• sample structure: loessic
100		+	+	-	-	+	• sample structure: loessic
110		+	+	-	-	+	• sample structure: loessic • whole molluscs
120		+	+	-	-	+	• large EBS • sample structure: loessic
130		+	+	-	-	+	• sample structure: loessic
140		+	+	-	-	+	• large EBS • sample structure: loessic
150		+	+	-	-	+	• large EBS • sample structure: loessic
160		-	+	-	-	+	• sample structure: loessic

b. Profile D:

Depth (cm)		HC	HC+CC	CC	CRC	EBS	Other remarks
102	Unit 2	+	-	-	+	+	• well-developed CRC with transparent cells • small concretions • sample structure: loessic
110		+	-	-	+	+	• sample structure: loessic
120		+	-	-	+	+	• sample structure: loessic
130		+	-	-	-	+	• sample structure: loessic, but

							contains aggregates and seems to be partly granular
140		+	-	-	+	+	• sample structure: loessic
150		+	-	-	-	+	• sample structure: loessic
160		+	-	-	-	+	• sample structure: loessic
170		+	-	-	-	+	• sample structure: loessic
180		+	+	-	-	+	• sample structure: loessic
190		+	+	-	-	+	• sample structure: loessic
200		+	+	-	+	+	• sample structure: loessic • whole molluscs
210		+	+	-	-	+	• sample structure: loessic
220		+	+	-	-	+	• EBS morphology: larger, elongated ones • sample structure: loessic • whole molluscs
230		+	+	-	-	+	• sample structure: loessic
240		+	+	-	-	+	• sample structure: loessic
250		+	+	-	-	+	• sample structure: loessic
260		+	+	-	-	+	• sample structure: loessic
270		+	+	-	-	+	• sample structure: loessic
280		+	+	-	-	+	• proofs of earthworm activity in the sample structure (aggregate discs) • sample structure: loessic
290		+	+	-	-	+	• sample structure: loessic
300	**Unit 3**	+	+	-	-	+	• sample structure: loessic
310		This part sampled only for bulk measurements (during the 2nd field campaign).					
320							

c. **Profile A:**

Depth (cm)		HC	HC+CC	CC	CRC	EBS	Other remarks
200	**Unit 4**	-	+	+	-	+	• HC+CC contains more calcite tubes in the inner channel • presence of Mn • mollusc shell fragments • detrital sample, signs of bioturbation
210		+	+	-	-	+	• HC+CC contains more calcite tubes in the inner channel • presence of Mn • mollusc shell fragments • detrital sample, signs of bioturbation
220		+	-	+	-	+	• small concretion: seems to be

							the cementation of small HC/CC channels
230		+	-	+	-	+	• EBS shows slight signs of breakage • whole molluscs + shell fragments
240		+	-	+	(+)	+	• CRC appeared only as an attachment to one HC
250		+	+	-	-	-	• large HC, some with more channel openings • soil aggregates
260	**Unit 5**	+	+	-	(+)	-	• CRC appeared only as an attachment to one HC • HC+CC contains more calcite tubes in the inner channel • soil aggregates + signs of bioturbation
270		+	+	-	-	-	• no special remarks
280		+	+	+	-	-	• large, opened-up HCs • CC main type • presence of Mn
290		+	+	-	-	+	• no special remarks
300		+	+	-	(+)	-	• CRC appeared only as an attachment to one HC – cells of CRC seems to be partly dissolved
310		+	+	-	-	-	• no special remarks
320		+	-	-	-	+	• no special remarks
330		+	+	-	+	+	• broken EBS with "patchwork"-style morphology
340		+	-	-	-	-	• detrital sample with strong signs of bioturbation
350		+	-	-	-	+	• no special remarks
360		+	-	-	-	+	• detrital sample with strong signs of bioturbation
370		-	+	-	-	+	• HC+CC are large and strongly cemented together, resembles the first phase of concretion development • detrital sample with strong signs of bioturbation
380		-	-	-	-	+	• some large EBS with "patchwork"-style morphology • detrital sample with strong signs of bioturbation
390		+	-	-	-	+	• some EBS are partly broken
400		+	-	-	-	+	• certain HC are more compact and resemble to first stage of concretion development
410		+	-	-	-	+	• some fibre-like features (not NFC) appeared

420		+	-	-	-	+	• some fibre-like features (not NFC) appeared • detrital sample with strong signs of bioturbation
430		+	-	-	-	+	• some broken EBS • HC with more channel openings • presence of **CC2** (chalky white, dense)
440		+	-	-	-	+	• soil aggregates + signs of bioturbation
450		+	-	-	-	+	• soil-like HC • soil aggregates + their colour refers to soil development • some fibre-like features (not NFC) • remains of **CC2** • signs of bioturbation
460	**Unit 6**	-	-	+	-	-	• soil aggregates + their colour refers to soil development • CC main type: not typical channel like, more as aggregates - signs of carbonate migration
470		-	-	-	+	+	• CRC with cell surfaces showing signs of dissolution

d. <u>Profiles B and C:</u>

Depth (cm)		HC	HC+CC	CC	CRC	EBS	Other remarks
480		+	-	-	-	+	• whole mollusc • loessic sample
490	**Unit 7**	+	-	-	-	+	• high amount of well-preserved HC
500		+	-	-	-	+	• no special remarks
510		+	+	-	-	+	• whole mollusc
520		+	+	-	-	+	• no special remarks
530		+	+	-	-	+	• no special remarks
540		+	-	-	-	+	• no special remarks
550	**Unit 8**	+	+	-	-	+	• contains large EBS with irregular morphology
560		+	-	-	-	+	• no special remarks
570		+	-	-	+	+	• CRC is thin, but cell structure is recognizable + partly contain Mn and/or grain cover • soil aggregates
580	**Unit 9**	+	+	-	-	+	• no special remarks
590		+	-	-	-	+	• no special remarks
600	**Unit 10**	+	-	-	-	+	• high amount of EBS

							• only few HC • soil aggregates • sample seems to be part of a transition zone and/or show signs of bioturbation
610		+	-	-	-	+	• whole molluscs
620	**Unit 11**	+	+	-	-	+	• whole molluscs
630		+	+	-	-	+	• whole molluscs
640		+	-	-	-	+	• whole molluscs
650	**Unit 12**	+	-	-	-	+	• whole molluscs
660	**Unit 13**	+	-	-	-	+	• whole molluscs
670		+	-	-	-	+	• whole molluscs
680	**Unit 14**	+	-	-	-	+	• whole molluscs
690		+	-	-	-	+	• whole molluscs
700	**Unit 15**	+	+	-	-	+	• whole molluscs
710		+	-	-	-	+	• whole molluscs
720		+	-	-	-	+	• broken EBS: possible translocation or just effects of bioturbation? • whole molluscs
730	**Unit 16**	This part sampled only for bulk measurements (during the 2nd field campaign).					
740							
750							
760							
770		-	-	-	-	-	• sample is detrital, shows possible signs of bioturbation
780		+	-	-	+	-	• soil-like HC • CRC seems to be recrystallized • soil aggregates • presence of many small minerals • high clay content
790		-	-	+	-	+	• main type CC, compact • soil aggregates
800		-	-	+	-	+	• main type CC, compact • soil aggregates
810	**Unit 17**	-	-	+	-	-	• main type CC, compact • small cemented concretions • soil aggregates
820		-	-	-	-	-	• small cemented concretions • soil aggregates
830	**Unit 18**	-	-	+	-	-	• soil aggregates • signs of bioturbation
840		-	-	+	+	+	• large EBS, fast transparent crystals, "patchwork"-style morphology • small concretion with small channel openings

850		+	-	-	-	+	• EBS of various morphology • HC of mixed loess and soil characteristics in grain composition
860		+	-	-	-	+	• small concretions
870	**Unit 19**	+	-	-	-	+	• no special remarks
880		+	-	-	-	+	• no special remarks
890		+	-	-	-	+	• no special remarks
900		+	-	-	-	+	• no special remarks
910	**Unit 20**	+	-	-	-	+	• no special remarks
920		+	-	-	-	+	• no special remarks
930		+	-	+	-	+	• concretions in different size • main type CC, compact

4. Verőce

a. Mean values of secondary carbonates at the Verőce section

		δ13C (VPDB ‰)				δ18O (VPDB ‰)			
		Max	**Min**	**Mean**	**SD mean**	**Max**	**Min**	**Mean**	**SD mean**
Aleurite	**A1-D**								
	HC	-7,58	-9,21	**-8,49**	*0,04*	-7,99	-10,54	**-9,68**	*0,06*
	CC	-7,03	-9,07	**-8,38**	*0,04*	-10,45	-12,03	**-11,24**	*0,08*
	CRC	-23,79	-27,49	**-25,87**	*0,04*	-15,12	-16,72	**-15,79**	*0,07*
	EBS	-11,45	-13,98	**-12,97**	*0,04*	-4,68	-11,14	**-8,14**	*0,07*
Paleosols	**P4-D**								
	HC	-5,53	-9,33	**-8,04**	*0,04*	-6,61	-9,80	**-7,88**	*0,08*
	HC+CC	-8,50	-9,06	**-8,78**	*0,04*	-8,32	-10,44	**-9,38**	*0,09*
	CC	-7,27	-9,49	**-8,69**	*0,04*	-7,91	-11,75	**-10,00**	*0,08*
	CRC	-15,28	-18,66	**-17,44**	*0,03*	-10,28	-12,26	**-11,47**	*0,08*
	P4-A								
	HC	-6,40	-10,39	**-8,72**	*0,03*	-8,00	-12,17	**-9,39**	*0,10*
	CC	-7,03	-9,07	**-8,38**	*0,04*	-10,45	-12,03	**-11,24**	*0,08*
	P4-C								
	HC	-8,53	-10,47	**-9,35**	*0,09*	-7,40	-11,44	**-9,76**	*0,12*
	P3-C								
	HC	-9,70	-10,25	**-9,91**	*0,04*	-8,31	-10,13	**-9,24**	*0,06*
	EBS	-11,63	-13,50	**-12,57**	*0,04*	-9,34	-9,41	**-9,38**	*0,06*
	P2-C								
	HC	-7,29	-10,00	**-8,79**	*0,04*	-6,54	-10,08	**-8,03**	*0,08*
	CC	-7,53	-9,64	**-9,00**	*0,03*	-8,61	-9,99	**-9,53**	*0,08*
	EBS	-9,82	-13,25	**-12,33**	*0,03*	-6,65	-11,77	**-8,48**	*0,07*
Loesses	**L5-D**								
	HC	-8,50	-9,91	**-9,45**	*0,04*	-8,72	-9,89	**-9,09**	*0,06*
	HC+CC	-8,84	-9,79	**-9,35**	*0,04*	-9,14	-10,25	**-9,69**	*0,06*
	CRC	-21,68	-24,84	**-22,59**	*0,04*	-14,59	-17,04	**-15,32**	*0,06*
	EBS	-11,97	-14,82	**-13,32**	*0,04*	-4,26	-9,78	**-8,20**	*0,06*
	L5-C								
	HC	-8,37	-9,95	**-8,98**	*0,09*	-6,64	-11,71	**-7,97**	*0,12*

	CRC	-26,49	-33,21	**-29,40**	*0,11*	-13,18	-16,68	**-15,25**	*0,13*
	EBS	-11,51	-14,51	**-12,83**	*0,09*	-1,46	-11,29	**-7,79**	*0,12*
	L4-C								
	HC	-8,26	-8,93	**-8,57**	*0,04*	-8,04	-9,50	**-8,83**	*0,05*
	EBS	-11,96	-14,19	**-12,90**	*0,04*	-7,76	-10,03	**-8,97**	*0,05*
	L3-C								
	HC	-8,42	-9,05	**-8,67**	*0,08*	-8,48	-10,25	**-9,36**	*0,17*
	CC	-8,63	-9,77	**-8,95**	*0,08*	-9,10	-9,91	**-9,47**	*0,17*
	EBS	-9,98	-14,29	**-13,13**	*0,08*	-6,51	-10,96	**-8,93**	*0,17*
Transition zones	**L4r/P4-C transition**								
	HC	-7,90	-8,96	**-8,44**	*0,06*	-8,41	-11,43	**-10,34**	*0,08*
	EBS	-11,97	-14,35	**-13,34**	*0,04*	-7,82	-12,41	**-9,43**	*0,06*
	P3/L4 transition								
	EBS	-12,84	-13,06	**-12,95**	*0,04*	-4,00	-10,18	**-7,09**	*0,05*
	L2r/P2 transition								
	HC	-8,47	-8,60	**-8,54**	*0,03*	-6,30	-8,15	**-7,22**	*0,17*
	EBS	-11,78	-13,49	**-12,63**	*0,02*	-5,25	-7,55	**-6,40**	*0,05*
Reworked layers	**L(r)?-A**								
	HC	-9,07	-9,25	**-9,16**	*0,03*	-8,88	-8,95	**-8,91**	*0,09*
	L4r-C								
	HC	-6,87	-9,83	**-8,69**	*0,04*	-7,66	-10,88	**-9,29**	*0,06*
	EBS	-11,37	-14,41	**-13,02**	*0,04*	-6,20	-10,04	**-7,64**	*0,05*
	L3r-C								
	EBS	-13,03	-13,94	**-13,38**	*0,04*	-4,75	-8,53	**-7,43**	*0,06*
	L2r-C								
	HC	-8,54	-9,06	**-8,88**	*0,02*	-7,64	-8,98	**-8,42**	*0,06*
	EBS	-11,01	-13,35	**-12,07**	*0,03*	-6,21	-8,77	**-7,32**	*0,14*

b. Tendencies of HC at the Verőce sequence, including site description (figure designed by BALÁZS BRADÁK)

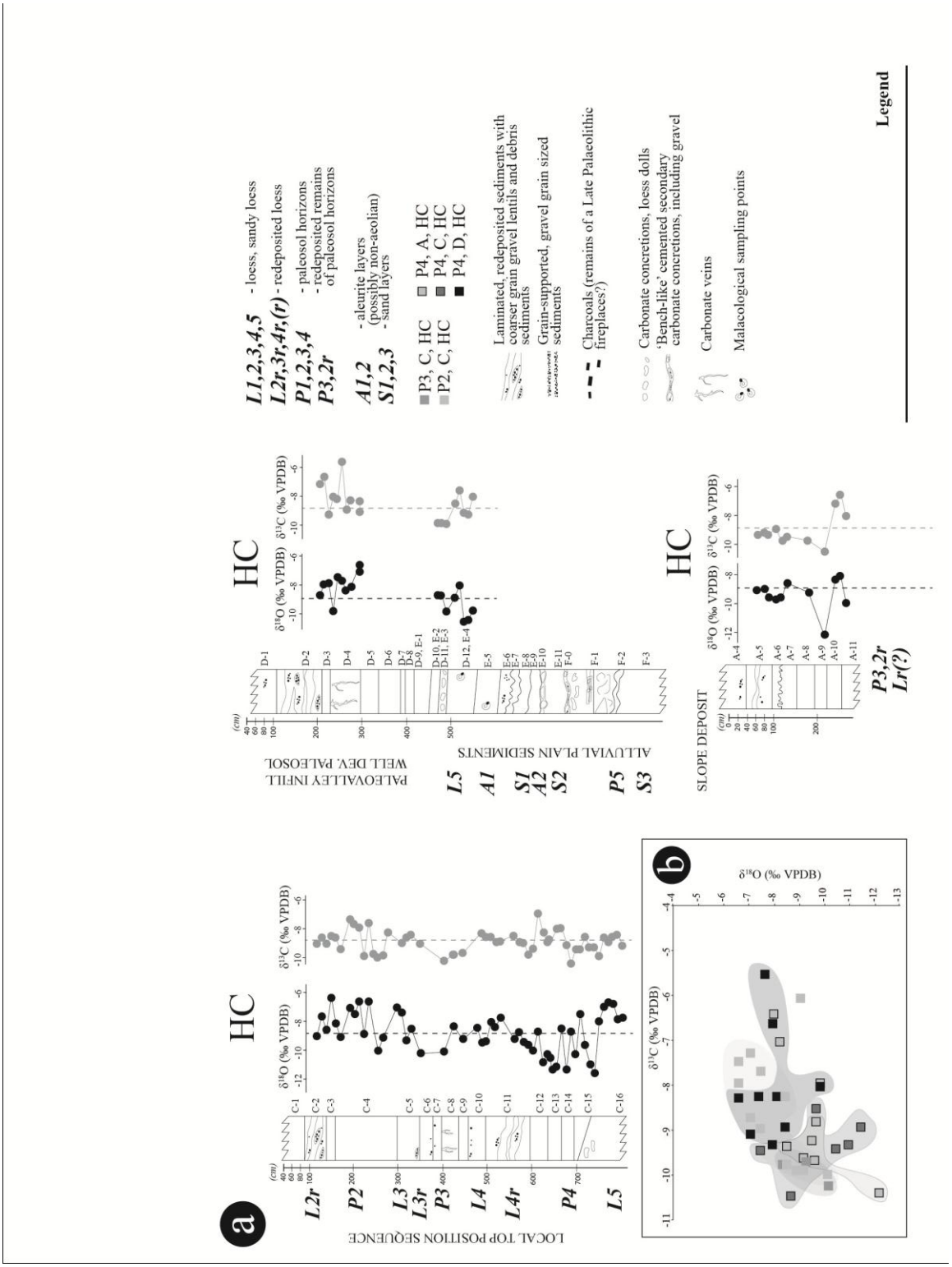

c. EBS curves of Verőce – profile C

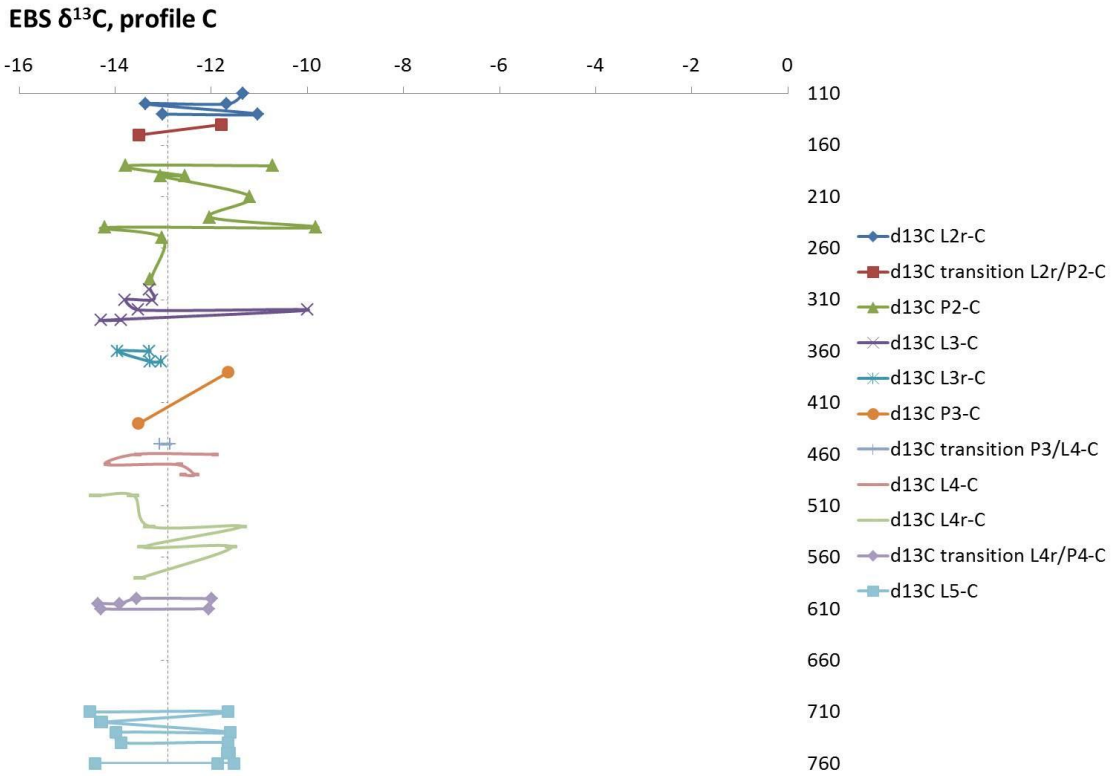

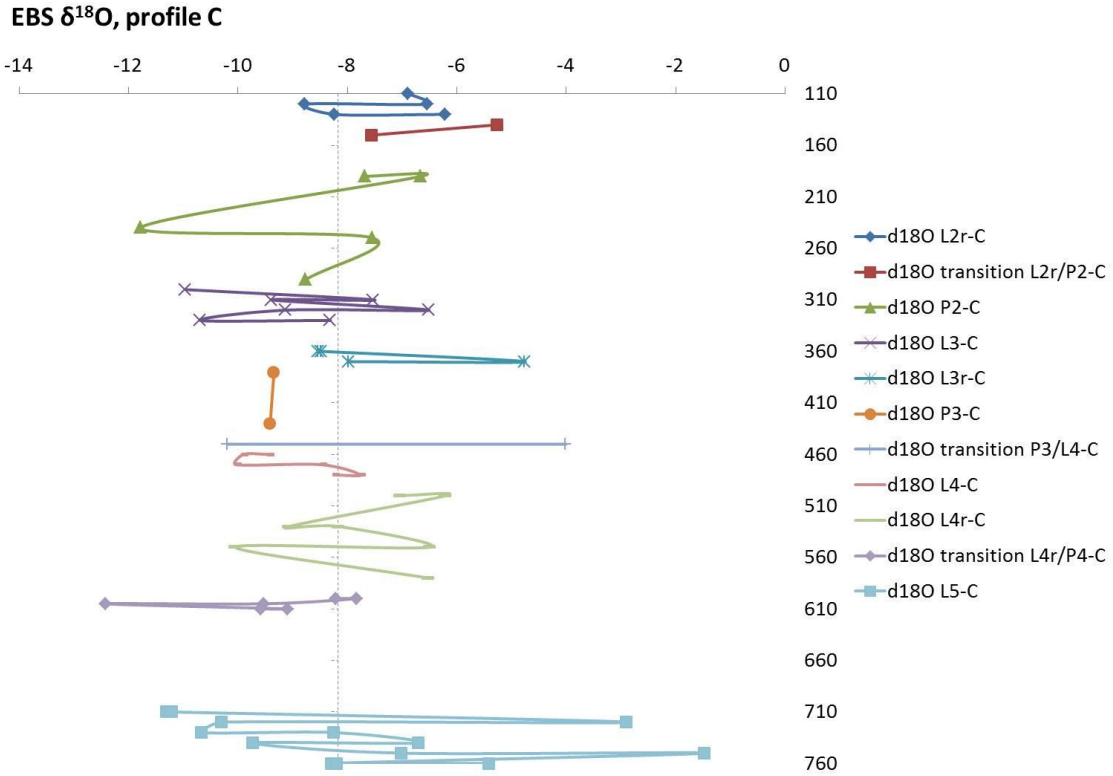

d. EBS curves of Verőce – profile D

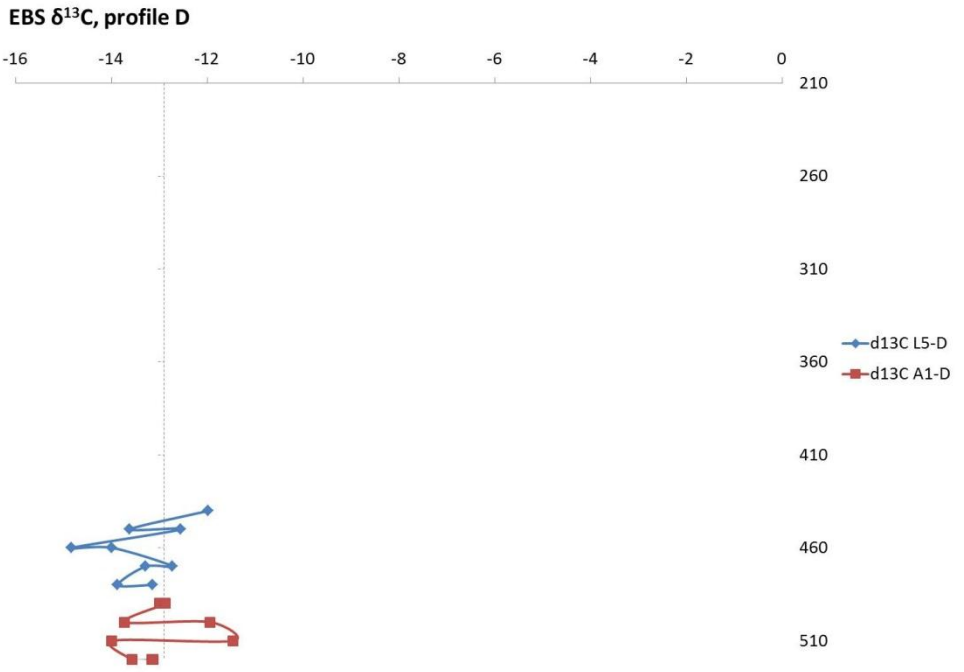

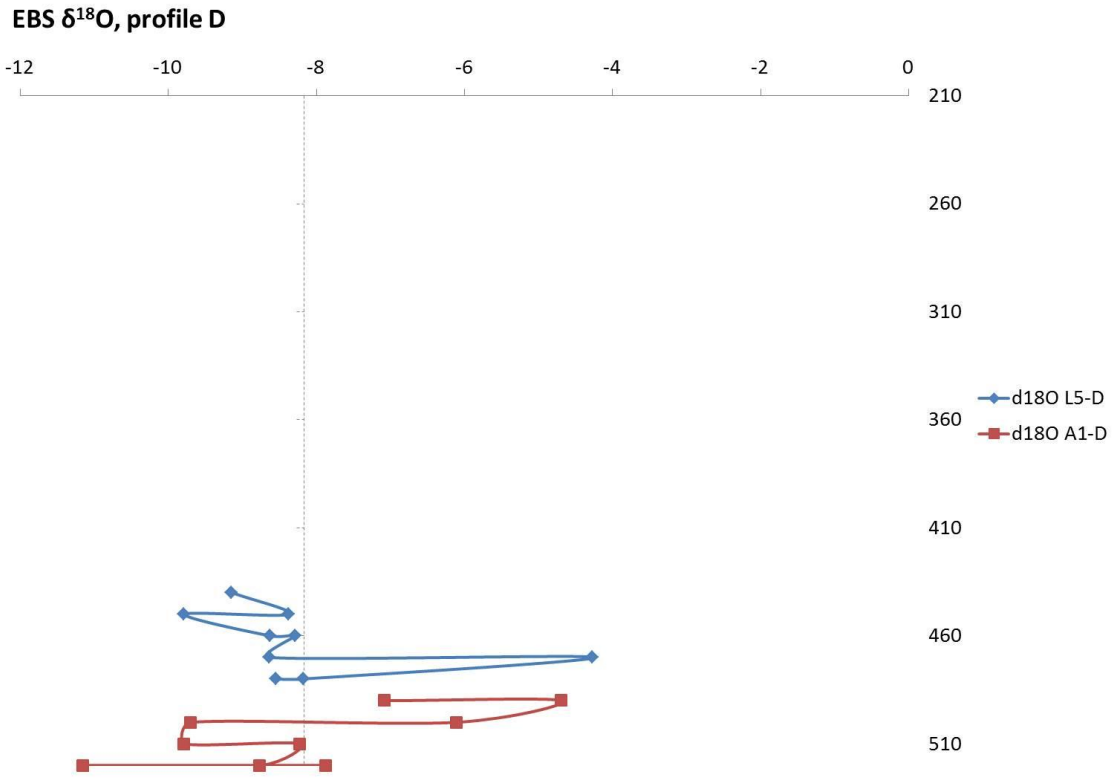

e. HC+CC curves of Verőce – profile D

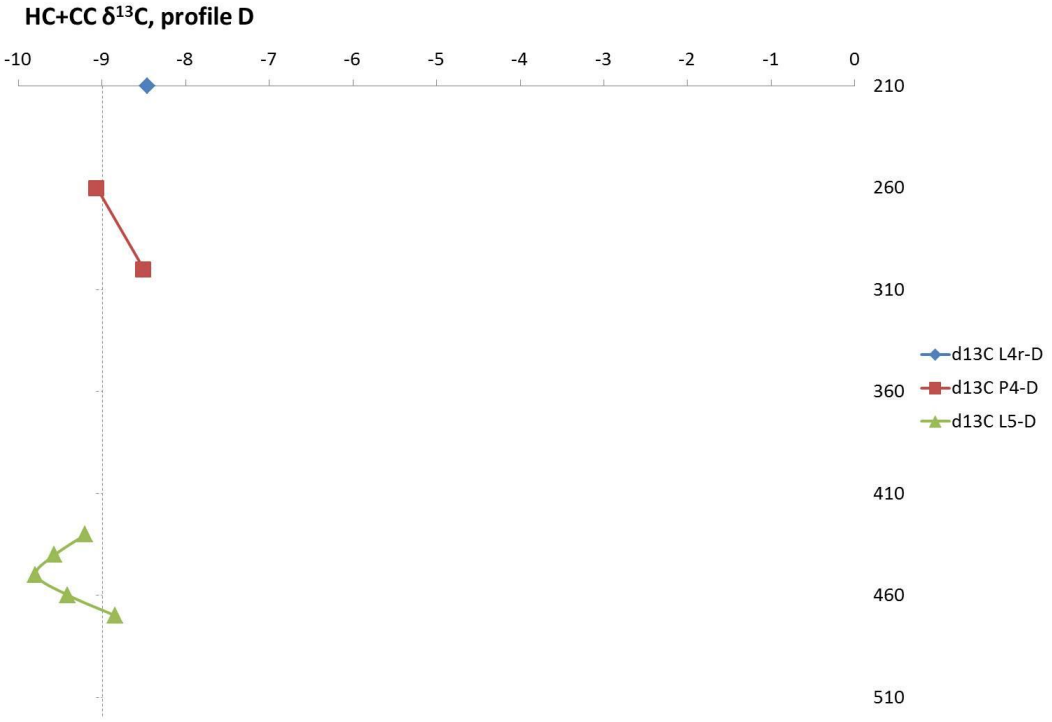

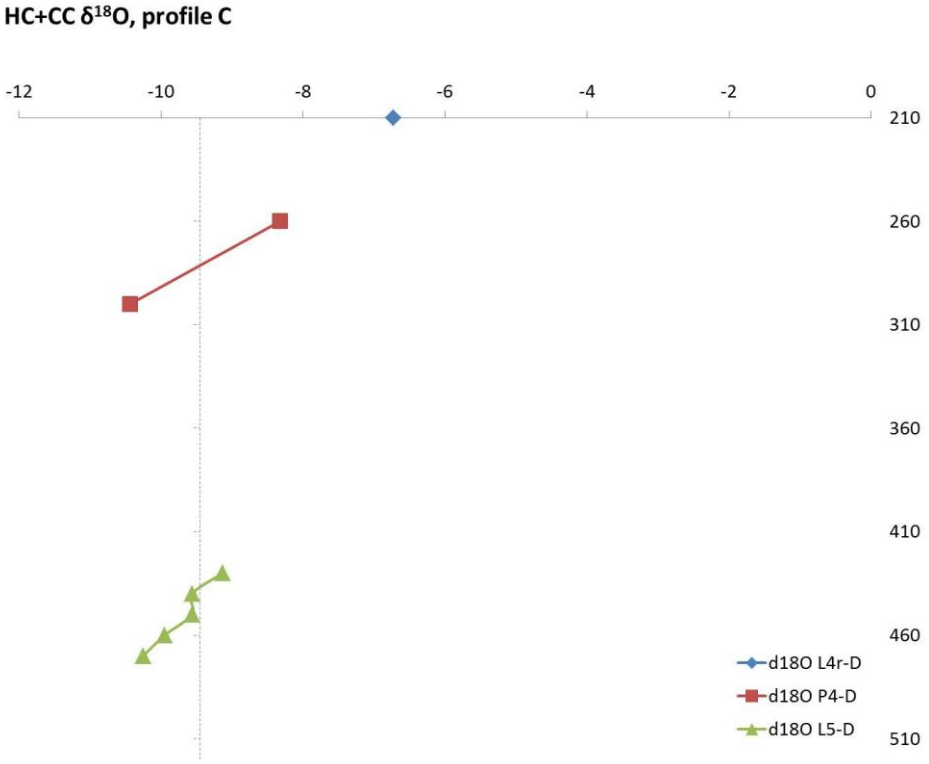

f. CRC curves of Verőce – profile C

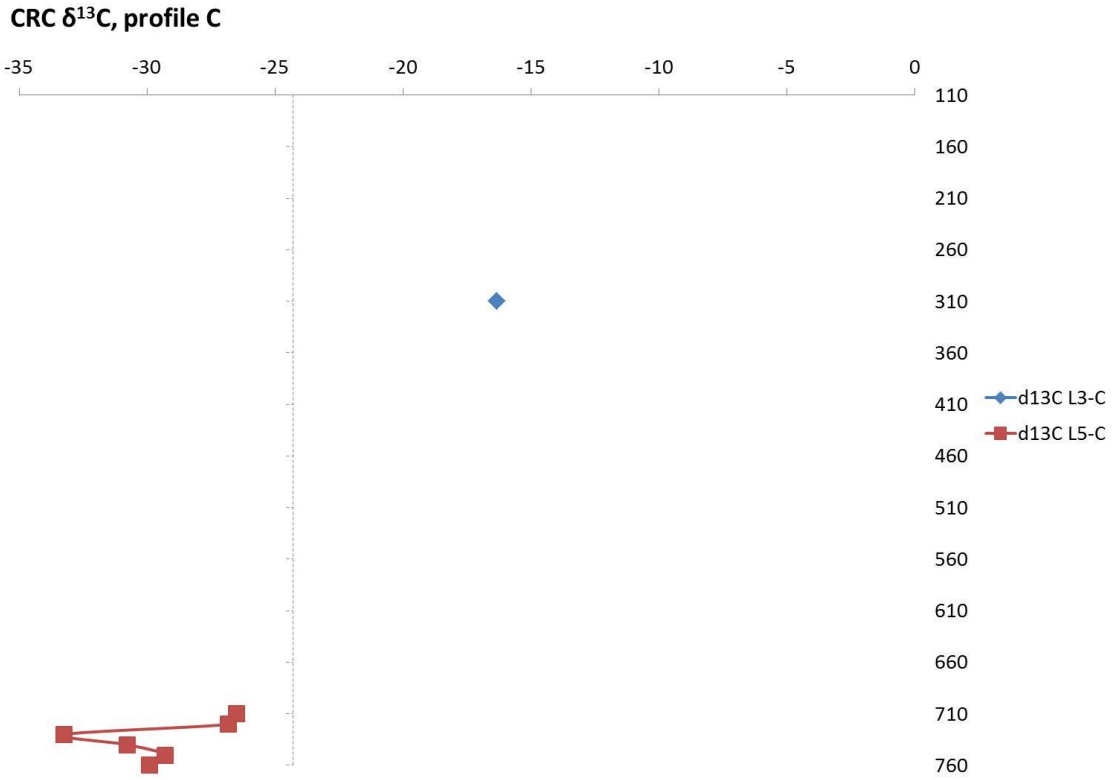

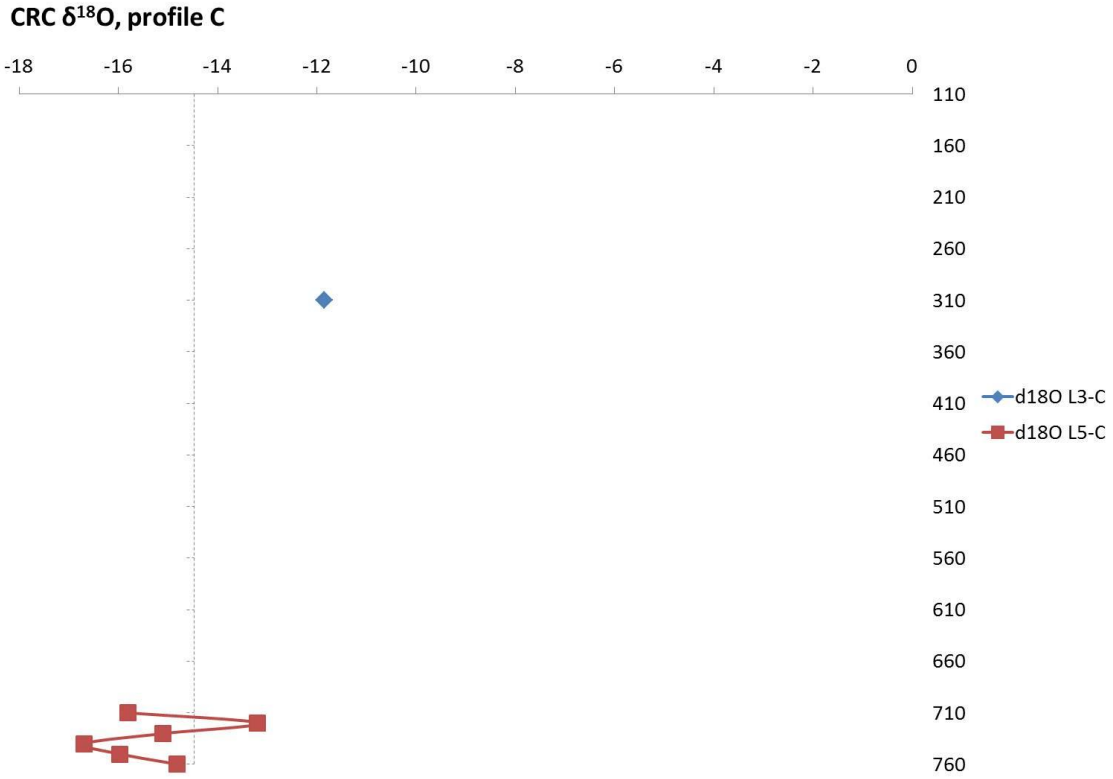

g. CRC curves of Verőce – profile C

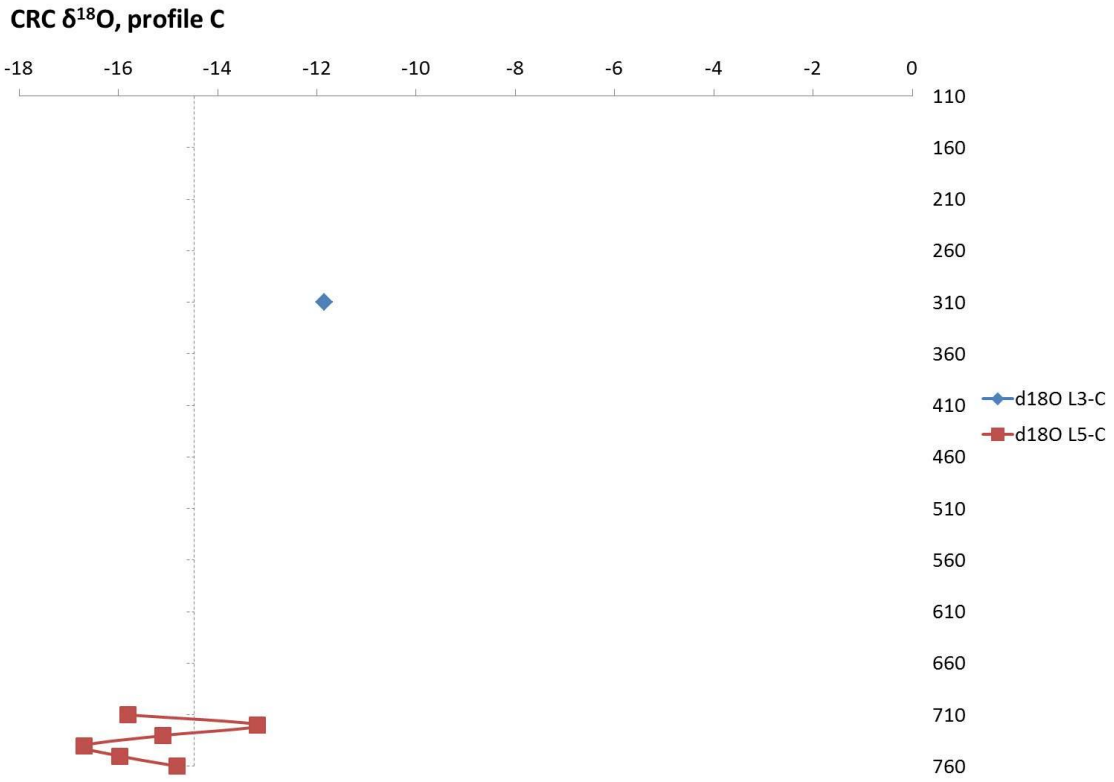

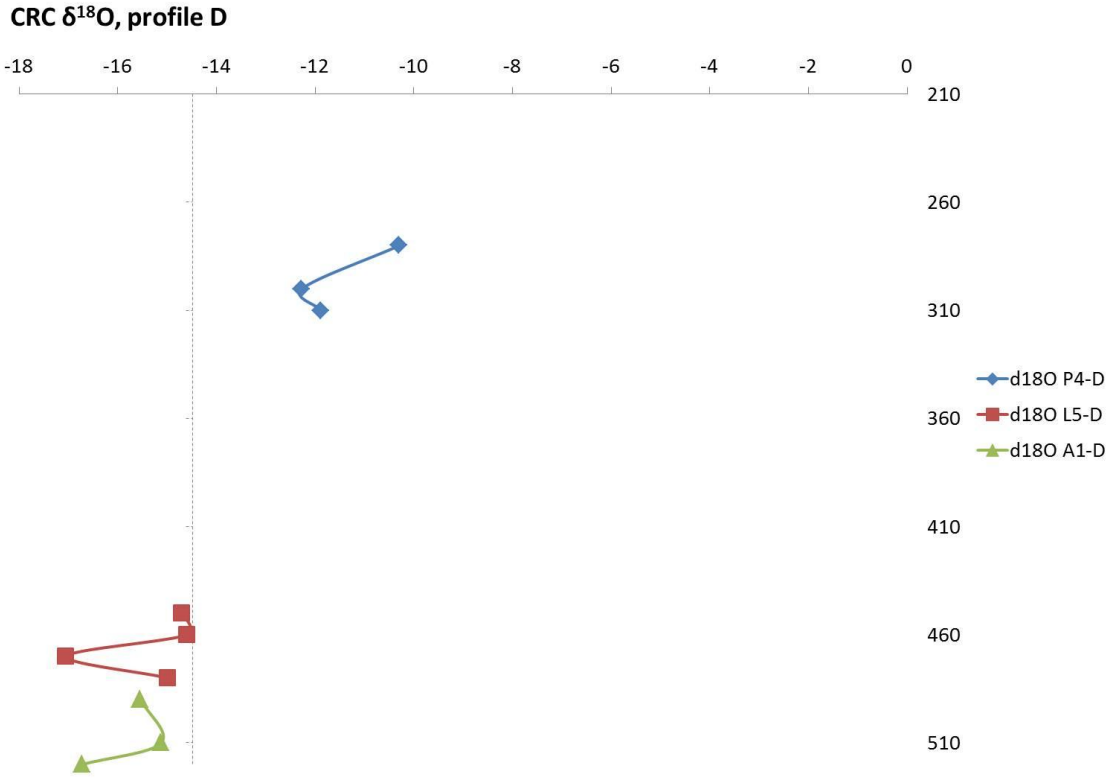

5. Paks

a. Mean values for bulk samples from the Paks sequence

	δ13C (VPDB ‰)				δ18O (VPDB ‰)			
	Max	Min	Mean	SD mean	Max	Min	Mean	SD mean
Unit 0	-2,63	-3,19	**-2,83**	*0,05*	-4,85	-5,31	**-5,06**	*0,13*
Unit 1	0,53	-2,45	**-0,50**	*0,04*	-2,97	-5,22	**-3,95**	*0,08*
Unit 2	-0,16	-1,53	**-0,60**	*0,02*	-3,91	-4,83	**-4,31**	*0,07*
Unit 3	0,23	-0,87	**-0,23**	*0,02*	-3,80	-4,41	**-4,10**	*0,07*
Unit 4	-0,27	-2,95	**-1,41**	*0,02*	-3,94	-5,33	**-4,60**	*0,10*
Unit 5	-0,70	-3,39	**-2,04**	*0,02*	-4,18	-4,87	**-4,52**	*0,10*
Unit 6	-1,90	-3,47	**-2,77**	*0,02*	-4,41	-4,90	**-4,62**	*0,11*
Unit 7	-2,96	-4,10	**-3,53**	*0,03*	-4,65	-5,20	**-4,85**	*0,08*
Unit 8	-4,63	-12,37	**-8,38**	*0,03*	-5,44	-9,18	**-7,31**	*0,06*
Unit 9	-6,94	-8,25	**-7,52**	*0,02*	-6,82	-7,50	**-7,16**	*0,07*
Unit 10	-6,33	-6,82	**-6,49**	*0,02*	-6,59	-7,04	**-6,79**	*0,07*

b. Bulk samples of Paks

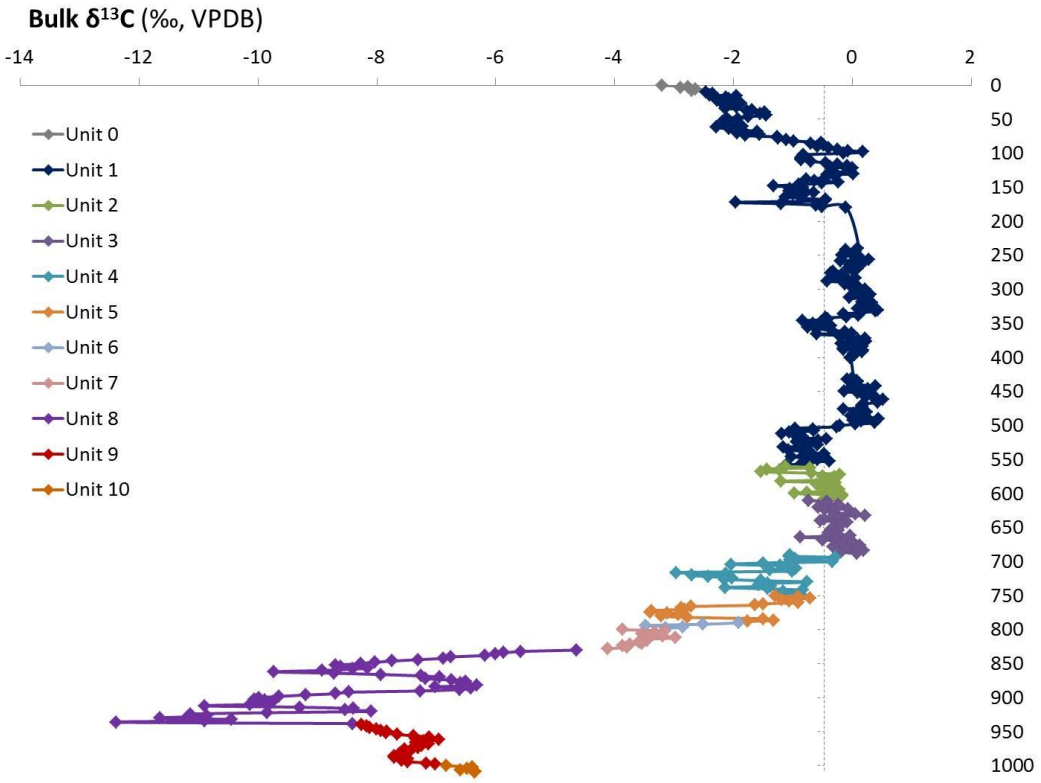

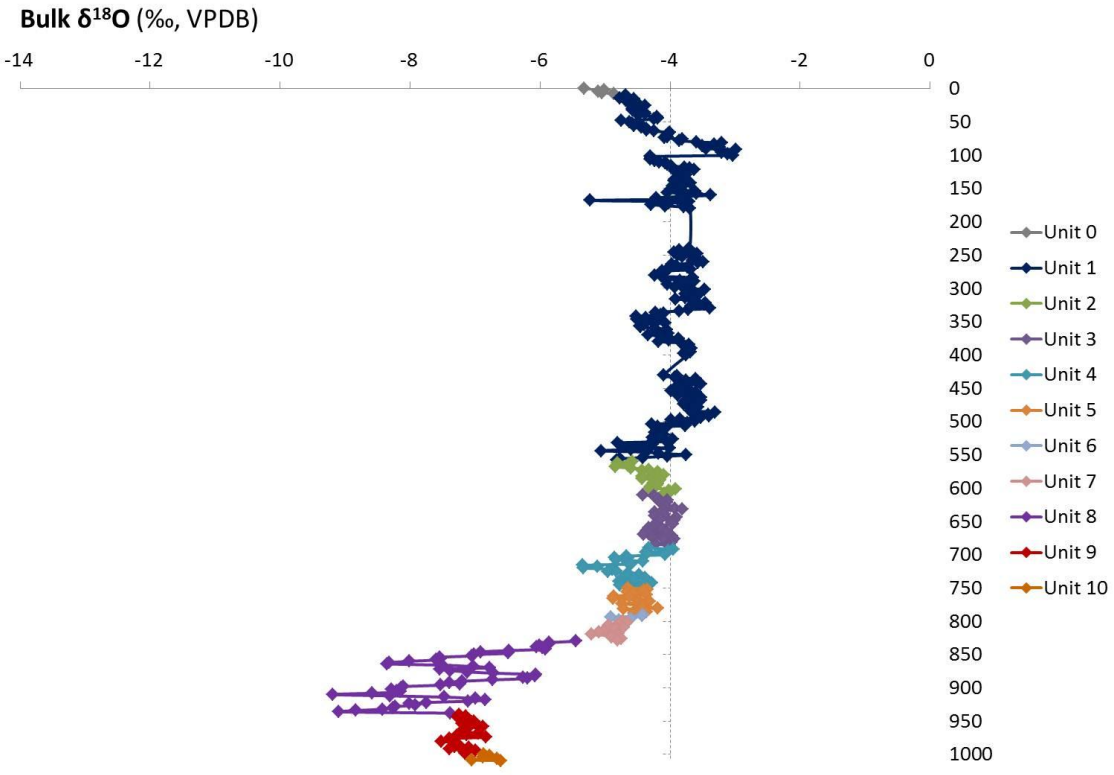

c. Bulk samples of Paks – Unit 1,2,3

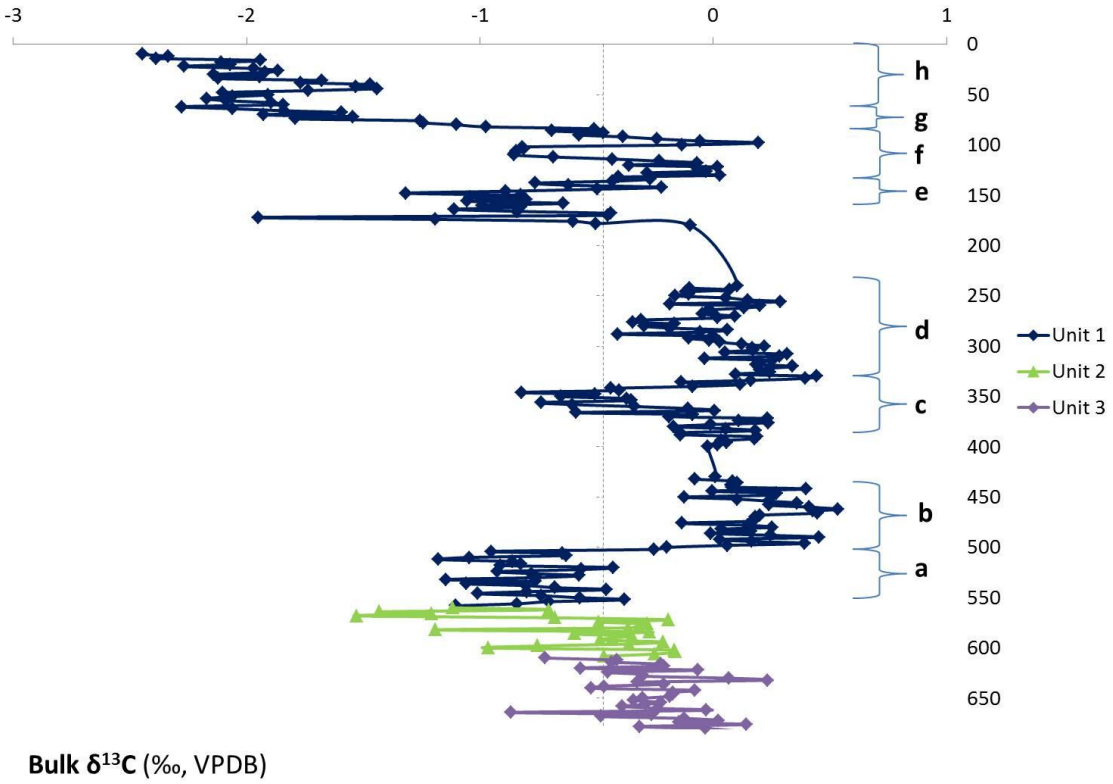

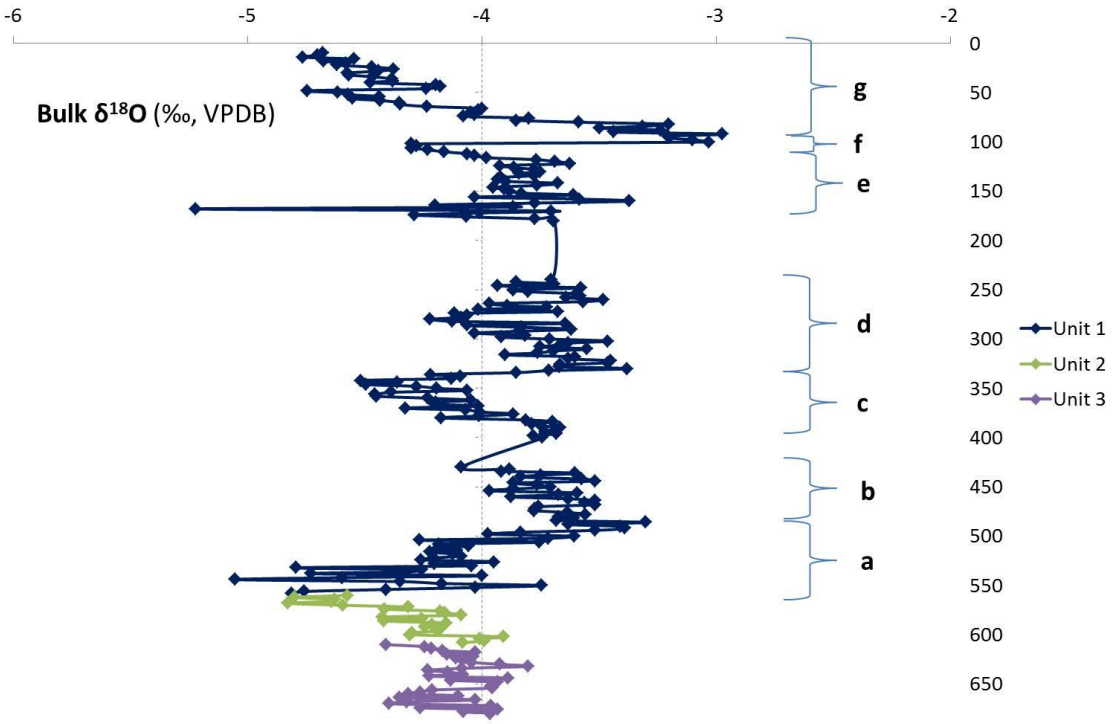

d. Bulk samples of Paks – Unit 2,3

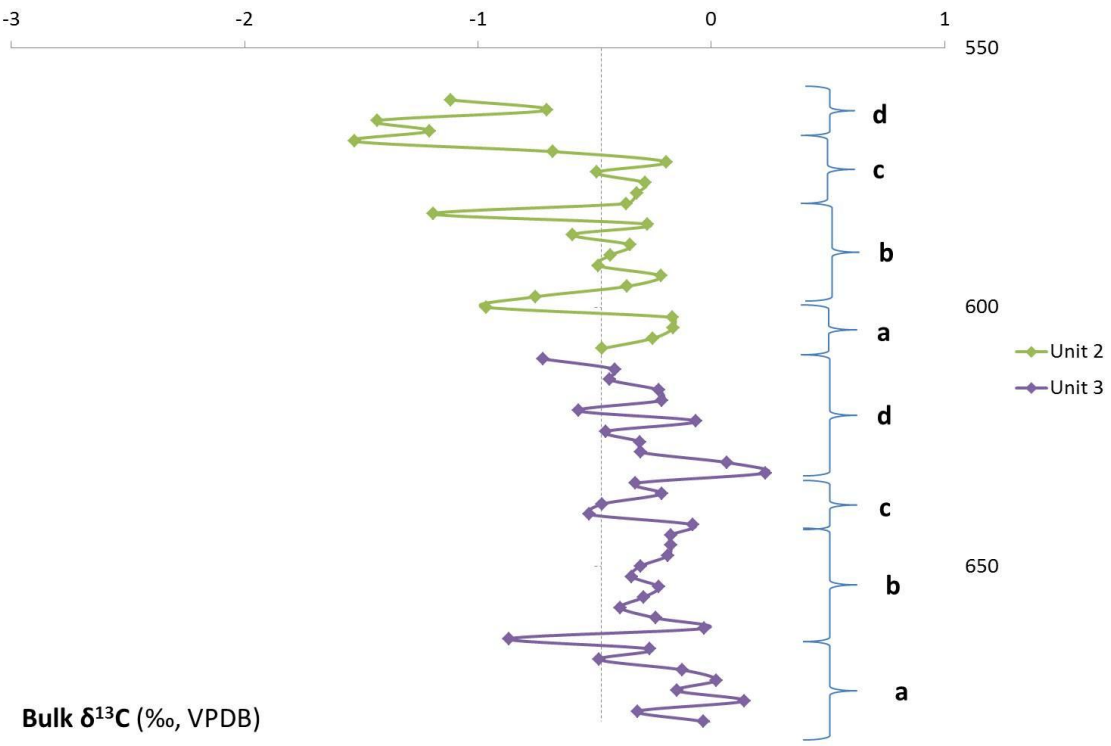

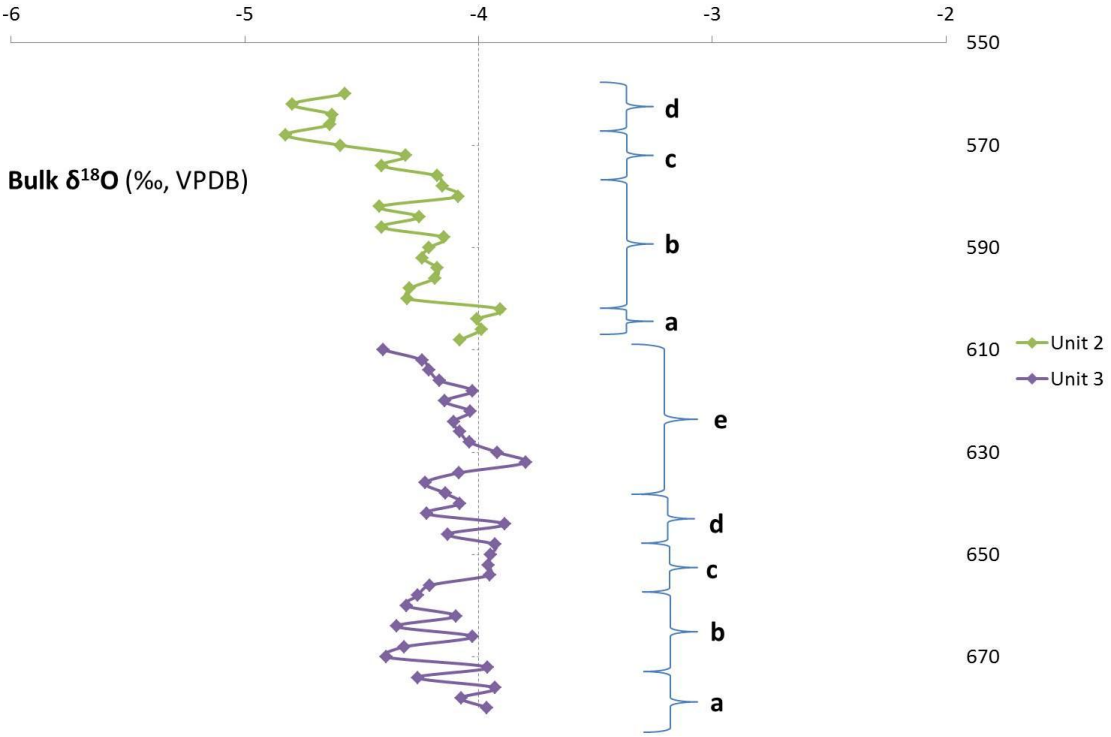

e. Bulk samples of Paks – Unit 4,5,6,7

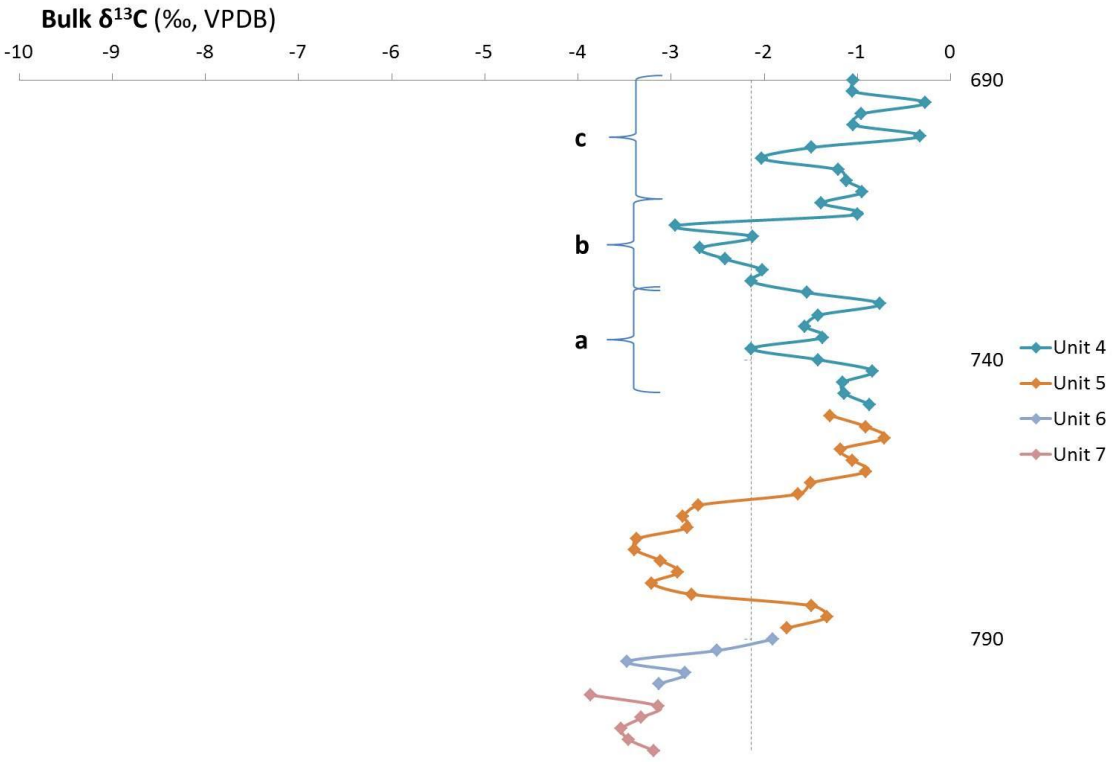

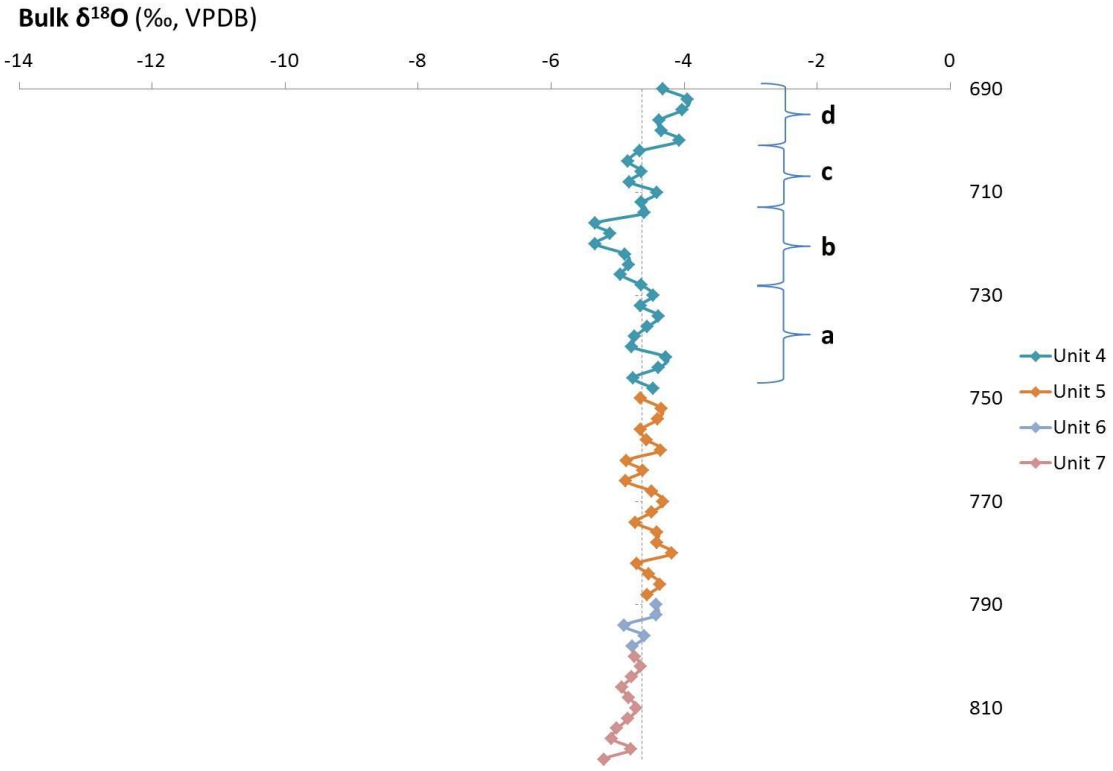

f. Bulk samples of Paks – Unit 8,9,10

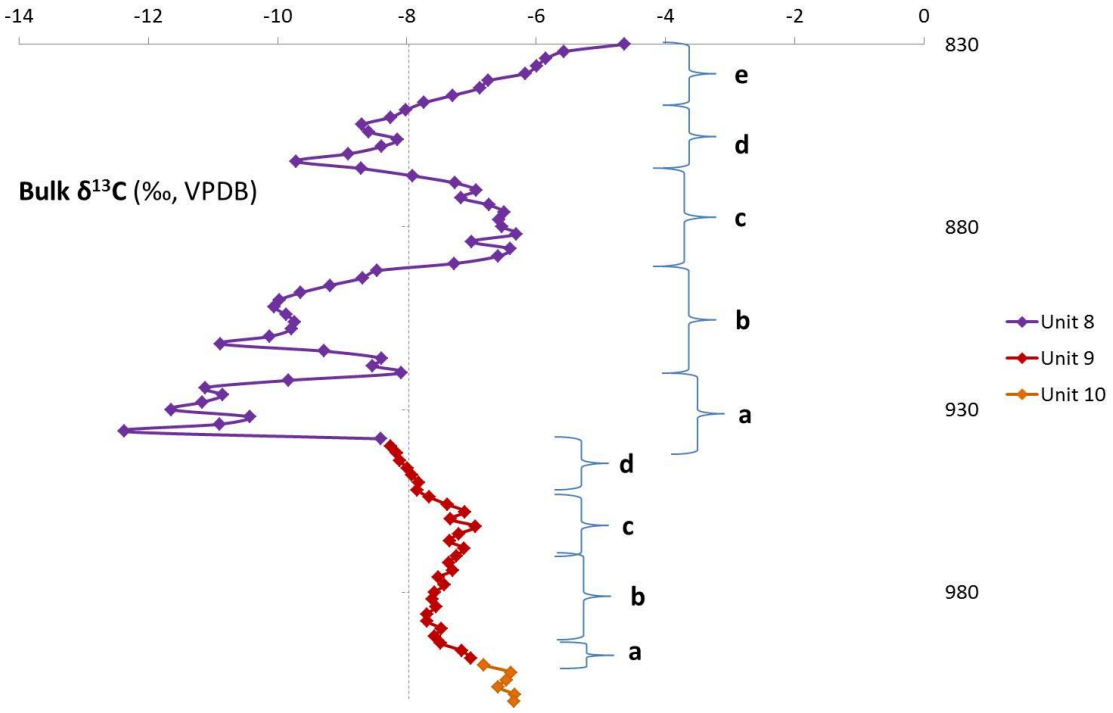

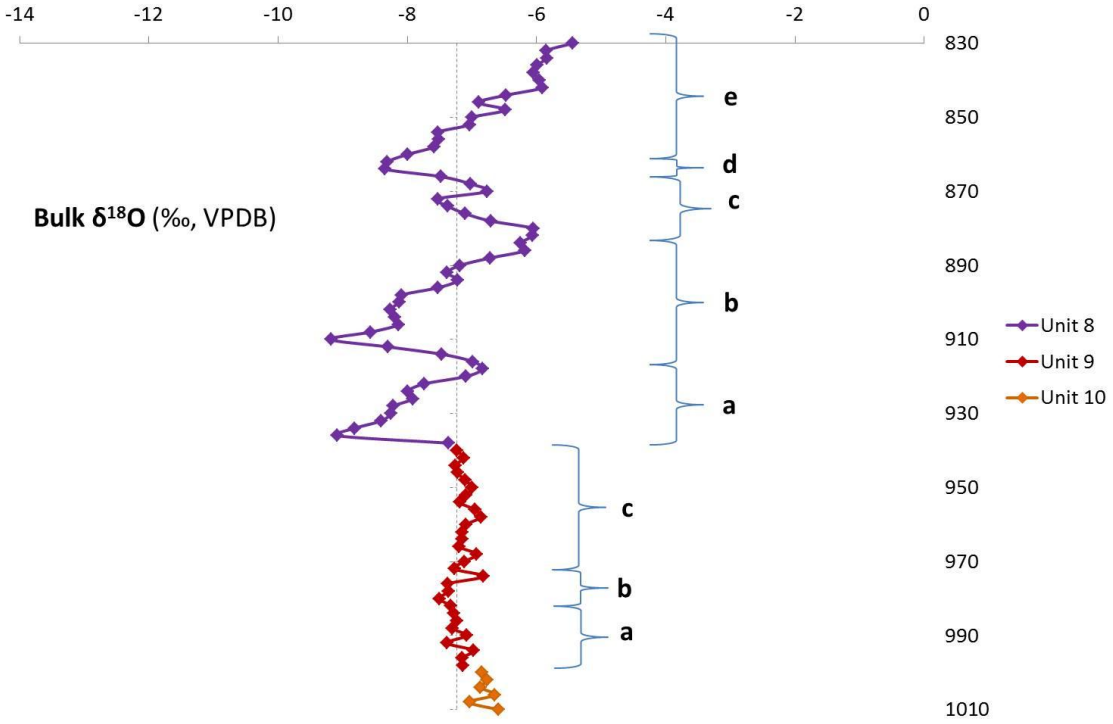

g. Hypocoatings of Paks

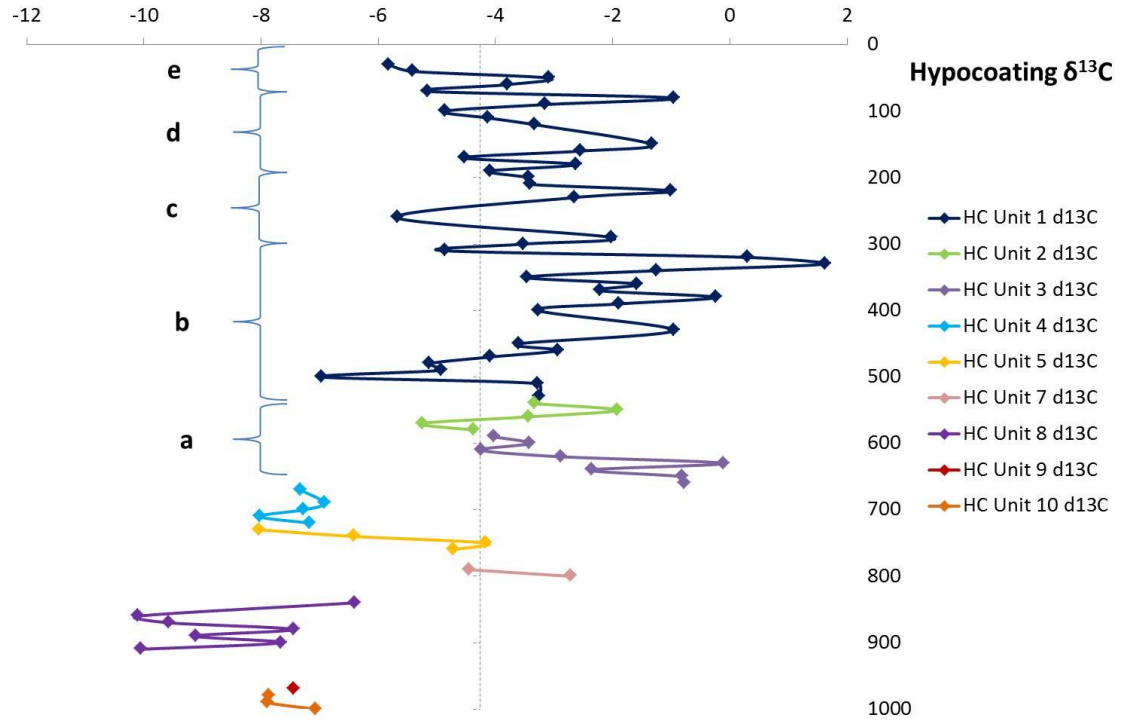

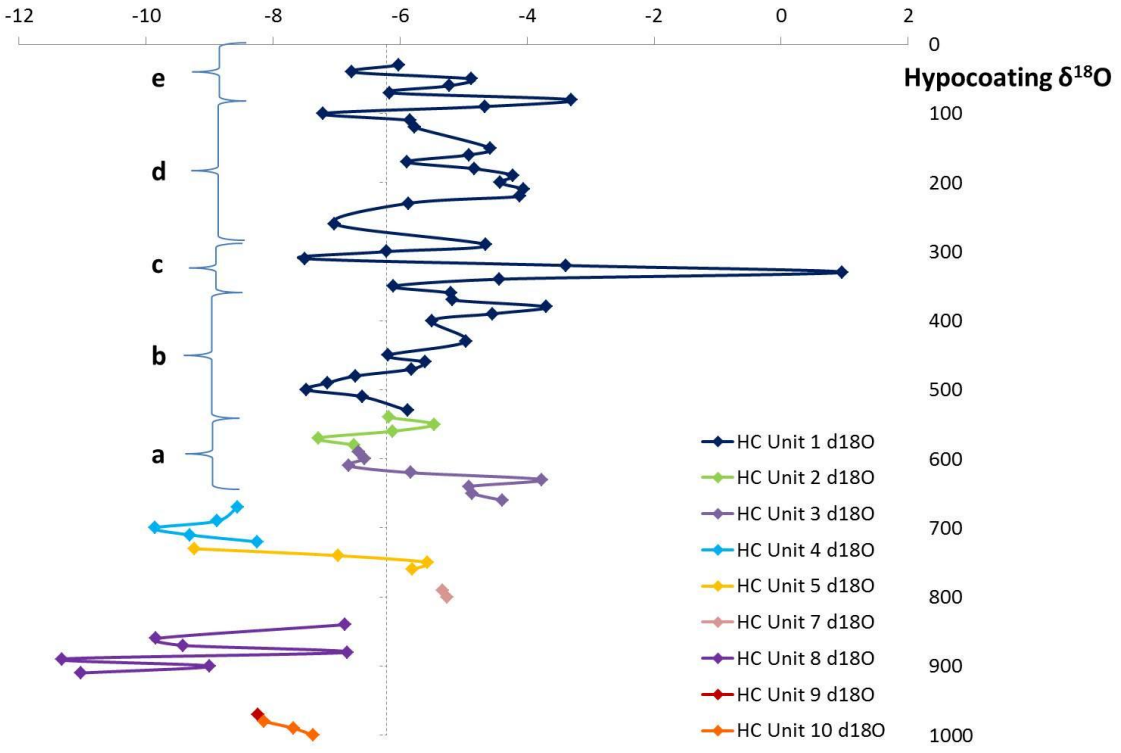

h. Earthworm biospheroids of Paks

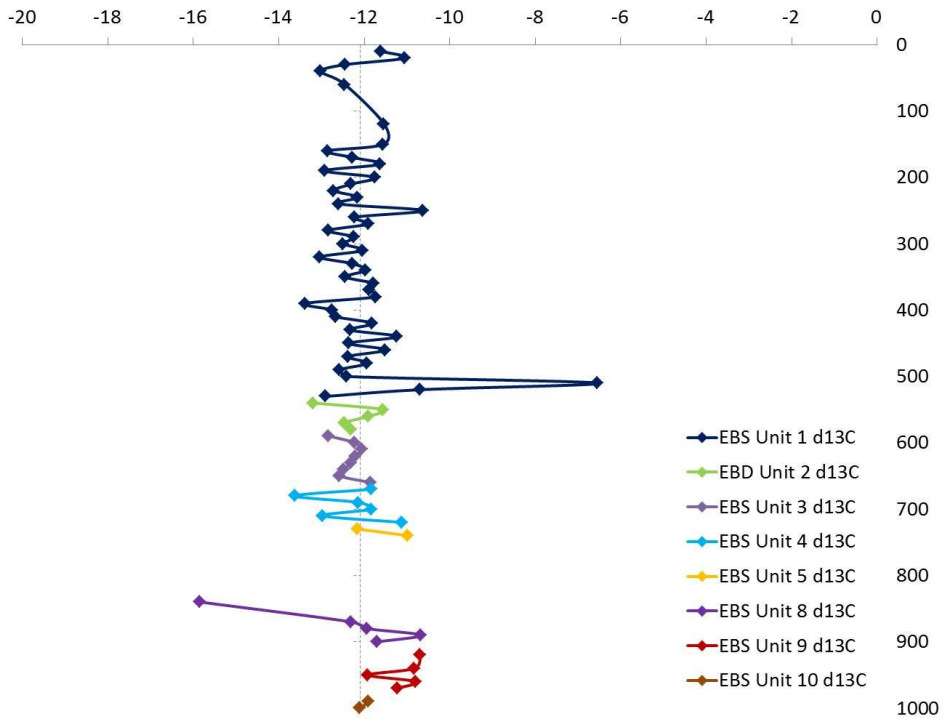

Earthworm biospheroid $\delta^{13}C$

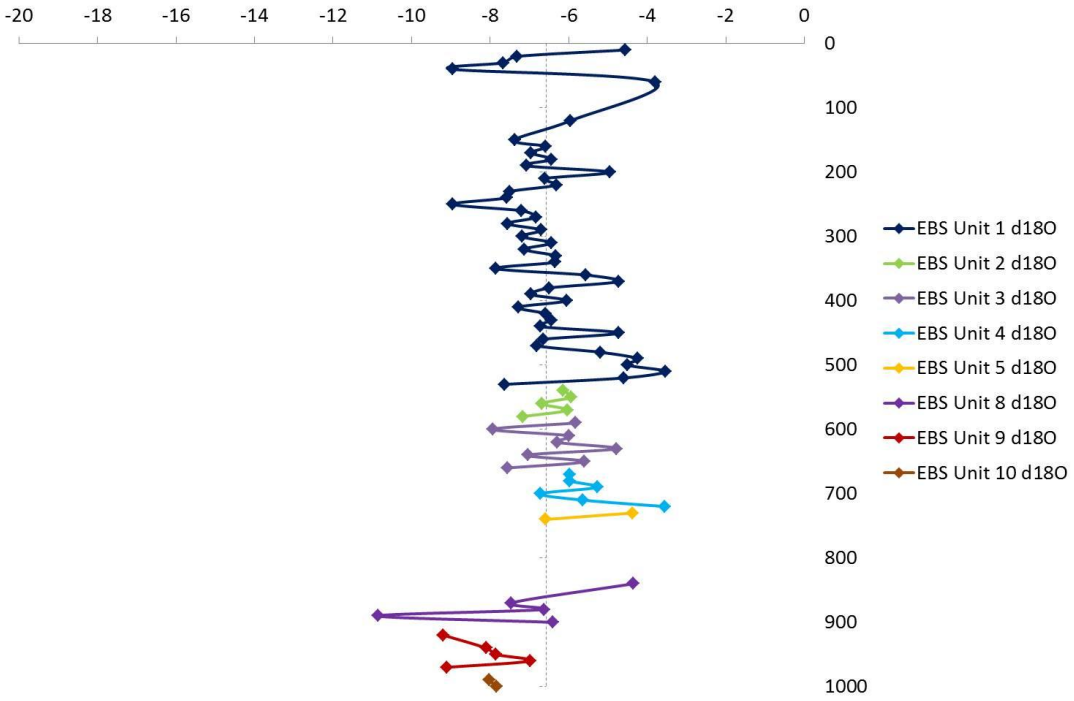

Earthworm biospheroid $\delta^{18}O$

i. Amount of EBS at Paks

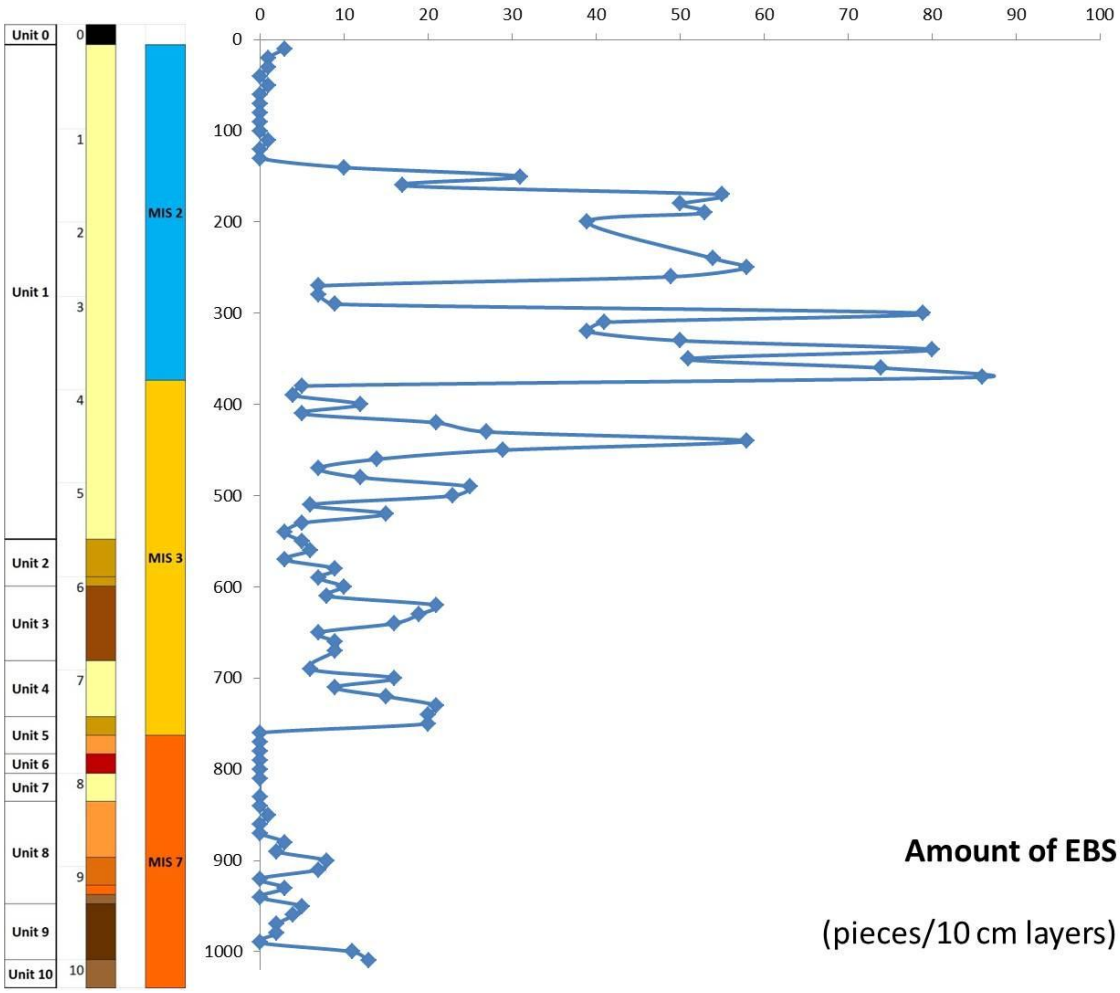

6. Villánykövesd

a. Mean values of bulk samples from the Villánykövesd sequence

	δ13C (VPDB ‰)				δ18O (VPDB ‰)			
	Max	**Min**	**Mean**	**SD mean**	**Max**	**Min**	**Mean**	**SD mean**
Unit 2	-2,02	-7,56	**-4,19**	*0,08*	-4,96	-6,42	**-5,76**	*0,11*
Unit 3	-1,95	-3,50	**-2,58**	*0,11*	-5,35	-9,12	**-6,28**	*0,18*
Unit 4	-1,16	-3,31	**-2,07**	*0,05*	-4,72	-6,27	**-5,53**	*0,13*
Unit 5	-0,91	-4,30	**-1,96**	*0,04*	-4,34	-6,53	**-5,11**	*0,08*
Unit 7	-3,14	-5,76	**-4,18**	*0,05*	-4,88	-6,85	**-5,61**	*0,08*
Unit 8	-4,81	-12,09	**-8,11**	*0,08*	-6,31	-11,89	**-8,87**	*0,08*
Unit 9	-7,70	-10,55	**-9,10**	*0,08*	-6,99	-9,38	**-7,91**	*0,08*
Unit 10	-6,97	-7,78	**-7,31**	*0,05*	-6,61	-7,24	**-6,92**	*0,07*
Unit 11	-7,99	-9,47	**-9,05**	*0,05*	-7,09	-7,98	**-7,67**	*0,06*
Unit 12	-8,34	-9,35	**-8,78**	*0,05*	-7,50	-7,91	**-7,71**	*0,07*
Unit 13	-8,50	-10,83	**-9,61**	*0,05*	-7,40	-9,60	**-8,37**	*0,07*
Unit 14	-10,63	-12,76	**-11,48**	*0,07*	-9,23	-12,28	**-10,53**	*0,09*
Unit 16	-10,22	-13,84	**-11,36**	*0,03*	-8,26	-11,14	**-9,45**	*0,08*
Unit 18								

	-9,20	-11,35	**-9,85**	*0,04*	-6,89	-9,59	**-7,87**	*0,08*
Unit 19								
	-7,43	-10,15	**-8,98**	*0,05*	-7,35	-8,88	**-7,87**	*0,06*
Unit 20								
	-9,88	-11,62	**-10,61**	*0,07*	-8,75	-10,33	**-9,49**	*0,07*

b. Mean values of secondary carbonates in the Villánykövesd sequence

	δ13C (VPDB ‰)				δ18O (VPDB ‰)			
	Max	**Min**	**Mean**	**SD mean**	**Max**	**Min**	**Mean**	**SD mean**
Unit 1								
EBS	-9,34	-13,94	**-11,76**	*0,03*	-4,26	-10,48	**-7,91**	*0,13*
HC	-8,59	-10,37	**-9,74**	*0,03*	-6,76	-8,24	**-7,26**	*0,09*
HC+CC	-9,17	-10,10	**-9,75**	*0,03*	-6,51	-8,37	**-7,31**	*0,08*
Unit 2								
EBS	-9,37	-13,73	**-12,36**	*0,06*	-4,93	-10,23	**-7,39**	*0,08*
HC	-7,04	-9,87	**-8,66**	*0,07*	-5,61	-8,08	**-7,20**	*0,08*
HC+CC	-8,21	-9,92	**-8,80**	*0,03*	-7,28	-8,17	**-7,86**	*0,06*
CRC	-28,47	-31,18	**-30,01**	*0,09*	-14,81	-16,12	**-15,80**	*0,10*
Unit 3								
EBS	-12,59	-13,22	**-12,90**	*0,01*	-4,79	-8,57	**-6,68**	*0,04*
HC	-6,23	-7,85	**-7,04**	*0,01*	-7,70	-7,79	**-7,75**	*0,04*
HC+CC	-8,70	-8,84	**-8,77**	*0,01*	-7,42	-7,84	**-7,63**	*0,04*
Unit 4								
EBS	-13,66	-15,10	**-14,29**	*0,02*	-4,59	-6,97	**-5,87**	*0,05*
HC	-8,43	-9,12	**-8,72**	*0,12*	-5,98	-7,40	**-6,87**	*0,09*
HC+CC	-8,10	-8,36	**-8,23**	*0,13*	-5,91	-6,48	**-6,19**	*0,07*
Unit 5								
EBS	-10,87	-13,84	**-11,91**	*0,02*	-4,59	-9,52	**-7,58**	*0,08*
HC	-4,94	-10,43	**-8,24**	*0,02*	-6,24	-7,61	**-6,94**	*0,07*
HC+CC	-6,37	-10,53	**-8,92**	*0,02*	-6,07	-7,21	**-6,56**	*0,09*
Unit 6								
EBS	-11,37	-12,23	**-11,92**	*0,04*	-5,79	-8,03	**-7,11**	*0,07*
Unit 7								
EBS	-10,02	-12,93	**-11,91**	*0,03*	-5,95	-10,08	**-8,73**	*0,03*
HC	-8,13	-9,11	**-8,68**	*0,03*	-6,83	-7,78	**-7,34**	*0,03*
Unit 8								
EBS	-11,49	-13,23	**-12,19**	*0,05*	-5,95	-7,76	**-6,89**	*0,03*
HC	-6,83	-9,10	**-8,09**	*0,05*	-6,49	-7,84	**-7,15**	*0,03*
HC+CC	-7,39	-8,85	**-8,31**	*0,05*	-6,80	-7,98	**-7,23**	*0,03*
Unit 9								
EBS	-11,40	-12,16	**-11,69**	*0,05*	-5,63	-9,21	**-7,55**	*0,04*
HC	-4,85	-7,62	**-6,41**	*0,06*	-7,31	-7,92	**-7,65**	*0,03*

Unit 10								
EBS	-12,77	-13,98	**-13,37**	*0,04*	-5,47	-6,40	**-5,94**	*0,06*
HC	-5,79	-8,26	**-7,02**	*0,04*	-6,67	-7,03	**-6,85**	*0,06*
Unit 11								
EBS	-12,14	-12,56	**-12,40**	*0,04*	-6,71	-9,61	**-8,04**	*0,05*
HC	-6,86	-7,89	**-7,38**	*0,04*	-5,01	-7,57	**-6,29**	*0,06*
Unit 13								
EBS	-13,03	-13,70	**-13,37**	*0,04*	-7,11	-7,45	**-7,28**	*0,06*
HC	-5,87	-6,23	**-6,05**	*0,04*	-6,66	-7,94	**-7,30**	*0,06*
Unit 14								
EBS	-12,63	-13,55	**-13,09**	*0,04*	-3,94	-6,09	**-5,02**	*0,06*
HC	-3,92	-6,30	**-5,11**	*0,04*	-4,82	-6,35	**-5,59**	*0,06*
Unit 15								
EBS	-13,02	-14,80	**-13,69**	*0,05*	-4,60	-6,16	**-5,25**	*0,07*
HC	-6,25	-8,65	**-7,29**	*0,05*	-5,00	-6,44	**-5,91**	*0,07*
Unit 16								
EBS	-12,71	-13,37	**-13,04**	*0,02*	-6,40	-8,12	**-7,26**	*0,02*
HC	-6,51	-6,53	**-6,52**	*0,01*	-5,91	-7,39	**-6,65**	*0,02*
Unit 17								
CC	-10,29	-10,81	**-10,55**	*0,02*	-6,96	-9,17	**-8,07**	*0,02*
Unit 18								
EBS	-10,72	-11,80	**-11,47**	*0,01*	-7,29	-9,28	**-8,39**	*0,02*
HC	-9,57	-9,83	**-9,73**	*0,01*	-7,32	-8,24	**-7,80**	*0,02*
Unit 19								
EBS	-10,76	-13,01	**-12,07**	*0,01*	-7,69	-10,96	**-9,58**	*0,02*
HC	-9,96	-10,23	**-10,08**	*0,02*	-7,21	-8,23	**-7,82**	*0,02*
Unit 20								
EBS	-10,72	-13,18	**-11,88**	*0,10*	-8,22	-10,22	**-9,05**	*0,12*
HC	-9,64	-10,34	**-10,07**	*0,06*	-8,14	-8,87	**-8,60**	*0,09*

c. Bulk values of Villánykövesd

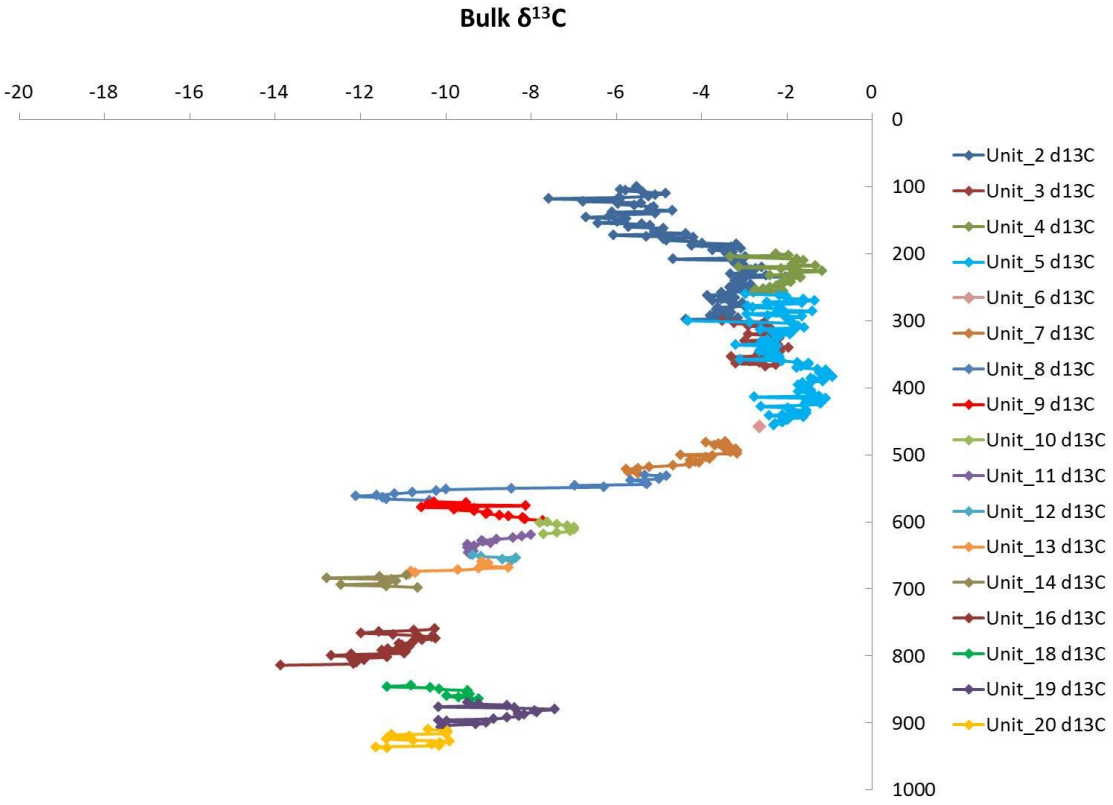

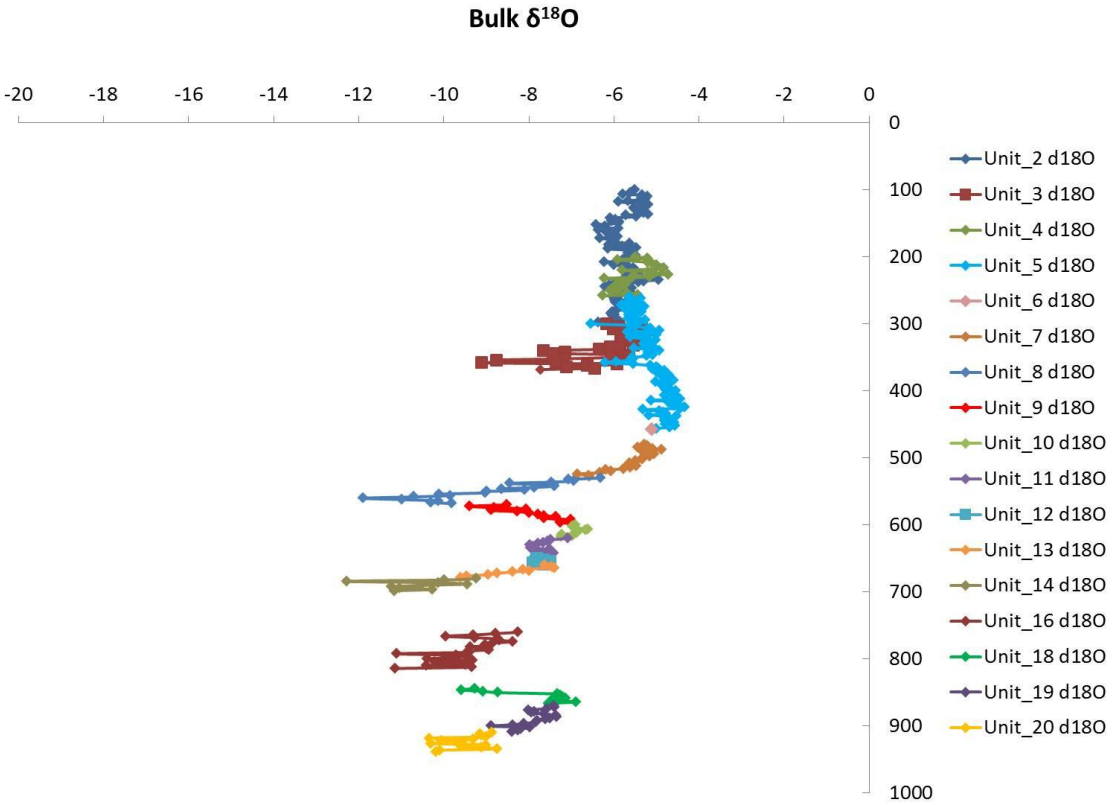

d. Bulk values of Villánykövesd – loess units

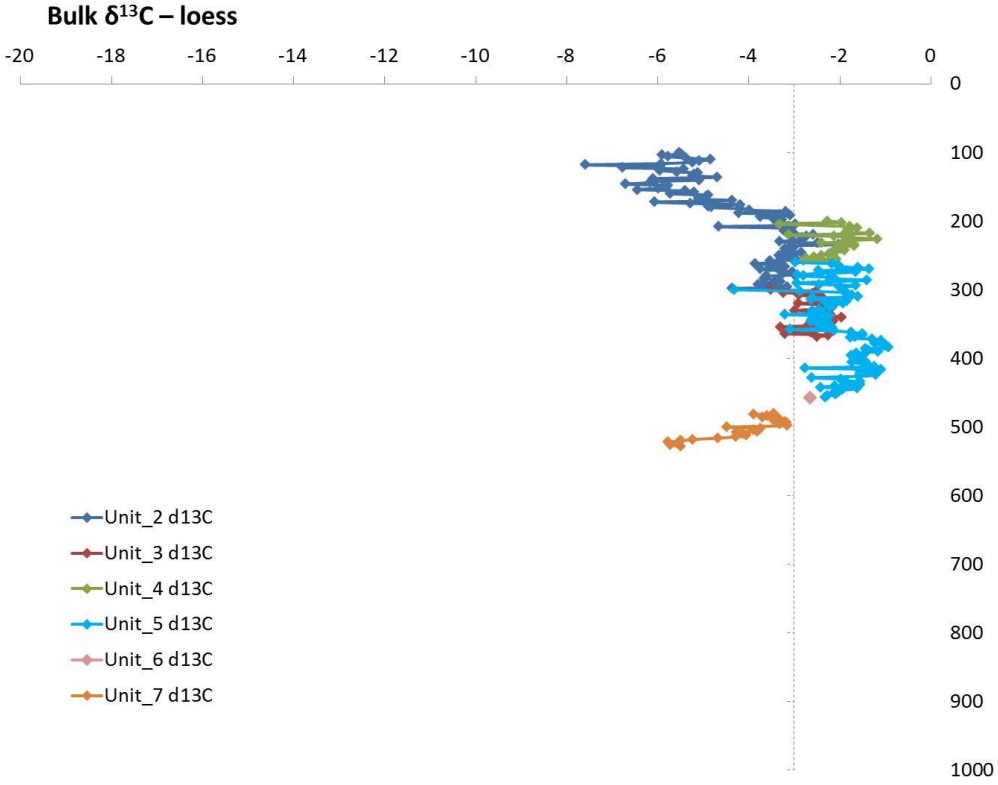

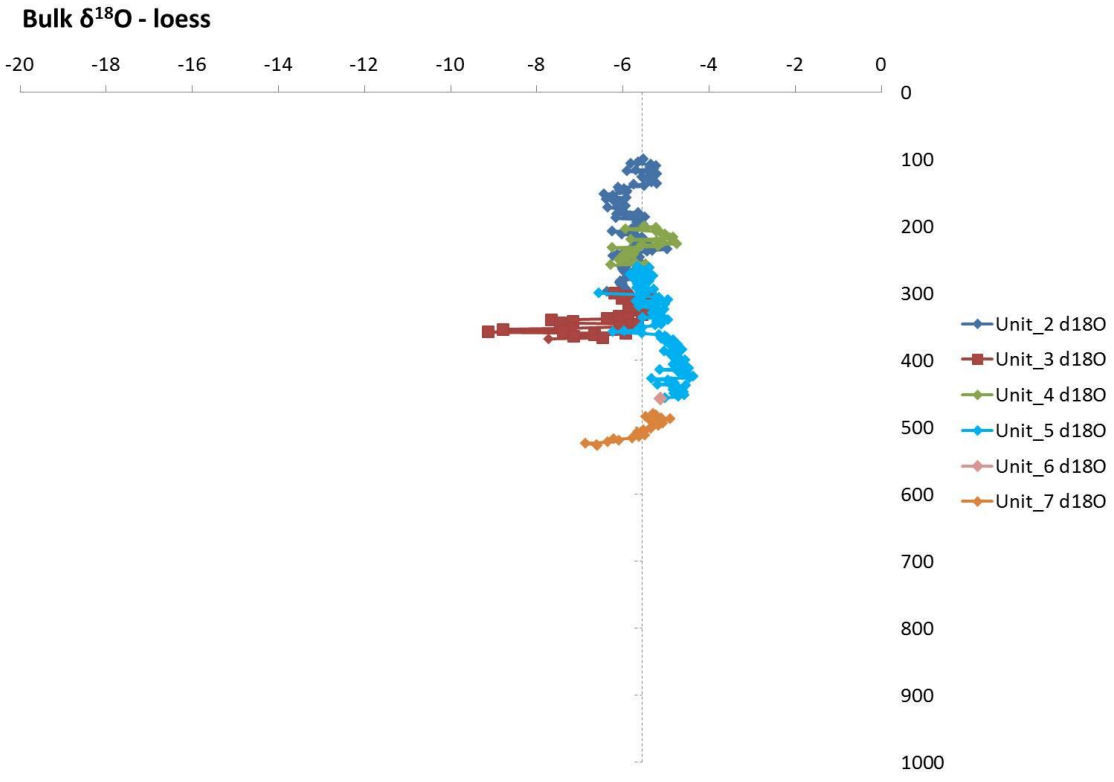

e. Bulk values of Villánykövesd – transition units + Unit 13 loess + Unit 18 loess

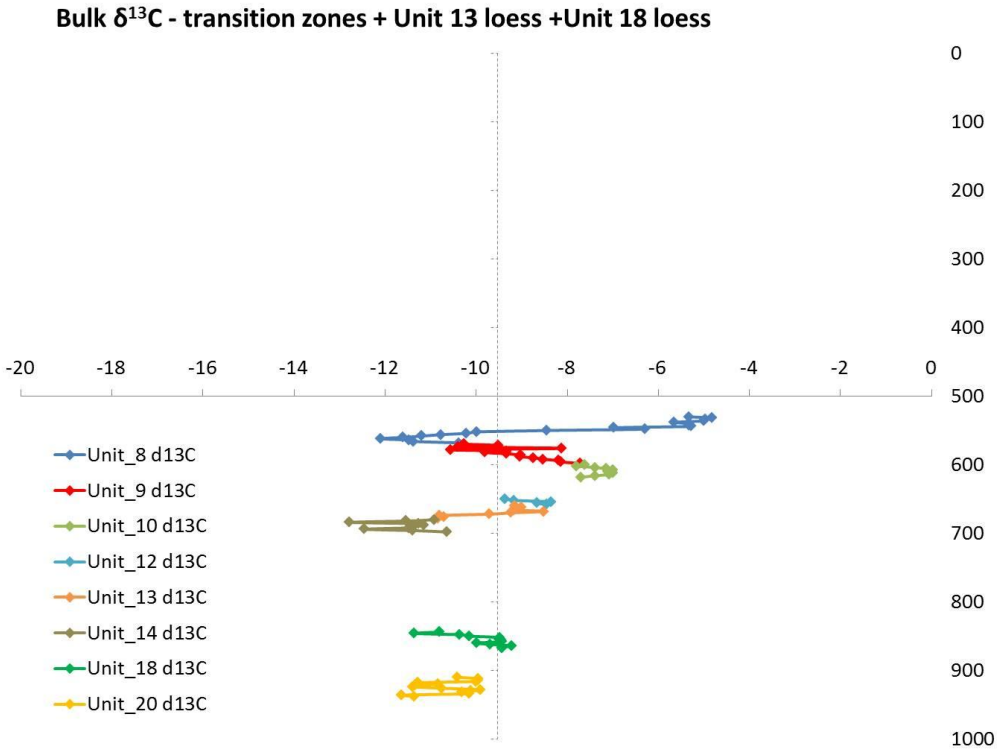

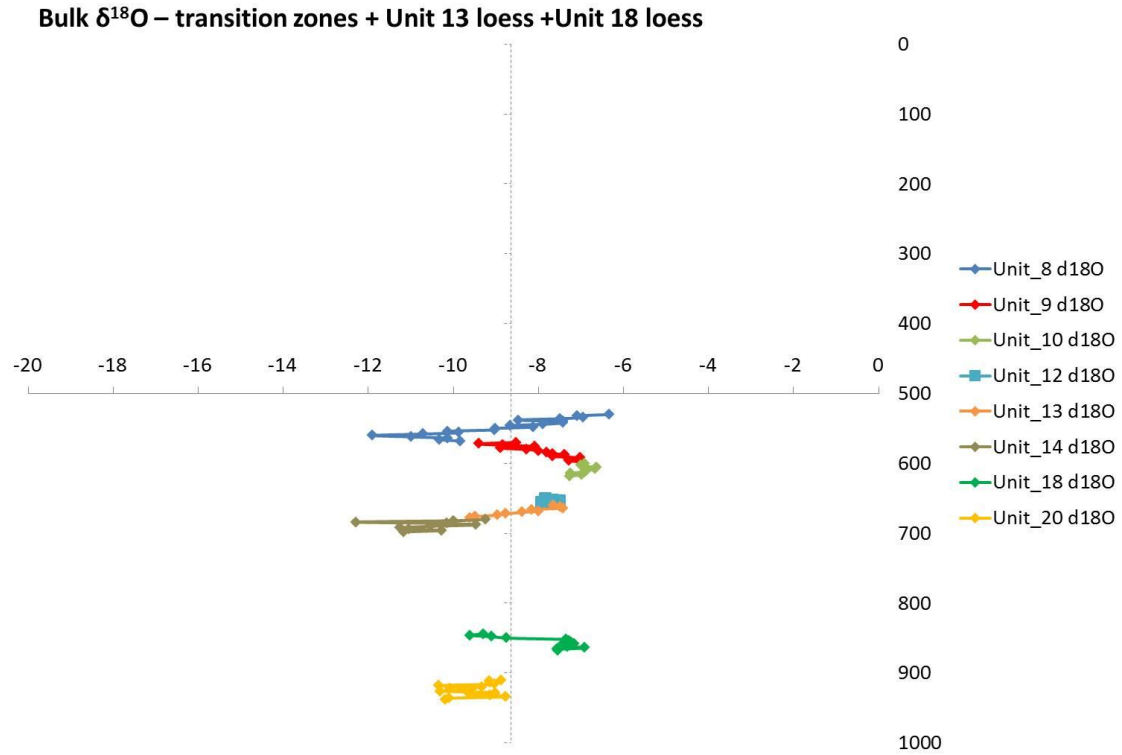

f. Bulk values of Villánykövesd – paleosols

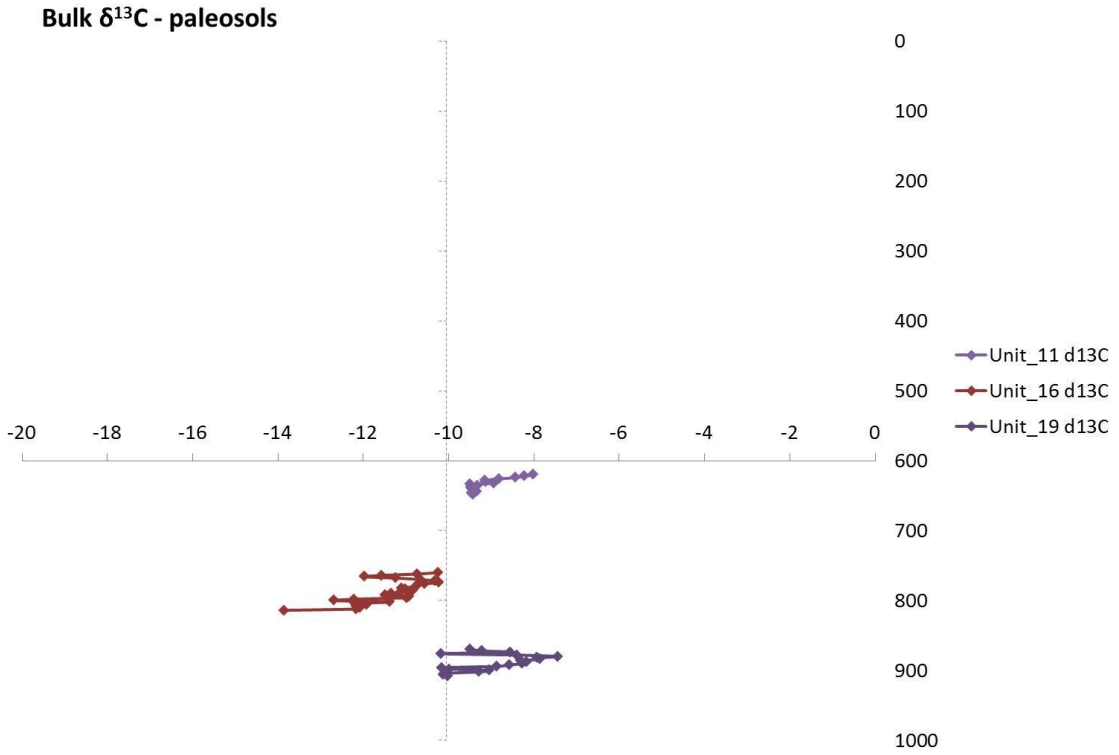

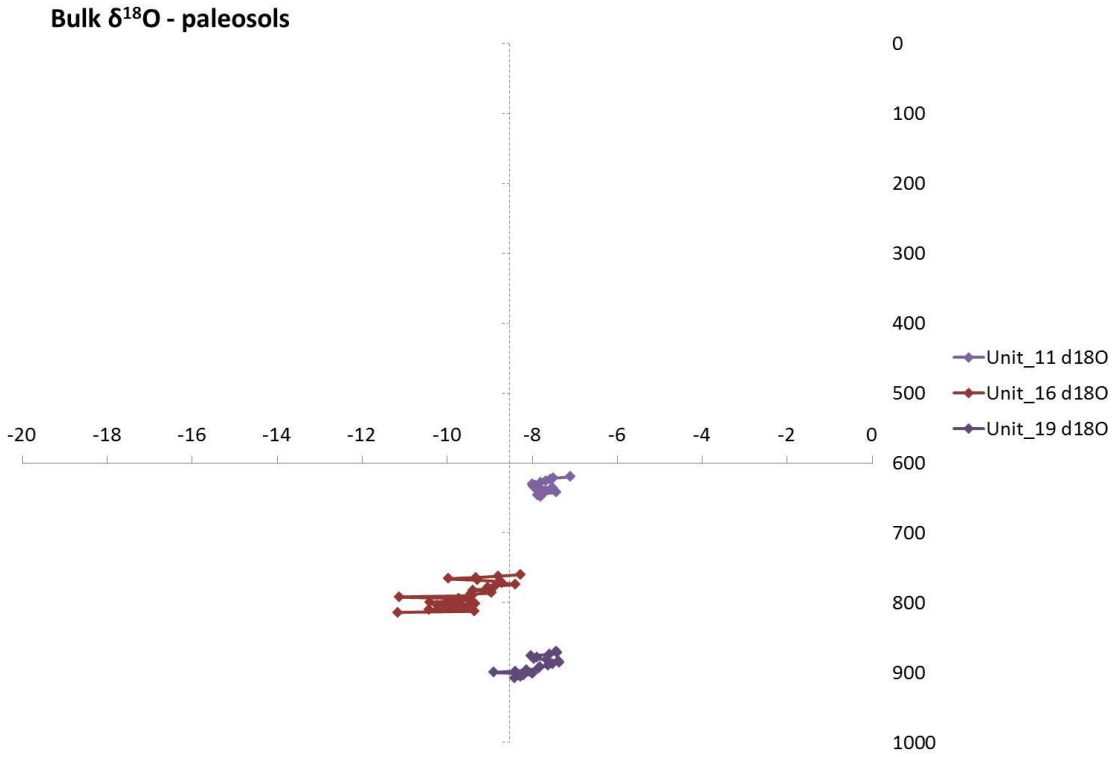

g. Hypocoatings of Villánykövesd

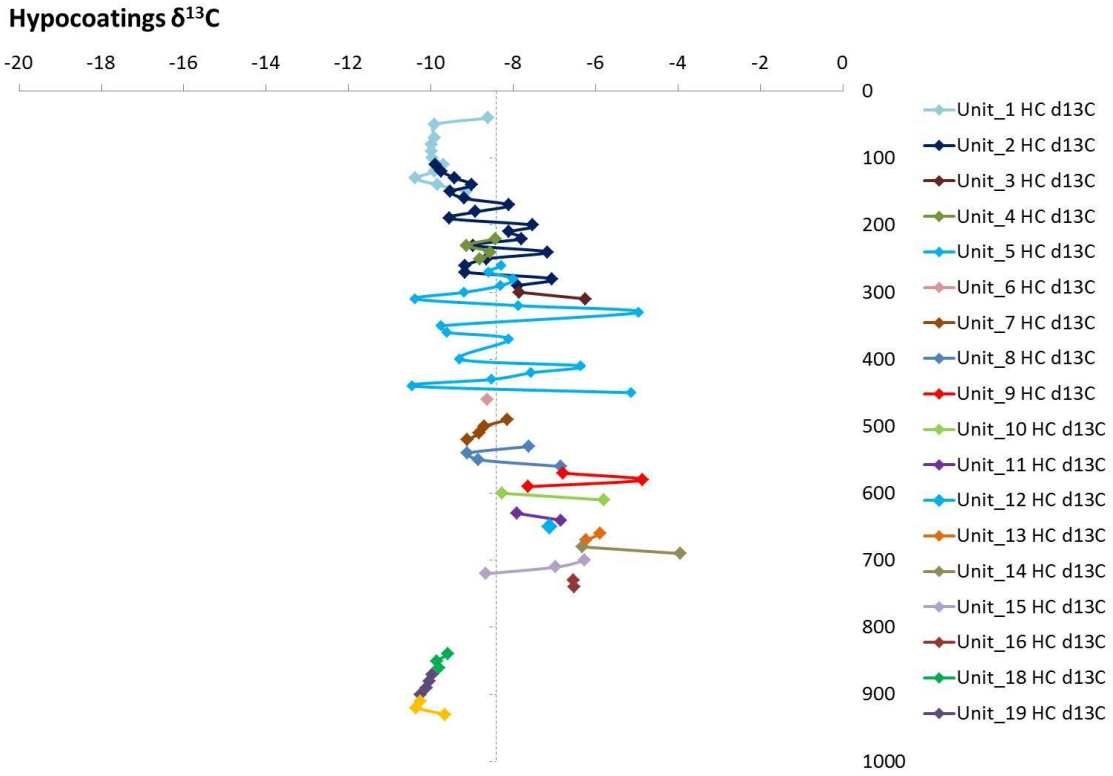

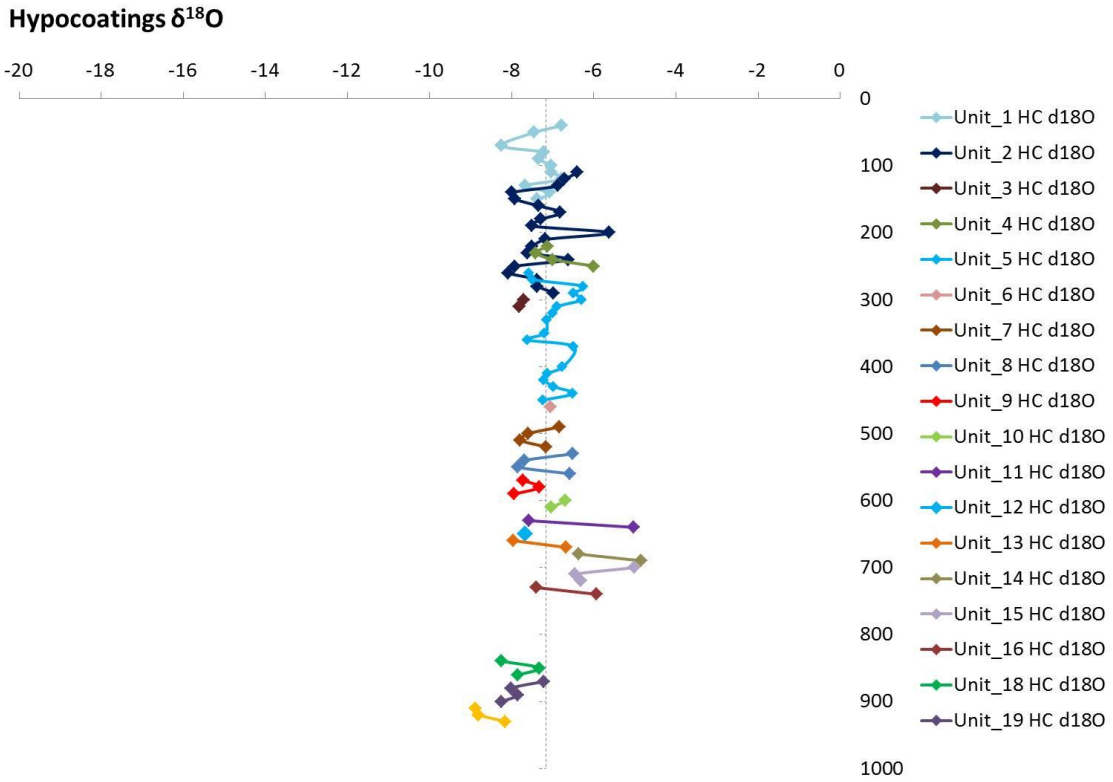

h. HC+CC of Villánykövesd

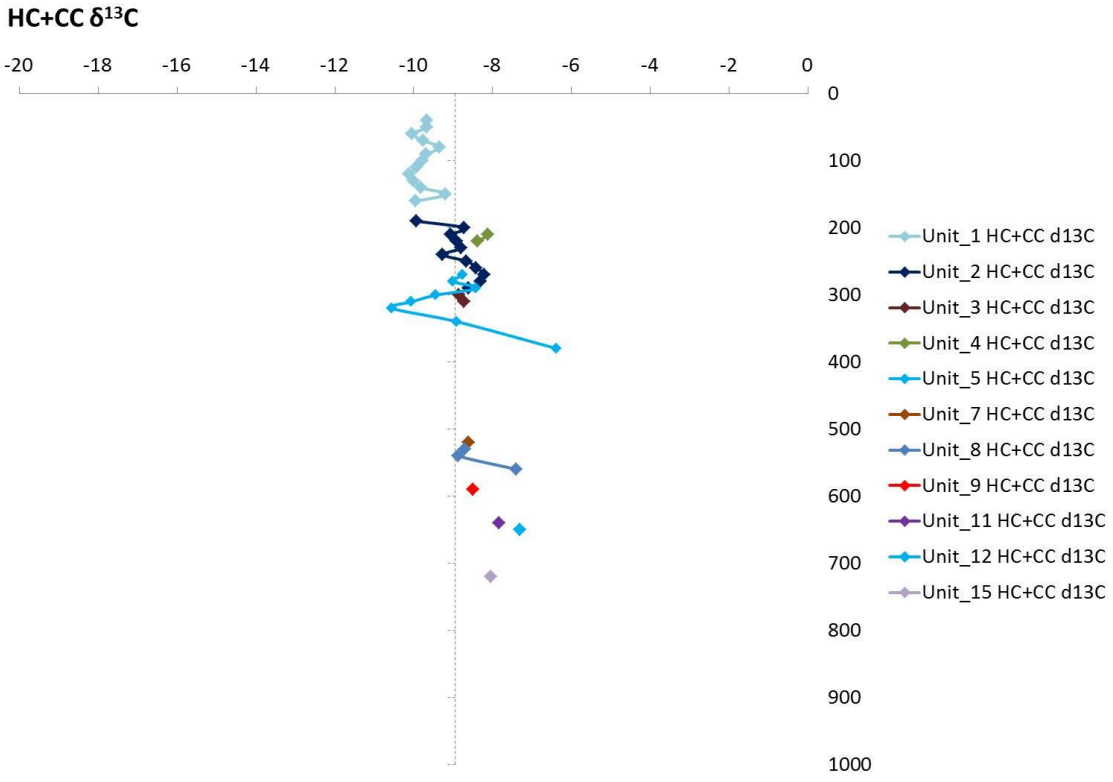

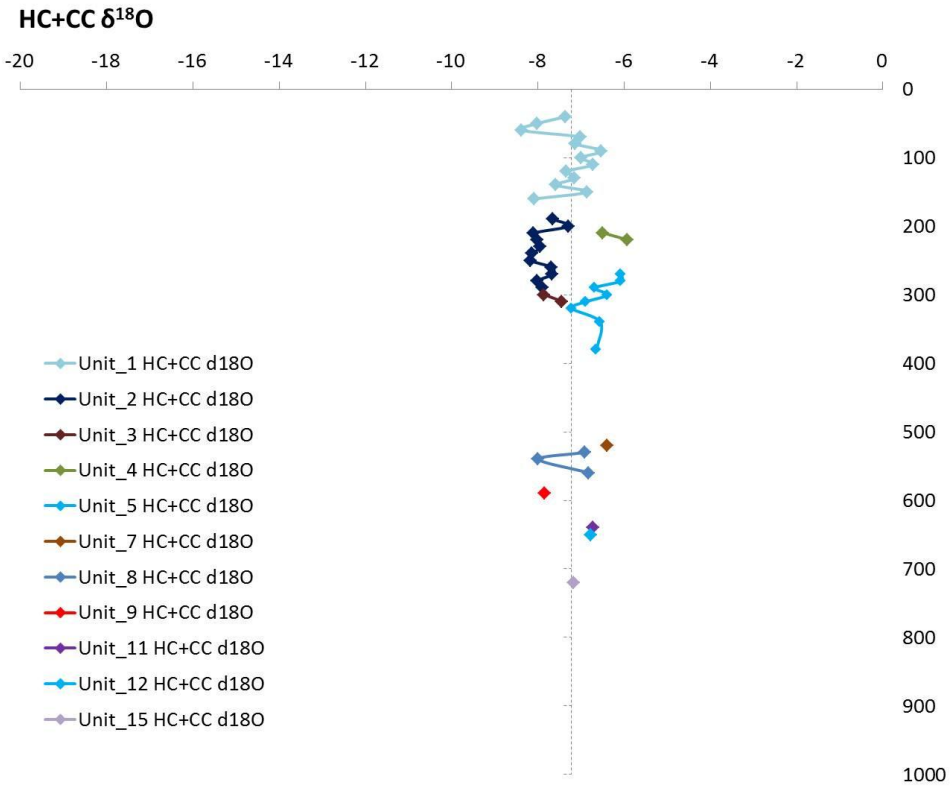

i. Earthworm biospheroids of Villánykövesd

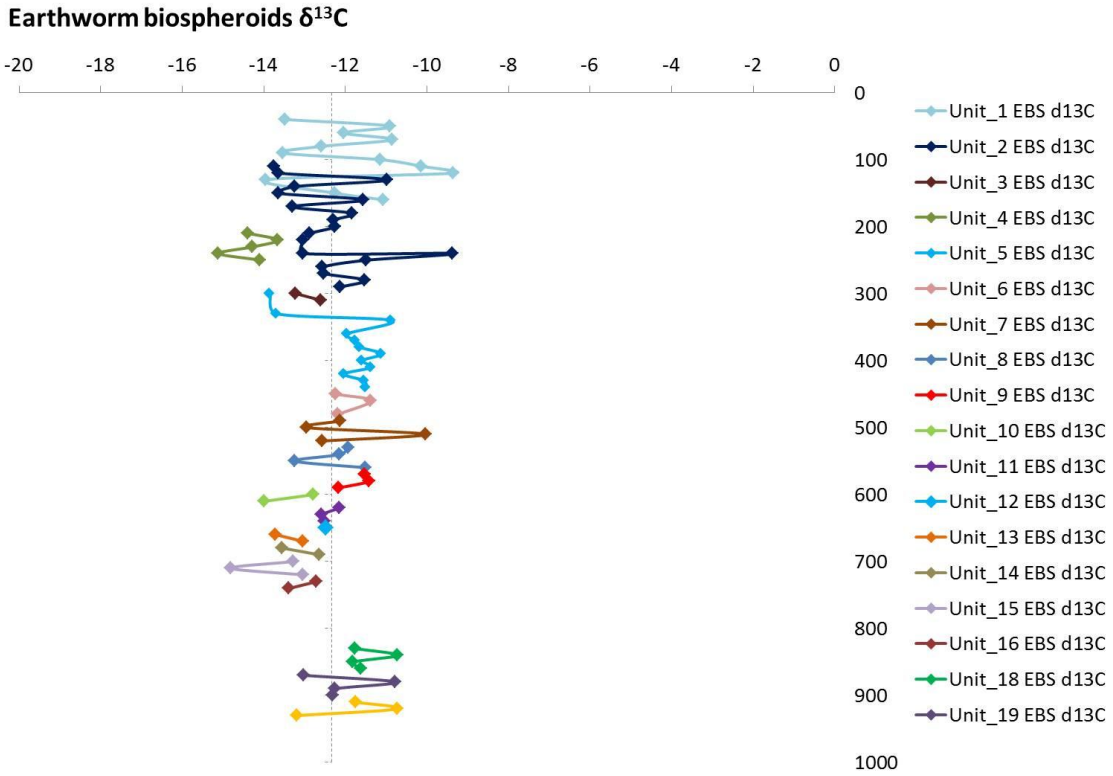

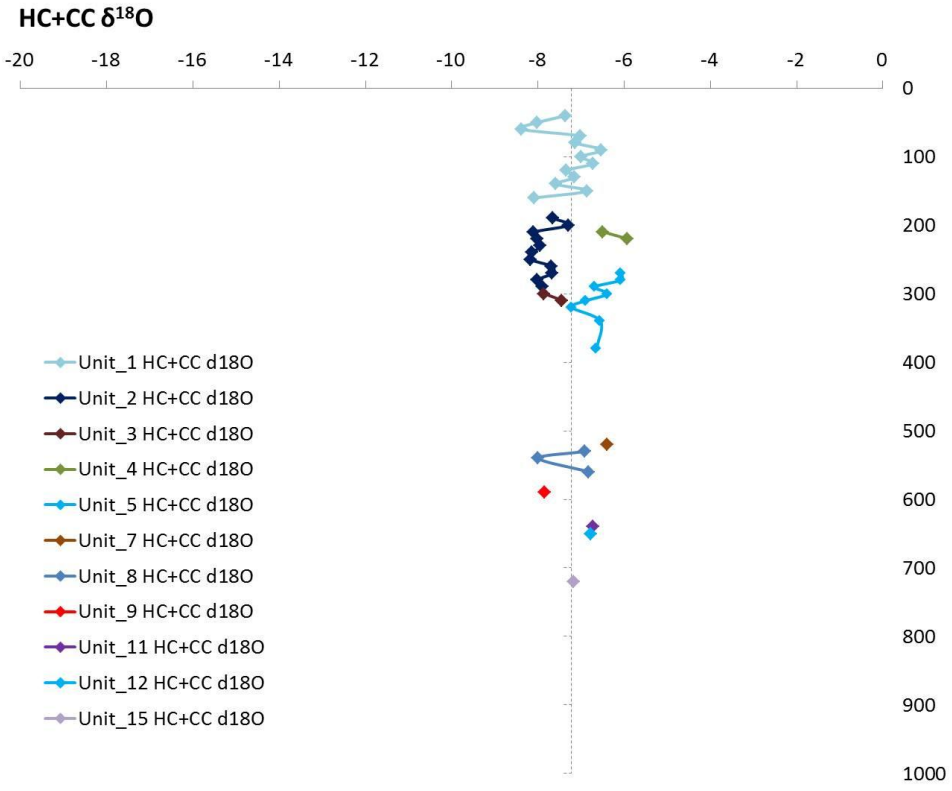

7. Applied terminology of microscale secondary carbonates based on BECZE-DEÁK, J. et al. (1997) and updated after BARTA, G. (2011a)

	Microscale secondary carbonate terminology based on BECZE-DEÁK, J. et al. (1997)	Correctly used terms	Comparison with differently described terms
Calcified root cells (CRC)		*Calcitic pseudomorphs of root cells* - LACKA, B. et al. (2009) *Calcified root cells* - JAILLARD, B. et al. (1991); KHOKHLOVA, O.S. et al. (2001); Phytomorphic calcite as part of *quasi structures* - STOOPS, G. (2003); DURAND, N. et al. (2010)	*Pseudomycelia*: as calcified root fragments - BOGUCKYI, A.B. et al. (2006) *Rhizolith*: calcite crystal infillings of root cells as pseudomorphs - SCHAEFLEIN, S. (2006) *Root petrification*: as the calcified cortex of roots - KLAPPA, C.F. (1980)
Earthworm biospheroids (EBS)		*Calcite biospheroids* – ANTOINE, P. et al. 2001 *Calcium carbonate granules* - CANTI, M.G. – PEARCE, T.G. (2003) *Earthworm biospheroliths* – ZAMANIAN, K. et al. (2016) *Earthworm granules* - DURAND, N. et al. (2010)	
Needle-fiber calcite (NFC)		*Needle-fiber (needle-fibre) calcite* - VERRECCHIA, E.P. – VERRECCHIA, K.E. (1994); LOISY, C. et al. (1999); CAILLEAU, G. et al. (2009a); MILLIERE, L. et al. (2011)	*Pseudomycelia*: biogenic structures in needle-fiber form calcite crystals (diameter of 1 µm), which are probably equal to calcified fungal hyphae - LACKA, B. et al. (2009) *Pseudomycelia*: acicular calcite crystals being of biogenic origin (connection to decaying roots) - WIEDER, M. – YAALON, D.-H. (1974, 1982) *Pseudomycelia*: this field description may be linked to NFC, since its presence is connected to hummus-rich horizons - ZHONGLI, D. et al. 1993; MARKOVIC, S.B. et al. 2007 *Pseudomycelium*: cotton-like accumulations composed of fine calcite needles - KOVDA, I. et al. (2009) *Pseudomycelium*: a) as loose crystal network on ped walls - KHOKHLOVA, O.S. et al. (2001)
Hypocoatings (HC)		*Hypocoating* - BULLOCK, P. et al. (1985); KEMP, R.A. (1995); STOOPS, G. (2003); DURAND, N. et al. (2010) *Quasi*: complex feature associated to calcification and decalcification of/and around root tissues. HC and quasicoatings are present in the form of perpendicular microchannels. - STOOPS, G. (2003); DURAND, N. et al. (2010) *Neocalcitan*: subcutan feature, which formed not on the channel wall, but around the channel. Its outer boundary may be diffuse – BLOCKHUIS, W.A. et al. (1968)	*Microrhizoliths* (formerly referred as *pseudmycelia*): small branching carbonate accumulations - GOCKE, M. et al. 2014a *Pseudomycelium*: as referring to hypocoatings during field description - DURAND, N. et al. (2010) *Pseudomycelium*: b) micritic calcite impregnations of matrix, which occur as thin coatings on voids - KHOKHLOVA, O.S. et al. (2001) *Rhizocretion*: a) thin tubes lined by micrite and/or filled with calcified root cell structures or root fragments; b) tube-like irregular concretions with empty channels - BOGUCKYI, A.B. et al. (2006) *Rhizoliths*: tube-form carbonate cementations in micritic size around rootlets - LACKA, B. et al. (2009). Similarity to HC also based on Fig. 9. in LACKA, B. et al. (2009). *Rhizoliths*: mentioned as coating of roots and cited equal to hypocoatings – UDVARI, G. et al. (2014) *Root tubules*: cemented micritic cylinders around root moulds, forming random or anastomosing structures; often built up of brown micrite and they could be filled up by low-Mg calcite in the vicinity of the root moulds - KLAPPA, C.F. (1980); ZHOU, J. – CHAFETZ, H.S. (2009a)

Carbonate coatings (CC)	***Carbonate coatings***: as intrusive pedofeatures on voids and peds, especially occur in root channels, cracks and other biopores – Antoine, P. et al. (2001); Stoops, G. (2003); Horvath, E. et al. (2007);. Appearance: a) main type (grey, built-up of more equal grains than HC); b) calcite tube; c) CC2 (possible paleocryogenic origin) – Barta, G. (2014)	***Pseudomycel***: (rapid) formation from percolating solutions, referred wrongly as hypocoatings – Zamanian, K. et al. (2016) ***Pseudomycelium***: powdery, white calcite infillings of root channels in loess, which may be due to repeating freeze-thaw cycles – Cilek, V. (2001) Possible connections to CC2 type - Barta, G. (2014).

8. Synthesis matrix for the interpretation of stable isotope values

more negative $\delta^{13}C$ – depletion in ^{13}C	more positive $\delta^{13}C$ – enriched in ^{13}C
Secondary carbonates are depleted in ^{13}C, when $\delta^{13}C$ values are shifted towards the more negative direction. This can be caused by the increase of mean annual precipitation, which affects plant-derived carbon and thus the composition of secondary carbonates (LIU, W. et al. 2011). In certain cases higher humidity may be combined with cooler conditions to indicate the same effect (PENDALL, E. – AMUNDSON, R.G. 1990). Negative $\delta^{13}C$ values are indicative of denser vegetation cover, enhanced biological activity and thus the effectiveness of organic matter mineralization (QUADE, J. et al. 1989; PENDALL, E. – AMUNDSON, R.G. 1990; BOGUCKYI, A.B. et al. 2006; LIU, W. et al. 2011): the reason of it can be found in the higher rate of root-respiratory CO_2 (WANG, H. – GREENBERG, S.E. 2007). Higher biological activity increases soil CO_2 and decreases the involvement of atmospheric CO_2 into the soil atmosphere (ALAM, M.S. et al. 1997). The presence of high vegetation density may refer to a warmer, interglacial period (RAO, Z. et al. 2006; CANDY, I. et al. 2012) and indicate at the same time humidity as an influencing factor (ALAM, M.S. et al. 1997; LIU, W. et al. 2011). This is especially true for secondary carbonates present in strongly developed paleosols (ALAM, M.S. et al. 1997). Extremely negative $\delta^{13}C$ values may refer to one component CO_2 systems (CO_2 derives only from the decomposition of organic matter), which are generally swampy, waterlogged soils/paleosols (SHELDON, N.D. – TABOR, N.J. 2009).	Secondary carbonates are enriched in ^{13}C, when $\delta^{13}C$ values are shifted towards the more positive direction. This phenomena has some reasons. Prevailing arid conditions and low productivity (low biological activity) of the soil-sedimentary environment generally cause a shift in $\delta^{13}C$ values of secondary carbonates towards more positive values (CERLING, T.E. 1984; ALAM, M.S. et al. 1997; KAAKINEN, A. et al. 2006; SHELDON, N.D. – TABOR, N.J. 2009; CANDY, I. et al. 2012). Water loss in the system will mainly be connected to the water loss of plants through evapotranspiration (QUADE, J. et al. 1989). Degassing of CO_2 is the consequence of evaporation, and since the lighter ^{12}C is removed in this process, the remaining solution has more positive $\delta^{13}C$ values (CANDY, I. et al. 2012). Enrichment in atmospheric CO_2 is especially characteristic of the uppermost soil horizon, when the climatic conditions are cold and/or arid (BOGUCKYI, A.B. et al. 2006). Arid conditions are guided by enhanced water stress during the growing season of plants, which leads to more positive $\delta^{13}C$ values for the organic matter – and thus may affect the isotopic composition of forming secondary carbonates as well (ALAM, M.S. et al. 1997; FOX, D.L. – KOCH, P.L. 2004). Sedimentation phases during glacials were exposed to such circumstances, since climatic conditions were colder and arid and vegetation density was relatively low (RAO, Z. et al. 2006; CANDY, I. et al. 2012). In certain cases closed forest canopy may cause differences in the CO_2 of the local atmosphere, which means that these

	plants can be more depleted in ^{13}C compared to those plants, which are the part of more opened vegetation systems (CERLING, T.E. – QUADE, J. 1993). Some other factors may cause the same effect, as the process of freezing lowers soil respiration rates, which leads to a possible enrichment of ^{13}C (CERLING, T.E. 1984). Enrichment may also be connected to the effect of microbial decomposition, since microorganisms prefer the useage of the lighter isotopes and leave the heavier ones in the system (GALIMOV, E.M. 1990). However, extreme seasonal changes can also lead to these properties (CERLING, T.E. 1984; CERLING, T.E. et al. 1991).
more negative $\delta^{18}O$ – depletion in ^{18}O	**more positive $\delta^{18}O$ – enriched in ^{18}O**
Meteoric water fallen during cool seasons is mainly depleted in ^{18}O (CERLING, T.E. – QUADE, J. 1993). By this means, temperature also affects the oxygen isotopic composition in precipitating carbonates: decreasing temperature leads to depletion in ^{18}O, while increasing temperature causes enrichment (HAYS, P.D. - GROSSMAN, E.L. 1991). The $\delta^{18}O$ values are shifted towards more negative values, when evaporation rates are lower and thus environmental conditions are moister (ALAM, M.S. et al. 1997). Freezing leads to enrichment of ^{16}O (according to RYSKOV, YA.G. et al. 1996). Isotopic signals can also be modified by infiltrating solutions, which reflect seasonal changes (QUADE, J. et al. 1989).	Evaporative effects lead to the enrichment of heavier isotopes in secondary carbonates developed under arid climatic conditions (KAAKINEN, A. et al. 2006): during evaporation the removal of the lighter isotope is easier and thus the heavier ^{18}O remains in the system (CERLING, T.E. – QUADE, J. 1993; SHELDON, N.D. - TABOR, N.J. 2009). This is especially true for near-surface evaporation during dry seasons (ŁĄCKA, B. et al. 2009). Low moisture availability causes more enhanced evaporation and high water stress conditions for the plants and thus leads to more positive $\delta^{18}O$ values in the precipitating secondary carbonates (ALAM, M.S. et al. 1997). Oxygen isotopic alteration due to evaporation may cause as +5‰ to +7‰ shifts in $\delta^{18}O$ values, especially close to the surface of the profile (SHELDON, N.D. - TABOR, N.J. 2009).

[38]**ADATLAP**

a doktori értekezés nyilvánosságra hozatalához

I. A doktori értekezés adatai

A szerző neve: **Barta Gabriella**

MTMT-azonosító: **10035374**

A doktori értekezés címe és alcíme: **Analysis of secondary carbonates from the young loess-paleosol sequences of the Carpathian Basin – especially regarding their paleoenvironmental role**

DOI-azonosító[39] 10.15476/ELTE.2016.044

A doktori iskola neve: **Földtudományi Doktori Iskola**

A doktori iskolán belüli doktori program neve: **Földrajz-Meteorológia Program**

A témavezető neve és tudományos fokozata: **Dr. Horváth Erzsébet**

A témavezető munkahelye: **Eötvös Loránd Tudományegyetem Természettudományi Kar**

II. Nyilatkozatok

A doktori értekezés szerzőjeként[40]

a) hozzájárulok, hogy a doktori fokozat megszerzését követően a doktori értekezésem és a tézisek nyilvánosságra kerüljenek az ELTE Digitális Intézményi Tudástárban. Felhatalmazom a Természettudományi Kar Tudományszervezési és Egyetemközi Kapcsolatok Osztályának ügyintézőjét Bíró Évát, hogy az értekezést és a téziseket feltöltse az ELTE Digitális Intézményi Tudástárba, és ennek során kitöltse a feltöltéshez szükséges nyilatkozatokat.

b) kérem, hogy a mellékelt kérelemben részletezett szabadalmi, illetőleg oltalmi bejelentés közzétételéig a doktori értekezést ne bocsássák nyilvánosságra az Egyetemi Könyvtárban és az ELTE Digitális Intézményi Tudástárban;[41]

c) kérem, hogy a nemzetbiztonsági okból minősített adatot tartalmazó doktori értekezést a minősítés *(dátum)*-ig tartó időtartama alatt ne bocsássák nyilvánosságra az Egyetemi Könyvtárban és az ELTE Digitális Intézményi Tudástárban;[42]

d) kérem, hogy a mű kiadására vonatkozó mellékelt kiadó szerződésre tekintettel a doktori értekezést a könyv megjelenéséig ne bocsássák nyilvánosságra az Egyetemi Könyvtárban, és az ELTE Digitális Intézményi Tudástárban csak a könyv bibliográfiai adatait tegyék közzé. Ha a könyv a fokozatszerzést követően egy évig nem jelenik meg, hozzájárulok, hogy a doktori értekezésem és a tézisek nyilvánosságra kerüljenek az Egyetemi Könyvtárban és az ELTE Digitális Intézményi Tudástárban.[43]

2. A doktori értekezés szerzőjeként kijelentem, hogy

a) az ELTE Digitális Intézményi Tudástárba feltöltendő doktori értekezés és a tézisek saját eredeti , önálló szellemi munkám és legjobb tudomásom szerint nem sértem vele senki szerzői jogait;

b) a doktori értekezés és a tézisek nyomtatott változatai és az elektronikus adathordozón benyújtott tartalmak (szöveg és ábrák) mindenben megegyeznek.

3. A doktori értekezés szerzőjeként hozzájárulok a doktori értekezés és a tézisek szövegének plágiumkereső adatbázisba helyezéséhez és plágiumellenőrző vizsgálatok lefuttatásához.

Kelt: Budapest, 2016. április 08.

Barta Gabriella

.....

a doktori értekezés szerzőjének aláírása

[38] Beiktatta az Egyetemi Doktori Szabályzat módosításáról szóló CXXXIX/2014. (VI. 30.) Szen. sz. határozat. Hatályos: 2014. VII.1. napjától.

[39] A kari hivatal ügyintézője tölti ki.

[40] A megfelelő szöveg aláhúzandó.

[41] A doktori értekezés benyújtásával egyidejűleg be kell adni a tudományági doktori tanácshoz a szabadalmi, illetőleg oltalmi bejelentést tanúsító okiratot és a nyilvánosságra hozatal elhalasztása iránti kérelmet.

[42] A doktori értekezés benyújtásával egyidejűleg be kell nyújtani a minősített adatra vonatkozó közokiratot.

[43] A doktori értekezés benyújtásával egyidejűleg be kell nyújtani a mű kiadásáról szóló kiadói szerződést.